# Conformational dynamics and pharmacology in transmembrane dimeric receptors

Jordi Haubrich

**THÈSE POUR OBTENIR LE GRADE DE DOCTEUR DE L'UNIVERSITÉ DE MONTPELLIER**

**En Biologie Santé**

École doctorale
**Sciences Chimiques et Biologiques pour la Santé**

Unité de recherche
**Institut de Génomique Fonctionnelle**

# Conformational dynamics and pharmacology in transmembrane dimeric receptors

**Présentée par Jordi HAUBRICH**
**Le 26 Novembre 2021**

**Sous la direction de Laurent PREZEAU et Jean-Philippe PIN**

**Devant le jury composé de**

| | |
|---|---|
| Pierre-Jean CORRINGER, Directeur de Recherche, Institut Pasteur UMR3571 | Rapporteur |
| Amandine HURBIN, Chargé de Recherche, IAB UMR5309 | Rapporteur |
| Jean-Louis BANÈRES, Directeur de Recherche, IBMM UMR5247 | Examinateur |
| Olivier CALVAYRAC, Chargé de Recherche, CRCT UMR1037 | Examinateur |
| Fabienne CHARRIER-SAVOURNIN, Product Manager, Cisbio/PerkinElmer | Examinateur |
| Laurent PRÈZEAU, Directeur de Recherche, IGF UMR5203 | Co-directeur de thèse |
| Jean-Philippe PIN, Directeur de Recherche, IGF UMR5203 | Co-directeur de thèse |

UNIVERSITÉ DE MONTPELLIER

# 1 ACKNOWLEDGEMENTS

I would like to start by thanking Jean-Philippe Pin and Laurent Prézeau for welcoming me in their team in 2017 as part of RSignal before being my directors of my thesis in 2018. I have enjoyed the freedom you have given me in my project and the guidance you have given when the project was a bit more challenging. Especially, the first 8 or 9 months were difficult project-wise, but luckily, we managed to reorganize the project and we could work on a "side-project". Jean-Philippe, I admire your qualities as a renowned researcher and it is much appreciated by me and many others in the team that you're very approachable to talk about science or about cycling/personal things. Also, the team meetings/barbecues at your place in Cazilhac were amazing and I think this tradition should be continued the coming years. Laurent, for you I have the same appreciation on the scientific level and on a personal level. It's easy to complain about life issues to you as you're very approachable and have some life lessons to share as well. That makes it easy to share stories with you, which helped me a lot. Thank you!

I would like to thank Pierre-Jean Corringer, Amandine Hurbin for being reviewer of my thesis and Jean-Louis Banères, Olivier Calvayrac and Fabienne Charrier-Savournin for taking up the role of jury member. The same goes for Christel Larbouret, Fabienne and Antonio Maraver who guided me during my thesis as members of my PhD committee during several official and non-official meetings.

A special thanks goes to professor Ad IJzerman and Elodie Dupuis for initiating my 4.5-year stay in the South of France. I'm glad Ad and Elodie came into contact, so I could become the first foreign Master student at Cisbio Bioassays.

Luckily, I was part of the EIDOS collaborative team of Cisbio and the IGF, as the monthly meetings (with free lunch) have helped me with my PhD a lot. I would like to thank Eric Trinquet a lot for his great advices and critics during the meetings. It has been highly appreciated as it improved my project. Also, I'm thanking the whole EIDOS team (Elodie, Thomas, Eric, JP, Laurent, Philippe, Sara, Julien, Alexandre, Salomé, Junke, Xue Li) for great discussions. Also, I would like to thank Jurriaan Zwier for scientific and personal advices, Robert Quast and Antonio Maraver for our scientific collaborations, the ARPEGE platform for using their facilities and La Région Occitanie and La ligue contre le cancer for financially supporting me.

En 2017, j'avais rencontré mes voisins Robert et Marceline à Codolet. Heureusement vous m'aviez invité pour l'anniversaire de Robert juste quelques semaines après mon arrivé à Codolet. Sans parler le français c'était une période difficile pour moi, mais Robert avait amélioré mon séjour dans le Gard énormément avec pleins soirées et des apéros. Robert, étant un vrai bon vivant, sait faire la fête. Quatorze juillet 2017 à Codolet était de loin le plus amusant quatorze juillet que j'ai eu avec le triathlon de Codolet.

J'aimerais aussi remercier Marie-Josée pour m'accueillir chez elle depuis janvier 2018. J'ai beaucoup aimé parler et discuter à propos pleins petits choses tous les jours et j'ai beaucoup apprécié que tu nous avais laissé la maison (et piscine) magnifique pour faire une « pool party » ou pour inviter des amies pour diner ensemble. Votre famille et les chiens sont aimables. Pablo (le chien le plus aimable) est devenu mon meilleur ami pendant le premier confinement. Tu vas me manquer et je te souhaite le meilleur et je viendrai te rendre des visites pendant mes vacances dans le sud de France.

Of course, I will miss Cédric as well! Thank you for great moments in the past years that started at the IGF after which we discovered that we had all kind of friends in common in the 'Erasmus' world. I've enjoyed it a lot to talk about football, because it's not easy to be Feyenoord supporter, but it may be even worse to be supporter of Olympique Marseille. It's been amazing to have you as a friend and I've enjoyed playing football and tennis, pubquizzes, drinking beers/wines, the ham party, the night I had to carry you home from the Pool party and organizing pool parties and barbecues.

Carole-Ann, my Belgian friend, thank you for laughing, gossiping, drinking (coffee/alcohol), eating and talking the past years. It's been great to be on the same wavelength on many things (hate and love for people, behaviour, good coffee) and at the same time being so different on many things as well (your love for coriander, insane spicy things/Korean noodles, cougar dresses, micheladas, crazy music taste).

Dear Alenca, it has been amazing to organize the Young Investigator Seminar Series with you. Your laugh is contagious and I've enjoyed to complain about all issues that living in France and working at the IGF may bring, including organizing the YISS. I've enjoyed our tea sessions, our jenever at work, strolling around the IGF ringing up people for the YISS, beers etc. etc. Thanks for all the fun we had!

Joan (or Mr. Johnny Fountain English), I'm happy we arrived in the same period at the IGF, because we spent great times at the institute and abroad. Thanks for the trips to Barcelona, parties (I love techno, legendary Panama nights), periquitos bastardos, science (how to work with nanobodies, our DN45 paper) and just being an awesome friend!

Matej, thank you for being partner in crime in Montpellier, Prague and Barcelona nightlife, for the smokes, the Italians, roadtrips to Spain, lavender, generosity and the chill aura that surrounds you. And thanks for being a great friend.

Xavi "*I am not a biologist*" and "*I have the answer to everything. But maybe it is not the correct answer.*", it's been great to complain about France, or Dutch accents with you. Thanks for the nice trips, good talks, introducing me to using PowerPoint to generate figures, good science and great friendship.

Alice and Jack, luckily you came to Montpellier and were part of my life here. I enjoyed our beers, pubquizzes at Shakespeare or on Zoom during covid, chill sessions, the visit to Amsterdam and the crazy house party.

Julie C., thanks for introducing me into "long-distance" cycling, good conversations, sharing a part of my music taste and just being a great person!

Maria R and Laura G, thanks for being part of the Spanish (and Catalan) enclave at the IGF. I've enjoyed our time together a lot and will not forget the nights at Panama and our visit to Prague.

Also, I'd like to thank the people that were in the Pin team during my stay and with who I worked together with great pleasure. Thank you, Fanny M, Michael, Xue Li, Ji-Yong, Julien S, Mathieu, Silvia, Carmen L and Marianne.

My last year in the lab has been really great, despite so many good friends leaving. So, thank you for being such nice people: Marta, Cyrielle, Kawthar, Jessica, Roxane, Alexandre, Leo, Mireille, Claire, Junke, Salomé, Anaïs, Isabelle, Pierre-André and Cécile.

Also, I'd like to thank other people that I came across at and around the IGF: the football squad (Kris, Anthony, Miguel, Yann), Bettina, Gavin, Tabitha, Philippe Marin and Muriel Asari.

Julie B., thank you for being such a great person during the last year of my PhD. I'm sure it would have been more difficult if you did not support me, like you did.

Juliette, thanks for our conversations. It's been easy to share the issues of life with you and I'm happy we could talk about our "great" diet.

Also, I would like to thank Linda K, San-Wei, Solveig and Vilde for the awesome first year I had in Montpellier. Thanks for all the nights out, the wintersport to the Pyrenees, the visit to Copenhagen and other times we went out.

Francesca, Matej, Valentina and Davide, thanks for the awesome second year I had in Montpellier. It's been great to hang out with "the Italians" and Matej. I will not forget the Panama, Rome, Les Arceaux and the Political Sciences gala. And Francesca, thank you for teaching me how to cook pasta and for spending so much time together.

Cas, Céline, Hilde, Ilse, Katja, Jonas and Cédric thanks for the awesome third year I had in Montpellier. It has been fun to hang around with some Dutch people, celebrate Sinterklaas and misbehave at the Erasmus gala.

Nicole, Harry and Joana, thank you for spending time after Covid, I've really enjoyed the dinner parties and the beers.

Ik wil ook graag Remy bedanken voor de support de afgelopen jaren. Zoals we inmiddels wel gewend zijn, zien we elkaar niet heel vaak, maar toch ben je altijd beschikbaar om te praten over alles wat me bezighoudt. Ik waardeer onze vriendschap enorm en ben blij dat we elkaar vaak goed begrijpen.

Graag wil ik m'n ouders, Erik, Rowen en Vincent bedanken voor de steun de afgelopen jaren, voor hun bezoekjes aan Montpellier en voor de vele overnachtingen die ik bij jullie heb mogen maken wanneer ik in Nederland was.

Then, a final shout-out to all the people that came to visit me (or wanted to til covid ruined the party): Waldo in Codolet, Laura M, Thijs S, Rick vd S+Anne S, Duif+vdE+Jongeleen, Rowen+Vincent, Erik, Pap, Mam, Pap+Mam, Suzanne+Maxime, Remy+Chantal, Francesca, Damy+Janna+Sophie, Kenny+Bruno+Maurits+Waldo, VdB+Leboux+Duif+Schaap+VdE (ruined by covid), Iris V, Remy

And the ones coming from far away to Montpellier to attend to my dissertation: Mam, Pap, Rowen Erik, Marc, Remy, vdB, Duif, Bruno, vdE, Huub, Thijs S, Romain, Xavi, Matej.

I can only say that the past 4 years and 9 months in France have been an amazing experience and I'm grateful for all the people I've met and the scientific environment that I've worked in.

Sinds mijn vertrek zijn er 4 personen die dicht bij ons gezin staan overleden. De ouders van mijn moeder: Janny en Frans van Oers en de zussen van mijn vader: Joke Haubrich-Mol en Ida Haubrich, dank jullie voor de belangrijke rol die jullie hebben gespeeld in ons leven.

# 2 SUMMARY (EN) & RÉSUMÉ (FR)

## 2.1 SUMMARY

**Biosensors for studying conformational dynamics and pharmacology in transmembrane dimeric receptors**

Transmembrane receptors are proteins that translate extracellular information into intracellular signals. These proteins are categorised based on the way they transduce signals through the plasma membrane. In many cases such transduction involves the formation of dimers, either ligand-induced or constitutive dimers. For example, while the enzyme-linked receptors, such as the Epidermal Growth Factor (EGF) receptor, may be ligand-induced dimers, the G protein-coupled receptors (GPCR) activated by the neurotransmitter glutamate are covalently linked constitutive dimers. Understanding how a signal can be transduced from the extracellular domain into the cell is important to develop novel drugs targeting such receptors.

The EGF receptor is a member of the receptor tyrosine kinase (RTK) class and is involved in cell differentiation and proliferation. Inhibition of the EGF receptor by medication is used as a successful treatment for a variety of cancers, but side effects and resistance to medication remain common major obstacles. The full-length EGF receptor crystal structure is unknown, which leaves ambiguity to the precise activation process and the effect of inhibitors. Its activation mechanism has been described as either ligand-induced dimerization or conformational changes within pre-assembled dimers. This is followed by phosphorylation of the intracellular domain of the receptor and the generation of intracellular signalling cascades. By generating a fluorescent conformational biosensor, we showed that the activation of the EGF receptor by its endogenous agonists results from ligand-induced dimerization. We also found that some non-competitive tyrosine kinase (TK) inhibitors also induce dimer formation, without activating the receptor, through a direct contact of the TK domains. Strikingly, internalization induced by its endogenous ligand is not blocked by the non-competitive inhibitors, demonstrating it does not require TK domain activity and is likely mainly dependent on receptor dimer conformation. This is supported by our observation that TK inhibitors promoting dimer formation slowed down the internalization process. This finding shows that the activation/dimerization process of the EGF receptor can be changed by inhibitors and that internalization of the EGF receptor is regulated by monomeric/dimeric conformations rather than by phosphorylation of the receptor.

In contrast to the EGF receptor, the metabotropic glutamate (mGlu) 4 receptor is a constitutive dimer that is important for the regulation of many synapses in the brain. Recently, an mGlu2-mGlu4 heterodimer was proven to exist in the brain, but its function remains unknown due to the lack of tools selectively controlling it. To further investigate mGlu4 homo- and heterodimers, an innovative nanobody that discriminates between these receptors was developed. The nanobody is selective for the human mGlu4 receptor, and stabilizes the active homodimer conformation, making it a full agonist. By combining molecular dynamics simulations and site-directed mutagenesis, the epitope and mechanism of action of the nanobody were identified, revealing a new way of activating mGlu receptors. Conversely, this nanobody is incapable of activating heterodimeric mGlu2-mGlu4, where it acts as positive allosteric modulator through asymmetric activation of the heterodimer. This nanobody is the first pharmacological tool that discriminates between homo- and heterodimers.

Overall, our studies revealed how important is the conformation of dimeric receptors to control their signalling, as shown with the TK inhibitors controlling to conformation of the TK domain-induced dimers and the internalization process of the EGF receptor, or by showing that nanobodies can control specifically a receptor dimer made of specific subunits. These findings show the importance of allosteric and asymmetric regulation of dimeric transmembrane receptors.

## 2.2 RESUME

**Biosenseurs pour l'étude des dynamiques des conformations et pharmacologie des récepteurs dimériques transmembranaires.**

Les récepteurs transmembranaires traduisent les informations extracellulaires en signaux intracellulaires sont classés en fonction de leur mécanisme de transmission des signaux à travers la membrane plasmique. Nombre de ces récepteurs sont assemblés en dimères constitutifs ou induits par le ligand. Si les récepteurs liés à une enzyme, tels que le récepteur du facteur de croissance épidermique (EGF), peuvent être des dimères induits par le ligand, les récepteurs couplés aux protéines G (RCPG) activés par le neurotransmetteur glutamate sont des dimères constitutifs liés de manière covalente. Il est important de comprendre comment ces récepteurs transmettent le signal pour développer des médicaments les ciblant.

Le récepteur de l'EGF est un récepteur à domaine tyrosine kinase (RTK) impliqué dans la différenciation et la prolifération des cellules. Son inhibition par des médicaments est utilisée dans le traitement de cancers, mais les effets secondaires et la résistance aux traitements restent des obstacles majeurs. Sa structure tridimensionnelle complète étant inconnue, son processus d'activation n'est pas complétement compris et résulterait soit d'une dimérisation induite par le ligand soit de changements de conformation au sein de dimères pré-assemblés. Ceci est suivi par la phosphorylation du domaine intracellulaire du récepteur et la génération de cascades de signalisation intracellulaire. En générant un biocapteur conformationnel fluorescent, nous avons démontré que l'activation du récepteur par l'EGF résulte de sa dimérisation induite par le ligand. Nous avons également découvert que certains inhibiteurs non compétitifs du domaine tyrosine kinase (TK) induisent la formation de dimères par un contact des domaines TK, mais sans activer le récepteur. Il est à noter que l'internalisation induite par l'EGF n'est pas bloquée par les inhibiteurs des TKs (ITK), ce qui démontre qu'elle ne nécessite pas l'activité du domaine TK et qu'elle dépend probablement de la conformation du dimère. Ceci est soutenu par l'observation que les ITKs favorisant la formation de dimères ralentissent l'internalisation. Ce résultat montre que le processus d'activation/dimérisation du récepteur de l'EGF peut être modifié par des ITKs et que son internalisation est régulée par sa conformation monomère/dimère plutôt que par sa phosphorylation.

Le récepteur métabotropique du glutamate (mGlu) 4 est un dimère constitutif qui joue un rôle important dans la régulation de nombreuses synapses dans le cerveau. Récemment, l'existence d'un hétérodimère mGlu2-mGlu4 a été prouvée dans le cerveau, mais sa fonction reste inconnue en raison du manque d'outils permettant de le contrôler sélectivement. Pour approfondir l'étude des homo- et hétérodimères mGlu4, un nanocorps innovant qui discrimine ces récepteurs a été développé. Ce nanocorps est sélectif pour le récepteur mGlu4 humain et stabilise la conformation active de l'homodimère, ce qui en fait un agoniste complet. En combinant des simulations de dynamique moléculaire et une mutagenèse dirigée, l'épitope et le mécanisme d'action du nanocorps ont été identifiés, révélant une nouvelle façon d'activer les récepteurs mGlu. À l'inverse, ce nanocorps est incapable d'activer les hétérodimères mGlu2-mGlu4, sur lesquels il agit comme un modulateur allostérique positif parune action asymétrique sur l'hétérodimère. Ce nanocorps est le premier outil pharmacologique qui permet de distinguer les homo- et les hétérodimères.

Nos études ont révélé l'importance de la conformation des récepteurs dimériques pour contrôler leur signalisation, comme le montrent les ITKs contrôlant la conformation des dimères induits par les domaines TK et le processus d'internalisation du récepteur de l'EGF, ou en montrant que les nanocorps peuvent contrôler spécifiquement un dimère de récepteur composé de sous-unités spécifiques. Ces résultats montrent l'importance de la régulation allostérique et asymétrique des récepteurs transmembranaires dimériques.

# 3 LAYMAN'S SUMMARY (EN), RESUME VULGARISE (FR) & SAMENVATTING VOOR LEKEN (NL)

**Layman's summary - Biosensors for studying conformational dynamics and pharmacology in transmembrane dimeric receptors.** The human body contains billions of cells that work together in order to maintain the organism alive and prevent or cure diseases. Each cell is surrounded by a lipid membrane that surrounds an aqueous environment. The membrane contains a big diversity of proteins, among them receptors. Receptors function by translating outside signals that are molecules (like medicines, chemical messengers or hormones), into messages for the cells that regulate their growth, secretion or life. In some diseases, receptors are too active or they don't function properly, resulting in a disbalance in messages into the cell. As a consequence, cells may keep growing uncontrollably (cancer) or generate a disbalance in chemical messengers in the brain (neuropathic diseases). Association of two receptors modifies their function and cellular action. Our study shows that association of two growth factor receptors (EGFR) can be modified by certain cancer medication, which perturbs the elimination of the receptor from the cell membrane. Moreover, we have developed an innovative molecule that differentially regulates the brain receptor, depending on whether it is associated to another receptor type or not. This allows us, for the first time, to selectively control activation of this brain receptor.

**Résumé vulgarisé - Biosenseurs pour l'étude des dynamiques des conformations et pharmacologie des récepteurs dimériques transmembranaires.** Le corps humain contient des milliards de cellules qui travaillent ensemble pour maintenir l'organisme en vie et prévenir ou guérir les maladies. Chaque cellule est constituée d'une membrane lipidique externe qui entoure un milieu aqueux intracellulaire. La membrane contient une grande diversité de protéines, dont des récepteurs. Les récepteurs fonctionnent en traduisant les signaux extérieurs qui arrivent sous forme de molécules (médicaments, messagers chimiques ou hormones) en messages destinés aux cellules, qui régulent par exemple leur croissance, leurs sécrétions ou leur mort. Dans certaines maladies, les récepteurs sont trop actifs ou ne fonctionnent pas correctement, ce qui entraîne un déséquilibre des messages dans la cellule. En conséquence, les cellules peuvent continuer à se développer de manière incontrôlée (cancer) ou générer un déséquilibre des messages chimiques dans le cerveau (maladies neuropsychiatriques). L'association de deux récepteurs modifient leurs fonctionnements et actions cellulaires. Ainsi, notre étude a montré que l'association du récepteur de facteur de croissance EGFR avec lui-même est modifiée par certains médicaments contre le cancer ce qui perturbe l'élimination du récepteur de la membrane cellulaire. De même, nous avons développé une molécule innovante qui permet de réguler différemment un récepteur cérébral selon qu'il est ou non associé avec un autre type de récepteur. Ceci permet, pour la première fois, de sélectivement contrôler les diverses actions cérébrales de ce récepteur.

**Samenvatting voor leken - Biosensoren voor de studie van conformationele dynamiek en farmacologie van dimere transmembraanreceptoren.** Het menselijk lichaam bevat miljarden cellen die samenwerken om het lichaam in leven te houden en ziekten te voorkomen of te genezen. Elke cel bestaat uit een intracellulair waterig medium dat is omgeven door een buitenmembraan van vetten. Het membraan bevat een grote verscheidenheid aan eiwitten, waaronder receptoren. Receptoren vertalen externe moleculaire signalen (geneesmiddelen, chemische boodschappers of hormonen) in berichten voor de cellen die hun groei, secretie of dood regelen. Bij sommige ziekten zijn de receptor te actief of functioneren ze niet goed, waardoor de berichten voor de cellen niet in balans zijn. Als gevolg daarvan, kunnen cellen ongecontroleerd blijven groeien (kanker) of is er geen balans in de hoeveelheid chemische boodschappers in de hersenen (hersenziektes). De functie van receptor hangt af van hun associatie met andere receptoren. In onze studie tonen we aan dat dit ook geldt voor de associatie van twee groeifactorreceptoren door bepaalde anti-kankermedicijnen: de verwijdering van receptoren van het celmembraan wordt verstoord. Daarnaast hebben we een innovatief molecuul ontwikkeld die het mogelijk maakt om een hersenreceptor te activeren afhankelijk van of deze geassocieerd is met een ander type receptor. Dit maakt het voor het eerst mogelijk verschillende functies van deze receptor te onderzoeken.

# 4 TABLE OF CONTENTS

# 5 PREFACE

During the past 4 years at the Institut de Génomique Fonctionnelle (IGF) I got the chance to work in a great scientific environment in the team of Jean-Philippe Pin, Laurent Prézeau and Philippe Rondard. This team is best known for their involvement in many discoveries involving dynamics and function of metabotropic glutamate (mGlu) receptors. In this preface I would like to give a small background about the thesis.

My interest in mGlu receptors started when I was doing my Bachelor and Master internships in the team of prof. IJzerman at the Universiteit Leiden on the residence time of positive allosteric modulators of the mGlu2 receptor. During my first Master internship, prof. IJzerman put me into contact with Elodie Dupuis from Cisbio Bioassays, so I could do my Master internship in their company. Guided by a bit of naivety, I spent 6 months in Codolet in France, where I learned a lot about antibodies, β-arrestins and French. The research team was part of a collaboration with the IGF, which brought me to the place where I am.

My thesis started as project to develop methods to measure G protein-coupled receptor (GPCR)-mediated transactivation of the EGF receptor. After 8 months of mostly failed experiments, we decided to dramatically change the subject and focus solely on the EGF receptor, thereby leaving the GPCR research field. After 2 years in my PhD, I came back to GPCR research, because the project involving an innovative nanobody for the mGlu4 receptor, needed extra hands. Together with Joan Font-Inglés and collaborators, we advanced the project and in August 2021 it was published in PNAS. The article of the study around the EGF receptor is in preparation, and the most advanced manuscript is included in this thesis.

# 6 INTRODUCTION

## 6.1 GENERAL INTRODUCTION

### 6.1.1 A short history of receptors

The first hypothesis about the existence of membrane receptors dates back to 1897 and was done by Paul Ehrlich. He formulated a theory in which immune cells have so-called "side-chains" that were binding nutrients in order to maintain life, the first description of a receptor (Witebsky 1954). The first hypothesis of receptors transferring an external signal inside cells was done by John Newport Langley in 1901 (Langley 1901). A few years later, in 1905, he proved dose-dependent regulation of cells by entities to which ligands bind on cells (Langley 1905). Paul Ehrlich was awarded the Nobel Prize in Physiology and Medicine in 1908[i] for his work on immunity and John Newport Langley was nominated several times for his work on the sympathetic nervous system, but never actually won a Nobel Prize.[ii] The first mathematical approach to describe drug-receptor interactions was done by Alfred Clark in 1933 (Clark 1933). He hypothesized that the effect of a drug is determined by the amount of drug bound to a receptor, the receptor occupancy theory. At this time, the idea that membrane receptors could be precisely regulated became accepted.

However, it was unknown what receptors looked like, thereby missing crucial information. It was not until the 2000s that the first full-length crystal structures of human membrane receptors were determined in detail. The first solved (atypical) G protein-coupled receptor (GPCR) structure was that of the rhodopsin receptor (Palczewski et al. 2000). In 2007, the first structure of a typical GPCR, the human β2-adrenergic receptor, was solved through X-ray crystallization (Rasmussen et al. 2007). By using computer power to visualize and model interactions between drug and receptor, interactions could now be calculated. By generating databases of protein and drug structures, *in silico*[iii] screenings could provide a fast way to predict drug interactions.

Despite major *in silico* advancements, the laboratory will remain an important part of drug research and testing drugs for interactions and effects on their target needs to be done *in vitro* and *in vivo* by researchers. Increasing computer power and new techniques that improve receptor crystallization, like cryogenic electron microscopy (cryo-EM), are the most recent milestones in drug discovery. Indeed, in the past years

[i] https://www.nobelprize.org/prizes/lists/all-nobel-laureates-in-physiology-or-medicine/
[ii] https://www.nobelprize.org/nomination/archive/show_people.php?id=5226
[iii] Experiments on a computer or with computer simulations

many high-resolution structures of receptors have been solved and published, which will lead to an increase in high-quality drug research and more detailed understanding of receptor mechanisms.

### 6.1.2 From DNA to receptor on the cell membrane

In 1990 the Human Genome project (HUGO) was launched with the goal to achieve the sequencing of a complete human genome within 15 years. The first draft of the human genome deoxyribonucleic acid (DNA) sequence was published within 11 years, making the project a success (Hood and Galas 2003). The human genome is full of regions of DNA that are coding for a protein or ribonucleic acid (RNA). These regions are called genes. Till today, it is not clear how many genes there are exactly and the latest estimates are around 21,000 genes. Partly, this is explained by the difficult definition of a gene, because large regions in the genome do not code for proteins or RNA, but are still important for cellular functions (Pertea et al. 2018).

#### *6.1.2.1 Gene regulation: transcription, splicing, translation, posttranslational modifications*

Gene expression is regulated by many steps among which transcription, the generation of RNA based on the gene sequence, is the first (Fig. 1A, 1.). Regulation of transcription involves the loosening of the condensed chromosomal structure, modifications of histones and supercoiling of the DNA. In the nucleus, after unwinding of the DNA and showing the promotor sequences on the DNA, a complex of proteins, that includes a transcription factor, binds to the DNA. Upon binding of the complex, RNA polymerase binds to the DNA and the protein complex, where it starts the transcription of DNA into pre-messenger RNA (pre-mRNA).

During a process called splicing, non-coding regions/introns are removed and coding regions/exons are joined together to form the messenger RNA (mRNA) (Fig. 1A, 2.). By alternative splicing, protein expression can be regulated. Different receptor splicing variants could be generated from the same DNA. This could result in constitutively active variants, like the exon 2 till 7-lacking EGFRvIII splicing variant, which is often overexpressed in glioblastoma multiforme (GBM) (Gan, Cvrljevic, and Johns 2013; Abou-Fayçal et al. 2017). On the other hand, some splicing variants can only be found in some tissues as is the case for an mGlu4 receptor splice variant that is only found on the tongue (Pal Choudhuri, Delay, and Delay 2016). Through splicing, the human transcriptome should contain over 100,000 transcripts.

After the mRNA is generated, it is transported from the nucleus to endoplasmic reticulum (ER) by a complex of transporter proteins (Fig. 1A, 3.). In the ER, the ribosomes are responsible for binding of transfer RNA (tRNA), a type of RNA that is coupled to amino acids. Following the mRNA sequence, a specific amino acid polymer is generated. Translation can be regulated by phosphorylation of initiation factors of translation or by secondary structures of RNA.

Importantly, proteins can also be modified through posttranslational modifications (Fig. 1A, 4.). These modifications often take place in the rough endoplasmic reticulum (RER). Post translational modifications include generation of disulphide bonds, proper folding, addition of saccharides (i.e. glycosylation), cleavage and organization of tertiary protein complexes (Fig. 1B). Misfolded proteins could be degraded and receptors with an intracellular KDEL or KKXX-sequence could be retained in the ER (Maurel et al. 2008). Lastly, many other protein modifications could occur that are classified as posttranslational modification. Some examples are phosphorylation, ubiquitination, acetylation, methylation. All these processes together are crucial for the correct functioning of receptors. For example, the mGlu4 receptor is a constitutive dimer through the formation of a disulphide bond, and the EGF receptor is a heavily glycosylated receptor (Zhen, Caprioli, and Staros 2003) (Fig. 2).

Overall, gene and subsequent receptor expression are regulated at the level of DNA transcription, splicing, translation and through posttranslational modifications.

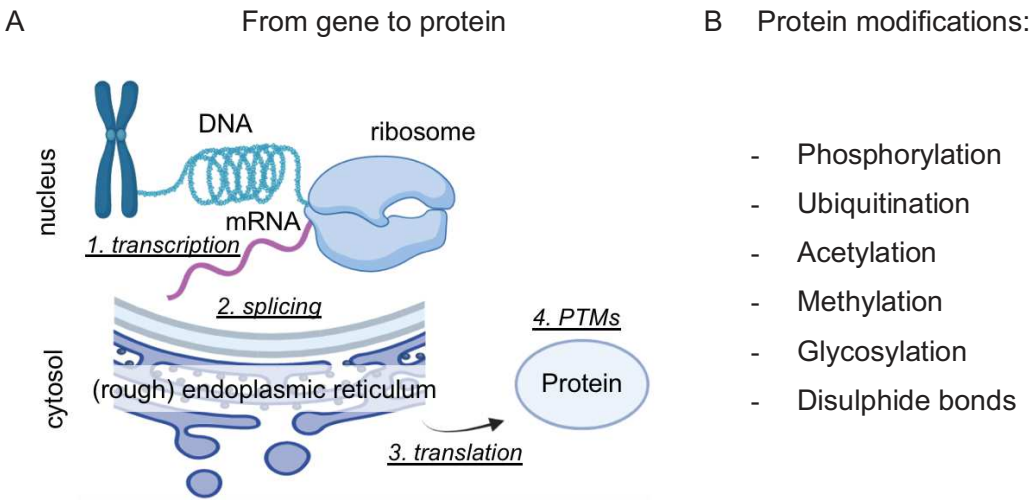


**Figure 1:** Schematic representation of cellular processes that regulate gene and protein expression. A) Global overview of the production of a protein inside a cell. B) Protein modifications that regulate its expression.

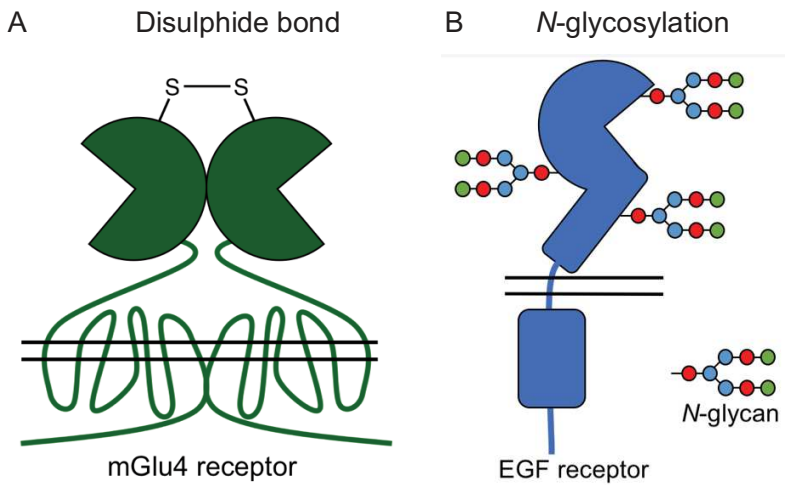


**Figure 2:** Receptor modifications in the (rough) endoplasmic reticulum regulate protein dimerization and folding. A) A disulphide bond covalently links two mGlu4 subunits to form the mGlu4 homodimeric receptor. B) *N*-glycosylation is important for EGF receptor folding. Figure 2B was adapted from Zhen *et al.* (2003).

### 6.1.3 The types of membrane receptors

There are three main types of cell surface receptors: ion-channel linked receptors, enzyme-linked receptors and G protein-coupled receptors (GPCRs) (Fig. 3). Generally speaking, these receptors have a similar function: they translate an external stimulus into an internal signal. External stimuli can be almost anything on the molecular, atomic or quantum level (e.g. photons, mechanical pressure, scent, small-molecule drugs, antibodies, ions) and can be specific for a type of receptor.

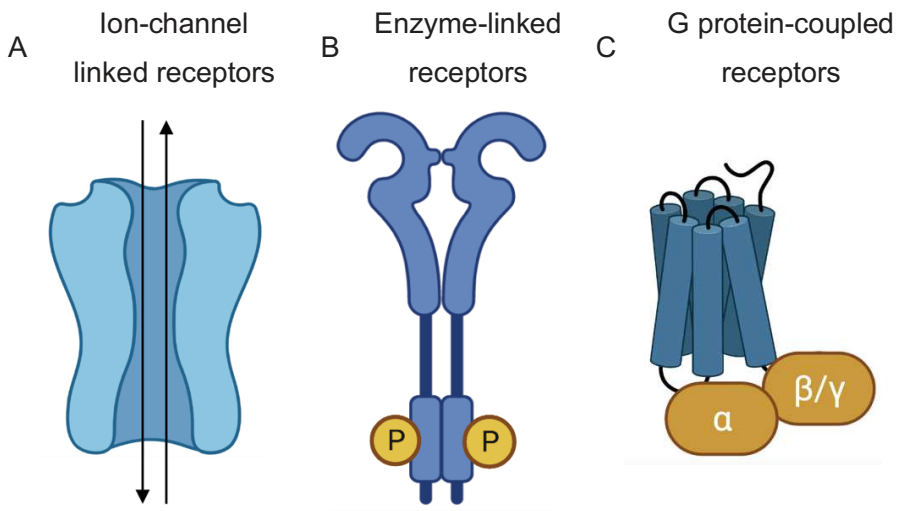


**Figure 3:** Three types of membrane receptors. A) Ion-channel linked receptors with a schematic ionotropic glutamate receptor as example. B) Enzyme-linked receptors with a receptor from the EGFR family as an example. C) G protein-coupled receptors (GPCR) with a class A GPCR as example.

#### *6.1.3.1 Ion-channel linked receptors*

Ion-channel linked receptors bind stimuli, resulting in conformational changes and opening or closure of the ion-channel. Ion-channels are crucial for changing the membrane potential by regulating influx or efflux of $Ca^{2+}$, $K^+$, $Na^+$ or $Cl^-$ ions. Within the group of ion-channel linked receptors, receptors are classified based on the stimulus that activates, or gates, them. Stimuli can be voltage, intracellular ions or extracellular ligands (e.g. neurotransmitters). Some well-described ligand-gated ion-channel linked receptors are the ionotropic glutamate receptors (e.g. AMPA and NMDA receptors) or the $GABA_A$ receptor (Briggs and Gopalakrishnan 2007).

#### *6.1.3.2 Enzyme-linked receptors*

There are several classes of enzyme-linked receptors. The main classes are receptor tyrosine kinases (RTKs), receptor serine/threonine kinases (RSTKs), tyrosine-kinase associated receptors, non-receptor

tyrosine kinases (nRTKs), receptor guanylyl cyclases, receptor tyrosine phosphatases and histidine-kinase-associated receptors (Alberts et al. 2002).

#### *6.1.3.3 Receptor tyrosine kinases*

RTKs consist of a variety of receptors that are being targeted by different secreted growth factors, hormones or receptors. There are around 20 RTK families identified based on molecular characteristics. Some of the most well-known classes are the EGFR class (i.e. EGF receptor, human epidermal growth factor receptor (HER) 2, HER3 and HER4), the insulin receptor (INSR) class, platelet-derived growth factor receptor (PDGFR) class, nerve growth factor (NGF) receptor class, mesenchymal-epithelial transition factor (MET) receptor/hepatocyte growth factor (HGF) receptor class and vascular endothelial growth factor (VEGF) receptor class (Ségaliny et al. 2015) (Table 1). These RTKs are involved in numerous cellular processes like cellular growth, migration, adhesion, metabolism, endocytosis, $Ca^{2+}$ signalling or survival. As such, RTKs are involved in physiological processes like development, wound healing, tissue renewal, regeneration and repair, vascularisation, proliferation of blood cells, metabolic homeostasis, immune cell proliferation, nerve cell proliferation and more. Besides, RTKs may be involved in tumorigenesis and many of the RTKs are druggable targets (Wee and Wang 2017). Despite many differences between RTKs, the EGFR family is usually referred to as the "prototypical" RTK class (Lemmon, Schlessinger, and Ferguson 2014).

| **Family** | **Members** |
|---|---|
| Epidermal growth factor receptor | EGFR, HER2, HER3, HER4 |
| Insulin receptor | INSR, IGFR |
| Met/hepatocyte growth factor receptor | MET |
| Nerve growth factor receptor | TrkA, TrkB, TrkC |
| Platelet-derived growth factor receptor | PDGFRα, PDGFRß, M-CSFR |
| Vascular endothelial growth factor | VEGFR1, VEGFR2, VEGFR3 |

**Table 1:** Examples of receptor tyrosine kinase families and members.

The main signalling by RTKs are Ras-Raf-MEK-ERK, PI3K-Akt-mTOR axes and Src, an nRTK, pathway leading to progression of the G1/S checkpoint in the cell cycle and activation of a plethora of transcription factors (Fig. 4A) (Ségaliny et al. 2015). Importantly, Src family members (i.e. Src, Lck, Hck, Fyn, Blk, Lyn, Fgr, Yes, Trk and Frk) modulate RTK signalling. They interact with many RTKs, like EGFR and PDGFR family members (Ishizawar and Parsons 2004). They can phosphorylate the EGF receptor (i.e. tyrosine

residue 845) and some of its downstream effector proteins (i.e. STAT3[iv], PDK1[v], Akt) (Warmuth et al. 2005). This can lead to enhanced signalling, but also receptor downregulation (Ishizawar and Parsons 2004). These mechanisms are often involved in cancer signalling and modulation of these pathways is being investigated as a treatment strategy (Warmuth et al. 2005).

One major difference between classes of the RTK family is the activation process: Within the RTK family, activation of the receptor is subsequent to ligand-induced dimerization (e.g. VEGFR family) (Fig. 4B) (Matsumoto and Mugishima 2006) or to ligand-induced conformational changes of a pre-formed dimer (Fig. 4C) (e.g. INSR family) (Uchikawa et al. 2019). Herein, a VEGF receptor agonist induces conformational changes and connects the two subunits (Fig. 4B), or an insulin receptor agonist induces conformational changes (Fig. 4C), both leading to association of the tyrosine kinase (TK) domains. Association of the TK domains leads to activation of these domains and subsequent phosphorylation of residues (i.e. tyrosine, serine, threonine) on the intracellular domain of the receptor. Phosphorylated tyrosine residues act as binding sites for adaptor proteins containing Src homology (SH) 2 and/or SH3 binding domains (e.g. Grb-2, Gab2, SHC1). Adaptor proteins are proteins that link other proteins with each other and could initiate downstream signalling (Flynn 2001).

[iv] Signal transducer and activator of transcription 3
[v] Pyruvate Dehydrogenase Kinase 1

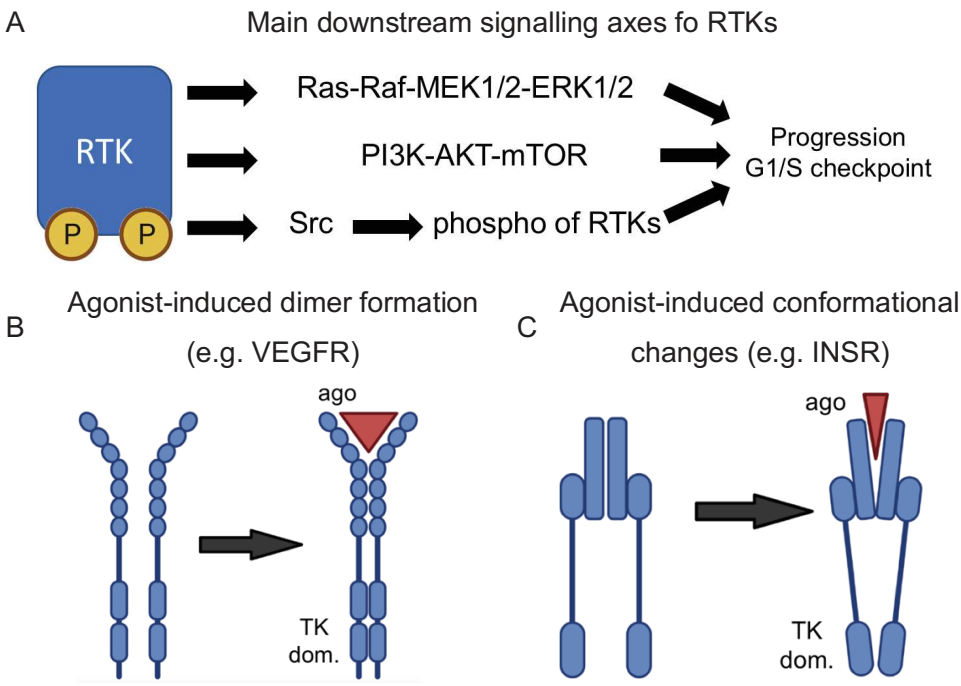


**Figure 4:** Activation and dimer formation of receptor tyrosine kinases. A) Main downstream signalling axes of RTKs. B) Agonists induce conformational changes of monomeric receptors, thereby inducing dimer formation. This is the case for some of the VEGFR family members. C) Agonists induce conformational changes that causes a pre-formed inactive dimer to become active. This is the case of the INSR family members. B-C) Agonists are represented in red.

#### *6.1.3.4 G protein-coupled receptors*

The GPCR superfamily consists of over 800 genes that contains many drug targets. In 2017, around 34% of all Federal Drug Administration (FDA)-approved drugs acted on 107 unique GPCR(-related) targets, making it the most drug-targeted gene family (Hauser et al. 2017). The GPCR superfamily is also referred to as seven transmembrane (7TM) receptors, due to the characteristic seven α-helices that pass through the membrane, connected by intra- and extracellular loops (Fig. 5A). The superfamily can be divided into six classes (class A till F) based on structure homology, ligands and function. Ligands could be small proteins or even photons[vi] and activation of the receptor induces conformational changes that lead to activation of the GPCR-bound heterotrimeric G protein (Bolander 2004).

There are many GPCRs and they are involved in numerous processes as they are expressed in every cell of the human body. Only a few receptors of the biggest class of GPCRs, class A, and the class of the mGlu4 receptor, class C, will be mentioned here. Firstly, class A rhodopsin-like receptors, are the largest class within the GPCR family and usually have a small extracellular and intracellular domain. Its agonist binding pocket is on the N-terminal side within the 7TM domain. Some examples of approved drugs, expression and physiological roles of class A GPCR drug targets are summarized in Table 2 (Sriram and Insel 2018; Berger, Gray, and Roth 2009). Class C GPCRs are a group of receptors with a large N-terminal domain, a 7TM domain and a C-terminal domain that varies in length per family member. Some of the most described families are the metabotropic glutamate (mGlu) receptor family, the γ-aminobutyric acid (GABA) receptor family, calcium-sensing receptor (CaSR) family and the taste receptor family. There are only two FDA-approved class C drugs, etelcalcetide, an allosteric agonist for the calcium-sensing receptor and baclofen, a $GABA_B$ receptor agonist (Sriram and Insel 2018). A short list with drugs, expression and physiological roles of these receptors is listed in Table 2.

[vi] Indirectly

| Class | GPCR family | FDA-approved drug example | Expression | Involved in physiological process |
|---|---|---|---|---|
| **A** | Opioid receptors | Morphine (δ, μ, κ-OR agonist) | CNS, immune system | Pain, immune cell proliferation and more. |
| **A** | Cannabinoid receptors | Tetrahydrocannabinol ($CB_1$, $CB_2$ partial agonist) | CNS, PNS | Cognition, inflammation, metabolism and more. |
| **A** | Adenosine receptors | Caffeine ($A_1$, $A_{2A}$ antagonist) | CNS, heart | Dopaminergic system, heart rate, vasodilatation and more. |
| **A** | Histamine receptors | Bilastine ($H_1$ antagonist) | CNS, immune system | Vasodilatation, immune response and more. |
| **C** | Metabotropic glutamate receptors | - | CNS, immune system | Cognition, immune system |
| **C** | Gammabutyric acid receptors | Bacoflen ($GABA_B$ agonist) | CNS | Sleep rhythm. |
| **C** | Calcium-sensing receptors | Etelcalcetide (CaSR allosteric agonist) | CNS, kidneys, parathryroid | |
| **C** | Taste receptors | - | Tongue, blood | Taste |

**Table 2:** Examples of class A and C GPCRs and FDA-approved drugs.

Activation of GPCRs causes G protein-mediated cellular responses. The G protein is a heterotrimeric protein consisting of an α, β and γ-subunit that dissociates into Gα and Gβγ when activated. The Gα-subunit is an enzyme that hydrolyses guanosine triphosphate (GTP), a GTPase. When Gα is GTP-bound, it interacts with other proteins and exert its function. The Gβγ-subunit is a regulatory protein that exerts its activity through protein-protein interactions (Wettschureck and Offermanns 2005). In general, the activation process can be divided into 5 steps (Fig. 5A):

1) In the inactive state, the G protein is heterotrimeric, in which the Gα-subunit is bound to guanosine diphosphate (GDP).
2) An activated GPCR undergoes conformational changes, thereby becoming available for G protein-binding. Activated GPCRs act as guanine exchange factor (GEF), that means that GDP is exchanged for guanosine triphosphate (GTP), upon binding of the heterotrimeric G protein to the receptor. A single receptor may activate more than 1 G protein.
3) The GTP-bound Gα-subunit and Gßγ-subunit are dissociated from each other, making them available for activation of their effectors. Both Gα as Gßγ-complexes activate distinct signalling pathways, depending on their subtype.
4) Once the GTP is hydrolysed to GDP, the Gα-subunit returns to its inactive state.
5) The Gα and Gβγ subunits re-associate.

GPCRs are characterized based on their Gα-coupling. There are 16 different human Gα-subunits, 5 different Gß-subunits and 12 Gγ-subunits (Wettschureck and Offermanns 2005). They are divided into 4 families: $G\alpha_s$, $G\alpha_q$, $G\alpha_i$ and $G\alpha_{12/13}$ (Fig. 5B). In short, the main effector of $G\alpha_s$ is adenylyl cyclase (AC), which hydrolyses adenosine triphosphate (ATP) into cyclic adenosine monophosphate (cAMP). cAMP is a second-messenger that activates many proteins, channels and enzymes. $G\alpha_i$-family members inhibit AC, causing cAMP levels to decrease. The main effector of $G\alpha_q$ is phospholipase C (PLC). PLC converts phosphatidylinositol 4,5-biphosphate ($PIP_2$) into inositol 1,4,5-triphosphate ($IP_3$), which is a second-messenger for $Ca^{2+}$-signalling, resulting in increased intracellular $Ca^{2+}$ levels and activation of $Ca^{2+}$-dependent pathways. The less-well studied $G\alpha_{12/13}$ principal effector is RhoGTPase (Inoue et al. 2019).

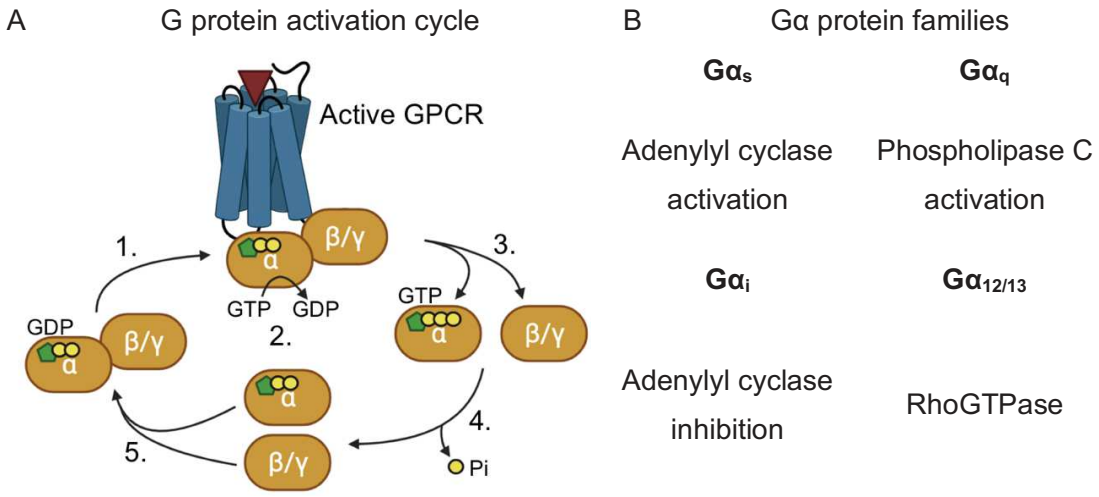


**Figure 5:** G protein activation. A) The G protein activation cycle has 5 mains steps: 1. Heterotrimeric G protein binds to activated GPCR; 2. GDP bound to Gα is exchanged for GTP; 3. Gα and Gβγ are dissociated and activate effectors; 4. GTP is hydrolysed into GDP; 5. GDP-bound Gα and Gβγ associate. B) The four Gα protein families with their main effectors.

In this subchapter, three types of receptors are summarized, viz. the ion-channel linked receptors, enzyme-linked receptors and GPCRs. Enzyme-linked receptors contain enzymatically active domains that are activated through interactions within the receptor. GPCRs activate a downstream activator, the G protein. Throughout the thesis, the focus will be on dimerization and activation mechanisms of the EGF receptor, an enzyme-linked receptor, and the mGlu4 receptor, a GPCR.

### 6.1.4 Pharmacology

To describe drugs and receptors, pharmacological concepts will be used. In this subchapter, concepts and definitions will be explained. Pharmacology is defined as the study to the effect of drugs on the human body. Drugs are defined as chemical substances that induce a physiological effect. Receptors are proteins that transfer extracellular signals into an intracellular signal. Drugs are classified, based on the biological response they induce, as follows: agonist, antagonist, inverse agonist, or allosteric modulator. Each effect will be discussed in the following subchapter.

#### *6.1.4.1 Agonists and inverse agonists*

Agonists are substances that induce a biological response (E) upon binding to their target. Agonists are generally divided into: full agonists, partial agonists and inverse agonists. Full agonists induce the maximal biological response of the receptor (Emax), whereas partial agonists only partially induce a biological response. The maximal biological response is called the efficacy. The concentration of agonist needed to induce 50% of its maximally induced response (EC50) is called the potency. Some receptors are activated in absence of agonist, this activity is called constitutive activity. Inverse agonists reduce constitutive activity of a receptor (Fig. 6A).

Receptors activate a variety of downstream signalling pathways. Some agonists may activate one pathway over another pathway, thereby inducing different cellular behaviours. This phenomenon is known as biased agonism or functional selectivity and may be crucial for some drug-specific effects (Kenakin 2011).

#### *6.1.4.2 Antagonists*

Antagonists are substances that block the effect of agonists, and inverse agonists, and do not induce receptor activity (Fig. 6B, C). Antagonists can block (inverse) agonist-induced responses in a “competitive” or “non-competitive” way.

In competitive antagonism, a reversible antagonist competes with the agonist for the same binding site. As a consequence, the measured EC50 is decreased, whereas the efficacy remains unchanged (Fig. 6B). When the EC50 of the agonist in absence and presence of multiple concentrations of a competitive antagonist is determined, the relationship between agonist and antagonist can be described with a Schild plot (Lazareno and Birdsall 1993). A Schild plot is used to describe the strength of the antagonist.

In non-competitive antagonism, the antagonist is either irreversibly occupying the agonist binding site or inhibiting the agonist-response by occupying a different binding site. In both cases, the antagonist reduces

the efficacy of the agonist, while the measured EC50 of the agonist remains unchanged (Fig. 6C). Non-competitive antagonists could also be allosteric modulators.

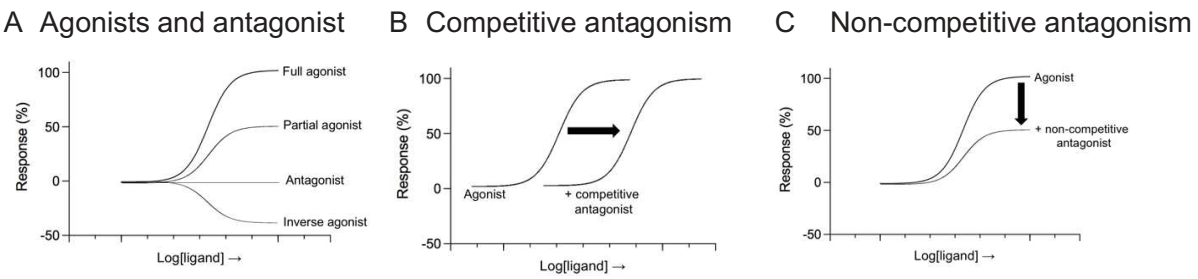


**Figure 6:** Agonism and antagonism in functional assays. A) Biological response to full, partial and inverse agonists and antagonists. B) Biological response to an agonist in presence of a competitive antagonist. C) Biological response to an agonist in presence of a non-competitive antagonist.

### *6.1.4.3 Allosteric compounds*

Compounds that bind on a different site than the orthosteric site are called allosteric modulators (Fig. 7A). Allosteric modulators are classified into silent, positive and negative allosteric modulators (SAM, PAM, and NAM, respectively). SAMs bind the receptor, but have no effect on the orthosteric-bound substance. PAMs ameliorate EC50 and/or efficacy and NAMs worsen EC50 and/or efficacy. Allosteric modulators that change the EC50 are α-allosteric modulators and allosteric compounds changing the efficacy are β-allosteric modulators (e.g. α-PAM or β-PAM) (Fig. 7B). Some PAMs or NAMs induce an agonistic effect themselves: they could be referred to as "agonist-PAM" or "agonist-NAM".

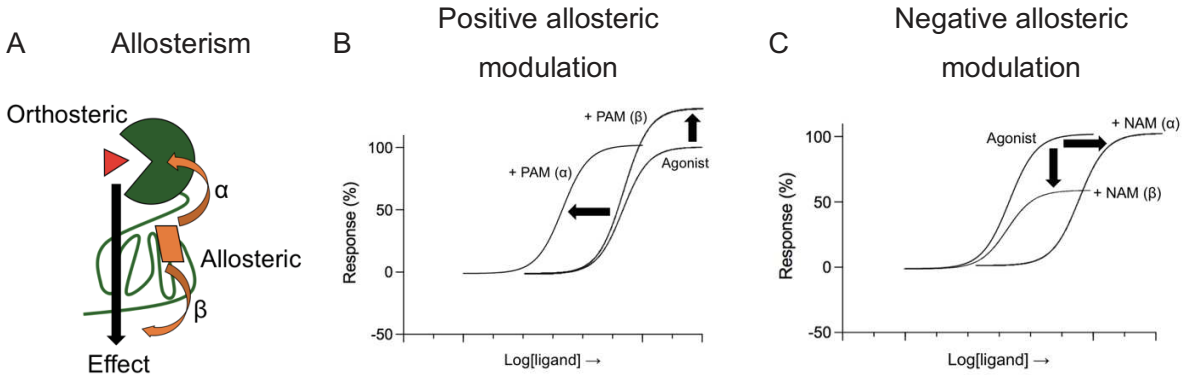


**Figure 7:** Allosteric modulation. A) Allosteric modulators bind a different pocket than the orthosteric binding site and can modulate the effect by changing the binding of the orthosteric compound, or changing its activation. B) Effect of positive allosteric modulation. C) Effect of negative allosteric modulation.

#### *6.1.4.4 Cheng-Prusoff and Hill coefficient*

Pharmacological characterization of agonists can be done by their biological response (i.e. EC50) or intrinsic binding affinity, based on the dissociation constant (Kd). The Kd is the concentration of a compound at which half of the available binding sites are occupied[vii].

Antagonists are characterized by the concentration of the compound that is needed to inhibit half of the biological response or binding of a competitor (IC50), or their intrinsic binding affinity, which is the dissociation constant of the inhibitor (Ki). The Ki can be calculated following the Cheng-Prusoff equation (Lazareno and Birdsall 1993) and depends on the concentration of the agonist ([A]), the Kd of the agonist and the experimental IC50 of a competitive ligand:

$$Ki = \frac{IC50}{1 + \frac{[A]}{Kd}}$$

When compound binding happens independently of the binding of other compounds, the Hill coefficient ($n$) is equal to 1. When compound binding becomes more favourable upon binding of previous compounds, there is positive cooperativity (i.e. $n$>1). Conversely, when compound binding becomes less favourable upon binding of previous compound, there is negative cooperativity (i.e. n<1). Depending on the $n$, the slope of the sigmoidal dose-response curve changes, following:

$$E = \frac{Emax}{1 + (\frac{EC50}{[A]})^n}$$

In this subchapter, the pharmacological principles that will be used throughout the thesis are introduced. Most of the compounds that are used in this thesis are classified as agonist (e.g. EGF, DN45) or antagonist (i.e. inhibitors of the mGlu4 and ATP-competitive inhibitors of the EGF receptor).

[vii] At equilibrium

## 6.2 EPIDERMAL GROWTH FACTOR RECEPTOR

### 6.2.1 History of the Epidermal Growth Factor Receptor

In 1986 Stanley Cohen and Rita Levi-Montalcini were awarded with the Nobel Prize in Physiology or Medicine for their discovery of ‘’growth factors’’. The discovery of the first growth factor, Nerve Growth Factor (NGF), was in the 1950s by Rita Levi-Montalcini, an Italian researcher working in St. Louis, Missouri at the Washington-University. While working on NGF, Stanley Cohen discovered another growth factor. Their observations linked this growth factor to epithelial growth, and therefore the name “Epidermal Growth Factor” (EGF) was given to the newly found growth factor. In the beginning of the 1970s, Cohen’s lab further elucidated the sequence and structure of EGF (C. R. Savage, Inagami, and Cohen 1972; R. C. Savage, Hash, and Cohen 1973). The finding that extracellular EGF binding caused intracellular tyrosine phosphorylation, lead to the discovery of the family of receptor tyrosine kinases (RTKs) (Cohen et al. 1982; Buhrow et al. 1983). Nowadays, RTKs are linked to many physiological (e.g. growth, tissue repair) and pathological processes (i.e. cancer, skin diseases, Alzheimer’s disease) (Wee and Wang 2017). This has led to many drugs acting on the EGF receptor and other RTKs. Despite many successes, the EGF receptor is not a perfect drug target due to resistance mechanisms, as will be discussed throughout this thesis.

### 6.2.2 *EGFR* gene and structure

The EGF receptor is a transmembrane receptor in the family of the RTKs. It has a mass of around 120 to 170 kDa depending on *N*-linked glycosylation of the extracellular domain (ECD). The *N*-linked glycosylation is important for the binding of its ligands and the activation of intracellular trafficking processes (Fernandes, Cohen, and Bishayee 2001; Slieker, Martensen, and Lane 1988; Kaszuba et al. 2015). The EGF receptor, also HER1[viii] or ErbB1[ix], is the prototypical receptor of the EGFR family. The three other members of the EGFR family (i.e. HER2, HER3, HER4) are shortly discussed later. The human *EGFR* gene is located on chromosome 7 in the p22 region of the short arm (Kondo and Shimizu 1983). The gene consists of 28 exons, in which exon 18 till 21 are coding for regions of the TK domain.

#### *6.2.2.1 Structure of the EGF receptor*

There are 1210 amino acid[x] residues in the human EGF receptor. The first 24 amino acids are coding for a signal peptide that is not present in the mature EGF receptor (Fig. 8A). The ECD of the EGF receptor consists of 620 amino acids (Fig. 8B). The ECD is divided into four subdomains. Of these four subdomains, subdomains I and III are lysine-rich and are considered to be the ligand-binding domains. Subdomains II

[viii] Abbreviation of Human Epidermal growth factor Receptor 1
[ix] Abbreviation of Erythoblastic leukemia viral oncogene homolog 1
[x] Signal peptide (24 aa), ECD (620 aa), TM (22 aa), JxD (41 aa), TKD (268 aa), C-tail (234 aa)

and IV are cysteine-rich domains and are responsible for stabilizing conformational rearrangements of the ECD and dimers/oligomers by the formation of disulphide bonds. A ~ 22 amino acid residue-long single transmembrane helix separates the ECD from the intracellular domain (ICD). The ICD consists of 3 subdomains: the juxtamembrane domain (JxD), TK domain and a carboxyterminal tail (Fig. 8A).

#### *6.2.2.2 Tyrosine kinase domain*

The TK domain is the enzymatic domain and consists of 268 residues (Fig. 8C). This domain is only active in an asymmetric dimeric conformation (i.e. 1 subunit is enzymatically active and 1 is inactive) (Brewer et al. 2009), as will be explained in more detail in the next subchapter. The TK domain has two lobes: the N and C-lobe in which the N-lobe has 8 β-sheets and 1 α-helix and the C-lobe has 3 β-sheets and 7 α-helices (R. J. Roskoski 2019). In the cleft between the two lobes, there is a binding pocket that stabilizes the adenine group of adenosine triphosphate (ATP). The enzymatically active subunit cleaves ATP, leading to phosphorylation of tyrosyls (Y) on the carboxyterminal tail of the inactive subunit. This process is called (trans-)autophosphorylation. Apart from autophosphorylation, other kinases like Src can phosphorylate tyrosine, serine or threonine residues of the EGF receptor (Sato 2013).

#### *6.2.2.3 Carboxyterminal tail*

The carboxyterminal tail (also C-tail) is a 234 residues region that is flexible and contains many tyrosyls[xi], among which there are 5 main autophosphorylation residues: Y992, Y1068, Y1086, Y1148 and Y1173. Once phosphorylated, these residues function as docking sites for adaptor proteins. Moreover, the carboxyterminal tail functions as an autoinhibitory domain. Indeed deletions in the carboxyterminal tail could lead to activation of the kinase activity (Dankort et al. 1997; Kovacs et al. 2015).

In summary, the EGF receptor is a single-pass transmembrane receptor with a large ECD containing the ligand-binding domains and a large ICD containing the enzymatical TK domain. Its carboxyterminal tail contains phosphorylatable residues, that may act as docking sites for adaptor proteins.

[xi] Y974, Y992, Y1045, Y1068, Y1086, Y1101, Y1114, Y1148, Y1173 (main autophosphorylation residues are underlined).

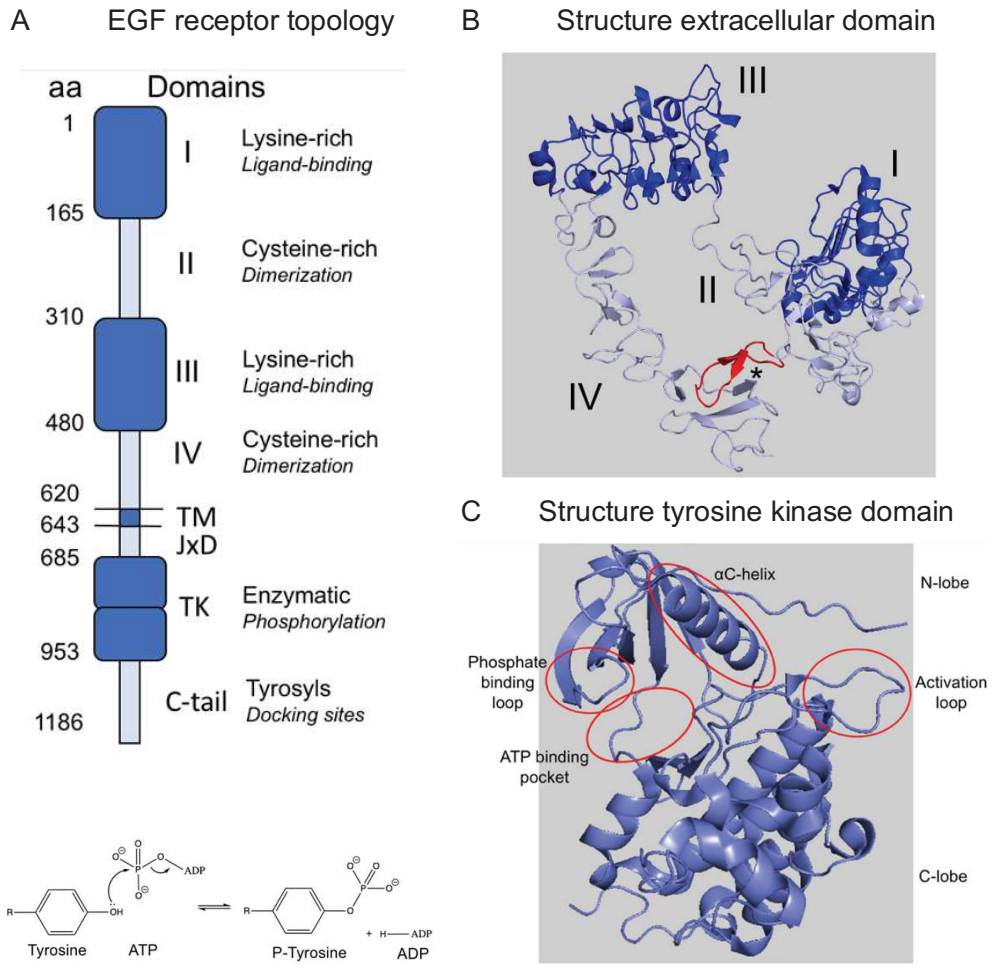


**Figure 8:** Structure of the EGF receptor and its tyrosine kinase domain. A) Topology of the EGF receptor in which domains and corresponding amino acids are mentioned. This figure is adapted from Ferguson *et al.* (2008). B) Representation of the crystal structure of the extracellular domain of the EGF receptor in inactive conformation. The dimerization arm is highlighted in red. This figure is adapted from Ferguson *et al.* (2003), protein database reference 1NQL. C) Representation of the crystal structure of the tyrosine kinase domain of the EGF receptor in active conformation. The phosphate binding loop, ATP binding pocket and unfolded activation loop are encircled. This figure is adapted from Stamos *et al.* (2002), protein database reference 1M17.

### 6.2.3 Activation process of the EGF receptor and downstream signalling

Activation of the EGF receptor is initiated upon ligand binding to the extracellular domain (ECD).

In ligand-free conditions, the ECD adopts a ‘’tethered’’ conformation (Fig. 9A). Herein, the asterisk represents a β-hairpin in subdomain II, which is called the dimerization arm. Interactions between the dimerization arm and subdomain IV stabilize the ECD in the tethered conformation (Ferguson et al. 2003). The ECD of the EGF receptor can also adopt a ligand-free ‘’extended’’ conformation, exposing the dimerization arm. Ligand-free inactive multimers with a variety of conformations could be stabilized through this mechanism (Zanetti-Domingues et al. 2018).

The epitope of agonists is on subdomains I and III, two subdomains that are always exposed. Upon binding of agonist, subdomain I of the ECD rotates 130° (Ferguson 2008). This allows for interactions between the ECDs of two EGF receptor subunits through the dimerization arm and subdomain IV (Fig. 9B).

As a result of these conformational changes, the transmembrane domain rotates, causing a reorientation of the juxtamembrane and TK domains. An asymmetric dimeric conformation of its TK domains is crucial for the EGF receptor to be enzymatically active. One of the TK subunits is in the inactive conformation, the activator conformation (Fig. 10A), whereas the other TK subunit is in the enzymatically active conformation, the receiver conformation[xii] (Fig. 10B). Following conformational changes, the C-lobe of an inactive TK subunit interacts with the N-lobe of the other TK subunit, stabilizing it in an enzymatically active conformation (Fig. 10A-C). More precisely, the αH-helix of the inactive subunit interacts with the αC-helix of the active subunit, thereby changing the orientation of the αC-helix from “in” to “out”. This generates a salt bridge between two residues in the N-lobe: lysine 745 (K745) and a residue in the αC-helix, glutamic acid 762 (E762). As a result: 1) interactions between E762 and leucine 858 (L858) are disrupted, resulting in the unfolding of the activation loop that contains L858 and 2) the movement of a DFG-motif (i.e. aspartic acid 855 (D855), phenylalanine 856 (F856) and glycine 857 (G857)) from “out” to “in” position (Fig. 10B) (R. Roskoski 2016). These re-orientations are crucial for the TK domain to be in an active conformation (Lemmon, Schlessinger, and Ferguson 2014). The TK domains remain dynamic, resulting in both TK domains adopting alternatively the active and inactive conformations, thereby inducing (trans-)autophosphorylation on the autophosphorylation sites on the carboxyterminal tail (Hubbard 2006).

In summary, the EGF receptor adopts a dimeric conformation through the ECD upon binding of an agonist. Subsequent allosteric modulations remove autoinhibitory structures in the intracellular TK domain. This leads to activation of the enzymatic activity and autophosphorylation on the carboxyterminal tail.

[xii] The inactive TK is called the activator. The active TK is called the receiver.

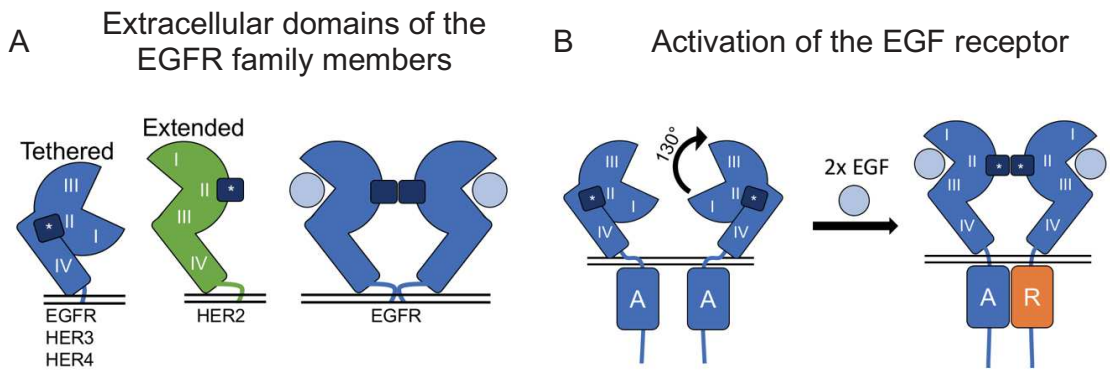


**Figure 9:** Conformation of ligand-free EGFR family members and dimerization of the EGF receptor. A) Ligand-free conformations of the extracellular domain of the four EGFR family members. EGFR, HER3 and HER4 are tethered and HER2 is extended. Figure is adapted from Maruyama *et al.* (2014). B) Activation of the EGF receptor upon binding of EGF. A 130° rotation of the extracellular domain, reveals the dimerization arm (*). The inactive (A) TK domains associate, resulting in an asymmetric TK domain consisting of an inactive and active (R) TK domain. Figure is adapted from Ferguson *et al.* (2008).

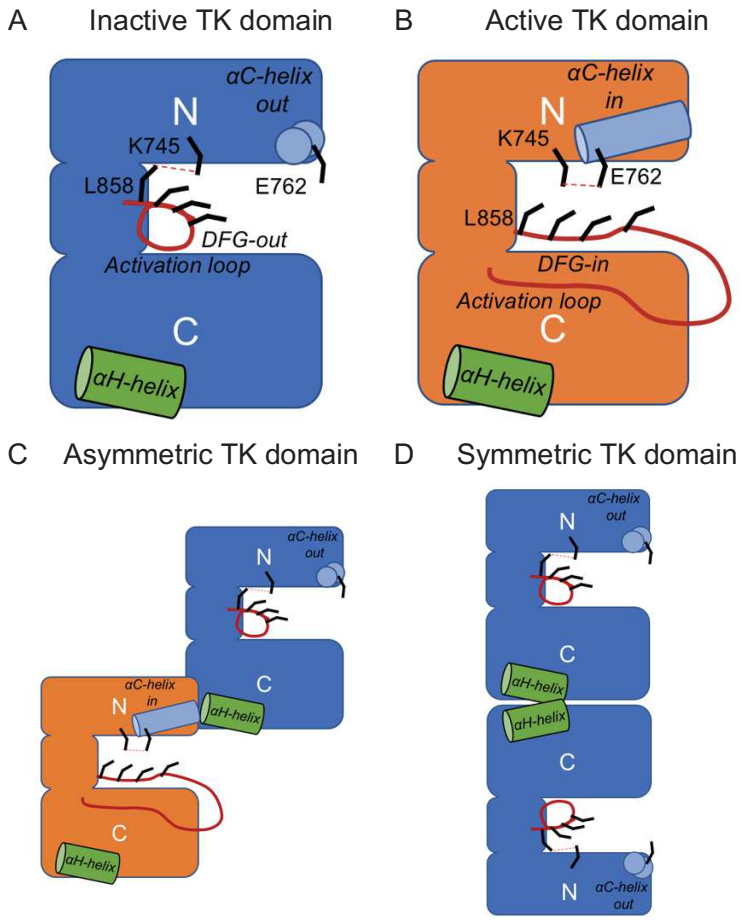


**Figure 10:** Molecular mechanism of TK domain activation. A) Schematic representation of the inactive TK domain or "activator". B) Schematic representation of the active TK domain or "receiver". C) Schematic representation of asymmetric TK domain. D) Schematic representation of symmetric TK domain. The red dotted line is an interaction between two residues. Figure is adapted from Lemmon *et al.* (2014).

### 6.2.4 Main downstream signalling pathways of the EGF receptor

The phosphorylated residues on the carboxyterminal tail act as docking sites for adaptor proteins that will initiate signalling and trafficking downstream of the EGF receptor. Two of the main signalling axes (i.e. Ras-ERK1/2 and PI3K-AKT-mTOR) (Fig. 11) and EGF receptor internalization (Fig. 12) are summarized below.

#### *6.2.4.1 ERK1/2 signalling*

The extracellular signal-regulated kinases (ERK) 1/2 signalling pathway is initiated by phosphorylation of tyrosine residue (Y) 1068 and Y1086 of the EGF receptor. Following, growth factor receptor-bound protein 2 (Grb2) associates to these tyrosyls through its SH2 and SH3 domains. Another adaptor protein, SHC1, associates to Y1148 and Y1173. Grb2 and SHC1 act as binding site of sons of sevenless (SOS1), which is a guanine exchange factor (GEF). SOS1 activates Ras-family proteins, a family of guanine triphosphatases (GTPase), by promoting the exchange of GDP for GTP. Hydrolysis of Ras-bound GTP, leads to phosphorylation and activation of Raf, a serine/threonine kinase. This leads to phosphorylation of MEK-1/2, a serine/threonine kinase. Next, ERK1/2, also a serine/threonine kinase, is phosphorylated and activated. ERK1/2 activation leads to subsequent activation of transcription factors (MYC, FOS, JUN), thereby increasing CYCLIN D expression. Elevated levels of CYCLIN D induce the formation of complexes with cyclin-dependent kinases (CDKs), which ultimately lead to progression of the cell cycle through activation of other regulatory proteins (Wee and Wang 2017).

#### *6.2.4.2 mTOR signalling*

The PI3K-AKT-mTOR axis is initiated by phosphorylation of Y1068 or Y1086 and association of Grb2. Next, Grb2 associated protein 2 (Gab2) binds to EGFR/Grb2. Subsequently, phosphoinositide-3 kinase (PI3K) associates to this complex and gets activated. This results in phosphorylation of phosphatidylinositol 4,5-biphosphate ($PIP_2$) to obtain phosphatidylinositol 3,4,5-triphosphate ($PIP_3$). $PIP_3$ localizes AKT to the cell membrane, where it promotes mTOR signalling complexes. Like ERK1/2 activation, mTOR signalling complex activation leads to CYCLIN D upregulation resulting in progression of the cell cycle (Meng, Frank, and Jewell 2018; Wee and Wang 2017).

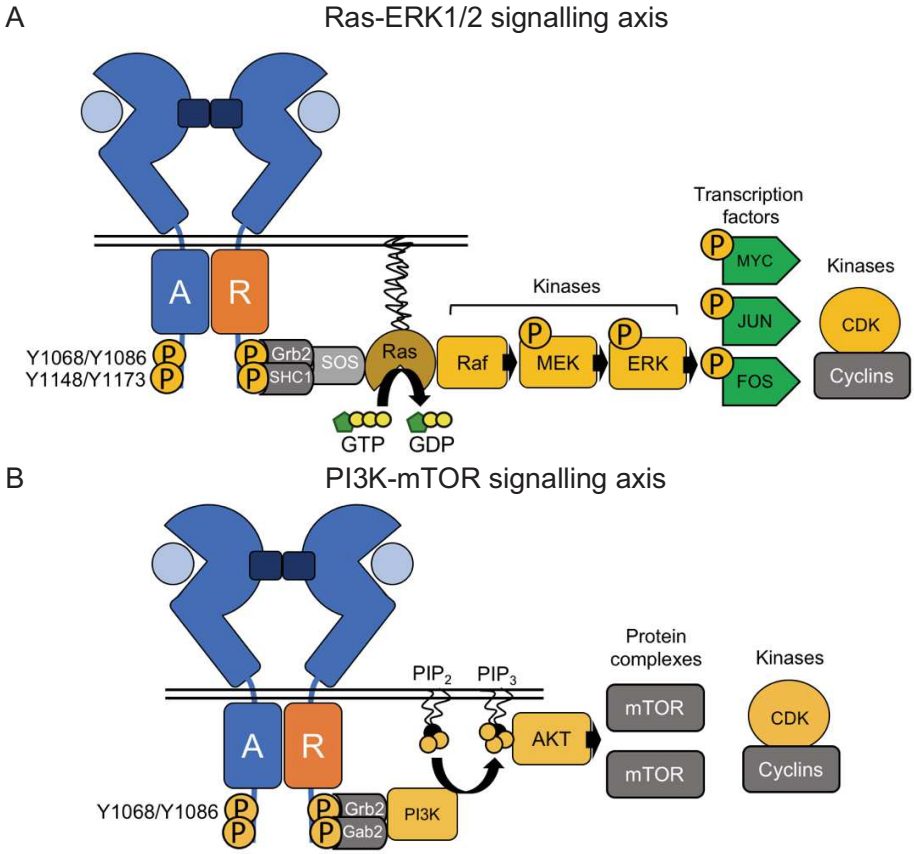


**Figure 11:** Main signalling axes of the EGF receptor. A) Schematic representation of the Ras-ERK1/2 signalling axis. Adaptor proteins are Grb2 and SHC1. SOS acts as GEF. Ras is a GTPase. Raf, MEK, ERK and CDK are kinases. MYC, JUN and FOS are transcription factors. Cyclins are regulatory proteins. B) Schematic representation of the PI3K-mTOR signalling axe. Grb2 and Gab2 are adaptor proteins. PI3K and AKT are kinases. $PIP_2$ and $PIP_3$ are phospholipids. mTORs are large protein complexes.

#### *6.2.4.3 Internalization*

The main internalization pathway of the EGF receptor is clathrin-mediated endocytosis (CME). However, depending on phosphorylation kinetics, ubiquitination and saturation of pathways, clathrin-independent endocytosis (CIE) mechanisms like fast endophilin-mediated endocytosis, micropinocytosis, caveolin-dependent endocytosis or lipid-raft endocytosis (Henriksen et al. 2013; Boucrot et al. 2015) may occur as well. Indeed, low levels of ubiquitination promote CME, whereas high levels of ubiquitination promote CIE (Sigismund et al. 2005).

The canonical CME is initiated by phosphorylation of Y1068/Y1086 and Y1045 (Fig. 12A) (F. Huang et al. 2006). Grb2 associates to phosphorylated Y1045 and one of the other phosphorylated tyrosyls. Consequently, Casitas B-lineage Lymphoma (Cbl), a ubiquitin ligase, is recruited to Grb2 and phosphorylated residue Y1045. Through conformational changes, Cbl recruits Cbl-interacting protein of 85K (CIN85) to form a complex. This complex is linked to endophilin, which is an initiator of the remodelling of the membrane that ultimately leads to membrane fission (Fig. 12B). Rapidly after activation, the EGF receptor gets ubiquitinated by Cbl, a process that determines whether the receptor gets recycled or degraded. During CME, the membrane will curve and adaptor proteins (i.e. adaptor protein 2 (AP-2), clathrin, dynamin) will associate to the complex, resulting in membrane fission and the generation of an early endosome (Fig. 12C). The early endosome gets sorted into recycling to the cell membrane or they become late endosome multivesicular bodies (MVB), which is sorted towards degradation upon fusion to the lysosome (F. Huang et al. 2006; Takei and Haucke 2001; Madshus and Stang 2009).

To summarize, the EGF receptor is subject to internalization through CME or CIE, regulated by a variety of cellular processes. During the internalization process, ubiquitination mediates sorting of the receptor towards recycling or degradation.

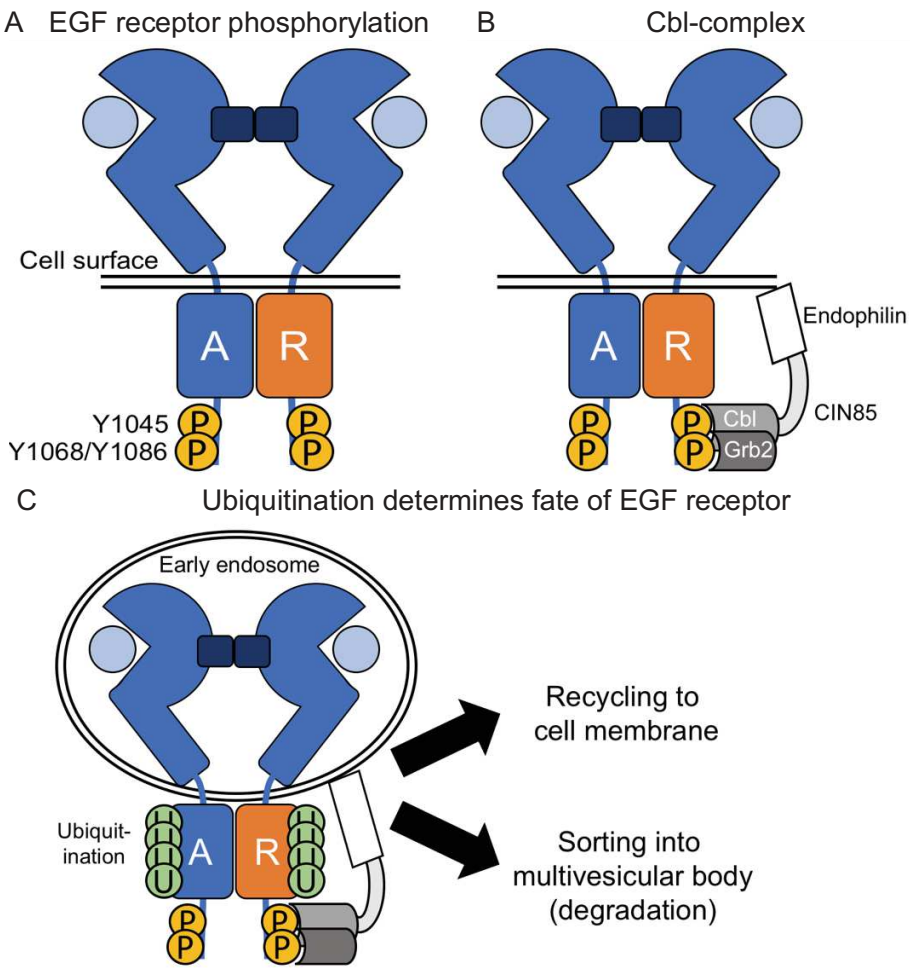


**Figure 12:** Canonical pathway of EGF receptor internalization. A) Main EGF receptor phosphorylation sites involved in internalization are Y1045, Y1068 and Y1086. B) A complex of Cbl, Grb2, CIN85 and endophilin is bound to the EGF receptor and the membrane. This complex induces receptor ubiquitination and membrane remodelling. C) The fate of the EGF receptor is determined in the early endosome, where it is sorted for recycling or degradation.

### 6.2.5 Agonists in the EGFR family

The EGF receptor can bind at least 7 endogenous ligands, which are all small proteins or peptides that bind the extracellular domain. EGF, a 6 kDa protein, is the prototypical agonist. Other EGF receptor agonists are Transforming Growth Factor-α (TGF-α), amphiregulin (AR), betacellulin (BTC), heparin-binding EGF-like growth factor (HB-EGF), epiregulin (EREG) and epigen (EPN) (B. Singh, Carpenter, and Coffey 2016). These ligands are expressed on the cell surface as membrane-inserted proteins that can be cleaved by a desintegrin and metalloproteinases (ADAMs) to release the ligands. BTC, HB-EGF and EREG also bind HER3 and HER4 and are therefore considered bispecific ligands (Wilson et al. 2009). There is also a class of small protein agonists that exclusively binds HER3 and HER4, called the neuregulins. EGFR family agonists could induce autocrine (i.e. cells that ligands are released from) or paracrine (i.e. neighbouring cells) activation (B. Singh, Carpenter, and Coffey 2016; Wee and Wang 2017).

All agonists act on the extracellular domain through interactions with subdomains I and III (Ogiso et al. 2002). However, some agonists induce more stable dimers than others. Full agonists EGF and TGF-α induce stable dimers, whereas partial agonists EREG and EPN induce less-stable dimers (Fig. 13). It was proposed that the stability of the dimer plays a role in signalling kinetics (Freed et al. 2017). Indeed, full agonists induce swift phosphorylation of the EGF receptor, leading to downregulation of the receptor, resulting in transient signalling. Conversely, activation of the EGF receptor by partial agonists is less rapid, causing less downregulation of the receptor and more sustained signalling (Freed et al. 2017). Consequently, transient signalling of the EGF receptor leads to more proliferation, whereas sustained signalling leads to more differentiation (Lemmon et al. 2016; Marshall 1995).

Till now, 7 endogenous agonists of the EGF receptor are discovered. All agonists bind to the extracellular domain of the EGF receptor, but the stability of the induced dimer may be different. By this way, different agonists may promote different kinds of signalling.

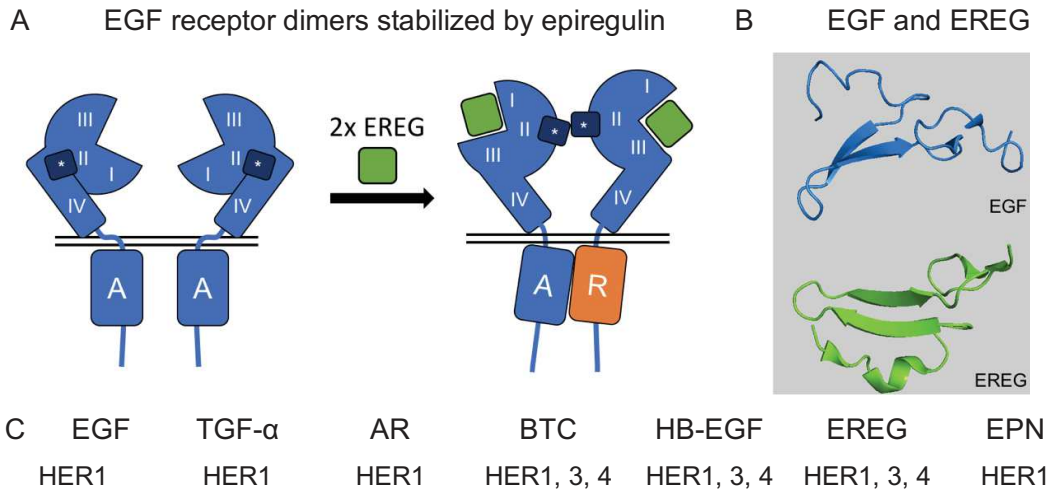


| C | EGF | TGF-α | AR | BTC | HB-EGF | EREG | EPN |
|---|---|---|---|---|---|---|---|
| | HER1 | HER1 | HER1 | HER1, 3, 4 | HER1, 3, 4 | HER1, 3, 4 | HER1 |

**Figure 13:** EGFR family agonists. A) Epiregulin (EREG) stabilizes dimers of the EGF receptor in a different conformation than EGF. Figure is adapted from Freed *et al.* (2017). B) Representation of crystal structures of EGF and EREG. EGF crystal structure is adapted from Lu *et al.* (2010), protein database reference 3NJP (Lu et al. 2010). EREG crystal structure is adapted from Kado *et al.* (2016, protein database reference 5E8D (Kado et al. 2016). C) Overview of EGFR agonists and their specificity to EGFR family members.

### 6.2.6 EGFR family members

Heterodimerization in the EGFR family is possible between all members of the EGFR family (Fig. 14) (Kennedy et al. 2016). Some heterodimers that are linked to physiological processes will be introduced here.

#### *6.2.6.1 Human Epidermal growth factor receptor 2 (HER2)*

In locally advanced breast cancer, an increased number of EGF receptor-HER2 heterodimers are correlated to poor clinical outcomes (Nieto et al. 2007), underlining the importance of heterodimer formation. Graus-Porta *et al.* described that depending on the ligand, the propensity of a member of the EGFR family to form heterodimers may change. Moreover, the HER2 plays a critical role as it is the preferred binding partner of all family members (Graus-Porta et al. 1997). As there is no high-affinity ligand for the HER2, the main function of this receptor is being exerted through formation of heterodimers (Kennedy et al. 2016).

#### *6.2.6.2 Human Epidermal growth factor receptor 3 (HER3)*

The kinase domain of the HER3 is locked in an inactive conformation that resembles the inactive conformations of the EGF receptor, HER2 and HER4 (Littlefield et al. 2015). Due to the lack of several key residues that modulate activation of the TK in the other EGFR family members, its TK domain remains inactive (Jura et al. 2009) or with weak activity (Shi et al. 2010). Nevertheless, HER3 is an allosteric modulator in heterodimers and was suggested as therapeutic target for treating brain metastases (Lyu et al. 2018).

#### *6.2.6.3 Human Epidermal growth factor receptor 4 (HER4)*

The role of HER4 is less clear than the other EGFR family members. Still, the receptor may be a favourable prognostic marker in breast cancer (Ghayad et al. 2010). The HER4 contains a kinase domain that can be activated, resulting in allosteric changes like for the EGF receptor (Mota et al. 2017).

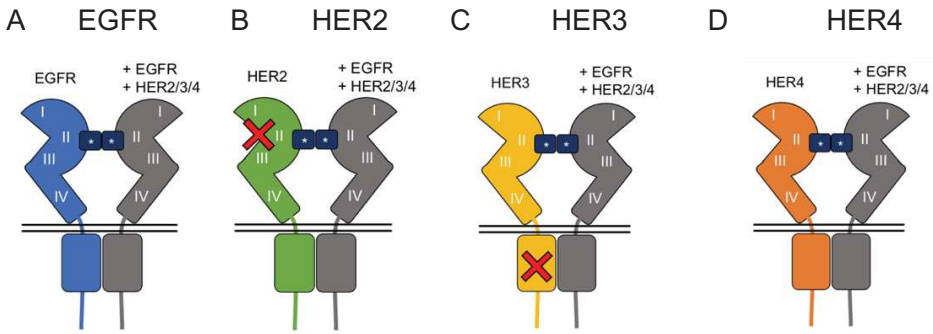


**Figure 14:** EGFR family members and their preferred binding partners. A) EGF receptor. B) HER2; the red cross represents the non-functional ligand binding domain. C) HER3. D) HER4; the red cross represents the inactive tyrosine kinase domain.

### 6.2.7 The EGF receptor in physiological processes

Mostly, the EGF receptor is implicated in mitogenic processes. As such, it is important in central nervous system (CNS) protection, vascularisation, lung function, kidney function, gastro-intestinal homeostasis, pancreatic function or reproductive system function. A few main processes will be introduced here.

#### *6.2.7.1 Embryogenesis, neuroprotection and skin repair*

The EGF receptor is expressed in all tissues in the human body, except in red blood cells. Especially during embryogenesis in the placenta, EGF receptor levels are high. This is not surprising when looking at its crucial role in embryogenesis: mice lacking EGF receptor had abnormalities in many tissues, including bone, brain, heart, skin, eyes and lung (Threadgill et al. 1995). In the earliest stages of life, the EGF receptor regulates uterine development, embryo implantation and growth and differentiation of the placenta (J. Chen et al. 2016). In postnatal development and organogenesis, absence of the EGF receptor can lead to a variety of abnormalities like dysfunctional or defect lungs, underdeveloped heart valves, delayed bone formation, decreased neuronal migration and cortical layer formation, and defects in development of renal ducts (J. Chen et al. 2016).

Also, in the brain, expression levels of the EGF receptor are high during early stages of life, but decreased at later stages in life. However, expression levels of the EGF receptor may go up in case of injuries in the CNS, where the EGF receptor induces tissue repair. Also, in Alzheimer's Disease, Parkinson's Disease and schizophrenia, the EGF receptor has a neuroprotective role as it protects against toxicity of neurotransmitters (i.e. glutamate) (Novak, Walker, and Kaye 2001; J. Chen et al. 2016).

The EGF receptor, HER2 and HER4 are well expressed in skin tissue, but especially the EGF receptor is linked to skin growth, repair and wound healing. EGFRs may be (trans-)activated by GPCRs or interleukins (i.e. interleukin-33 (IL-33)) and can suppress expression of chemokines, thereby reducing skin inflammation. Conversely, inhibition of IL-33 could lead to skin problems that resemble those of patients treated with TK inhibitors for the EGF receptor (Gangemi et al. 2013).

To summarize, EGF receptor expression levels are high in the first stages of life, where it is important for the correct development of many tissues. Throughout later stages of life, expression levels of the EGF receptor may be upregulated during certain neurological disorders or skin repair and wound healing.

### 6.2.8 Non-small cell lung cancer

The EGF receptor being implicated in so many fundamental physiological processes, is a central player in tumorigenesis as well. Often, the EGF receptor and its ligands are overexpressed in cancerous tissues. In normal cells, it has been estimated that there are between 40,000 to 100,000 receptors per cell, whereas in cancerous cells there could be over 1,000,000 receptors per cell (Carpenter and Cohen 1979). In combination with overexpressed ligands that induce expression of the EGF receptor and themselves, positive feedback loops could be generated, leading to gene amplification (William et al. 2017).

#### *6.2.8.1 Introduction to lung cancer*

Lung cancers are categorized into small cell lung cancers (SCLC) and non-small cell lung cancer (NSCLC). Around 85% of lung cancers is NSCLC and around 15% is SCLC. In this thesis, the focus is on NSCLC. NSCLC is a category of cancers in and around the lung that are histologically categorized into two main groups: squamous cell carcinomas and non-squamous cell carcinomas (i.e. adenocarcinoma and large cell cancer). Squamous cell carcinomas are often related to smoking or external factors, whereas non-squamous adenocarcinoma, the most common NSCLC, is more often related to genetics and could be overrepresented in certain ethnic groups. Around 75% of all lung cancer patients have a history of smoking. In the other 25% of patients, external factors as air pollution, second-hand smoking or genetic factors may have been of influence. The average age of discovery of NSCLC is 65 years and it is one of the deadliest cancers in the world with an average 5-year survival rate of 17% (Ettinger et al. 2015).

#### *6.2.8.2 Stages of non-small cell lung cancer*

NSCLC can be diagnosed by several methods: computed tomography (CT) imaging, biopsy of potentially cancerous lung tissue or cytology of coughed up fluid, the sputum (Boerckel et al. 2019). Depending on the spread and size of the cancer in the lungs and lymph nodes, there are multiple stages of NSCLC (Fig. 15). At stage I, there is cancerous tissue in the lung and there is no metastasis. At stage II, cancerous tissue can be found in the lung and nearby lymph nodes. In stage III cancerous tissue can be found in the lung and lymph nodes in the middle of the chest. In stage IIIA, the cancer is present in the lymph nodes on the same side where the cancer was found first. In stage IIIB, the cancer is present in the lymph nodes on the opposite side of where the cancer started growing or above the collarbone. In the final stage, stage IV, the cancer has metastasized and can be found in other parts of the body. The more advanced the cancer is, the more the expected 5-year survival rate decreases (Ettinger et al. 2015).

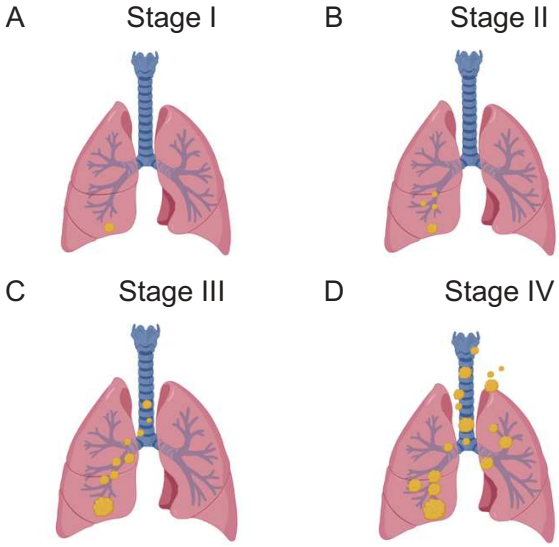


**Figure 15:** Four stages of non-small cell lung cancer. A) Stage I: tumour is between 1 and 4 cm and not metastasized. B) Stage II: tumour is between 3 and 7 cm and could be present in lymph nodes close to the lungs. C) Stage III: tumour could be bigger than 7 cm and present in multiple lymph nodes close to the lungs. D) Stage IV: tumour has metastasized. Figure is adapted from American Cancer Society: Non-small cell lung cancer stages. www.cancer.org/cancer/non-small-cell-lung-cancer/detection-diagnosis-staging/staging.html (2019).

#### *6.2.8.3 Driver gene mutations*

A common step for determining the treatment strategy is genotyping the cancer (Ettinger et al. 2015). In NSCLC, there are 3 genes that often carry driver mutations: *KRAS*, *ALK* and *EGFR*. Driver mutations in these genes promote cancerous cell growth. *KRAS* driver mutations are found in 25% of all NSCLC patients. Rearrangement of anaplastic lymphoma kinase (ALK), i.e. fusion between the *ALK* gene and an oncogenic driver gene, are found in 8% of NSCLC patients. Activating mutations in the *EGFR* gene are found in 17% of NSCLC patients. Usually, *EGFR*, *ALK* and *KRAS* mutations are mutually exclusive (Kris et al. 2014). Lastly, therapy against programmed cell death protein (PD1) or programmed death-ligand 1 (PD-L1), so-called immunotherapy, could be considered for cancer cells expressing PD-L1 (Ribas and Hu-Lieskovan 2016). Inhibitors specifically targeting K-Ras, ALK, EGFR or PD-L1 are currently available on the drug market.

#### *6.2.8.4 EGFR driver mutations and resistance to treatment*

Almost exclusively, *EGFR* mutations are somatic mutations and will not be passed to future generations. This does not exclude that genetics play a major role for *EGFR* driver mutations. It was found that females and Asian people are overrepresented in the group of NSCLC patients bearing *EGFR* mutations. Light or non-smokers are overrepresented in this group as well (Pao et al. 2004).

In NSCLC, the *EGFR* mutations can be found in the exons 18 to 21, that are coding for the TK domain. Herein, exon 21 codes for the activation loop that is crucial for the inhibition of the TK domain (Fig. 10). In exon 21, the most common mutation is the substitution of L858 with arginine (L858R), resulting in a TK domain that is always in the active conformation (Fig. 16A). Another common mutation is the deletion of residues 746 till 750 in exon 19 (exon19del). This deletion causes the displacement of the activation loop, also causing the TK domain to be in the active conformation. L858R and exon19del are considered primary, activating EGF receptor-mutations and they account for over 90% of the primary mutations in the TK domain (Shigematsu et al. 2005). Often, patients bearing these mutations are treated with TK inhibitors, a group of ATP-competitive antagonists that will be discussed in more detail in the next subchapter. There are three generations of TK inhibitors that are on the drug market (Table 3). First-generation TK inhibitors act on *wild-type* EGF receptor and EGF receptors with a primary activating mutation. Second-generation TK inhibitors are pan-EGFR family inhibitors. Third-generation TK inhibitors are designed for a specific EGF receptor mutant, but also have affinity for *wild-type* EGF receptor, as will be discussed here.

EGF receptors bearing a primary activating mutation have an increased sensitive to treatment by first-generation TK inhibitors (Pao et al. 2004) and second-generation TK inhibitor dacomitinib (Lau et al. 2019). Through a plethora of mechanisms, drug resistance to first-generation TK inhibitors will inevitably appear after 9-13 months of treatment (Cortot and Jänne 2014). Importantly, the appearance of drug-induced *EGFR* mutations is very common (Wang et al. 2016). Common other resistance mechanisms are: bypassing of EGF receptor-signalling through HGF receptor or HER2, *PI3KCA* mutations or histological changes (i.e. SCLC transformation or epithelial-mesenchymal transition) (Tan et al. 2018). Moreover, over the course of time, cancers become more heterogenous due to temporal, spatial and drug-induced heterogeneity. Tumour heterogeneity could abolish initial responses to drugs due to increased complexity of the tumour (Fig. 16B). Combination or pan-inhibition of oncogenes could therefore be beneficial in NSCLC treatment (Dagogo-Jack and Shaw 2018).

Especially in patients treated with first-generation TK inhibitors, the appearance of a secondary *EGFR* mutation *in cis*[xiii] is common. During treatment with first-generation TK inhibitors, drug resistance through

[xiii] *In cis* means on the same allele and thus in the same protein

the substitution of threonine 790 with methionine (T790M) appears in around 50% of patients (Fig. 16) (Nosaki et al. 2016). The bulky methionine sterically hinders first-generation TK inhibitors (Pao et al. 2005). Moreover, it increases enzymatic activity of ATP hydrolysis (Yun et al. 2008). Because, the T790M mutation renders resistance to many of the existing TK inhibitors, it is also called the gatekeeper mutation (Yun et al. 2008).

Drugs specifically designed for the inhibition of the T790M-containing EGF receptor are third-generation TK inhibitors. Third-generation TK inhibitors are ATP-competitive and form a covalent bond with cysteine 797 (C797). Generally, patients treated with these inhibitors have a better overall survival (Ohe et al. 2019) and a higher progression-free survival (Jiang et al. 2018) than first-generation TK inhibitors. Despite high initial response rates to osimertinib, patients will develop new resistance mechanisms of which a substitution of cysteine 797 with serine (C797S) is common (Fig. 16) (Heydt et al. 2018). Patients bearing C797S in combination with an activating mutation (e.g. L858R or exon19del) and the gatekeeper mutation (i.e. T790M), have acquired resistance to all FDA-approved TK inhibitors of the EGF receptor. A new generation of (allosteric) inhibitors, targeting the triple-mutated (i.e. L858R/T790M/C797S) EGF receptor, is in development. First results revealed synergy between EGFR allosteric inhibitor 045 (EAI045) and cetuximab, a monoclonal inhibitory antibody, on mice bearing the triple-mutated EGF receptor (Jia et al. 2016).

To summarize, NSCLC is a group of cancers in the lung and belongs to the deadliest cancers in the world. Common mechanisms leading to NSCLC are driver mutations, among which the *EGFR* driver mutation is one of the most frequent ones. *EGFR* driver mutations are more common for Asians and females and less common in smokers. *EGFR* driver mutations are caused by a combination of genetic background, environment and other factors. Initial inhibition of the primary-mutated EGF receptor is relatively successful, till the appearance of drug-induced resistance mutations, like the gatekeeper mutation T790M and C797S.

| EGF receptor mutation | Drug sensitivity | Drugs | Mechanism of action |
|---|---|---|---|
| *None (wild-type)* | 1st generation TK inhibitors<br>2nd generation TK inhibitors | Erlotinib, gefitinib<br>Lapatinib | ATP-competitive<br>ATP-competitive |
| L858R or exon19del | 1st generation TK inhibitors<br>2nd generation TK inhibitors | Erlotinib, gefitinib<br>Lapatinib, dacomitinib | ATP-competitive<br>Daco.: cov. to C797 |
| T790M | 3rd generation TK inhibitors | Osimertinib | Covalent to C797 |
| C797S | Allosteric TK inhibitors? | EAI045 | Stabilizes inactive TK domain |

**Table 3:** EGF receptor mutations and drug sensitivity. Cov. means covalent.

A Main mutated residues in the EGF receptor TK domain

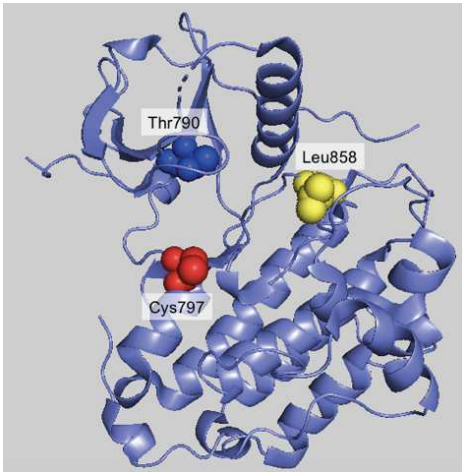


B Drug-induced resistance

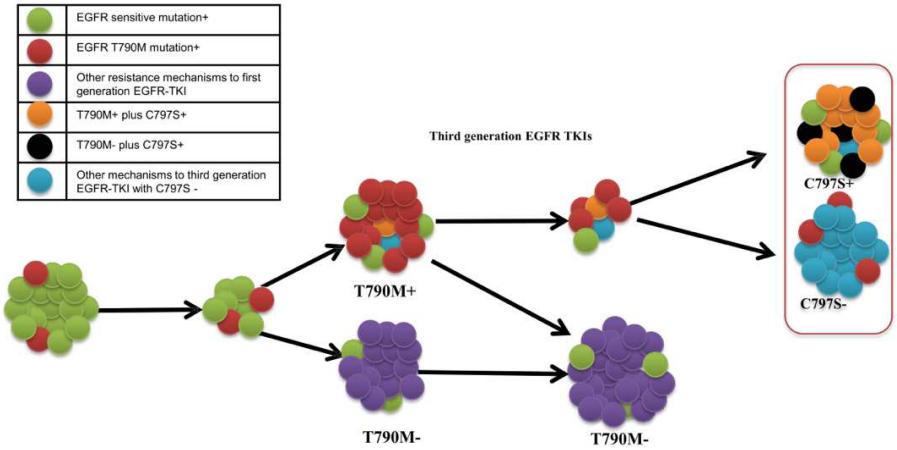


**Figure 16:** Drug-induced resistance to TK inhibitors. A) EGF receptor TK domain (active). This figure is adapted from Stamos *et al.* (2002), protein database reference 1M17. B) Drug-induced resistance to first-generation TK inhibitors. This figure is copied from Wang *et al*. (2016), with permission from Springer Nature.

### 6.2.9 Generations of EGF receptor TK inhibitors

TK inhibitors have been shortly introduced in the last subchapter. In this subchapter the characteristics of each generation are presented. TK inhibitors can be classified in a few ways, but the most common way is to distinguish them based on their generation in which they are designed. All TK inhibitors are not competitive to agonists. There are three generations of TK inhibitors that are FDA-approved and each generation was developed with a specific purpose. An experimental fourth-generation TK inhibitor is in the testing phase.

#### *6.2.9.1 First-generation TK inhibitors*

First-generation TK inhibitors are reversible ATP-competitive compounds. This generation includes compounds like gefitinib (Iressa, FDA approved in 2003), erlotinib (Tarceva, FDA approved in 2004), PD153035 and AG1478 (Fig. 17A-C, J). These compounds are efficacious on *wild-type* EGF receptor and EGF receptor with a primary mutation (e.g. L858R or exon19del) (Karachaliou et al. 2019). First-generation TK inhibitors occupy the ATP-binding pocket and form hydrogen-bonds with M793 in a hinge region at the entry of the TK domain. The hydrophilic part of these compounds points outside of the TK domain into the solvent. The hydrophobic part of these molecules is stabilized through hydrophobic interactions inside the TK domain (R. Roskoski 2016). These compounds do not extend into the back of the ATP cleft. As a result, the DFG-motif is in an inward position and the activation loop is unfolded. Therefore, first-generation TK inhibitors stabilize the active conformation of the TK domain (Dar and Shokat 2011). Additionally, the inactive conformation of the TK domain is stabilized as well by first-generation TK inhibitors (J. H. Park et al. 2012).

#### *6.2.9.2 Second-generation TK inhibitors*

Second-generation TK inhibitors are ATP-competitive compounds that have slow or irreversible binding kinetics (E. R. Wood et al. 2004). Some examples of second-generation TK inhibitors are lapatinib, GW583340, dacomitinib (Fig. 17D-F, K) and afatinib. Second-generation TK inhibitors are pan-EGFR TK domain inhibitors that are designed for inhibiting the EGF receptor and HER2, in for example breast cancer (i.e. lapatinib) and/or NSCLC (i.e. dacomitinib and afatinib). All compounds of this generation form hydrogen bonds with the hinge region comprising M793. Lapatinib and GW583340 have a large hydrophobic group pointing inside the TK domain. These compounds displace the DFG-motif, thereby stabilizing the inactive conformation of the TK domain. On the other hand, dacomitinib does not extend in the back of the TK domain, thereby stabilizing the active (and inactive) conformation of the TK domain. Unlike lapatinib and GW583340, dacomitinib and afatinib are irreversible inhibitors by forming a covalent bond with C797 (Niederst et al. 2015).

#### *6.2.9.3 Third-generation TK inhibitors*

Third-generation TK inhibitors are ATP-competitive compounds that form covalent bonds with C797 (Wang et al. 2016). Osimertinib and rociletinib are well known third-generation TK inhibitors (Fig. 17G, H, L). These compounds have an increased affinity (i.e. 200 times) for double-mutated (i.e. L858R/T790M) EGF receptor over *wild-type* EGF receptor, thereby reducing *wild-type* EGF receptor-associated side effects (Burtness et al. 2009). Nevertheless, toxic effects on the skin or gastrointestinal tract are often observed (Jänne et al. 2015). Importantly, the pharmacological profile of osimertinib is advantageous over first and second-generation TK inhibitors as the blood-brain barrier penetration is higher, making osimertinib more efficacious against brain metastases (Le and Gerber 2019). Osimertinib and rociletinib stabilize the inactive conformation of the TK domain.

#### *6.2.9.4 Experimental fourth-generation TK inhibitors*

Because of additional resistance mechanisms, the search for newer generations of TK inhibitors is ongoing. A "fourth-generation" TK inhibitors could be allosteric binders like EAI045. EAI045 binds in an allosteric pocket next to the αC-helix of the TK domain of mutated EGF receptor and is not ATP-competitive (Zhao et al. 2018). Importantly, it has an increased affinity (1000 times) for the EGF receptor bearing T790M over *wild-type* EGF receptor and does not bind to the TK domain bearing exon19del (Jia et al. 2016). Its structure can be described as a three-bladed propeller, in which one blade is in between the gatekeeper mutation (i.e. M790) and K745, a second blade occupies a hydrophobic pocket in the back of the ATP cleft and the third blade is next to the αC-helix forming interactions with the DFG-motif (Fig. 18) (L. Chen et al. 2018). Its inhibitory activity was increased when combination with cetuximab (Jia et al. 2016)

To summarize, first-generation TK inhibitors are inhibitors of *wild-type* and mutated (i.e. L858R or exon19del) EGF receptor. Second-generation TK inhibitors are considered pan-EGFR TK inhibitors with generally slow or irreversible binding kinetics. Third-generation TK inhibitors are irreversible mutant-specific (i.e. T790M) inhibitors. Experimental fourth-generation TK inhibitors inhibit the EGF receptor through an allosteric binding site which is not ATP competitive.

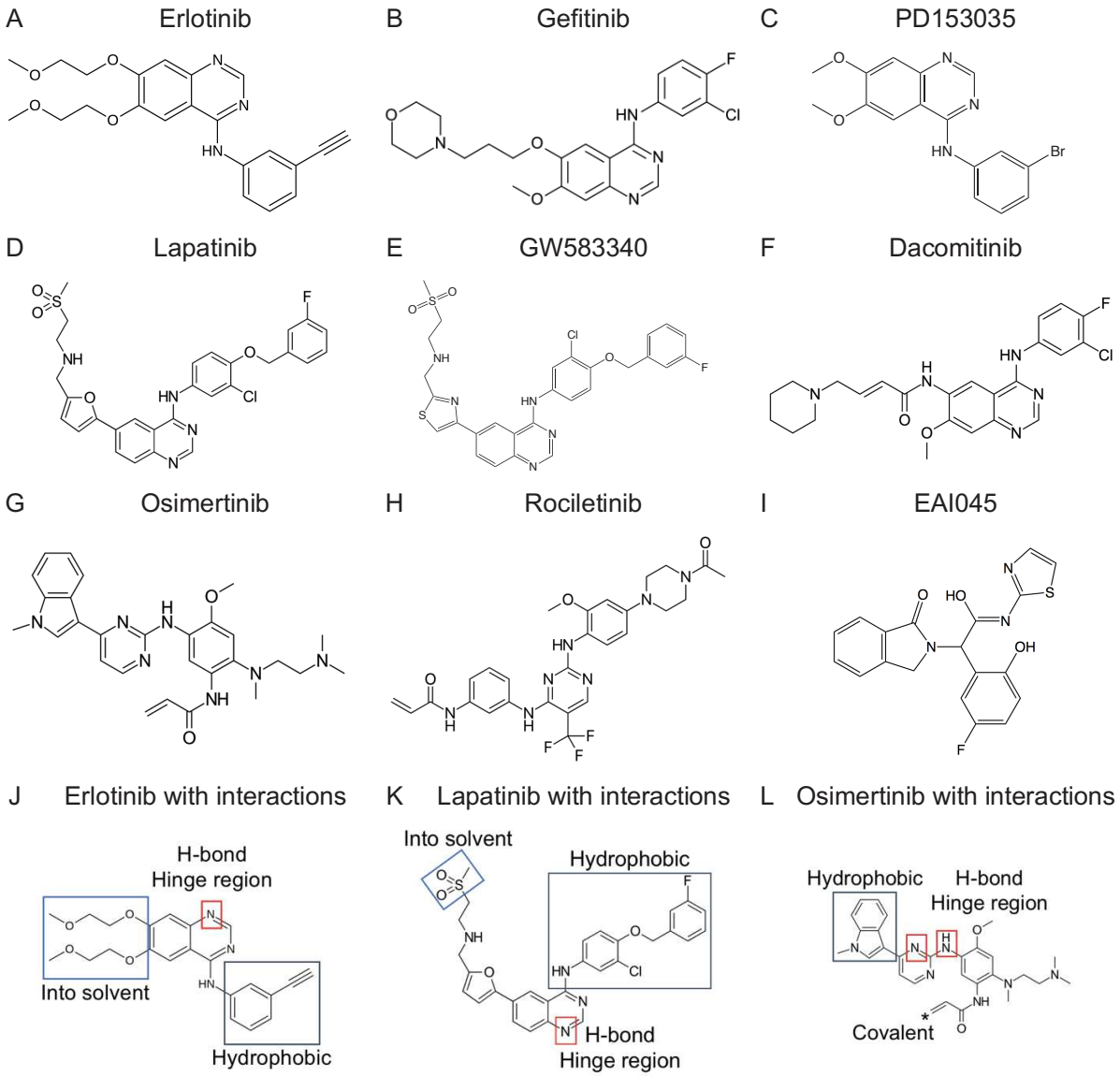


**Figure 17:** Structures of four generations of tyrosine kinase inhibitors. A) Erlotinib. B) Gefitinib. C) PD153035. D) Lapatinib. E) GW583340. F) Dacomitinib. G) Osimertinib. H) Rociletinib. I) EAI045. J-L) Erlotinib, lapatinib and osimertinib with the interactions with their pharmacophores highlighted. The H-bonds in the hinge region is formed with M793. The covalent interaction of osimertinib is formed with C797. Figure 17J-L are adapted from Roskoski *et al.* (2016).

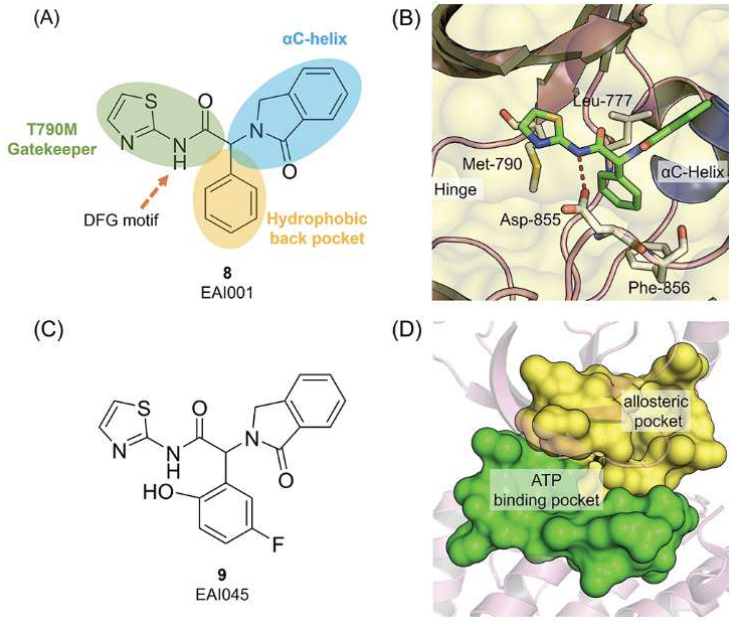


**Figure 18:** Mode of binding of allosteric TK inhibitors. A) Chemical structure of EAI001. B) Mode of binding into allosteric binding pocket of the inactive, mutated (T790M/V948R) TK domain. Protein database reference 5D41 (Jia et al. 2016). C) Chemical structure of EAI045. D) ATP binding pocket and allosteric pocket of the TK domain are highlighted. This figure was copied from Chen *et al*. (2018) with permission of American Chemical Society.

### 6.2.10 Summary of the introduction of the EGF receptor

Since the discovery of receptor tyrosine kinases (RTKs) and the EGF receptor in the 1950s, the EGFR family has become the prototypical RTK class. The EGF receptor is a single transmembrane receptor linking a large extracellular domain with an enzymatic intracellular domain, the tyrosine kinase domain. Its agonists are small proteins and induce dimer formation/conformational changes in order to activate the receptor. Activation of the receptor leads to progression of the cell cycle. The EGF receptor has a key role in embryogenesis and is involved in many physiological processes like skin repair and neuroprotection. As such, it is also involved in tumorigenesis and several drugs are targeting the (overactive) EGF receptor and other EGFR family members. For many non-small cell lung cancer patients, the EGF receptor is a therapeutic target that is inhibited by different generations of TK inhibitors. Unfortunately, resistance mechanisms occur, among which drug-induced appearance of mutations in the TK domain are common. Ultimately, this leads to acquired resistance to all FDA-approved drugs. Innovation of therapy could be succeeded by the generation of new generations of TK inhibitors, or by optimizing therapies. In this thesis, we did an effort to increase understanding of the effect of TK inhibitors on the EGF receptor.

## 6.3 METABOTROPIC GLUTAMATE RECEPTOR SUBTYPE 4

### 6.3.1 History of the metabotropic glutamate receptors

The first discovered glutamate receptors are the ion-channel linked ionotropic glutamate receptors. In 1985, another kind of glutamate receptor, with different downstream signalling, was discovered (Sladeczek et al. 1985). In the years that followed, other glutamate receptors of the same kind were discovered, establishing a new family of receptors that was named the metabotropic glutamate (mGlu) receptor family. As the members of the mGlu receptor family are coupled to G proteins, they became a new family of the GPCR superfamily (Bockaert, Pin, and Fagni 1993). Within the mGlu receptor family, there are 8 subtypes (and more if splicing variants are considered) divided into 3 groups. Group I mGlu receptors are mGlu receptor subtype 1 (mGlu1) and 5 (mGlu5), mainly coupled to the $G\alpha_q$ protein, as was discovered by Sladeczek in 1985 (Sladeczek et al. 1985). Group II mGlu receptors are the mGlu2 and mGlu3 receptor. Their main G protein family coupling is $G\alpha_i$ and $G\alpha_o$. Group III mGlu receptors are mGlu4, 6, 7 and 8 receptors. Their main coupling is to $G\alpha_i$ and $G\alpha_o$.

#### *6.3.1.1 Group-selective modulation of mGlu receptors*

All mGlu receptors can be activated by the endogenous orthosteric agonist glutamate, though with different potencies (J. P. Pin and Duvoisin 1995). Moreover, group-selective compounds (i.e. agonists, antagonists, allosteric modulators) have been developed for group I (Salt, Turner, and Kingston 1999), II (Simmons et al. 2002) and III (Lopez et al. 2007) mGlu receptors. These compounds act either on the orthosteric site in the N-terminal extracellular domain or within the 7TM domain on the allosteric binding site. In 1999, an allosteric binding site was discovered in the 7TM domain of class C GPCRs. This binding site resembles that of the orthosteric binding site of class A GPCRs (Litschig et al. 1999).

#### *6.3.1.2 Homo- and heterodimeric structures of mGlu receptors*

Before, the members of the mGlu receptor family were believed to be (mainly) constitutive homodimers (Romano, Yang, and O'Malley 1996). Only ten years ago, it was shown that mGlu receptors within group I or within group II and III have the propensity to form heterodimers with each other (Doumazane et al. 2011). Later, the existence of pharmacologically active mGlu2-4 heterodimers was proven in native tissue (Yin et al. 2014). The precise mechanisms of activation of heteromeric mGlu receptors are not clear yet, but insights in the structure of mGlu receptors bound to activators or inhibitors could help deciphering the activation mechanisms. In 2000, the structure of the Venus Flytrap (VFT) domain of the mGlu1 receptor was solved (Kunishima et al. 2000) and in 2014, the first 7TM domain of an mGlu receptor structure was solved; also that of the mGlu1 receptor (H. Wu et al. 2014). In 2019, the first 'full-length' mGlu5 agonist-bound receptor structure was solved with crystallography and cryo-EM (Koehl et al. 2019). A next milestone

was the solving of the structures of the mGlu2 and mGlu4 (Fig. 19A) (Lin et al. 2021). Notably, the dimers are asymmetric and only one subunit of each dimer binds a G protein, as was proposed by biochemical approaches by Pin's team (Hlavackova et al. 2005; Goudet et al. 2005). This information will be crucial for explaining the asymmetric activation of an mGlu2-4 heterodimer, as was shown in 2017 (J. Liu et al. 2017). The only published cryo-EM structure of a heterodimeric mGlu receptor is the inactive mGlu2-7 heterodimer, in which it was shown that G protein activation is strictly through the mGlu7 subunit (Du et al. 2021), revealing that G protein coupling is differently regulated between different dimers.

Overall, tremendous progress in mGlu receptor research has been made since their discovery in 1985. There are now orthosteric and allosteric compounds to selectively control the different groups of mGlu receptors. Once, mGlu receptors were believed to be exclusively homodimers, whereas a functional mGlu2-4 receptor and the cryo-EM structure of the mGlu2-7 heterodimer are the ultimate prove against. The next challenge is to decipher the physiological role of these heterodimeric receptors.

### 6.3.2 Structure of metabotropic glutamate receptors subtype 4

The mGlu4 receptor is a ~130 kDa *N*-glycosylated membrane protein consisting of a large N-terminal domain, a 7TM domain and C-terminal domain (Fig. 19A-B). The receptor has 880 amino acids after cleavage of its 32 amino acid signal peptide (Rosemond et al. 2002). The N-terminal domain resembles the venus flytrap plant and has around 553 residues (Fig. 19C). It consists of a Venus Flytrap (VFT) domain and a cysteine-rich domain (CRD). The VFT domain contains the orthosteric binding site and is well conserved within the mGlu receptor family (Rosemond et al. 2002). The 7TM domain is a 261-residue domain consisting of seven transmembrane α-helices, connected by three intra- and three extracellular loops. The binding pocket in between the transmembrane helices is the allosteric binding site and is less well conserved (M. R. Wood et al. 2011). The intracellular loops between the α-helices regulate G protein coupling (Jean Philippe Pin, Galvez, and Prézeau 2003). The carboxyterminal tail may very between splicing variants and may change the potency of glutamate (Niswender and Conn 2010).

In summary, the mGlu4 receptor is a transmembrane receptor with a large N-terminal domain that contains the conserved orthosteric binding site. The allosteric binding site is in the 7TM domain. The intracellular loops of mGlu receptors control G protein activity.

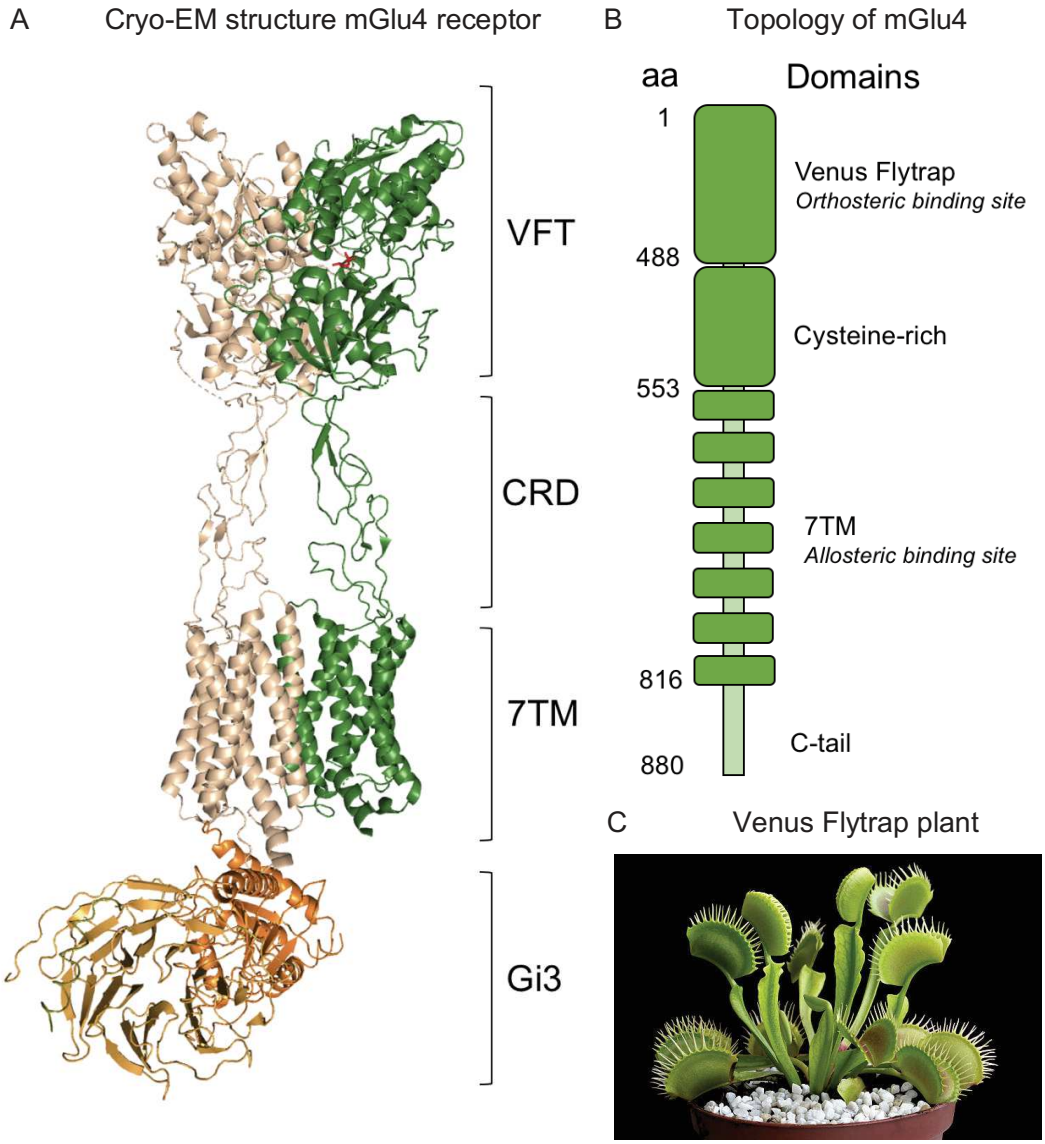


**Figure 19:** Structure and topology of the mGlu4 receptor. A) Model of the cryo-EM structure of an mGlu4 homodimer in active conformation bound to the Gi3 protein. This figure is adapted from Lin *et al.* (2021), protein database: 7E9H. B) Topology of the mGlu4 receptor. This figure is adapted from https://gpcrdb.org/protein/grm4_human/. C) Photo of Venus Flytrap plants. This image is from https://pixabay.com/images/search/venus%20flytrap/ and is not protected by copyright.

### 6.3.3 mGlu4 expression and function

The mGlu4 receptor is expressed in different areas in the human body like bone, skin, pancreas, tongue and the brain. Importantly, cellular responses to activation of the mGlu4 receptor depend on the tissue. In bone and skin, the mGlu4 receptor is involved in cellular differentiation and proliferation (Chang et al. 2005). In the pancreas it regulates insulin secretion (Brice et al. 2002). On the tongue, the mGlu4 receptor (i.e. splice variant) forms heteromeric complexes with taste receptors and is involved in sensing umami and glutamate taste (Pal Choudhuri, Delay, and Delay 2016).

However, the role of the homodimeric mGlu4 receptor has been mostly investigated for its function in the brain. The mGlu4 receptor is mainly expressed in the cortex, basal ganglia (amygdala, striatum), cerebellum, thalamus, olfactory bulb, substantia nigra and some hippocampal areas (Fig. 20) (Corti et al. 2002; Ferraguti and Shigemoto 2006). In neuronal tissue, the mGlu4 receptor is involved in signal transmission by regulating glutamate release from GABAergic and glutamatergic neurons (Corti et al. 2002; Charvin 2018; Ishkakova and Smith 2016). The mGlu4 receptor has a regulatory role during neuroinflammation, where it decreases glutamate release in peripheral dendritic cells in the brain (Fazio et al. 2018; Fallarino et al. 2010). In the amygdala, the mGlu4 receptor regulates pain sensitivity (Zussy et al. 2018), whereas in the nucleus accumbens, the mGlu4 is involved in the reward pathways (Ebrahimi et al. 2021). Unlike the homodimeric mGlu4 receptor, there is no knowledge about the function of mGlu4-containing heterodimers (McCullock and Kammermeier 2021).

#### *6.3.3.1 The mGlu4 receptor regulates synaptic glutamate release*

The mGlu4 receptor is a pre-synaptic receptor that is expressed in glutamatergic and GABAergic neurons. During signal transmission (i.e. activation of a neuron), glutamate levels in the synaptic cleft could be up to 1 mM (Dzubay and Jahr 1999). This activates the mGlu4 receptor and initiates mGlu4 receptor signalling (i.e. EC50 of glutamate for mGlu4 is in µM range) (J. P. Pin and Duvoisin 1995). Activation of the mGlu4 receptor leads to activation of its main signalling pathway through inhibition of adenylyl cyclase by $G\alpha_i$, which will be discussed in more detail in the next subchapter. Importantly, in neurons this leads to inhibition of calcium influx and subsequent reduced release of glutamate into the synaptic cleft via vesicular glutamate transporters (VGLUT) (Fig. 20B) (Tao Li, Ghishan, and Bai 2005). Glutamate concentrations in the synaptic cleft are also regulated by other mGlu receptors and glutamate transporters like the excitatory amino acid transporters (EAAT) (Conti et al. 1998).

Overall, the mGlu4 receptor is expressed in various tissues throughout the body, being involved in a variety of processes. In the brain, the receptor has a regulatory role, as activation leads to reduced vesicular glutamate release and subsequent decreased signal transmission.

A Expression of mGlu4 in mouse brain

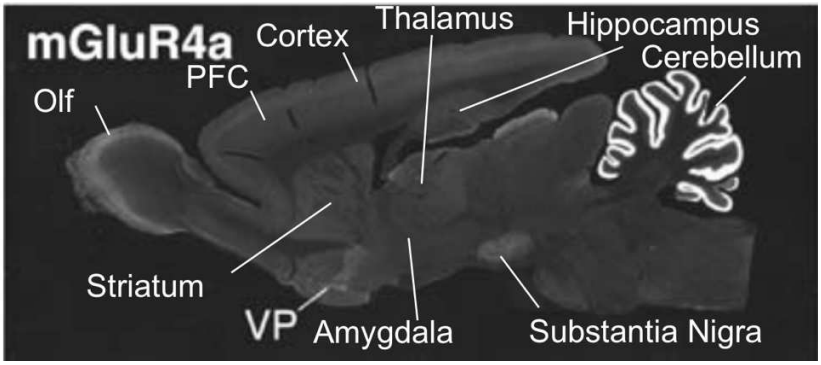


B Overview of mGlu receptor function in the brain

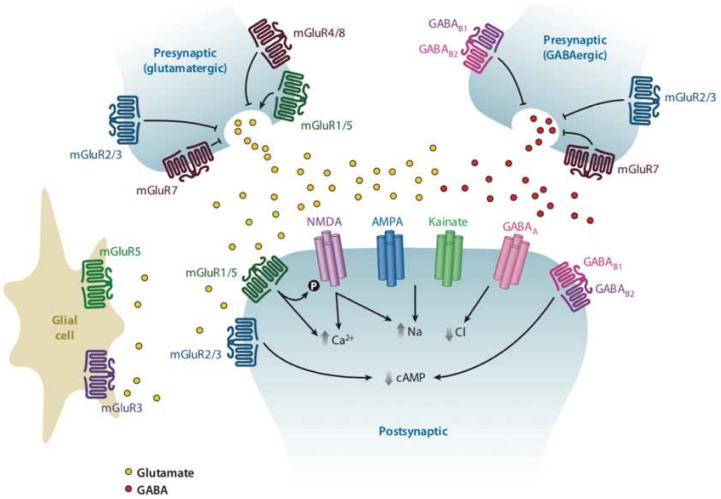


**Figure 20:** Expression and physiology of the mGlu4 receptor. A) Expression levels of the mGlu4 receptor in different brain regions. Levels are especially high in the cerebellum, substantia nigra and olfactory bulb (Olf). PFC means prefrontal cortex. B) Scheme of synapses of glutamatergic and GABAergic neurons with ionotropic and metabotropic glutamate receptors and GABA receptors highlighted. Figure A was copied and adapted from Ferraguti *et al.* (2006) with permission from Springer Nature. Figure B was copied from Niswender *et al.* (2010) with permission from Annual Reviews.

### 6.3.4 mGlu4 receptor activation mechanism

Upon binding of an agonist in the orthosteric site, the VFT domains close and the subunits rotate around each other. This causes the CRDs to re-orientate, inducing a movement and rotation in the 7TM domain like for the calcium-sensing receptor (CaSR) (Fig. 21A). The re-orientation of the 7TM from ligand-free (apo) to active receptor causes the intracellular tips of helices III and IV to be available for G protein binding (Fig. 21B, C) (Lin et al. 2021). Coupling of the GDP-bound $G\alpha_i$-protein to the agonist-bound receptor, leads to the exchange of GDP for GTP in the G protein. Upon exchange of GDP for GTP, the heterotrimeric G protein will dissociate into two parts: $G\alpha_i$ and $G\beta\gamma$. Both parts interact with effector proteins (Fig. 21D):

- $G\alpha_i$ inhibits adenylyl cyclase (AC), which leads to a decrease in levels of second messenger cAMP and less subsequent activation of downstream kinases that are cAMP-dependent (e.g. cAMP-dependent protein kinase A (PKA)). PKA phosphorylates other proteins or transcription factors, thereby regulating their activity.
- $G\beta\gamma$ inhibits G-protein-gated inwardly rectifying $K^+$ (GIRK) channels (Kofuji, Davidson, and Lester 1995) and $Ca^{2+}$ion-channels (Herlitze et al. 1996) by interacting with them.
- $G\beta\gamma$ also activates phospholipase C (PLC)-ß (D. Park et al. 1993) and Src-proteins (Shajahan et al. 2004). PLC-β is an enzyme involved in generation of $IP_3$, a second messenger. Src-proteins are kinases that phosphorylate a variety of proteins, among them the EGF receptor.

It was suggested that regulation of mGlu4 receptor is through deactivation by phosphokinase C (Mathiesen and Ramirez 2006) or by trafficking to inactive domains in the synapse (Siddig et al. 2020).

In summary, the re-orientation of the 7TM domain of the mGlu4 after ligand binding resembles that of other class C GPCRs like the CaSR and mGlu5 receptor. The main downstream signaling pathways are through $G\alpha_i$ (i.e. inhibition of AC) and $G\beta\gamma$ (i.e. inhibition of ion-channels and activation of kinases/enzymes).

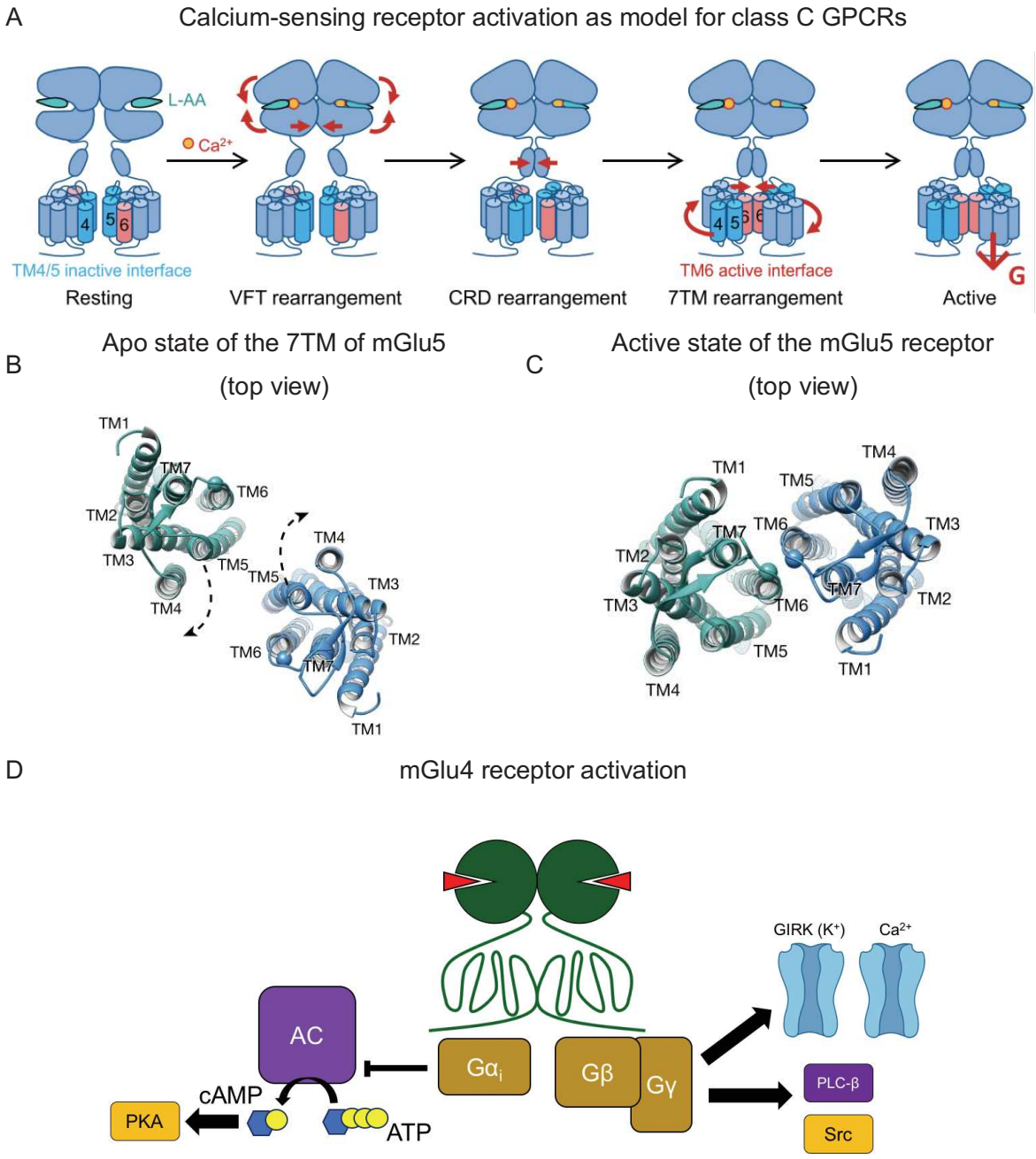


**Figure 21:** Activation of class C GPCRs. A) Activation of the calcium-sensing receptor as model for class C GPCR activation. B) Apo state of the mGlu5 7TM domain. The arrows point towards the direction the 7TM domain rotates. C) Active state of the mGlu5 7TM domain. The TM6s of each subunit are interacting in the active state. D) Scheme of main signalling pathways of the mGlu4. The mGlu4 is in green. Figure A is copied from Liu *et al.* (2019) with permission from Proceedings of the National Academy of Sciences of the United States of America. Figures B and C are copied from Koehl *et al.* (2019) with permission from Springer Nature.

### 6.3.5 Parkinson's disease, pain and cancer

Because of its regulatory role in the CNS, the mGlu4 receptor has been suggested as therapeutic target for Parkinson's Disease (PD) (Charvin 2018; Niswender et al. 2016) or pain (Vilar et al. 2013; Zussy et al. 2018). Also, the mGlu4 was found to be overexpressed in multiple cancers (i.e. colorectal cancer, malignant melanoma and laryngeal and breast carcinomas) and is correlated to poor disease-free survival (Chang et al. 2005). The role of the mGlu4 receptor in PD, pain and cancer will be shortly discussed.

#### *6.3.5.1 mGlu4 receptor in Parkinson's Disease*

PD is characterized by slow movement (i.e. bradykinesia), rigidity and tremors due to decreased dopaminergic signalling and increased glutamatergic transmission in corticostriatal neurons [xiv] and GABAergic neurons in the basal ganglia (i.e. globus pallidus internus (GPi) and globus pallidus externus (GPe)) (Fig. 22). PD is also characterized by increased levels of glutamate in subthalamic neurons (STN), substantia nigra pars compacta (SNpc) and substantia nigra pars reticulata (SNpr). Since, glutamate causes excitotoxicity, it worsens the disease progress (Finlay and Duty 2014).

Current treatment of PD focuses on the shortage of dopamine, by administration of L-DOPA, a dopamine precursor. Initially, this treatment greatly improves the quality of life of patients, but after 5 years of treatment, higher dosage regimes are required to maintain efficacy (Olanow, Stern, and Sethi 2009). The increase in dose leads to adverse effects like L-DOPA-induced dyskinesia (LID) and neurodegeneration due to increased levels of glutamate over-time (Mellone and Gardoni 2018). Moreover, periods in which PD symptoms return despite antiparkinsonian treatment, so-called OFF periods, occur more often (Tanner 2020).

The reasoning behind activating the mGlu4 receptor as treatment strategy, is that glutamatergic transmission is reduced in a direct (i.e. SNpr) and indirect (i.e. GPe-STN-SNpc/SNpr) way, thereby reducing motor symptoms and dopaminergic cell death (Fig. 22).

#### *6.3.5.2 mGlu4 receptor in pain*

The mGlu4 receptor is expressed in spinal neurons that are involved in pain sensation. The mGlu4 receptor modulates hypersensitivity in inflammatory or neuropathic pain models of mice. Therefore, the mGlu4 receptor could be targeted for future treatment of pain (Vilar et al. 2013).

#### *6.3.5.3 mGlu4 receptor in cancer*

In colorectal cancer, the mGlu4 receptor was found to be overexpressed and was suggested as poor prognostic factor due to its neuroprotective role (Chang et al. 2005). In glioblastoma cancer cells, the mGlu4

[xiv] Neurons connecting the cortex and striatum

receptor suppresses proto-oncogenes (Z. Zhang et al. 2018) and in medulloblastomas, the mGlu4 inhibits cancer growth (Iacovelli et al. 2006).

Modulation of the mGlu4 receptor has been proposed as innovative treatment strategy in PD in order to reduce glutamate transmission and excitotoxicity. Nevertheless, the mGlu4 receptor has shown potential as drug target in hypersensitivity or cancer as well.

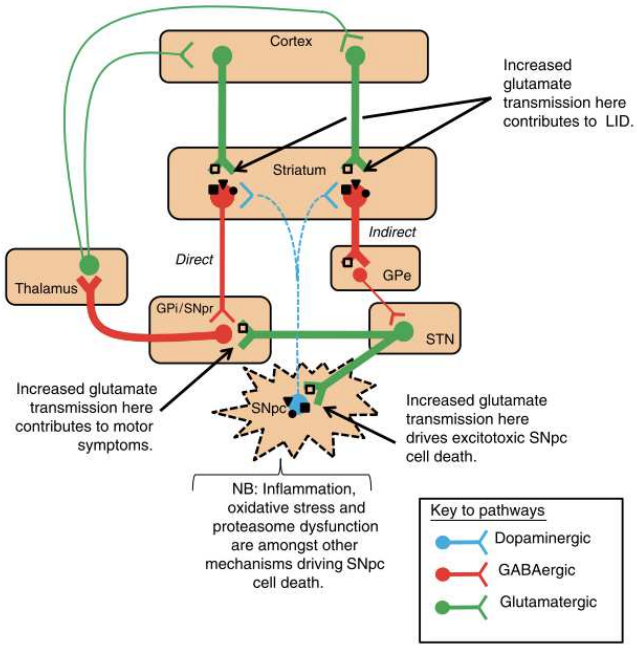


**Figure 22:** Scheme of the activity of pathways in the basal ganglia motor circuit in Parkinson's Disease. GPe is globus pallidus externus, GPi is globus pallidus internus, SNpr is substantia nigra pars reticulata, SNpc is substantia nigra pars compacta, STN is subthalamic nucleus. Group II and III mGlu receptors are open squares. Group I mGlu receptors are black squares. In the dopaminergic (blue), GABAergic (red) and glutamatergic (green) transmission, thick lines represent increased and thin lines represent decreased transmission. This figure is copied from Finlay *et al.* (2014) with permission of Springer.

### 6.3.6 Compounds targeting the mGlu4 receptor

Despite extensive research, no drugs are on the market for the mGlu4 receptor, yet. So far, the only mGlu4-targeted compound tested in a clinical trial was foliglurax, a positive allosteric modulator for the treatment of Parkinson's Disease. Efficacy criteria in the 2nd phase were not met and further investigations by Lundbeck and Prexton were aborted (Doller et al. 2020). Since, there are no new clinical investigations for mGlu4 receptor compounds ongoing. Nevertheless, there are many compounds binding the mGlu4 receptor that are being used in research and throughout this thesis.

#### *6.3.6.1 mGlu4 receptor endogenous compounds*

Firstly, mGlu4 endogenous orthosteric agonists are glutamate (L-glutamic acid) (Fig. 23A), L-aspartic acid and L-serine-O-phosphate. These compounds bind the orthosteric binding site and are not selective for the mGlu4 receptor as they have affinity for other mGlu receptor subtypes as well (Acher and Tocris 2006). These compounds have micromolar potencies and as they are amino acids, they are hydrophilic, making them not very suitable as drugs for brain diseases.

#### *6.3.6.2 mGlu4 receptor designed orthosteric compounds*

Secondly, mGlu4 receptor designed orthosteric agonists are L-2-amino-4-phosphonobutyric acid (L-AP4) (Eriksen and Thomsen 1995) (Fig. 23B), a group III mGlu receptor agonist, and LSP4-2022 (Goudet et al. 2012), a mGlu4-selective agonist. Both compounds have potencies in the high nanomolar range for the mGlu4 receptor.

Thirdly, mGlu4-designed orthosteric antagonists are LY341495 (Kingston et al. 1998) (Fig. 23C), a group II mGlu receptor antagonist, with some affinity for group III mGlu receptors as well (high micromolar range). (S)-2-methyl-2-amino-4-phosphonobutanoate (M-AP4) (Han and Hampson 1999) is a group III mGlu receptor-specific antagonist with affinities in the high micromolar range, but does only bind rodent mGlu4.

#### *6.3.6.3 mGlu4 receptor designed allosteric compounds*

Fourthly, there are several PAMs targeting the mGlu4 receptor, among them 2-methyl-6-(2-phenylethynyl)pyridine (MPEP) (Mathiesen et al. 2003) and VU0155041 (Niswender et al. 2008), both with potencies in the micromolar range. The only published mGlu4 NAM is OptogluNAM4.1, which is used in studies with photopharmacology techniques (Rovira et al. 2016).

#### *6.3.6.4 mGlu4 receptor nanobodies*

The latest development in mGlu4 receptor drugs are camelid single-domain heavy chain antibodies (nanobodies). Nanobodies represent an innovative group of molecules that are selective for their target, as will be discussed in the next subchapter. Previously, nanobodies that are allosteric modulators of the mGlu2

receptor were published (Scholler, Nevoltris, et al. 2017). In this thesis, DN45 is presented, the first nanobody with agonist activity for a class C GPCR (i.e. mGlu4 receptor).

Overall, clinical trials for compounds targeting the mGlu4 receptor have not been successful. Nevertheless, a plethora of compounds is used in research. In this thesis, a nanobody for the mGlu4 receptor is represented.

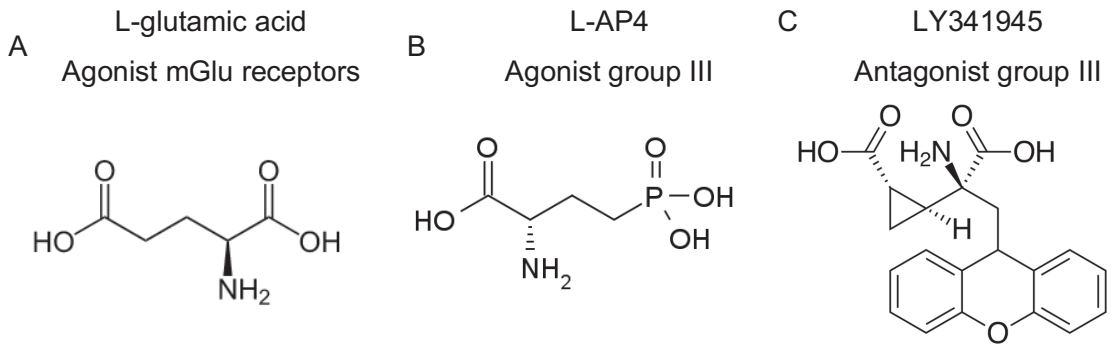


**Figure 23:** Orthosteric ligands for metabotropic glutamate receptors. A) L-glutamic acid. B) L-AP4. C) LY341945.

### 6.3.7 Nanobodies

Nanobodies are single-domain camelid antibodies. More specifically, a nanobody is the single variable domain on a heavy chain ($V_HH$) recognition domain of a camelid heavy chain-only antibody (HcAb) (Fig. 25A) (C. S. et al. 2016). The recognition domain of conventional immunoglobulin G (IgG) antibodies (e.g. cetuximab, trastuzumab) is a heavy chain ($V_H$) domain which is stabilized by a light chain ($V_L$) domain (Fig. 25B). Unlike $V_H$ domains, $V_HH$ domains are more hydrophilic and thus stable in an aqueous environment, making them more suitable for recombinant expression (Cromie and Boutton 2015). Nanobodies have a molecular weight of around 15 kDa, which makes them much smaller than conventional antibodies (~150 kDa). Nanobodies have three target recognition areas, the complementarity-determination regions (CDRs) (Fig. 25C). Given their small size, nanobodies may have more chance of passing through the blood-brain-barrier (BBB) than conventional antibodies (Tengfei Li et al. 2012). Nevertheless, passing of the BBB remains difficult or unknown for most nanobodies.

#### *6.3.7.1 Advantages of nanobodies in drug research*

A major advantage of nanobodies (and antibodies) over most small molecule drugs is that they have a high specificity for a molecular target. This, in combination with the possibility to label the nanobody directly (e.g. fluorophores, radiolabels) or indirectly (e.g. secondary antibodies), makes them ideal for localization of receptors on for example brain slices and cultured neurons (Scholler, Nevoltris, et al. 2017). Additionally, $V_HH$ nanobodies are relatively easy to modify: unnatural amino acids can be added for labelling, and they can be made bivalent or bi-paratopic for targeting heterodimers. Moreover, due to their small size and long CDRs, nanobodies are prone to reach cavities in proteins. Hence, nanobodies could stabilize an active or inactive conformation, thereby acting as agonist or antagonist/inverse agonist. Examples of modulating nanobodies are PAMs for the mGlu2 (Scholler, Nevoltris, et al. 2017) and an agonist nanobody for the angiotensin receptor (McMahon et al. 2020). This property is also useful for crystallization studies, as was demonstrated for the mGlu5 receptor. A nanobody that potentiates agonist binding was used to stabilize the active conformation of the mGlu5 receptor (Fig. 26) (Koehl et al. 2019).

#### *6.3.7.2 Nanobodies as innovative therapies*

Only one nanobody, caplacizumab, has made it as a drug so far (Duggan 2018). This bivalent nanobody is used for the treatment of patients with acquired thrombotic thrombocytopenic purpura by binding to von Willebrand factor (vWF), thereby blocking platelet aggregation. Caplacizumab shows that nanobodies can be used as selective therapeutic inhibitors. However, it may be even more interesting to develop nanobodies that are selectively modulating receptor activity. This is especially relevant for related receptors in which the binding sites are well conserved (e.g. orthosteric binding site of mGlu receptors). For these receptors, selective nanobodies could overcome the lack of selectivity of orthosteric binders.

To summarize, nanobodies are the antigen binding domain of camelid HcAbs. Their 3 CDRs allow them to be selective and modify protein activity. So far, one nanobody is approved as a drug. Nanobodies could overcome a lack of selectivity of receptors with conserved agonist binding sites.

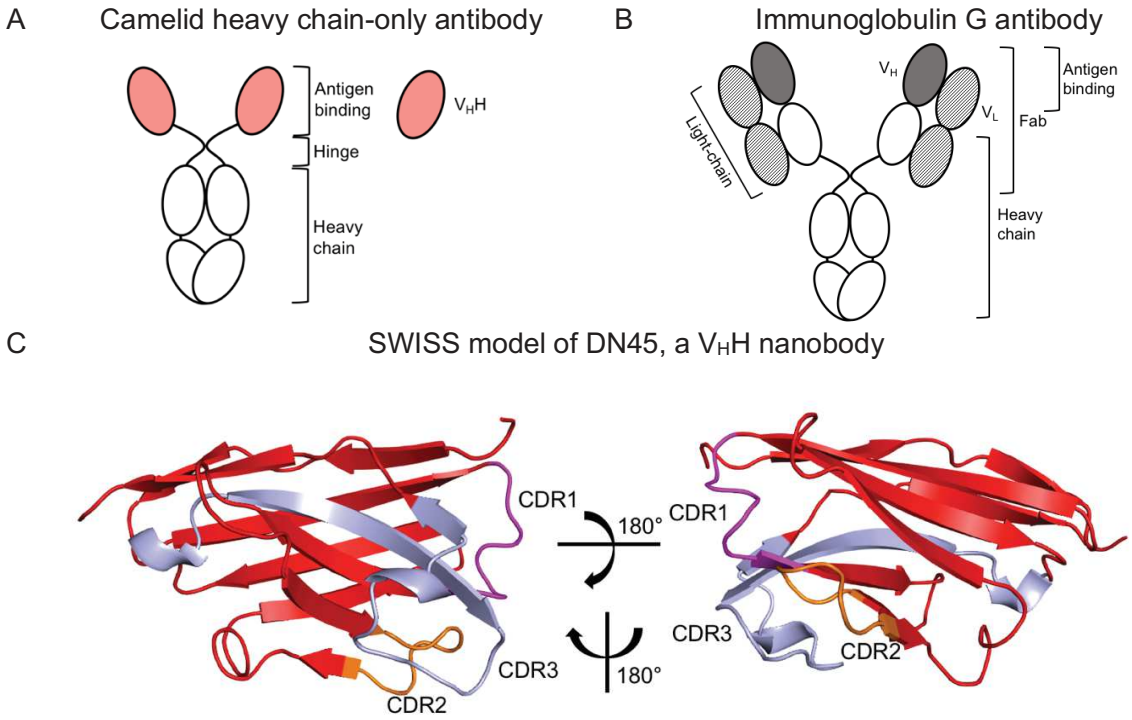


**Figure 25:** Scheme of structures of IgG and camelid HcAb. A) IgG. B) HcAb and $V_HH$. C) Model of DN45 generated by SWISS model. The complementarity-determination regions (CDRs) are highlighted. CDR1 is purple, CDR2 is orange and CDR3 is silver.

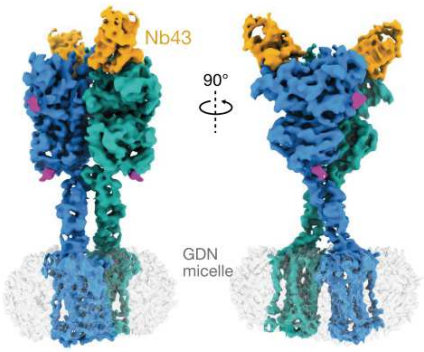


**Figure 26:** A nanobody stabilizing the mGlu5 receptor for cryo-EM crystallization. This image was copied from Koehl *et al.* (2019) with permission from Springer Nature.

### 6.3.8 Summary of the introduction of the mGlu4 receptor

Since the discovery of the first mGlu receptors in the 1980s, much progress has been made in understanding the function of these class C GPCRs. Within the mGlu receptor family, there are 3 groups containing 8 receptor subtypes. All of them are characterized by a large VFT domain and a 7TM domain. Group III mGlu receptors, which include the mGlu4 receptor, are coupled to the inhibitory $G\alpha_i$ protein. The mGlu4 receptor has been proposed as drug target in Parkinson's Disease, pain sensitivity and cancer. Importantly, the mGlu4 can form heterodimers with the mGlu2, but its function is unknown. When targeting the mGlu4 receptor with orthosteric agonists, a lack of specificity may occur due to the well conserved binding site. New compounds, like nanobodies, that selectively activate the mGlu4 receptor could overcome this problem.

## 6.4 DIMERS

### 6.4.1 EGF receptor ligand-induced dimerization or conformational changes

The EGF receptor is a well-studied receptor, but some fundamental questions cannot be answered as there is no full-length crystal/cryo-EM structure available due to flexible domains like the JxM domain (Diwanji, Thaker, and Jura 2019). Therefore, the dimerization dynamics of the EGF receptor remains a debated subject.

#### *6.4.1.1 Conformational changes in the extracellular domain*

Within the RTK superfamily, receptors may follow different dimerization processes. RTKs are categorized in receptors that follow ligand-induced conformational changes (e.g. insulin receptor) or ligand-induced dimerization (e.g. VEGF receptor). It is not fully clear to which category the EGF receptor belongs. Before highlighting the main arguments for each category, it is important to discuss the dimerization process of the EGF receptor that is generally agreed on. Both the extracellular domain (ECD) and intracellular domain (ICD) are involved in stabilizing dimeric conformations. In the ECD, subdomain II and its dimerization arm is the main dimerization force (± 90%), whereas subdomain IV is a secondary dimerization force (Dawson et al. 2005). X-ray crystal structure data of the ECD showed that the monomeric EGF receptor subunit is in a tethered conformation, in which the dimerization arm is hidden (Burgess et al. 2003). Conversely, subdomains I and III are available for EGF binding. Binding of EGF leads to revealing of the dimerization arm and subsequent dimerization and activation of the EGF receptor through the asymmetric association of the TK domains (Ferguson 2008).

#### *6.4.1.2 Pre-formed dimers*

There are several arguments that the EGF receptor is a pre-formed dimer that is activated following conformational changes, like the example of the insulin receptor. In 2002, Yu *et al.*, first described that dimerization and activation are separable events and that the EGF receptor forms ligand-free dimers through its TK domain (Yu et al. 2002). Later, it was shown with a (mutated) EGF receptor constitutive dimer that only minor rearrangements of the ECD are necessary for activation of the TK domain (Freed, Alvarado, and Lemmon 2015). These rearrangements are taking place due to a rotation of the transmembrane (TM) domain. As a consequence, the auto-inhibited TK domain becomes more flexible and adopts its active asymmetric conformation. Because of the rotation of the TM domain, this model is called the “rotation model” (I. N. Maruyama 2015). Importantly, studies based on FRET (Bader et al. 2009), fluorescence correlation spectroscopy (P. Liu et al. 2007; Yavas, Macháň, and Wohland 2016) and total internal reflection fluorescence (TIRF) (Teramura et al. 2006) prove the existence of pre-formed EGF receptor dimers at

physiological expression levels. Purba *et al.* even conclude that all EGFR molecules are present in a dimeric form in living cells (Purba, Saita, and Maruyama 2017).

#### *6.4.1.3 Ligand-induced dimers*

Nonetheless, there are also arguments that suggest that the EGF receptor follows ligand-induced dimerization. According to Zhang *et al.*, the EGF receptor is mainly monomeric and dimerization promotes removal of auto-inhibitory structures (X. Zhang et al. 2006). Accordingly, it was suggested that dimer formation could be induced by TK inhibitors (Gan et al. 2007) or that it is an intermediate step for the removal of the auto-inhibited conformation (Bublil et al. 2010). A recent study proposes several kinase-mediated ligand-free conformations: side-to-side, back-to-back, and stalk-to-stalk (Fig. 27) (Zanetti-Domingues et al. 2018). A quantum-dot approach on the single molecule level, provides evidence that the EGF receptor fluctuates between monomers and dimers, which could be regulated by expression or localization (Chung et al. 2010). It was suggested that the mono-dimer equilibrium of the EGF receptor could be shifted with first-generation TK inhibitors like gefitinib and erlotinib (Coban et al. 2015). Moreover, several studies suggested that there is a mixture of monomers and dimers prior to agonist binding (D. R. Singh et al. 2020; Yamashita et al. 2015; Kozer and Clayton 2019).

#### *6.4.1.4 TK inhibitors and their role on dimerization*

First-generation TK inhibitors have been described to stabilize the active and inactive conformations of a TK domain (Stamos, Sliwkowski, and Eigenbrot 2002; J. H. Park et al. 2012), whereas second-generation TK inhibitors[xv] only stabilize the inactive conformation (E. R. Wood et al. 2004). Consequently, first-generation TK inhibitors stabilize the asymmetric TK domain of an EGF receptor homodimer (Coban et al. 2015). It has been proposed that these dimers alter the EGF binding to the extracellular domain (Hajdu et al. 2020), but the physiological consequences remain elusive. Some explanation could be that dimerization plays a role in sorting the EGF receptor towards degradation, and not recycling (Tanaka et al. 2018). Another possibility is that second-generation, and not first-generation, TK inhibitors prime the EGF receptor to form oligomeric signalling platforms (Claus et al. 2018). These signalling pathways are believed to increase activity of the EGFR family members due to increased density of docking sites for downstream adaptor proteins (Y. Huang et al. 2016) Overall, it remains unclear how these ligand-free dimers are regulated in a cellular environment, how often they are present and what is their precise role. Therefore, studies with full-length EGF receptors in a cellular environment are necessary to clarify these points.

Based on the current knowledge about the dimerization process of the EGF receptor, there are two main subjects that are discussed in this thesis. Firstly, the activation process at physiological expression level will

[xv] Except dacomitinib and afatinib, because they also stabilize the active conformation of the TK domain

be determined. Secondly, the effect of TK inhibitors is evaluated on this process and we try to dive into the physiological relevance of these observations.

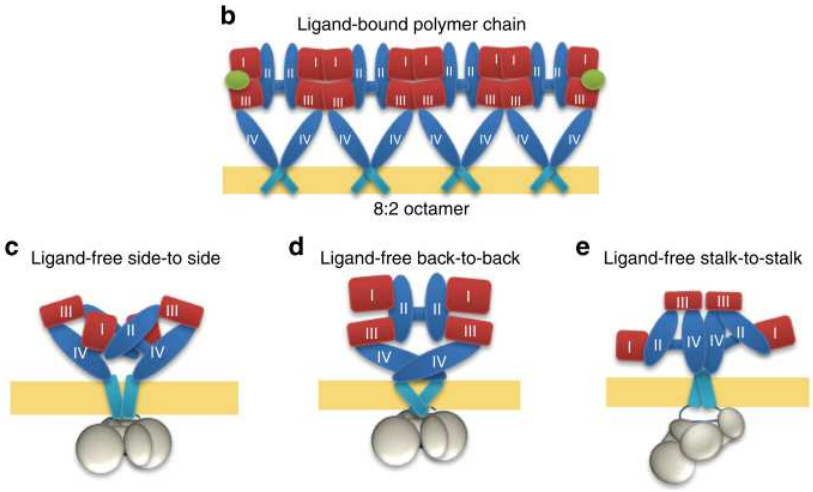


**Figure 27:** Ligand-free conformations of the EGF receptor. This image is copied from Zanetti-Domingues *et al.* (2018) with permission from Nature.

### 6.4.2 Asymmetry in G protein-coupling in class C GPCRs: 1 subunit a time.

In the last subchapter of the introduction, recent discoveries of asymmetric activation of class C GPCRs are described. For a long time, receptors were considered to be acting mainly as a monomer. Nowadays, this view has changed dramatically and it becomes clearer that there is a big diversity of dimers. This is also the case for the GPCR superfamily in which class A receptor may be active as a monomer or dimer (Dijkman et al. 2018) and class C GPCRs are functional as constitutive dimers.

#### *6.4.2.1 Allosteric control of receptor activity*

Pharmacology and formation of heterodimers of class C GPCRs have retained much attention in the past years (J. Liu et al. 2017; Doumazane et al. 2011; Lee et al. 2020). Generally, receptors are activated in an asymmetric way. This means that the G protein only binds to one of the subunits (Fig. 28). Between receptors, there are differences in how strict this G protein coupling is. In the case of the $GABA_B$ receptor, the $GABA_{B1}$ subunit contains the agonist-binding domain and the G protein coupling is strictly to the $GABA_{B2}$ subunit. Within the $GABA_{B2}$ subunit, a lipid binding pocket regulates receptor activation (Papasergi-Scott et al. 2020). Moreover, an additional allosteric binding pocket on the interface between the 7TM domains was suggested (Freyd et al. 2017), showing that the $GABA_B$ receptor activation is controlled by intersubunit interactions (Xue et al. 2019). Much can be learned from these interactions when looking at other receptors, as these mechanisms could be extrapolated to other receptors.

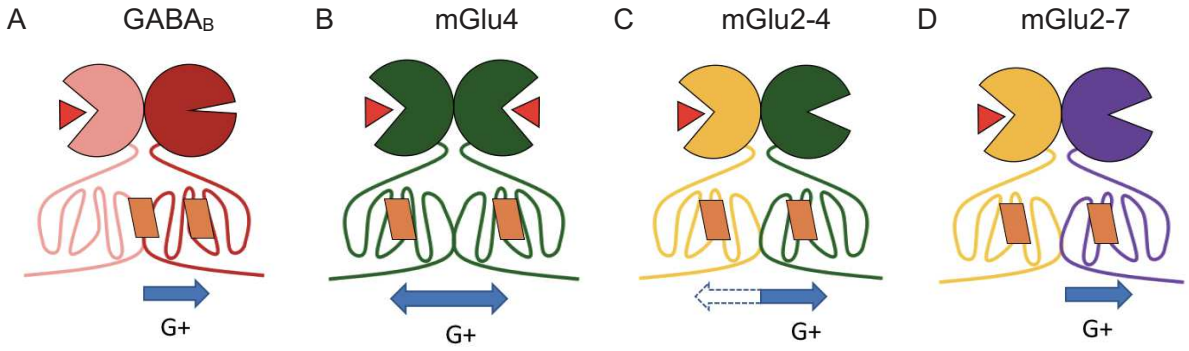


**Figure 28:** Asymmetric activation of class C GPCRs. A) $GABA_B$ receptor. $GABA_{B1}$ subunit is in pink and $GABA_{B2}$ subunit is in dark red, the agonist is in red, allosteric binding pockets are in orange. G protein coupling is restricted to the $GABA_{B2}$ subunit. B) mGlu4 receptor. Only 1 G protein can couple at the same time to either of the subunits. C) mGlu2-4 receptor. mGlu2 subunit is in yellow. G protein coupling is to the mGlu4 subunit, but can be shifted to mGlu2 with mGlu2 PAMs or mGlu4 NAMs. D) mGlu2-7 receptor. mGlu7 subunit is in purple. G protein coupling is strictly to the mGlu7 subunit.

#### *6.4.2.2 G protein coupling to mGlu receptor heterodimers*

An investigation on dimer formation of mGlu receptors revealed that some of the mGlu receptors have a higher propensity to form heterodimers than their respective homodimers (Doumazane et al. 2011). This is the case for the mGlu4 (i.e. mGlu2-4 and mGlu3-4) and mGlu7 (mGlu2-7 and mGlu3-7), suggesting that these heterodimers may be more favourable than homodimers in physiological conditions (Lee et al. 2020; Doumazane et al. 2011). These findings could be considered ground-breaking as it changes our view on this family of receptors, that was believed to be mainly homomeric before. A recent pharmacological demonstration has shown that G protein coupling in mGlu4 homodimers and mGlu2-4 heterodimers is not so different (Fig. 28B-C): G protein coupling occurs to 1 subunit of a dimer at a time (Lin et al. 2021). In the mGlu4 homodimer, 1 mGlu4 subunit is prone to coupling and activation of the G protein. In the mGlu2-4 heterodimer, G protein coupling is principally to the mGlu4 subunit. However, allosteric modulators of the mGlu2 and mGlu4 (i.e. mGlu2 PAM or mGlu4 NAM) may redirect G protein coupling to the mGlu2 subunit (J. Liu et al. 2017). This is the opposite of what was seen for the mGlu2-7 heterodimer, in which G protein coupling was strictly to the mGlu7 subunit (Fig. 28D) (Du et al. 2021). This revealed that even within the group III mGlu receptors, receptors have distinct properties when in a dimer. These differences may be driven by differences in interactions between 7TM domains of subunits (Thibado et al. 2021). Nevertheless, the lack of knowledge about the physiological role of heterodimers and the lack of the mechanism of regulation of dimer formation puts science in front of many new challenges.

#### *6.4.2.3 mGlu2-4 heterodimer in the brain*

Such challenges need to be addressed with innovative research tools that could discriminate between homo- and heterodimers. So far Yin *et al.* have proven the existence of a functional mGlu2-4 heterodimer in rat and mice brain tissue by using selective allosteric modulators to modulate signalling (Yin et al. 2014). The mGlu2-4 heterodimer was later proven to exist in human lateral performant path terminals (Delgado et al. 2017) and medial prefrontal cortex (Xiang et al. 2021). Animal models revealed that the mGlu2-4 heterodimer, unlike the mGlu4 homodimer, is likely not a target for treatment of Parkinson's Disease (Niswender et al. 2016). The complexity to generate heterodimer-specific ligands and research tools certainly plays a role in the ambiguity of the role of the heterodimer (Fulton et al. 2020).

Overall, we can say that after seven years since the discovery of functional mGlu2-4 heterodimers, progress has been made in understanding allosteric interactions in the dimer and its pharmacology. However, innovative tools are necessary for discovering the role of the mGlu2-4 in the brain. A first step is to discover in what regions the heterodimer is expressed. Pharmacological studies revealed that mGlu2 and mGlu4 are co-expressed in some brain regions: hippocampus (Delgado et al. 2017), striatum (cortical synapses) (Yin et al. 2014).

The challenge for discovering the physiological role of the mGlu2-4 heterodimer is to develop tools that are specific for the heterodimer and not for mGlu2 or mGlu4 homodimers. These tools could be used to localize heterodimers in brain regions. After localization, these receptors could be controlled in the brain regions and animal studies could give insights in effects.

# 7 OBJECTIVES

The past chapters have described the history of the discovery of membrane receptors, showing that perspectives on drug-receptor and receptor-receptor interactions are changing continuously. The work presented in this thesis focuses on two well-known dimeric receptors: one is very well-studied receptor and a proven druggable target (i.e. the EGF receptor) and one is a receptor that has been extensively researched (i.e. mGlu4 receptor), but it has never led to marketed drugs. By studying the conformational dynamics and pharmacology of these receptors, the role of dimerization is investigated. Two major research themes for specific dimeric membrane receptors are addressed in this thesis: 1) what is the link between drug action and dimerization of the EGF receptor and 2) how to selectively control the activity of a homodimeric mGlu4 receptor versus that of a heterodimeric mGlu2-4 receptor.

To reach these objectives, (innovative) techniques measuring aspects of receptor activation are necessary. Therefore, we utilized/developed measuring systems, so-called biosensors, to evaluate these processes. Our biosensors are compatible with the use of homogenous time-resolved fluorescence (HTRF®), a highly sensitive technique based on Förster resonance energy transfer (FRET) as discussed in '*Chapter 8: Materials and Methods'*. For the EGF receptor, we made use of biosensors that are capable of measuring receptor subunit association based on FRET. For the mGlu4 receptor we developed a nanobody to control activity of the mGlu4 receptor and used FRET techniques for a characterization of its effect.

## 7.1 THE LINK BETWEEN DRUG ACTION AND DIMERIZATION OF THE EGF RECEPTOR

In the first research chapter, the objective is to describe the link between TK-inhibitor induced dimerization and drug action on the EGF receptor. As mentioned, TK inhibitors induce a dimeric TK domain conformation, of which its physiological relevance remains unclear. Firstly, this study evaluates for multiple TK inhibitors if they induce dimer formation. Secondly, FRET-techniques are used to describe the conformational dynamics of the full-length EGF receptor during activation and how TK inhibitors interfere in this process. Thirdly, TK inhibitors are pharmacologically characterized in order to determine a possible link between dimerization of the EGF receptor and drug action. This study provides important information that could be considered for future drug research, as it reveals that the dimeric TK domains that are induced by some TK inhibitors may have a physiological relevance.

## 7.2 SELECTIVE CONTROL OF A HOMODIMERIC MGLU4 RECEPTOR VERSUS HETERODIMERIC MGLU2-4.

In the second research chapter, the objective is to selectively control homodimeric mGlu4 and heterodimeric mGlu2-4. Primarily, an innovative pharmacological tool, a nanobody, is developed and characterized. The nanobody is a selective agonist for the human mGlu4 receptor. Its mode of binding and mechanism of action are explained with both biochemical approaches as molecular dynamics studies. Indeed, its mode of action reveals a new way to activate a class C GPCR. In addition, we reveal that DN45 has a distinct pharmacological profile for mGlu2-4 heterodimers.

To summarize, these studies highlight the importance of asymmetry in the activation mechanism of dimeric transmembrane receptors. On the one hand, we show that TK inhibitors differentially regulate the EGF receptor depending on their capability of inducing asymmetric inactive dimers. On the other hand, we develop a pharmacological tool that can be used to control activity of mGlu4 homo- and heterodimers differently.

# 8 MATERIALS AND METHODS

## 8.1 FÖRSTER RESONANCE ENERGY TRANSFER

The main technique that has been used in this thesis is Homogenous Time Resolved Fluorescence (HTRF®). HTRF® is based on Förster Resonance Energy Transfer (FRET) and is developed by Cisbio Bioassays. In principle, HTRF® is FRET between lanthanide-complexes and a compatible FRET-acceptor in a homogenous format (i.e. no separation step of bound and unbound fluorescent compounds). This combination results in a technique that is high-throughput screening (HTS) compatible with a low background signal.

FRET is named after German physicist Theodor Förster for his contributions in understanding FRET. In the 1940s, he discovered that upon excitation of a donor fluorophore, it could transfer energy to an acceptor fluorophore with an overlapping absorption spectrum that is in close proximity (i.e. less than 10 nm). The energy transfer between donor and acceptor fluorophore results in a shift of the wavelength of the emitted light, the Stokes' shift (Fig. 29A). The energy transfer depends on the quantum yield of the donor, the relative orientation and distance between the fluorophores. The quantum yield is a ratio between the number of photons emitted and number of photons absorbed by the donor and could be different in different media. The relative orientation between fluorophores is dependent on multiple factors among which the protein-protein interactions, when the fluorophores is inserted in the protein, play an important role. Typically, FRET compatible fluorophore pairs have an energy transfer of 50% between 4 and 6 nm, this distance is called the Förster distance ($R_0$) (Fig. 29B) (Arts, Aper, and Merkx 2017).

There is a variety of different FRET-based techniques, each with its advantages and disadvantages. In the current studies, most of the experimental work was performed with lanthanide-based luminescence resonance energy transfer (LRET), which includes HTRF® and single-molecule FRET (smFRET). Moreover, bioluminescence resonance energy transfer (BRET) was used. BRET is based on the use of fluorescent proteins that are found in sea pansies (Renilla reniformis).

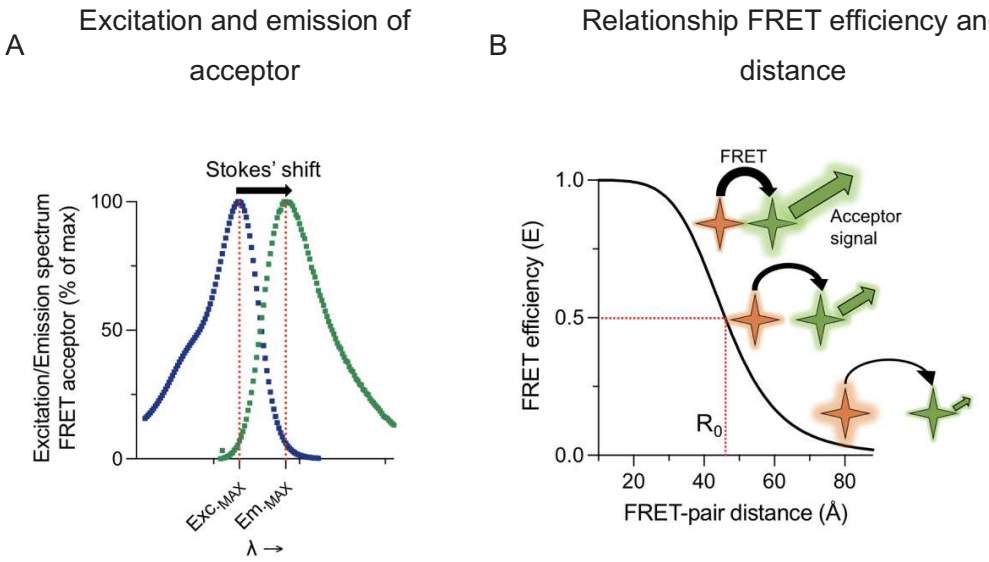


**Figure 29:** FRET principles. A) Excitation and emission of an acceptor. The Stokes' shift, maximal excitation ($Exc._{MAX}$) and maximal emission ($Em._{MAX}$) are highlighted in the graph. B) Relationship between FRET efficiency and FRET-pair distance. The FRET donor is in orange, FRET acceptor in green. FRET is a black arrow and acceptor emission is a green arrow.

### 8.1.1 Lanthanide-based luminescence resonance energy transfer

#### *8.1.1.1 Lanthanide cryptates as FRET donors*

Lanthanides are a group of silvery soft metals that are considered rare-earth elements due to their low abundance on our planet. All 15 lanthanides have fluorescent properties, but only the ions of 4 of them, Samarium, Europium, Terbium (Tb), and Dysprosium are useful for LRET (Soini, Lövgren, and Reimer 1987). By themselves these lanthanides do not have favourable properties as a fluorescent probe, as they have a very low absorption cross section. This means that they do not easily absorb energy from photons and are therefore hard to excite, making them difficult to use in a biological setting. However, the low absorption cross section also leads to an emissive lifetime that is relatively long (i.e. millisecond range) compared to FRET acceptors (i.e. nanosecond range), which is useful for time-resolved measurements (Zwier et al. 2014). To improve the properties of the lanthanides, their ions can be chelated in an organic macrocyclic complex called a cryptate. In the case of Lumi4-Tb, the cryptate is an octadentate cage with a bound $Tb^{3+}$ (Fig. 30) (Xu et al. 2011). The cryptate surrounding the ion has several functions: it works as an antenna to absorb light and transfer the energy to the lanthanide-ion, it changes the emission spectrum of the complex and it protects the ion against quenching by water-molecules (Cottet et al. 2012; Selvin 2002). Lastly, the cage can be modified by addition of a linker in order to allow specific molecule labelling, including proteins (Zwier et al. 2014), which will be discussed later in this chapter.

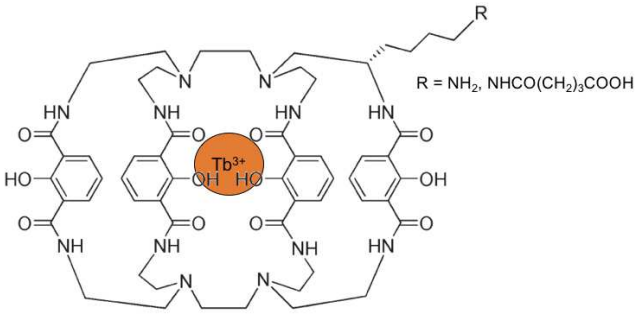


**Figure 30:** Structure of Lumi4-Tb. This figure is copied and adapted from Xu *et al.* (2011) with permission from Springer.

### *8.1.1.2 Spectral and temporal selectivity in LRET*

Some well-known FRET acceptors that are compatible with Lumi4-Tb are d2 or XL665 in the red spectrum or Green (a fluorescein derivative) in the green spectrum (Zwier et al. 2014). As mentioned before, the emission spectrum of Lumi4-Tb should be overlapping with the excitation spectrum of the acceptor (Fig. 31). Lumi4-Tb is excited between 320-380 nm and has multiple emission peaks (i.e. 490, 548, 587 and 621 nm). Red acceptors are excited in the range of 600-650 nm and emit maximally at 670 nm. Green acceptors are excited in the range of 450-495 nm and emit maximally at 520 nm (Cottet et al. 2012). Typically, when measuring the emission of an excited donor or acceptor fluorophore, their emission is measured at the following wavelengths: Lumi4-Tb at 620 nm, red acceptor emission at 665 nm and green acceptor emission at 520 nm. At these wavelengths (λ) there is no overlap from the emission spectra of the other present fluorophores. Through this way, it is possible to precisely determine the emission of excited Lumi4-Tb and emission by the excited acceptor. The observed emission consists of two parts: 1) short-lived fluorescence and 2) FRET-induced fluorescence (Zwier et al. 2014). Short-lived fluorescence is a combination of emission of the acceptor and components in the matrix (e.g. cells, media, plastic) induced by the initial excitation and is considered to be non-specific. Because Lumi4-Tb has a much longer excited-state lifetime, short-lived fluorescence can be excluded by a measurement delay of typically 50 µs after excitation of the donor (i.e. time-resolved measurement). The signal that is present after 50 µs consists of: 1) the FRET-induced fluorescence of the acceptor (i.e. 520 or 665 nm) and 2) the emission of the Lumi4-Tb that is not in FRET (i.e. 620 nm). By exploiting the long emissive lifetime of Lumi4-Tb, background signals are reduced.

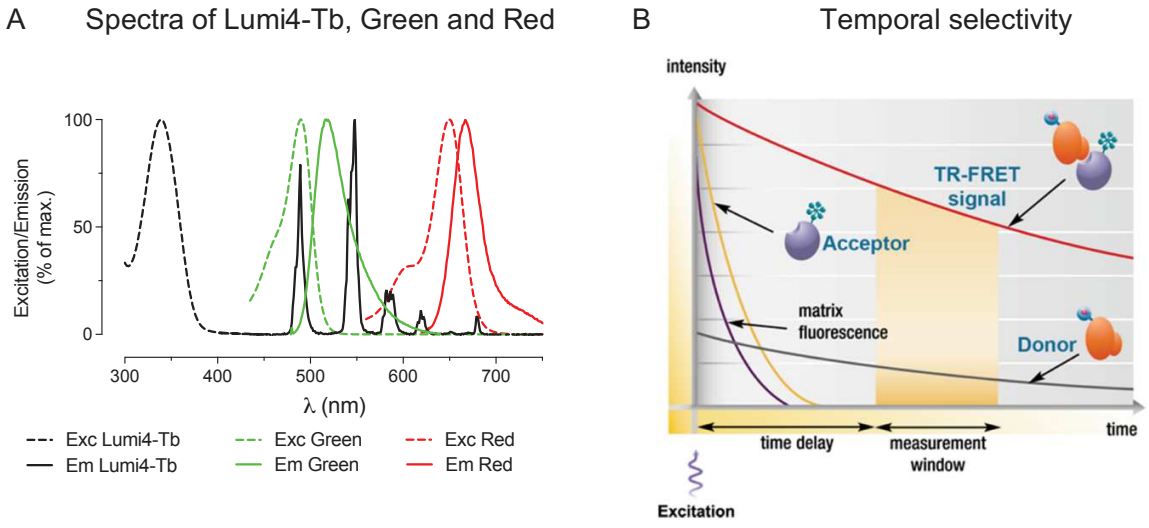


**Figure 31:** Spectral and temporal selectivity in HTRF®. A) Excitation and emission spectra of Lumi4-Tb, Green and Red. Figure is adapted from Cottet *et al.* (2012). B) Emissive signals in a HTRF®-based experiment. After a time-delay, there is no signal from unbound acceptor or matrix components. Figure is copied from Zwier *et al.* (2014) with permission from Springer.

*8.1.1.3 Spatial selectivity by specific protein labelling*

One approach to gain spatial selectivity is by covalently linking the fluorophore to the protein of interest (POI) (Fig. 32). This approach is possible by modifying the protein of interest by addition of a SNAP-tag, an enzymatic tag derived from $O^6$-guanine nucleotide alkyltransferase that reacts with guanine (Keppler et al. 2003). Since, the reagents are not cell permeable, only protein expressed on the cell surface is labelled (Maurel et al. 2008). In our studies, we make use of $O^6$-benzylguanine (BG or SNAP) linked to Lumi4-Tb with a flexible linker. After labelling, the benzyl-group and fluorophore are covalently linked to the SNAP-tag (Maurel et al. 2008). One variation to the SNAP-tag is the CLIP-tag. The principle for the two tags is the same, except CLIP-tag reacts with $O^6$-benzylcytosine (BC or CLIP) (Gautier et al. 2008). These labelling techniques are widely applicable as was shown by Scholler *et al.*, describing a tool kit for measuring conformational dynamics of mGlu homo- and heterodimers and 9 RTKs[xvi] (Scholler, Moreno-Delgado, et al. 2017).

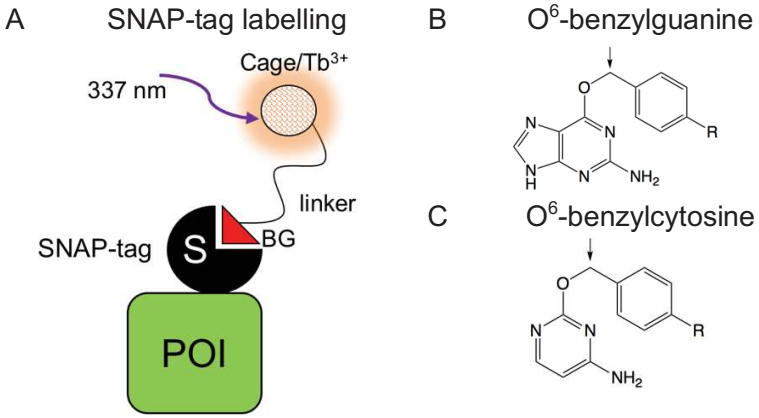


**Figure 32:** Specific labelling of protein of interest. A) Scheme of labelling of the SNAP-tag on a protein of interest (POI). Highlighted in the picture are the SNAP-tag in black, $O^6$-benzylguanine (BG) in red, a linker as a black curved line, the octadentate cage complex with $Tb^{3+}$ in orange and an ultraviolet laser signal in purple. B) Structure of $O^6$-benzylguanine (BG). C) Structure of $O^6$-benzylcytosine (BC). B-C) The arrow points to the atom that is covalently linked to the SNAP-tag or CLIP-tag. R is the linker.

[xvi] EGFR, Insulin receptor, PDGFRA, PDGFRB, FGFR1, VEGFR2, TrkA, TrkB, TrkC

## 8.2 ANALYSIS OF FLUORESCENT SIGNALS

There are many ways to analyse the obtained data and there is much information that can be retrieved. Therefore, I will discuss what kind of data is used to answer specific questions. First of all, for determining expression levels of the labelled protein of interest, we analysed the emission of Lumi4-Tb at 620 nm. Secondly, to determine the amount of FRET, we calculated the HTRF®-ratio with the emission levels of Lumi4-Tb at 620 nm and Green at 520 nm or d2 and XL665 at 665 nm. Thirdly, for deriving receptor dynamics, we looked at the excited-state lifetime of the signal at 520 nm of green acceptor in FRET. Fourthly, we determined rearrangement of proteins by measuring bioluminescence of Renilla-luciferin 2-monooxygenase (RLuc) at 530 nm and Venus (i.e. an improved version of yellow fluorescent protein (Nagai et al. 2002)) at 485 nm.

Typically, for FRET measurements the PHERAstar® FS microplate reader (BMG Labtech) was used. This reader has a UV-pulsed nitrogen laser with a wavelength of 337 nm. The analysis of signals was done by MARS Data Analysis Software (BMG Labtech). For BRET measurements, the Mithras LB 940 multimode plate reader (Berthold technologies) was used. This reader has a xenon flash lamp with a large range of wavelengths.

### 8.2.1 Expression level of labelled protein of interest

Expression levels of the labelled protein were determined by measuring the signal of Lumi4-Tb at 620 nm. Integration of the signal was between 50 and 450 µs after excitation with 30 flashes.

### 8.2.2 HTRF®-ratio

The HTRF®-ratio is a ratio between the signal of the acceptor and the signal of the donor that is calculated to correct for variability in the quality of the sample between experiments (Zwier et al. 2014). The HTRF®-ratio was calculated for measuring dimerization and phosphorylation of the EGF receptor and phosphorylation of ERK1/2. For most assays, the signal is integrated between 50 and 450 µs after excitation of the donor:

$$HTRF® - ratio = \frac{\int_{450}^{50} Signal\ at\ 520\ or\ 665\ nm}{\int_{450}^{50} Signal\ at\ 620\ nm}$$

### 8.2.3 Excited-state emission of the donor in FRET/Sensitized acceptor emission

The excited-state lifetime of Lumi4-Tb changes when in FRET. The more efficient the FRET, the shorter the excited-state lifetime of the Lumi4-Tb signal. The FRET efficiency (E) is inversely proportional to the 6$^{th}$ power of the distance between the FRET donor and acceptor (D):

$$FRET\ Efficiency\ (E) \propto \frac{1}{D^6}$$

Because of the very short lifetime of FRET acceptors, the lifetime of Lumi4-Tb in FRET can be determined by measuring the lifetime of the acceptor signal in a time-resolved way (Fig. 31B). To determine lifetimes of the donor in FRET, the excited-state of the acceptor is measured, the sensitized emission approach (Heyduk and Heyduk 2001). The excited-state signal of the sensitized acceptor is measured during 5 ms and follows a bi-exponential decay. The precise nature of the bi-exponential decay is unknown, but could be due to multiple Lumi4-Tb conformations that induce FRET (Selvin 2002). The excited-state lifetime of the donor at 620 nm ($\tau_D$) and excited-state lifetime of the acceptor at 520 nm ($\tau_{DA}$) are defined as the lifetime of the slow phase. The $\tau_D$ is determined in complete absence of FRET acceptors.

The FRET efficiency can be calculated as follows:

$$E = 1 - \frac{\tau_{DA}}{\tau_D},$$

D can be calculated by determining E following:

$$E = \frac{1}{1+(\frac{D}{R_0})^6},$$

where the $R_0$ of Lumi4-Tb and Green is 46 Å. Therefore, changes of the FRET efficiency (E) correspond to proportional changes of the distance between the FRET donor and acceptor (Doumazane et al. 2011). That information can be used to define receptor conformations as will be discussed in chapter 9.

## 8.3 ADDITIONAL MATERIALS & METHODS

The optimization of an HTRF®-based assay to measure internalization of the EGF receptor is found in annex III, the generation of HEK293 cell stably expressing SNAP-EGFR is found in annex IV. All materials and methods belonging to chapters 9 and 10 can be found in annexes VIII and IX. Additional methods that were performed to generate data for figures in the annexes is explained in the corresponding annex.

# 9 DIMER FORMATION AND CONFORMATION OF EPIDERMAL GROWTH FACTOR RECEPTOR CONTROL ITS ACTIVITY AND INTERNALIZATION

Receptor tyrosine kinases (RTKs) are a class of transmembrane receptors that may have different mechanisms of activation. Some RTKs are pre-formed as a dimeric receptor and are activated through conformational changes induced by an agonist (e.g. insulin receptor). Other RTKs are monomeric and form dimeric receptors upon agonist-binding, resulting in receptor activation (e.g. VEGF receptor).

The first subject of this chapter is the activation process of the EGF receptors. The precise mechanism of EGF receptor activation is unclear and has been described as the example of the insulin receptor (i.e. ligand-induced conformational changes), but also as the example of the vascular endothelial growth factor receptor (i.e. ligand-induced dimerization). By using HTRF® and the sensitized acceptor approach, we demonstrate that it follows mainly ligand-induced dimerization.

A second subject of this chapter is the role of TK inhibitors on the activation process. Some TK inhibitors induce dimer formation, thereby altering the mechanism of activation of the EGF receptor. By measuring TK inhibitor function and internalization, pharmacological profiles are generated. These profiles reveal a link between dimerization and internalization.

Overall, we show that dimerization is necessary, but not sufficient for EGF receptor activation. Moreover, we report that TK domains that are stabilized in an asymmetric conformation may not be internalized.

# Dimer formation and conformation of Epidermal Growth Factor Receptor control its activity and internalization

**Jordi Haubrich[a], Jurriaan M. Zwier[b], Fabienne Charrier-Savournin[b], Laurent Prézeau[a,1], and Jean-Philippe Pin[a,1]**

[a]Institut de Génomique Fonctionnelle, University of Montpellier, CNRS, INSERM, 34094 Montpellier Cedex 5, France
[b]Cisbio Bioassays-PerkinElmer, Parc Marcel Boiteux – BP 84175, 30200 Codolet, France
[1]To whom correspondence may be addressed. Email: laurent.prezeau@igf.cnrs.fr or jean-philippe.pin@igf.cnrs.fr.
Author contributions: J.H., L.P. and J.-P.P. designed research and wrote the paper; F.C.-S. and J.M.Z. designed research; J.H. performed research and analyzed data.
Keywords: Epidermal Growth Factor Receptor | activation | TK inhibitors | internalization | conformation

**The activation process of the EGFR and the action of various subtypes of tyrosine kinase (TK) inhibitors are still a matter of debate despite the importance of this target in the development of anti-cancer drugs. Here, we analyze the effects of agonists and therapeutic TK inhibitors used for the treatment of non-small cell lung cancer (NSCLC) on the EGFR conformation and activity. Using time resolved (TR)-Förster resonance energy transfer (TR-FRET)-based techniques we show that agonists act by promoting EGFR dimer formation, and that all TK inhibitors inhibit EGFR phosphorylation and downstream signaling. Erlotinib-related compounds, unlike lapatinib-related ones, promote EGFR dimers through the intracellular TK domains, independently of the conformation of the extracellular domain. Surprisingly, TK inhibitors do not inhibit EGF-induced EGFR internalization, only TK inhibitors promoting dimers could slow down this process. These results reveal that the conformation of the intracellular TK dimer, rather than EGFR phosphorylation is critical for EGFR internalization. These results show clear differences in the mode of action of TK inhibitors on the EGFR.**

In the group of receptor tyrosine kinases (RTKs) the Epidermal Growth Factor Receptor (EGFR) is one of the most-studied receptors. The EGFR is expressed in many tissues and plays a vital role in biological processes as apoptosis, cell growth and differentiation, migration and more (1).

The EGFR has seven endogenous agonists, that are all small proteins (2). Upon binding to the extracellular domain, EGFR activators promote allosteric processes between two assembled EGFRs leading to the association of the intracellular tyrosine kinase (TK) domains, and the activation of one of them. Whether this process results from ligand-induced dimerization (3) or from conformational changes within pre-formed dimers (4) is still a matter of debate. EGFR activity is exclusively occurring when the two TK domains adopt an asymmetric conformation, i.e. there is an enzymatically inactive (Activator) and active (Receiver) domain (5). The Receiver domain initiates ATP-dependent phosphorylation of tyrosine residues on the intracellular domain of the Activator. Phosphorylation of its carboxy-tail residues leads to downstream signaling events such as activation of ERK1/2 and PI3K/AKT/mTOR (6). Conversely, receptor trafficking may be both dependent (7) as independent of phosphorylation of carboxy-tail residues (8, 9).

*EGFR* gene mutations or amplification are found in many cancers, among which non-small cell lung cancer (NSCLC) has one of the lowest survival rates (10). Depending on histological and genotypical analysis of NSCLC, different and combinatorial treatment strategies are being used. The treatment strategy for patients with sensitizing EGFR mutations like a substitution of leucine for arginine at position 858 (L858R) involves ATP-competitive reversible first-generation TK inhibitors (e.g. erlotinib) (11). Resistance mechanisms occurring after treatment with first-generation TK inhibitors are common. In around 50% of these patients the apparition of a secondary mutation in the *EGFR* gene is prevalent (e.g. the substitution of a threonine for a methionine at position 790 (T790M)) (12). This mutation desensitizes first-generation TK inhibitors and induces higher enzymatic activity of the EGFR (13). Treatment options for L858R and T790M double-mutated EGFR ($EGFR_{NSCLC}$) involves irreversible second and third-generation TK inhibitors (i.e. dacomitinib and osimertinib, respectively) (14, 15).

We have used techniques based on time-resolved (TR) Förster resonance energy transfer (TR-FRET) to analyze the mode of action of EGFR agonists and various types of TK inhibitors. We provide clear evidence that EGFR agonists promote dimer formation through direct contact between the extracellular domains, resulting in receptor phosphorylation and internalization. We show that first-generation TK inhibitors and dacomitinib induce EGFR dimer formation, but not for the mutated EGFR ($EGFR_{NSCLC}$), through a direct association of the TK domains, independently of the conformation of the extracellular domain. Surprisingly, TK inhibitors do not inhibit

EGF-induced EGFR internalization, demonstrating EGFR phosphorylation is not required for this process. Importantly, TK inhibitors inducing dimers slow down EGF-induced internalization of the EGFR, revealing a link between TK inhibitor-induced EGFR conformation and EGFR trafficking. These data reveal that differential effects induced by TK inhibitors can result from different conformation of the EGFR dimers.

## Results

### Intersubunit FRET induced by agonists and group I TK inhibitors through the TK domain.

Intersubunit FRET was measured after randomly labelling the SNAP-tags with SNAP-Lumi4-Tb (donor) and SNAP-Green (acceptor) (Fig. 1A) (16) in monoclonal stable cell lines expressing SNAP-EGFR or SNAP-EGFR$_{NSCLC}$. Cells were stimulated with agonist or TK inhibitors for 30 minutes. Both agonists, dacomitinib, erlotinib and PD153035 (group I TK inhibitors) induced intersubunit FRET (Fig. 1B, C and Suppl. Fig. 2 and 3A). Since FRET efficiency is related to distance of the FRET-pair, total FRET levels may change depending on conformational changes and on the number of molecules in FRET. Group I TK inhibitors induced a lower amount of TR-FRET signal than agonists, raising the question whether this is due to a different conformation or due to a lower number of induced dimers. In contrast, the other TK inhibitors, GW583340 and lapatinib (group II inhibitors), osimertinib, cetuximab (i.e. an inhibitory antibody) and AG1024 (i.e. an insulin-like growth factor receptor inhibitor) did not induce intersubunit FRET (Fig. 1C and Suppl. Fig. 2 and 3A).

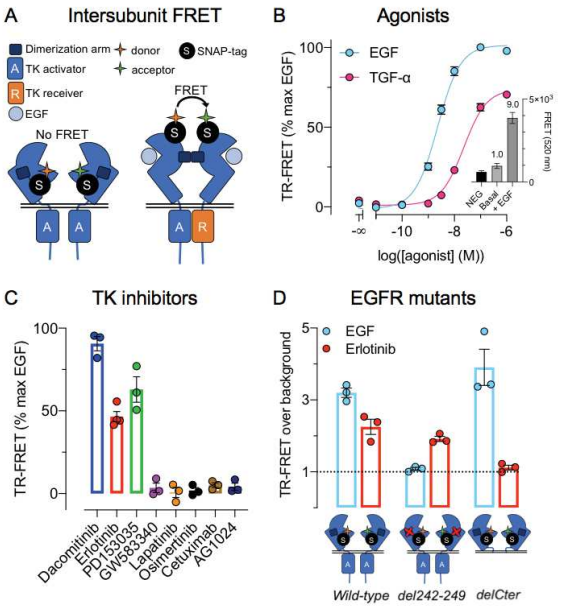


**Fig. 1.** Intersubunit FRET is induced by group I TK inhibitors through the TK domain. *(A)* Cartoon representing a TR-FRET-based EGFR intersubunit FRET assay. EGFR subunits were randomly labelled with 125 nM acceptor and 100 nM donor. *(B)* Intersubunit FRET of EGFR in presence of EGF (blue) or TGF-α (pink). Representative raw FRET values and fold increase of specific FRET are shown in a subgraph. *(C)* EGFR intersubunit FRET induced by saturating concentration of TK inhibitors. *(D)* EGFR intersubunit FRET of *wild-type* EGFR or EGFR mutants induced by 100 nM EGF (blue) or 100 µM erlotinib (red). Data in *B-D* are mean ± SEM of three or more individual experiments.

To determine whether the group I TK inhibitor-induced FRET between two EGFRs also occurs independently of the extracellular domain, we measured intersubunit FRET of an EGFR mutant with a disrupted dimerization arm (EGFR$_{del242-249}$) and an EGFR mutant with a deletion of its intracellular domain (EGFR$_{delCter}$) (17). When stimulated with EGF, no intersubunit FRET was observed for SNAP-EGFR$_{del242-249}$ (Fig. 1D and Suppl. Fig. S3C). However, erlotinib induced intersubunit FRET for this mutant, demonstrating it is independent of the dimerization arm. On the contrary, EGF and not erlotinib induced intersubunit FRET on SNAP-EGFR$_{delCter}$ (Fig. 1D and Suppl. Fig. S3D). This showed that erlotinib induces intersubunit FRET of the EGFR through the TK domain independently of the dimerization arm located in the extracellular domain. This was confirmed for the full-length EGFR, when exposure of the dimerization arm was prevented by cetuximab (Fig. 2A).

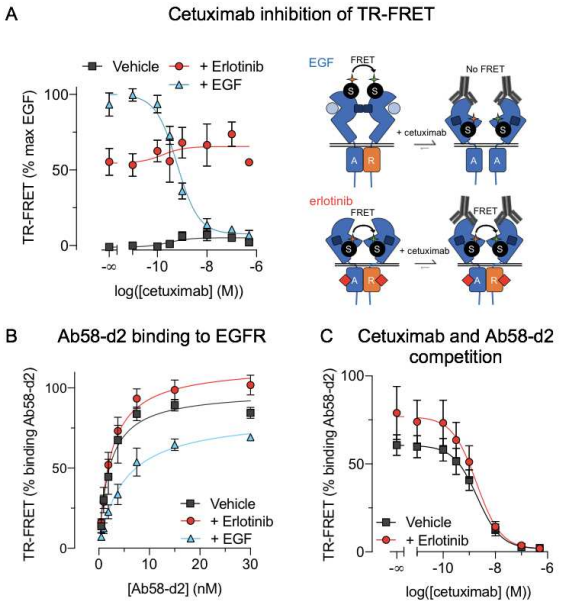


**Fig. 2.** Erlotinib-induced dimers are not inhibited by cetuximab. *(A)* EGFR intersubunit FRET in presence of cetuximab with vehicle (gray), EGF (blue), or erlotinib (red) and a schematic interpretation of the data. *(B)* Binding of Ab58-d2 to SNAP-EGFR that is labelled with 125 nM donor and pre-incubated with saturating concentrations of erlotinib (red) or EGF (blue) or vehicle (gray). *(C)* Binding of Ab58-d2 in presence of cetuximab with (red) or without (gray) erlotinib. Data in *A-C* are mean ± SEM of three or more individual experiments.

Moreover, the TR-FRET did not change in the presence of cetuximab, suggesting that an increase in intersubunit FRET is a measure for dimerization rather than conformational changes of the extracellular domain. The absence of effect of cetuximab is not due to a specific conformation stabilized by erlotinib that could prevent cetuximab binding. Indeed, cetuximab could still inhibit binding of antibody 58 labelled with d2 (Ab58-d2) in the presence of erlotinib (Fig. 2B, C).

**Group I TK inhibitors induce less dimers than agonists**

Whether EGF acts by allowing dimer formation, or through conformational changes within pre-formed dimers is still a matter of debate (4). The absence of effect of cetuximab, or of the deletion of the dimerization arm on TK inhibitor-induced intersubunit FRET is more consistent with ligand-induced dimerization. To further study this possibility, we examined why TK inhibitors induced a lower maximal FRET signal than agonists. This can be due either to a different conformation of the EGFR dimer, which would be consistent with pre-formed dimers, or to a lower proportion of receptors in FRET than with agonist. To determine this, we analysed the excited-state lifetime of sensitized acceptor (i.e. the donor in FRET) emission ($\tau_{DA}$) as an indication of the conformational state of the receptor, as $\tau_{DA}$ is related to the distance between the fluorophores.

As a control for this approach, we co-expressed SNAP-metabotropic glutamate (mGlu) 4 receptor and CLIP-mGlu2 receptor known to form a constitutive heterodimer, both subunits being linked by a disulphide bond (18). In that case, a change in FRET cannot be due to a different proportion of dimers, and then only rely on a change in distance due to conformational changes within these constitutive dimers. The C termini of the subunits were modified by addition of the endoplasmic reticulum retention sequences of the $GABA_{B2}$ (C2) and $GABA_{B1}$ (C1) to the respective receptors, so that only heterodimeric receptors were expressed at the cell surface (Suppl. Fig. S4A) (19). We labelled each mGlu2-4 heterodimer with SNAP-Lumi4-Tb (donor) and CLIP-Green (acceptor), and measured the FRET signal.

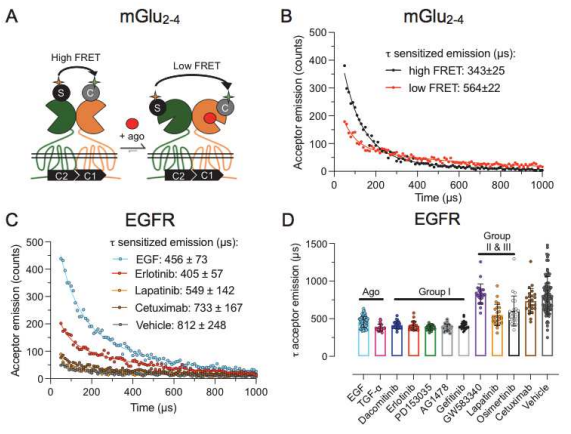


**Fig. 3.** Sensitized emission reveals that higher FRET levels correspond to more receptors in FRET rather than closer proximity of FRET-pair. *(A)* Intersubunit FRET between an mGlu2 (orange) and mGlu4 (green) constitutive dimer labelled with acceptor and donor. *(B)* Representative data of excited-state sensitized acceptor emission of mGlu2-4 intersubunit FRET assay in presence of vehicle (black) and 100 µM LY379268 (red). *(C)* Representative data of excited-state sensitized acceptor emission of EGFR intersubunit FRET assay in presence of 100 nM EGF (blue), 10 µM erlotinib (red), 10 µM lapatinib (orange), 100 nM cetuximab (brown) and vehicle (gray). *(D)* Summary of excited-state sensitized acceptor emission of EGFR intersubunit FRET assay. Data in *D* are individual values ± SD of at least 23 data points obtained in at least three individual experiments. Statistical test in *C* is one-way ANOVA with Dunnett's multiple comparison (Suppl. Table S3).

In principle, the excited-state lifetime of the FRET donor emission ($\tau_D$) is in the millisecond range, and decreases when the donor's excited state is subject to other deactivation pathways such as FRET. As the $\tau_{DA}$ is proportional to the distance between a FRET donor and acceptor, distinct FRET donor-acceptor distances can be determined. The $\tau_{DA}$ is measured in a time-resolved manner to discriminate between non-specific and specific signal (20).

In the basal mGlu2-4 condition, $\tau_{DA}$ was 343 ± 25 µs, corresponding to a high FRET conformation. The $\tau_{DA}$ was largely increased to 564 ± 22 µs in the presence of the mGlu2 agonist LY379268, indicating a low FRET conformation (Fig. 3A and B) (17, 21). These data confirm that a conformational change within constitutive dimers can be detected by measuring the $\tau_{DA}$ values.

For the SNAP-EGFR, the $\tau_{DA}$ measured in the presence of agonists or group I TK inhibitors were not significantly different (Fig. 3C and D, Suppl. Table S3), despite differences in TR-FRET intensity (Suppl. Fig. 4B). This suggests that the larger TR-FRET level measured with agonists is due to a higher proportion of receptors in FRET, rather than to a distinct donor-acceptor distance. Such data are then consistent with TK inhibitors stabilizing less EGFR dimers than agonists.

**Inhibition of EGF-induced phosphorylation of EGFR and ERK1/2 by TK inhibitors**

We then evaluated the efficacy of the inhibitors for EGF-induced phosphorylation of either EGFR or ERK1/2. Phosphorylation of tyrosine residue 1068 of the EGFR (Y1068) and of threonine residue 202 and tyrosine residue 204 of ERK1/2, as detected by the HTRF® signals in an antibody-based sandwich assay (Fig. 4A and Suppl. Fig. 5), are inhibited efficiently by group I, group II TK inhibitors and cetuximab and less efficiently by group III TK inhibitor osimertinib. Conversely, irrelevant TK inhibitor AG1024 did not inhibit phosphorylation of EGFR or ERK1/2 (Fig. 4B, C and Suppl. Fig. 5B, D).

**TK inhibitors stabilizing dimers slow down EGF-induced EGFR internalization**

Then, we setup an internalization assay for the EGFR based on diffusion-enhanced resonance energy transfer (DERET) (22). In principle, SNAP-EGFR is labelled with Lumi4-Tb and an excess of fluorescein is added to each well, thereby generating DERET and quenching Lumi4-Tb emission. Upon internalization of the EGFR, the Lumi4-Tb signal is recovered (Fig. 4D) allowing the detection of EGFR internalization in living cells over time.

We observed a basal internalization in the absence of agonist, but EGF largely increases EGFR internalization, that reaches a plateau after 39 min, followed by a decline, suggesting receptor recycling to the cell surface. Cetuximab fully inhibited EGF-

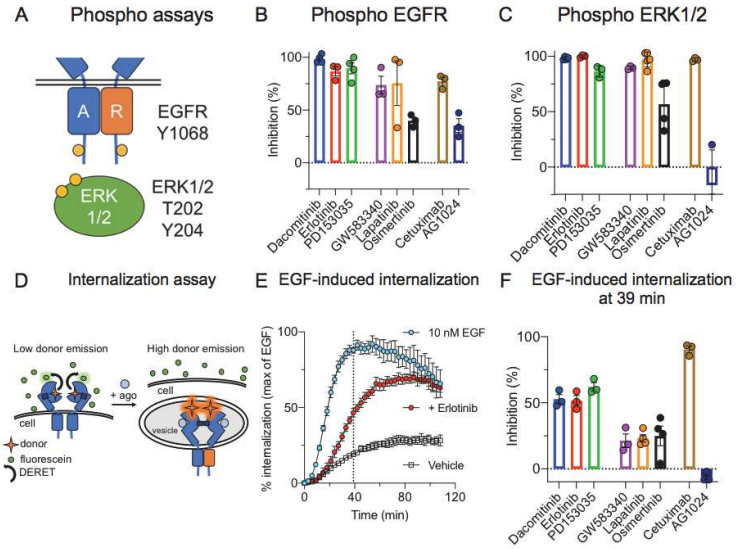


**Fig. 4.** Phosphorylation of EGFR and ERK1/2, and internalization of EGFR. *(A)* Scheme of antibody-based sandwich assays to measure EGFR and ERK1/2 phosphorylation. *(B)* Inhibition of EGF-induced (10 nM) EGFR phosphorylation by 1 μM of dacomitinib, erlotinib, PD153035, lapatinib, osimertinib and AG1024, 0.3 μM GW583340 or 100 nm cetuximab. Inhibitors were pre-incubated for 30 minutes and phosphorylation was measured 30 minutes after stimulation with EGF. *(C)* Inhibition of EGF-induced (10 nM) ERK1/2 phosphorylation by 1 μM of dacomitinib, erlotinib, PD153035, lapatinib, osimertinib and AG1024, 0.3 μM GW583340 or 100 nm cetuximab. Inhibitors were pre-incubated for 30 minutes and phosphorylation was measured 5 minutes after stimulation with EGF. *(D)* Scheme of DERET-based EGFR internalization assay. *(E)* Representative data for EGFR internalization assay in presence of 10 nM EGF (blue), EGF and 1 μM erlotinib (red) or vehicle (gray). *(F)* EGF-induced EGFR internalization in presence of 1 μM of dacomitinib, erlotinib, PD153035, lapatinib, osimertinib and AG1024, 0.3 μM GW583340 or 100 nm cetuximab. Inhibitors were pre-incubated for 2 hours and EGF-internalization was measured after 39 minutes. Data in *B-C* and *F* are mean ± SEM of at least three individual experiments. Data in *E* is represented as mean ± SD.

induced internalization but not the basal internalization (Suppl. Fig. 7). Surprisingly, TK inhibitors did not inhibit EGFR internalization (Fig. 4F and Suppl. Fig. 7) as group I TK inhibitors only slowed down EGF-induced EGFR internalization (Fig. 4E), whereas others had no effect (Suppl. Fig. 7).

Despite not inhibiting internalization, it is clear that group I TK inhibitors were more efficacious in slowing down EGFR internalization than the group II and III TK inhibitors and irrelevant TK inhibitor AG1024 (Fig. 4F and Suppl. Fig. 7). We compared internalization of EGFR with fluorescence microscopy, showing comparable results (Suppl. Fig. 6).

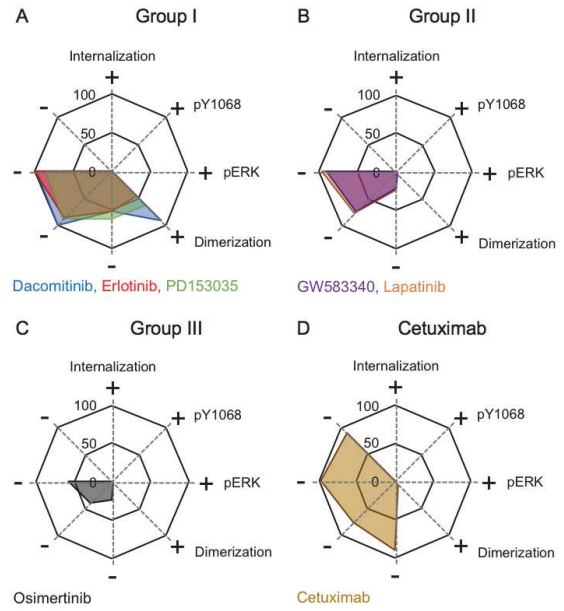


**Fig. 5.** Pharmacological profile of TK inhibitors. *(A)* Group I TK inhibitors dacomitinib (blue), erlotinib (red), PD153035 (green). *(B)* Group II TK inhibitors GW583340 (purple) and lapatinib (orange). *(C)* Group III TK inhibitor osimertinib (gray). *(D)* Cetuximab (brown). All data are from figures 1-4.

The combined data of the 4 assays revealed a different pharmacological profile of each group of compounds for the wild-type EGFR as represented in Figure 5 (Suppl. Fig. S8). Moreover, bias plots for the agonists demonstrated that EGF and TGF-α are more potently inducing internalization and phosphorylation of ERK1/2 (Suppl. Fig. S9). Among the TK inhibitors, only PD153035 more potently inhibited phosphorylation of Y1068 than ERK1/2 (Suppl. Fig. S10).

### NSCLC-mutated EGFR is insensitive to TK inhibitor-induced dimerization

$EGFR_{NSCLC}$ has an increased activity within the asymmetric dimer (23) and it was suggested that the presence of $EGFR_{NSCLC}$ could increase dimer formation (24). To investigate if $EGFR_{NSCLC}$ has an increased propensity to induce dimer formation, we developed an intersubunit FRET assay specifically detecting heterodimers of *wild-type* EGFR and $EGFR_{NSCLC}$ or homodimers of $EGFR_{NSCLC}$ (Fig. 6A). For both the heterodimer as the homodimers, EGF induced dimer formation with a similar potency as for *wild-type* EGFR (Fig. 6B).

As the $EGFR_{NSCLC}$ is resistant to erlotinib-like TK inhibitors due to the T790M substitution in the ATP binding pocket (13), we were curious whether erlotinib could induce dimer formation in presence of this mutant. Interestingly, erlotinib could not induce formation of dimers containing $EGFR_{NSCLC}$, suggesting that both subunits of an asymmetric TK domain need to be bound by TK inhibitors to induce TK domain dimer formation (Fig. 6C and Suppl. Fig. S11).

## Discussion

Although of clinical importance, several aspects of EGFR activation and the mode of action of various TK inhibitors remain unclear. This study brings clear evidence for the agonist-induced dimer formation model of EGFR activation. It also reveals that formation of dimers can be induced by some TK inhibitors through interaction of the TK domains,

resulting from a specific conformation of the TK dimer. Eventually, our data show that EGF-induced internalization is mainly driven by a specific conformation of the EGFR dimer, and not by the phosphorylation of the receptor, allowing some, but not all TK inhibitors to slow down this process.

Despite years of research on EGFR two models of receptor activation were still discussed (4). One model proposes that agonists like EGF act by promoting dimer formation (25), while the other proposes that agonists stabilize a specific conformation of a pre-formed EGFR dimer (26). Our data strongly support the first model. Indeed, through FRET measurements between N-terminal tags, with cell surface receptors labelled exclusively, we detected a very low FRET signal under basal condition, in the cell line stably expressing SNAP-EGFR (Suppl. Fig. S1). This signal is largely increased (9-fold) in the presence of agonist (Fig. 1B). The low FRET under basal condition is unlikely due to pre-formed dimers with a conformation leading to a large distance between the N-termini carrying the SNAP-tags, for two main reasons. First, although a very low FRET was measured under the basal condition, the estimated $\tau_{DA}$ is only twice of that measured with the active dimer (Fig. 3C), consistent with the low FRET resulting mainly from a very low number of dimers. Such finding is also consistent with the distances between the N-termini of the proposed inactive and active dimers (24). Second, when dimers were stabilized through their TK domains using some TK inhibitors, the extracellular domains do not appear to interact via the dimerization arm, and are then likely in an inactive conformation possibly similar to that proposed by others for the pre-formed dimers (24). If so, such pre-formed dimers should generate a FRET signal with a $\tau_{DA}$ similar to that obtained with the EGF bound EGFR dimers. Accordingly, the FRET signal measured under our basal condition should be related to the proportion of pre-formed inactive dimers. Our data indicate they represent a very small proportion of the EGFR subunits at the cell surface, either because of a low proportion of pre-formed dimers, or because of random collisions of EGFR monomers.

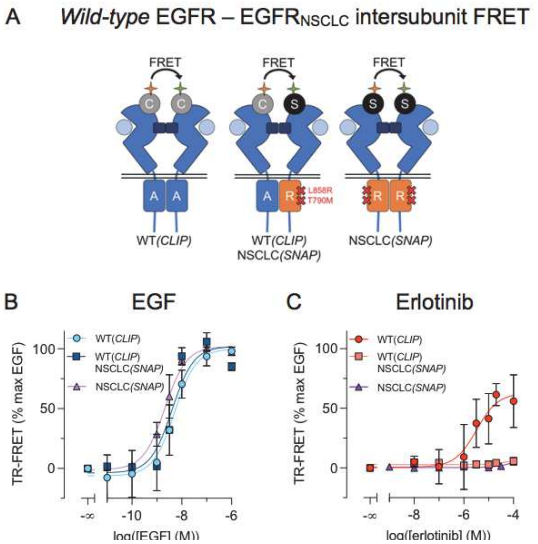


**Fig. 6.** TK domain-induced dimers need binding of two TK inhibitors. *(A)* Scheme of assays to measure intersubunit FRET of the *wild-type* CLIP-EGFR homodimer, CLIP-EGFR + SNAP-EGFR$_{NSCLC}$ heterodimer and SNAP-EGFR homodimer. *(B)* EGF-induced intersubunit FRET. *(C)* Erlotinib-induced intersubunit FRET. Data in *B-C* are represented as mean ± SEM of at least three individual experiments.

Consistent with previous studies (27–29), we found that some TK inhibitors can also induce dimer formation. Because the dimerization arm is not necessary, it suggests a main role of the TK domain interaction in this process. It is interesting to note that TK inhibitors inducing dimer formation can bind either to the Activator-like or the Receiver like TK domain (30) (Fig 7), thereby allowing the formation of an asymmetric TK domain dimer, as expected in the active form of the EGFR dimer (31). The proportion of the Activator and Receiver forms may then dictate the number of possible dimers – i.e. the higher the number of one species (i.e. Activator or Receiver), the lower the number of possible Activator-Receiver dimers. This explains the TK inhibitors not being able to promote the formation of the same amounts of dimers as EGF (Suppl. Fig. S4). In contrast, TK inhibitors stabilizing a specific conformation of the TK domain do not favor dimer formation, revealing the critical importance of the effect of TK inhibitors on the TK domain conformation.

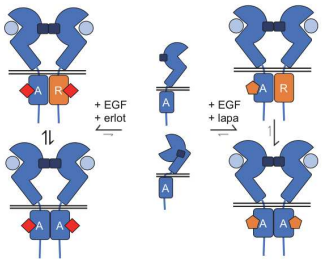


**Fig. 7.** Schematic hypothesis of stabilized dimers by group I and group II TK inhibitors in presence of EGF. Group I TK inhibitors stabilize both Activator and Receiver conformations and group II TK inhibitors only Activator conformations of the TK domain. In presence of erlotinib there are more inactive Activator-Receiver dimers than in presence of lapatinib.

As already reported (32), we confirmed that EGFR can rapidly engage into internalization upon agonist activation, though the number of internalized receptors rapidly declined after a peak, possibly due to receptor recycling to the cell surface. However, we show here that this process does not require receptor phosphorylation, as it is not prevented by any of the TK inhibitors tested despite their full inhibitory effect on agonist-induced receptor phosphorylation. As such, the internalization process may likely be the result of a specific conformation of the dimer. This is well supported by the differential effect of TK inhibitors, as those promoting dimer formation, can slow down this process, while those without effect on EGFR dimerization have no effect on internalization. However, it is surprising to see that TK inhibitors promoting EGFR dimer formation, do not promote internalization.

To explain these apparently contradictory results, one should consider the possible conformation

of the intracellular part of the receptor. Indeed, TK inhibitors that stabilize the Activator state of the TK domain, such as lapatinib, do not promote dimer formation, and do not affect EGF-induced internalization (Fig 7). This suggests that a symmetric EGFR dimer in which both TK domains are in the inactive Activator state, are perfectly prone to internalization after direct association of the extracellular domains. In contrast, TK inhibitors like erlotinib that can stabilize either the Activator or the Receiver state (Fig 7), promote dimer formation likely through a stable asymmetric TK domain dimer composed of an Activator and Receiver TK domain. They do not induce receptor internalization, while they only slow down EGF-induced internalization. As such, one is tempted to propose that the asymmetric Activator-Receiver dimer is not prone to internalization. Such hypothesis explains our results, but would certainly need further support to be fully validated.

Previously, agonist-induced conformational models of the EGFR (33, 34) and the role of agonist binding kinetics in ligand bias have been described (35, 36). For TK inhibitors such studies are less well known, whereas it could improve understanding of their mode of action. Generation of pharmacological profiles and bias plots has recently been proposed as mode to improve EGFR drug design (37). Techniques for determining pharmacological profiles or ligand bias are more common in the research field of G protein-coupled receptors (GPCRs) and contributing to GPCRs being the most targeted family of receptors by drugs on the market (38, 39). In this study, such techniques have been adapted for a study on the EGFR.

Efforts to expose functional selectivity induced by EGFR ligands indicated that agonists have different signalling kinetics by stabilizing different conformations of the extracellular domain (34). Bias plots for agonists EGF and TGF-α reveal that they are more potent for phosphorylation of ERK and internalization than dimerization and phosphorylation of Y1068 (Suppl. Fig. S9). Moreover, we found that most TK inhibitors inhibit phosphorylation of Y1068 and ERK with similar potency, except for PD153035, which more potently inhibits phosphorylation of Y1068 (Suppl. Fig. S10C).

Some TK inhibitors may impact EGF binding through allosteric modulation of the EGFR conformation (33, 40). We show that TK inhibitors stabilize distinct dimers, resulting in altered EGFR trafficking. Previous reports linked dimerization to improved cellular survival (29) and decreased efficacy for some TK inhibitors (41). Moreover, disruption of dimerization could be an antitumoral mechanism as well (42), confirming its significance. The role of internalization in tumour survival is not fully clear, nonetheless it has been suggested that *wild-type* NSCLC patients (i.e. no resistance mutations) could benefit from blocking clathrin-mediated endocytosis of EGFR (43, 44). This implies that ligands that reduce EGFR internalization (i.e. dacomitinib, erlotinib, PD153035) could induce positive outcomes for *wild-type* EGFR in NSCLC patients.

To our best knowledge there are no reports of TK inhibitors inducing dimerization of the $EGFR_{NSCLC}$ or heterodimers of *wild-type* EGFR and $EGFR_{NSCLC}$. In our model we do not observe pre-formed homo- and heterodimers containing $EGFR_{NSCLC}$, as the dimers are inducible by EGF and TGF-α. The potencies for dimerization are not significantly different from *wild-type* EGFR (Suppl. Table S2). None of the tested TK inhibitors induces dimerization, suggesting there is a direct or indirect loss of potency for the heterodimer due to altered binding (45, 46) or increased affinity for ATP (47). In tumor cells of NSCLC patients, different populations of EGFR heterodimers could exist, among them the *wild-type* EGFR-$EGFR_{NSCLC}$ heterodimer (13) and EGFR-ErbB2 heterodimers (48). Investigations on the effect of drugs on these heterodimeric receptors, could help improving treatment strategy as they may function as additional drug targets. Another approach could be the use of allosteric modulators to decrease off-target effects (15). The use of allosteric compounds like EAI045 for treating NSCLC has recently been reviewed (10).

Overall, this study reveals the importance of the conformational state of the TK domains within the EGFR dimer in signalling and trafficking. As TK inhibitors have various effect on such conformations, this may explain their biased effects on dimerization and internalization, properties that may have some importance in the cellular physiology of EGFRs.

## Materials and methods

Reagents and the protocols for cell culture, cell preparation for experiments, generation of SNAP-$EGFR_{NSCLC}$ and CLIP-EGFR plasmids, lipofectamine transfection for experiments, generation of HEK293 cells stably expressing SNAP-EGFR and SNAP-$EGFR_{NSCLC}$, intersubunit FRET, binding and displacement of Ab58-d2, ERK1/2 phosphorylation, phosphorylation of tyrosine residue 1068 of the EGFR (Y1068), internalization, fluorescence microscopy and data analysis can be found in the supplementary information.

Monoclonal stable cell lines stably expressing SNAP-EGFR or SNAP-$EGFR_{NSCLC}$ were generated by lipofectamine transfection. Positive cells were selected by G418 and single cells were sorted with fluorescence-activated cell sorting. An estimated 256,000 individual SNAP-EGFRs (i.e. 4-fold lower than A341 squamous carcinoma) are present on the cell surface and expression levels were stable over time (Suppl. Fig. S1).

**Excited state-lifetime of sensitized acceptor emission to determine receptor conformations**

At 24 hours after lipofectamine transfection (for SNAP-mGlu4-C2-KKXX and CLIP-mGlu2-C1-KKXX constructs) or transfer of cells stably expressing SNAP-EGFR into a 96-wells plate, medium was

replaced by ice-cold DMEM containing SNAP-Lumi4-Tb (100 nM) and SNAP-Green (125 nM) for SNAP-labelling and CLIP-Lumi4-Tb (1 µM) and CLIP-Green (1 µM) for CLIP-labelling. Cells were incubated for 90 minutes at 4 °C and carefully washed four times with ice-cold Tag-Lite buffer. LY379268 (100 µM), EGF (100 nM), TGF-α (100 nM), dacomitinib (10 µM), erlotinib (10 µM), PD153035 (10 µM), AG1478 (10 µM), GW583340 (5 µM), lapatinib (10 µM), osimertinib (10 µM), cetuximab (10 nM) or vehicle was incubated in ice-cold Tag-Lite buffer for 30 minutes at 4 °C. Luminescence decay at 520 nm was measured after 150 flashes/well with the UV-pulsed nitrogen laser (337 nm) of the PHERAstar FS microplate reader. Decay was measured from 50 to 5000 µs and was fitted using the biexponential decay function in GraphPad Prism software (version 9.0.1.), which is the preferred model in an extra sum-of-squares F-test compared to a mono-exponential decay function. The excited-state lifetime of the sensitized acceptor emission ($\tau_{DA}$) was calculated with a least-squares fit. The apparent amplitude of slow ($A_s$) and fast ($A_f$) components of the biexponential decay may vary due to adaptation to multiple conformations or interactions with the antenna, increasing the complexity of its decay (49). Typically, the apparent $A_f$ was larger than $A_s$ whereas this value is likely overestimated and should be corrected (20). The true fraction of the slow decay species ($\alpha_{DA}$) is based on the resonance energy transfer rate constant, as described by Heyduk *et al.*(20). After applying this correction, $\alpha_{DA}$ is in the range of 0.75-0.88 for all conditions (Suppl. Table S1).

**ACKNOWLEDGEMENTS.** We thank the ARPEGE platform facilities at the Institut de Génomique Fonctionnelle for all fluorescence-based assays and the MRI platform facilities at the Institut de Génétique Humaine for FACS and microscopy assays. We thank dr. Robert Quast for discussions. J.-P.P. was supported by la Fondation pour la Recherche Médicale (ref. DEQ20170336747), Cisbio Bioassays (EIDOS collaborative team IGF-CISBIO, ref. 039293), the Fond Unique Interministériel of the French government (FUI, Cell2Lead project), the Agence Nationale pour la Recherche (ANR 18-CE11-0004-01) and LabEx MAbImprove (ref. NR-10-LABX-5301). J.-P.P. and L.P. were further supported by the Centre National de la Recherche Scientifique and the Institut National de la Santé et de la Recherche Médicale. J.H. was supported by a fellowship from la Région Occitanie and Cisbio Bioassays (TransACT, ref. 156544) and la Ligue contre le cancer (PhD grant, ref. IP/SC-16487).

1. P. Wee, Z. Wang, Epidermal growth factor receptor cell proliferation signaling pathways. *Cancers (Basel).* **9**, 1–45 (2017).
2. R. C. Harris, E. Chung, R. J. Coffey, EGF receptor ligands. *Exp. Cell Res.* **284**, 2–13 (2003).
3. H. Yamashita, Y. Yano, K. Kawano, K. Matsuzaki, Oligomerization-function relationship of EGFR on living cells detected by the coiled-coil labeling and FRET microscopy. *Biochim. Biophys. Acta - Biomembr.* **1848**, 1359–1366 (2015).
4. E. Purba, E. Saita, I. Maruyama, Activation of the EGF Receptor by Ligand Binding and Oncogenic Mutations: The "Rotation Model." *Cells* **6**, 13 (2017).
5. E. Kovacs, *et al.*, Analysis of the Role of the C-Terminal Tail in the Regulation of the Epidermal Growth Factor Receptor. *Mol. Cell. Biol.* **35**, 3083–3102 (2015).
6. M. C. Mendoza, E. E. Er, J. Blenis, The Ras-ERK and PI3K-mTOR Pathways: Cross-talk and Compensation. *Trends Biochem. Sci.* **36**, 320–328 (2011).
7. F. Huang, D. Kirkpatrick, X. Jiang, S. Gygi, A. Sorkin, Differential regulation of EGF receptor internalization and degradation by multiubiquitination within the kinase domain. *Mol. Cell* **21**, 737–748 (2006).
8. J. Tong, P. Taylor, M. F. Moran, Proteomic Analysis of the Epidermal Growth Factor Receptor (EGFR) Interactome and Post-translational Modifications Associated with Receptor Endocytosis in Response to EGF and Stress. *Mol. {&} Cell. Proteomics* **13**, 1644–1658 (2014).
9. S. Vergarajauregui, A. San Miguel, R. Puertollano, Activation of p38 mitogen-activated protein kinase promotes epidermal growth factor receptor internalization. *Traffic* **7**, 686–698 (2006).
10. S. Maity, K. S. R. Pai, Y. Nayak, Advances in targeting EGFR allosteric site as anti-NSCLC therapy to overcome the drug resistance. *Pharmacol. Reports* **72**, 799–813 (2020).
11. R. Porta, *et al.*, Brain metastases from lung cancer responding to erlotinib: The importance of EGFR mutation. *Eur. Respir. J.* **37**, 624–631 (2011).
12. F. Morgillo, C. M. Della Corte, M. Fasano, F. Ciardiello, Mechanisms of resistance to EGFR-targeted drugs: Lung cancer. *ESMO Open* **1**, 1–9 (2016).
13. M. R. Brewer, *et al.*, Mechanism for activation of mutated epidermal growth factor receptors in lung cancer. *Proc. Natl. Acad. Sci. U. S. A.* **110**, 3595–3604 (2013).
14. C. Brzezniak, C. A. Carter, G. Giaccone, Dacomitinib, a new therapy for the treatment of non-small cell lung cancer. *Expert Opin. Pharmacother.* **14**, 247–253 (2013).
15. Y. Jia, *et al.*, Overcoming EGFR T790M and C797S resistance with mutant-selective allosteric inhibitors. *Nature* **534**, 129–132 (2016).
16. E. Doumazane, *et al.*, A new approach to analyze cell surface protein complexes reveals specific heterodimeric metabotropic glutamate receptors. *FASEB J.* **25**, 66–77 (2011).
17. P. Scholler, *et al.*, HTS-compatible FRET-based conformational sensors clarify membrane receptor activation. *Nat. Chem. Biol.* **13**, 372–380 (2017).
18. P. Rondard, *et al.*, Coupling of agonist binding to effector domain activation in metabotropic glutamate-like receptors. *J. Biol. Chem.* **281**, 24653–24661 (2006).
19. J. Kniazeff, *et al.*, Closed state of both binding domains of homodimeric mGlu receptors is required for full activity. *Nat. Struct. Mol. Biol.* **11**, 706–713 (2004).
20. T. Heyduk, E. Heyduk, Luminescence energy transfer with lanthanide chelates: Interpretation of sensitized acceptor decay amplitudes. *Anal. Biochem.* **289**, 60–67 (2001).
21. E. Doumazane, P. Scholler, L. Fabre, J. M. Zwier, E. Trinquet, Illuminating the activation mechanisms and allosteric properties of metabotropic glutamate receptors. *Proc. Natl. Acad. Sci.* **110**, 1416–1425 (2013).
22. A. Levoye, *et al.*, A broad G protein-coupled receptor internalization assay that combines SNAP-tag labeling, diffusion-enhanced resonance energy transfer, and a highly emissive terbium cryptate. *Front. Endocrinol. (Lausanne).* **6** (2015).
23. Z. Ruan, N. Kannan, Altered conformational landscape and dimerization dependency underpins the activation of EGFR by αC–β4

loop insertion mutations. *Proc. Natl. Acad. Sci. U. S. A.* **115**, E8162–E8171 (2018).
24. L. C. Zanetti-Domingues, *et al.*, The architecture of EGFR's basal complexes reveals autoinhibition mechanisms in dimers and oligomers. *Nat. Commun.* **9**, 4325 (2018).
25. I. Chung, *et al.*, Spatial control of EGF receptor activation by reversible dimerization on living cells. *Nature* **464**, 783–787 (2010).
26. I. Maruyama, Mechanisms of Activation of Receptor Tyrosine Kinases: Monomers or Dimers. *Cells* **3**, 304–330 (2014).
27. H. K. Gan, *et al.*, The epidermal growth factor receptor (EGFR) tyrosine kinase inhibitor AG1478 increases the formation of inactive untethered EGFR dimers: Implications for combination therapy with monoclonal antibody 806. *J. Biol. Chem.* **282**, 2840–2850 (2007).
28. E. M. Bublil, *et al.*, Kinase-mediated quasi-dimers of EGFR. *FASEB J.* **24**, 4744–4755 (2010).
29. O. Coban, *et al.*, Effect of phosphorylation on EGFR dimer stability probed by single-molecule dynamics and FRET/FLIM. *Biophys. J.* **108**, 1013–1026 (2015).
30. J. H. Park, Y. Liu, M. A. Lemmon, R. Radhakrishnan, Erlotinib binds both inactive and active conformations of the EGFR tyrosine kinase domain. *Biochem. J.* **448**, 417–423 (2012).
31. K. M. Ferguson, Structure-based view of epidermal growth factor receptor regulation. *Annu. Rev. Biophys.* **37**, 353–373 (2008).
32. H. Björkelund, L. Gedda, M. Malmqvist, K. Andersson, Resolving the EGF-EGFR interaction characteristics through a multiple-temperature, multiple-inhibitor, real-time interaction analysis approach. *Mol. Clin. Oncol.* **1**, 343–352 (2013).
33. T. Hajdu, *et al.*, Comprehensive Model for Epidermal Growth Factor Receptor Ligand Binding Involving Conformational States of the Extracellular and the Kinase Domains. *Front. Cell Dev. Biol.* **8**, 1–16 (2020).
34. D. M. Freed, *et al.*, EGFR Ligands Differentially Stabilize Receptor Dimers to Specify Signaling Kinetics. *Cell* **171**, 683–695 (2017).
35. A. Kiyatkin, I. K. van Alderwerelt van Rosenburgh, D. E. Klein, M. A. Lemmon, Kinetics of receptor tyrosine kinase activation define ERK signaling dynamics. *Sci. Signal.* **13**, eaaz5267 (2020).
36. K. J. Wilson, J. L. Gilmore, J. Foley, M. A. Lemmon, D. J. Riese 2nd, Functional selectivity of EGF family peptide growth factors: implications for cancer. *Pharmacol. Ther.* **122**, 1–8 (2009).
37. K. Karl, M. D. Paul, E. B. Pasquale, K. Hristova, Ligand Bias in Receptor Tyrosine Kinase Signaling. *J. Biol. Chem.* **295**, 18494–18507 (2020).
38. T. Kenakin, Functional selectivity and biased receptor signaling. *J. Pharmacol. Exp. Ther.* **336**, 296–302 (2011).
39. A. S. Hauser, M. M. Attwood, M. Rask-Andersen, H. B. Schiöth, D. E. Gloriam, Trends in GPCR drug discovery: New agents, targets and indications. *Nat. Rev. Drug Discov.* **16**, 829–842 (2017).
40. J. L. Macdonald-Obermann, L. J. Pike, Allosteric regulation of epidermal growth factor (EGF) receptor ligand binding by tyrosine kinase inhibitors. *J. Biol. Chem.* **293**, 13401–13414 (2018).
41. A. Oashi, *et al.*, Monomer preference of EGFR tyrosine kinase inhibitors influences the synergistic efficacy of combination therapy with cetuximab. *Mol. Cancer Ther.* **18**, 1593–1601 (2019).
42. J. Cho, *et al.*, Cetuximab response of lung cancer-derived EGF receptor mutants is associated with asymmetric dimerization. *Cancer Res.* **73**, 6770–6779 (2013).
43. B. Kim, *et al.*, Clathrin-mediated EGFR endocytosis as a potential therapeutic strategy for overcoming primary resistance of EGFR TKI in wild-type EGFR non-small cell lung cancer. *Cancer Med.* **10**, 372–385 (2021).
44. U. Jo, *et al.*, EGFR endocytosis is a novel therapeutic target in lung cancer with wild-type EGFR. *Oncotarget* **5** (2014).
45. S. Kobayashi, *et al.*, *EGFR* Mutation and Resistance of Non–Small-Cell Lung Cancer to Gefitinib. *N. Engl. J. Med.* **352**, 786–792 (2005).
46. M. Bello, Binding mechanism of kinase inhibitors to EGFR and T790M, L858R and L858R/T790M mutants through structural and energetic analysis. *Int. J. Biol. Macromol.* **118**, 1948–1962 (2018).
47. C.-H. Yun, *et al.*, The T790M mutation in EGFR kinase causes drug resistance by increasing the affinity for ATP. *Proc. Natl. Acad. Sci.* **105**, 2070–2075 (2008).
48. J. Zhao, Y. Xia, Targeting HER2 Alterations in Non–Small-Cell Lung Cancer: A Comprehensive Review. *JCO Precis. Oncol.*, 411–425 (2020).
49. P. R. Selvin, Principles and biophysical applications of lanthanide-based probes. *Annu. Rev. Biophys. Biomol. Struct.* **31**, 275–302 (2002).

**Supplementary figures**

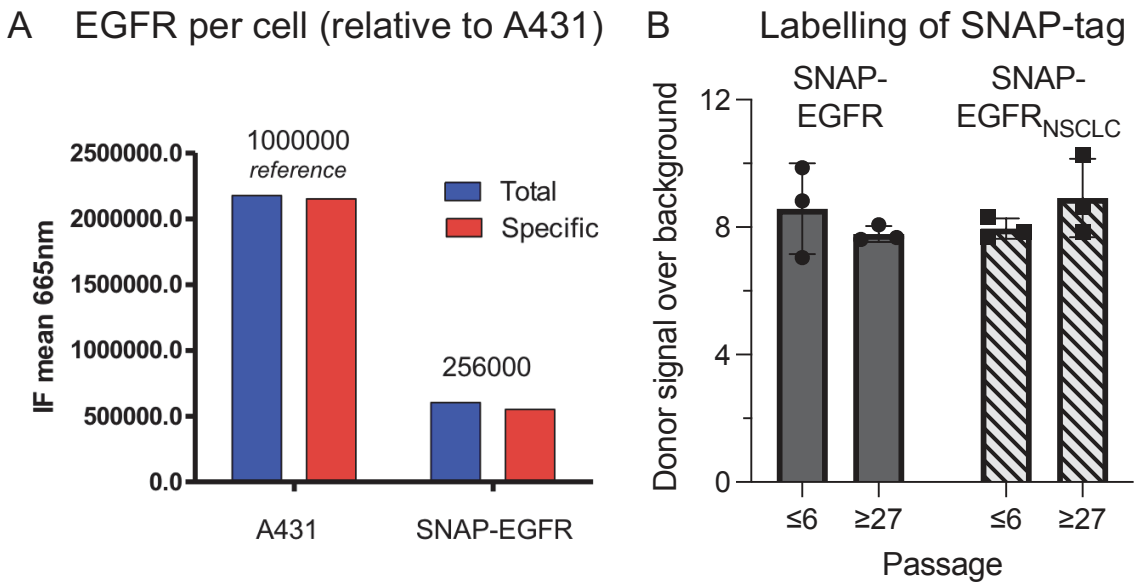


**Suppl. Fig. S1.** Expression levels of SNAP-EGFR. *(A)* FACS analysis of EGF-red labelled EGFR. *(B)* Signal over noise of Lumi4-Tb labelled SNAP-EGFR. Data in *B* is mean ± SD of representative experiment.

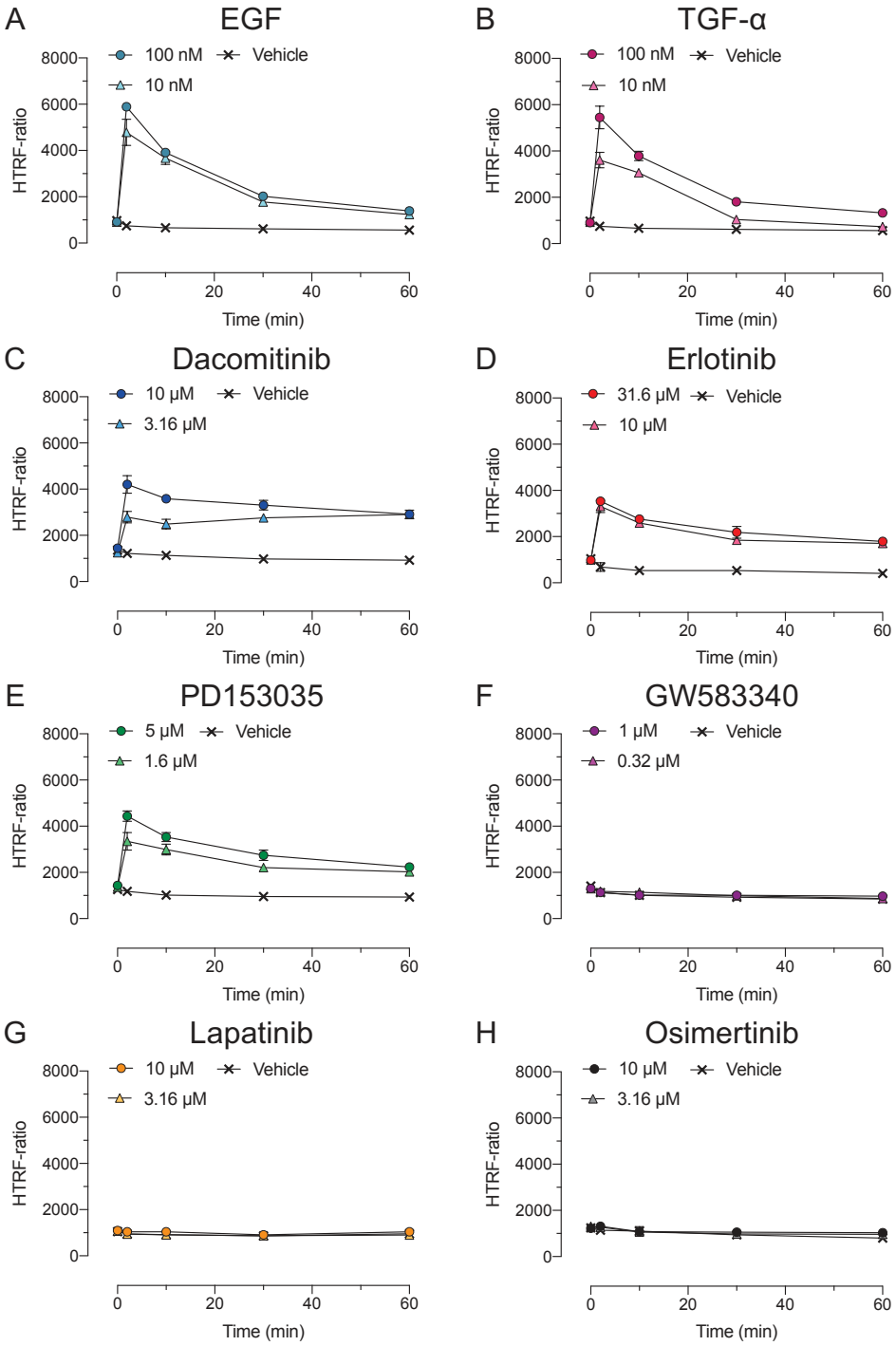


**Suppl. Fig. S2.** Intersubunit FRET for *wild-type* SNAP-EGFR. Intersubunit FRET is represented by HTRF-ratio. Data in *A-H* is mean ± SD of representative experiments.

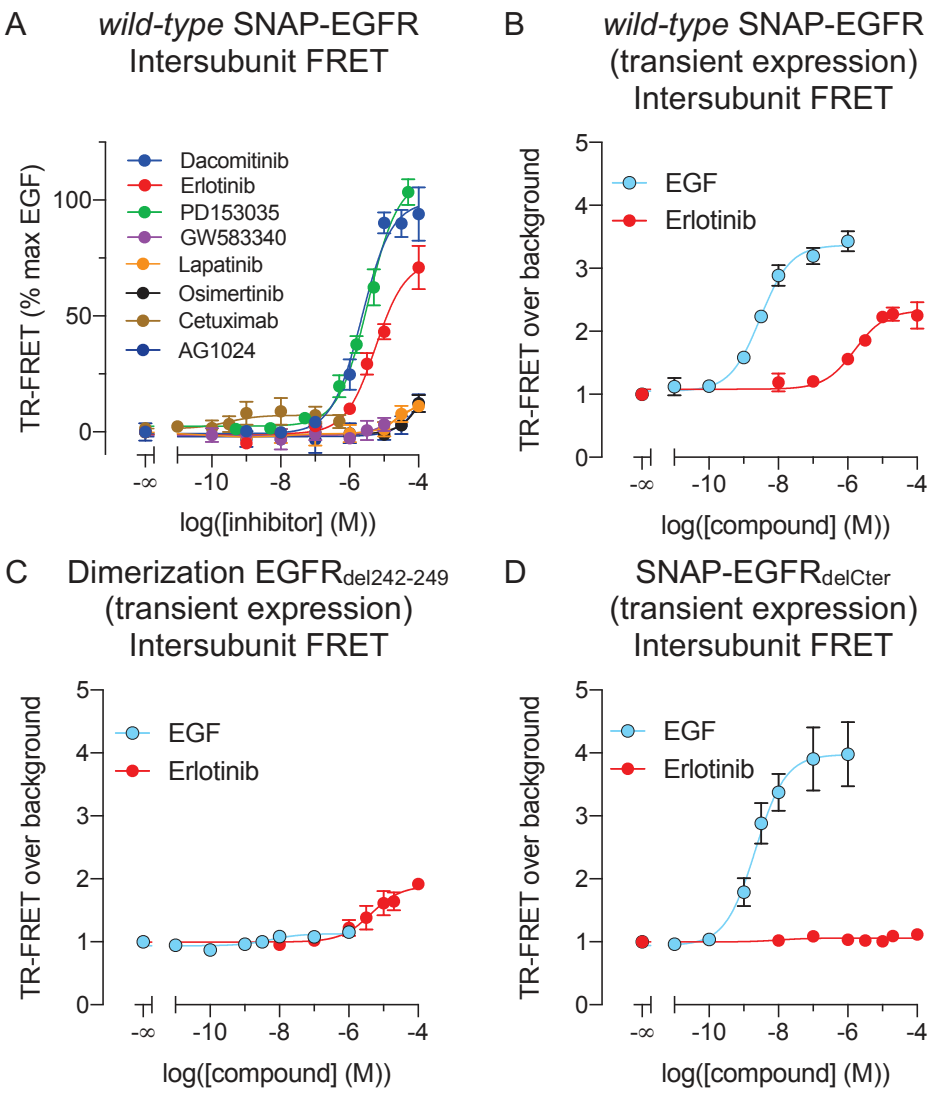


**Suppl. Fig. S3.** Intersubunit FRET assays. *(A)* TK inhibitor-induced intersubunit FRET. *(B)* Intersubunit FRET of transiently expressed *wild-type* SNAP-EGFR. *(C)* Intersubunit FRET of transiently expressed SNAP-EGFR$_{del242-249}$. *(D)* Intersubunit FRET of transiently expressed SNAP-EGFR$_{delCter}$. Data in *A-D* are mean ± SEM of at least three individual experiments.

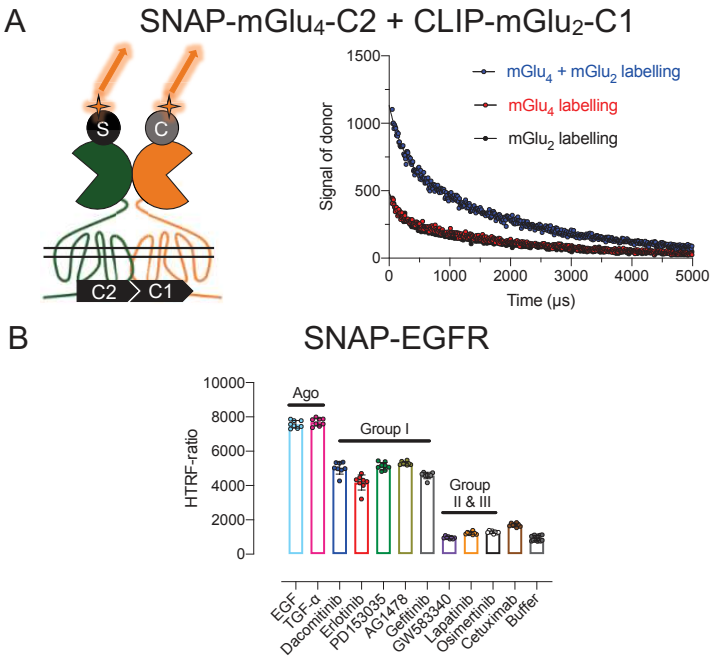


**Suppl. Fig. S4.** Expression levels of mGlu subunits in mGlu2-4 heterodimer and intersubunit FRET of *wild-type* SNAP-EGFR at 4 °C. *(A)* Scheme of mGlu2-4 labelling with donor and signal of the donor. *(B)* Intersubunit FRET of *wild-type* SNAP-EGFR at 4 °C represented by HTRF-ratio. Data in *A* are individual data points of a representative experiment. Data in *B* are mean ± SD of a representative experiment.

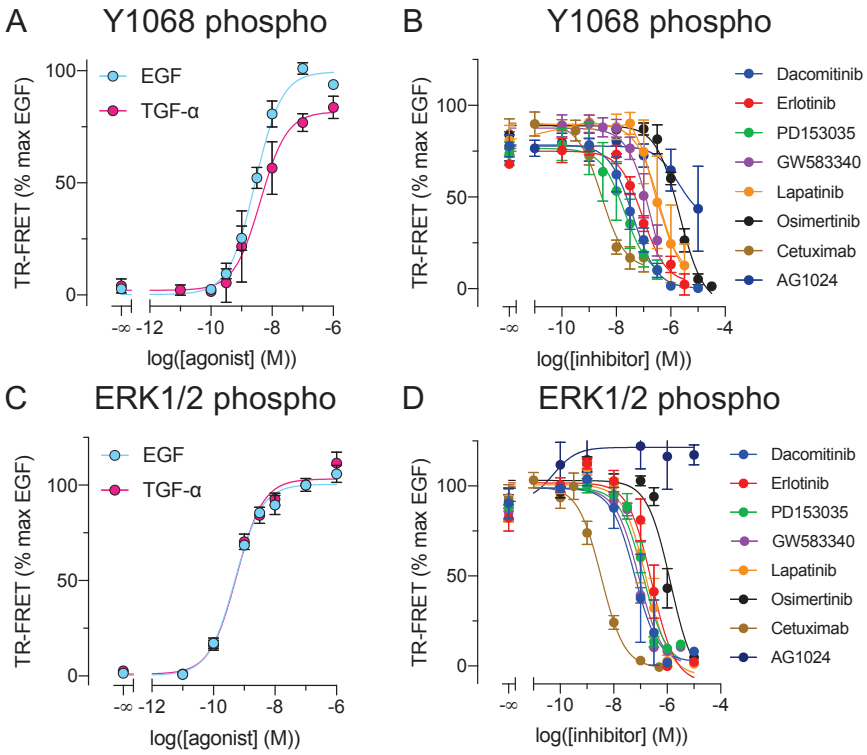


**Suppl. Fig. S5.** Phosphorylation of Y1068 of the EGFR and Thr202/Tyr204 of ERK1/2. *(A)* Phosphorylation of Y1068 of the EGFR induced by agonists. *(B)* EGF-induced Y1068 of the EGFR phosphorylation (10 nM) inhibited by inhibitors. *(C)* Phosphorylation of ERK1/2 induced by EGFR

agonists. *(D)* EGF-induced phosphorylation (10 nM) of ERK1/2 inhibited by inhibitors. Data in *A-D* are the mean ± SEM of at least three individual experiments.

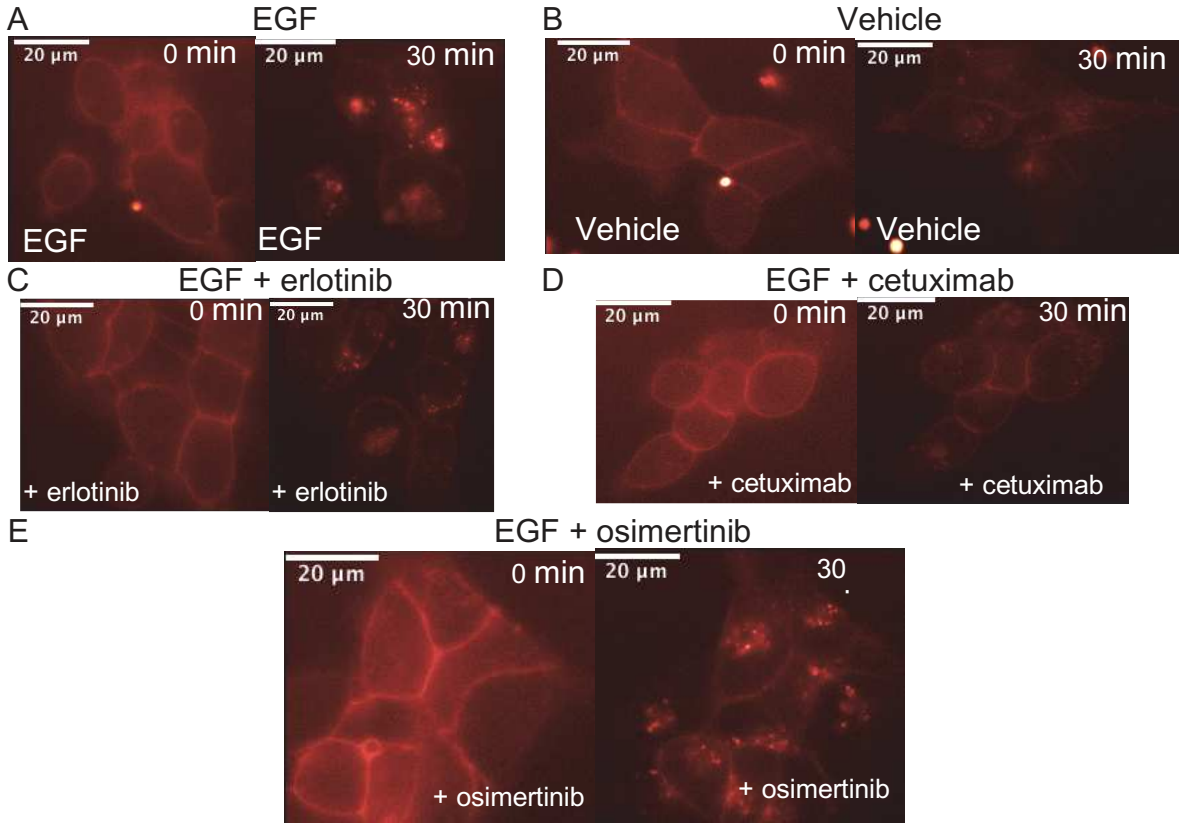


**Suppl. Fig. S6.** Internalization of the *wild-type* SNAP-EGFR labelled with SNAP-Red represented by two snapshots right before addition of compounds and 30 minutes after. *(A)* 10 nM EGF. *(B)* Vehicle. *(C)* 1 µM erlotinib pre-incubated for 2 hours and 10 nM EGF. *(D)* 100 nM cetuximab pre-incubated for 2 hours and 10 nM EGF. *(E)* 1 µM osimertinib pre-incubated for 2 hours and 10 nM EGF. Snapshots in *A-E* are from a representative experiment.

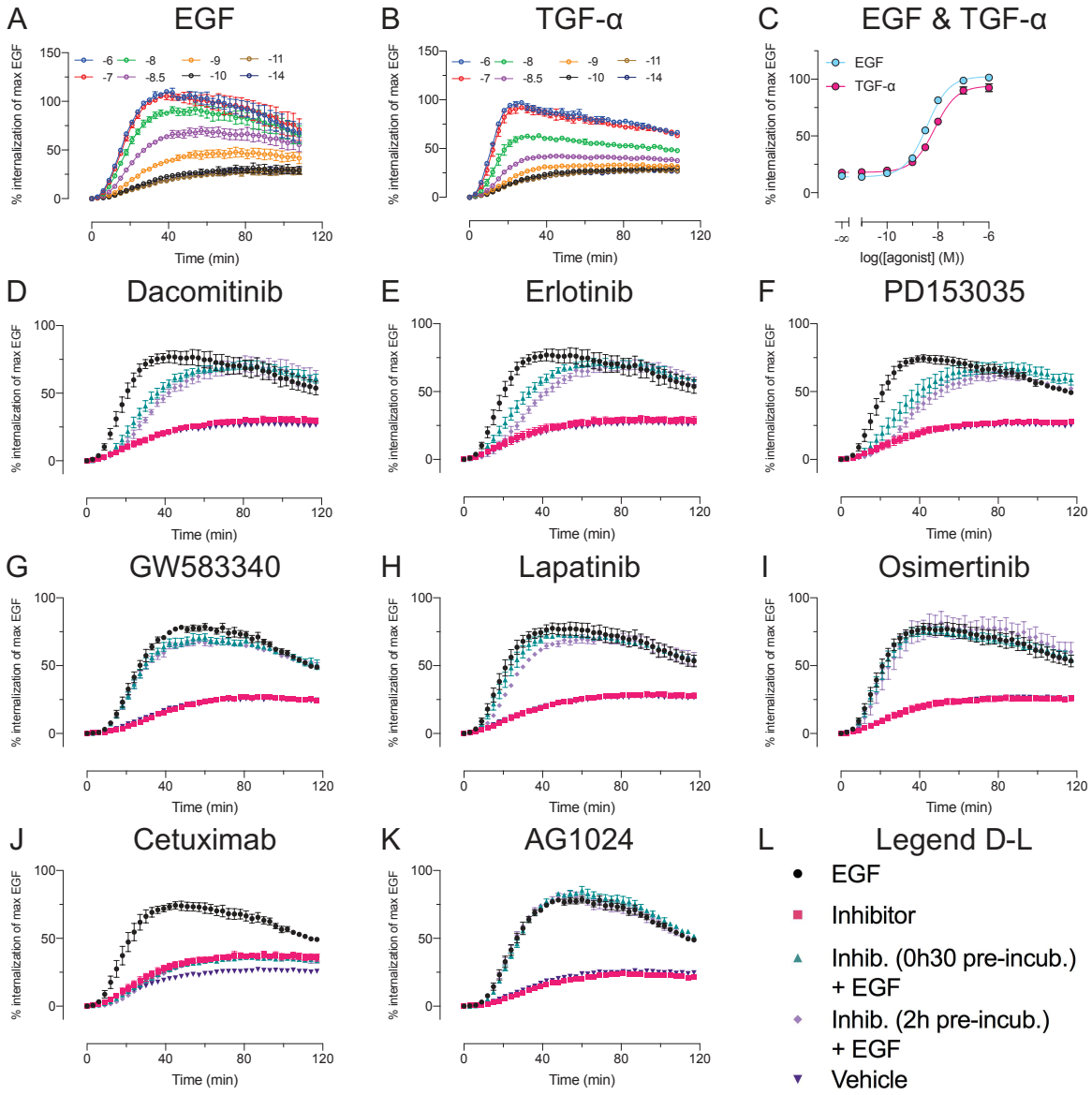


**Suppl. Fig. S7.** Internalization of the *wild-type* SNAP-EGFR labelled with SNAP-Lumi4-Tb represented by kinetic curves. *(A, B)* Agonists. *(C)* Dose-response curve of agonists. *(D-L)* Internalization of EGFR in presence of pre-incubated inhibitors and EGF. Data in A-B and D-K are mean ± SEM of at least three individual experiments.

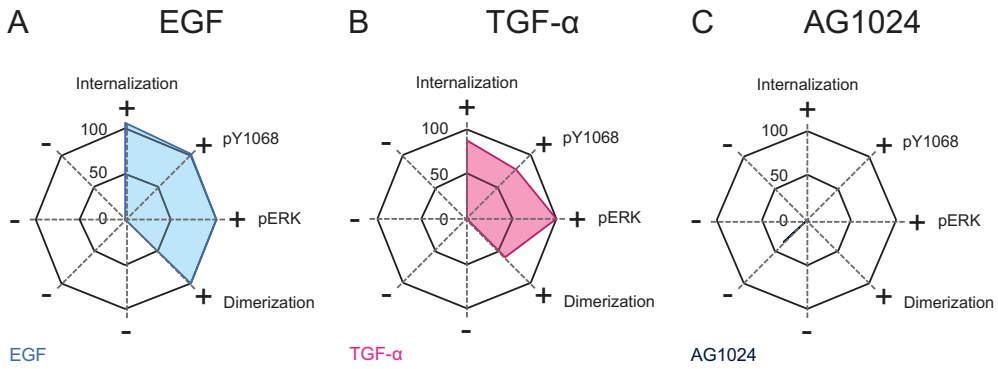


**Suppl. Fig. S8.** Pharmacological profile of compounds. (A) EGF. (B) TGF-α. (C) AG1024. All data are from figures 1-4.

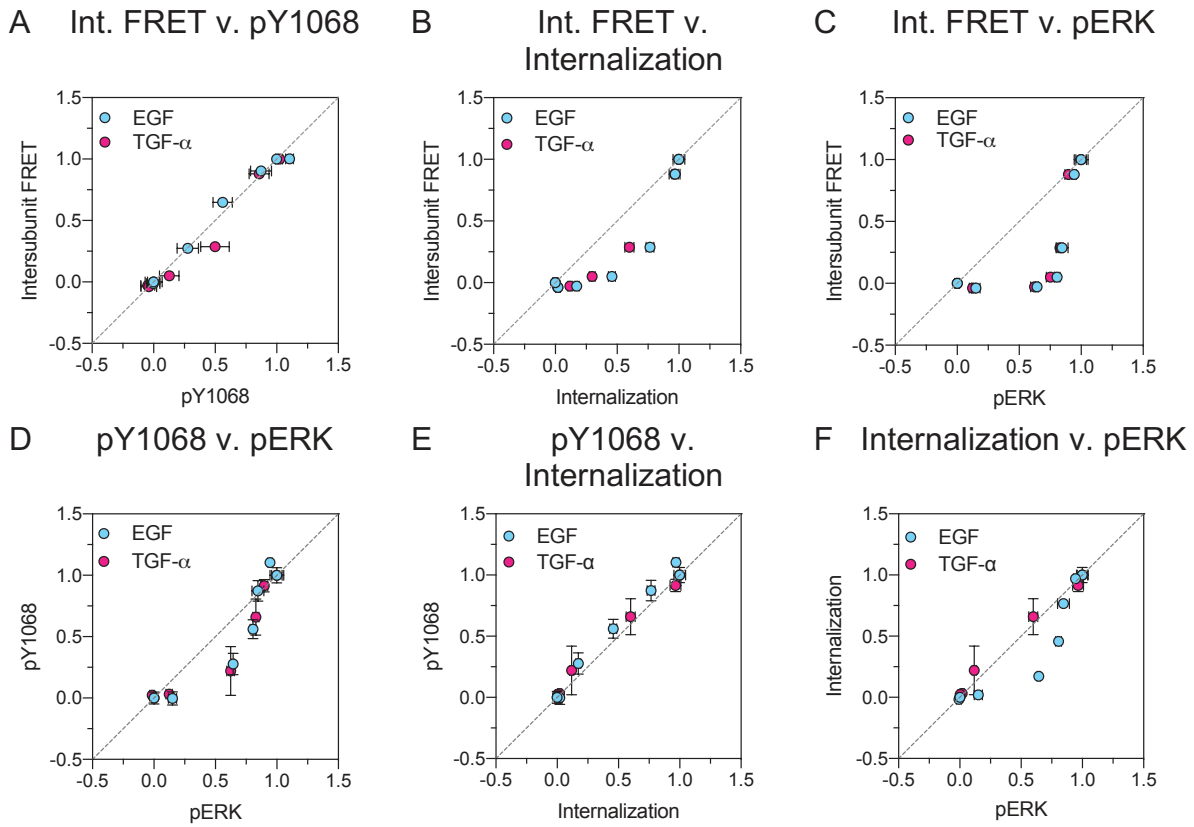


**Suppl. Fig. S9.** Bias plots for EGFR agonists. *(A)* Intersubunit FRET v. phosphorylation Y1068 of the EGFR. *(B)* Intersubunit FRET v. Internalization. *(C)* Intersubunit FRET v. phosphorylation ERK. *(D)* phosphorylation Y1068 of the EGFR v. phosphorylation of ERK1/2. *(E)* phosphorylation Y1068 of the EGFR v. Internalization. *(F)* Internalization v. phosphorylation Y1068 of ERK1/2. All data are mean ± SEM of at least three individual experiments.

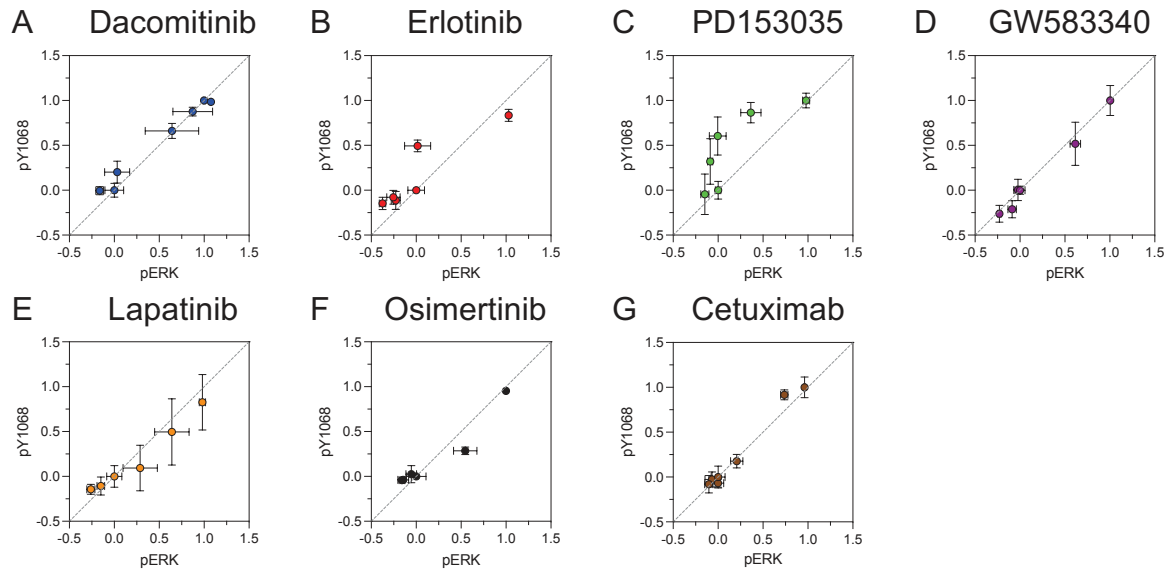


**Suppl. Fig. S10**. Inhibition of EGF-induced phosphorylation of the EGFR or ERK1/2 by TK inhibitors.

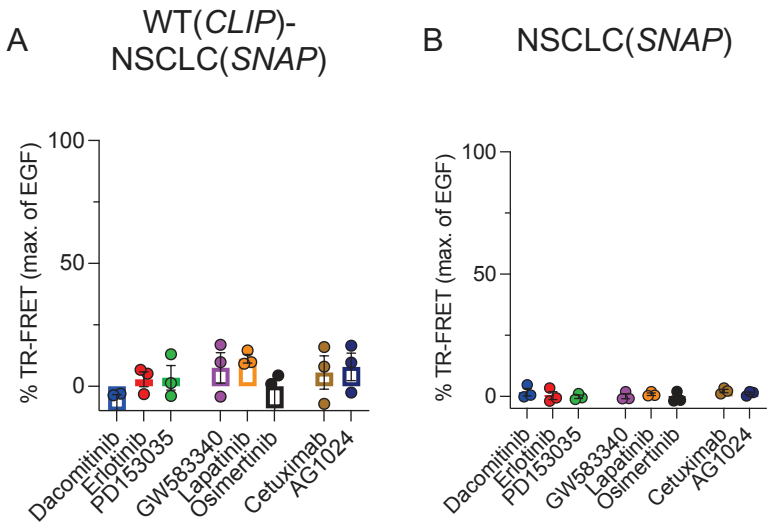


**Suppl. Fig. S11.** Effect of inhibitors on *wild-type* EGFR – $EGFR_{NSCLC}$ intersubunit FRET assay. *(A) Wild-type* CLIP-EGFR + SNAP-$EGFR_{NSCLC}$ heterodimer. *(B)* SNAP-$EGFR_{NSCLC}$ homodimer. Data A-B are mean ± SEM of three individual experiments.

**Supplementary tables**

| Ligand | $\alpha_{DA}$ | SD | $A_s$ | SD |
|---|---|---|---|---|
| AG1478 | 0.84 | 0.04 | 0.40 | 0.07 |
| Dacomitinib | 0.85 | 0.06 | 0.49 | 0.11 |
| Erlotinib | 0.84 | 0.06 | 0.41 | 0.08 |
| Gefitinib | 0.84 | 0.05 | 0.43 | 0.10 |
| PD153035 | 0.84 | 0.03 | 0.38 | 0.08 |
| GW583340 | 0.82 | 0.03 | 0.16 | 0.02 |
| Lapatinib | 0.75 | 0.09 | 0.16 | 0.06 |
| Osimertinib | 0.81 | 0.12 | 0.25 | 0.13 |
| EGF | 0.75 | 0.04 | 0.31 | 0.07 |
| TGF-α | 0.77 | 0.04 | 0.35 | 0.04 |
| Cetuximab | 0.88 | 0.04 | 0.30 | 0.11 |
| Vehicle | 0.80 | 0.15 | 0.20 | 0.11 |

**Suppl. Table S1.** The true fraction of the slow decay species ($\alpha_{DA}$) after the Heyduk and Heyduk correction.

| pEC50 ± SEM | EGF | N | TGF-α | N |
|---|---|---|---|---|
| $EGFR_{WT}$ | 8.636 ± 0.039 | 9 | 7.636 ± 0.019 | 3 |
| $EGFR_{NSCLC}$ | 8.705 ± 0.204 | 4 | 8.131 ± 0.164 | 3 |
| WT + NSCLC | 8.384 ± 0.040 | 3 | 7.484 ± 0.251 | 3 |
| P value | NS (P = 0.1690) | | NS (P = 0.0860) | |

**Suppl. Table S2.** Summary of potencies of EGF and TGF-α for $EGFR_{WT}$, $EGFR_{NSCLC}$ and $EGFR_{WT}$ + $EGFR_{NSCLC}$. Potency values are represented as pEC50 ± standard error of the mean (SEM) of 3 or more individual experiments. The used statistical test is ordinary one-way ANOVA. NS means not significant.

| Ligand | Mean ± SD | N | P value |
|---|---|---|---|
| Erlotinib | 405.2 ± 57.0 | 24 | 0.6972 |
| Gefitinib | 412.9 ± 52.8 | 24 | 0.8606 |
| PD153035 | 383.1 ± 33.8 | 24 | 0.2186 |
| AG1478 | 384.6 ± 43.9 | 24 | 0.2408 |
| Dacomitinib | 414.3 ± 48.3 | 24 | 0.8844 |
| GW583340 | 828.2 ± 133.8 | 24 | <0.0001 |
| Osimertinib | 601.6 ± 199.2 | 23 | 0.0002 |
| Lapatinib | 549.2 ± 142.2 | 24 | 0.0483 |
| EGF | 456.8 ± 72.8 | 84 | - |
| TGF-α | 382.0 ± 46.6 | 24 | 0.2016 |
| Cetuximab | 733.3 ± 167.6 | 24 | <0.0001 |
| Vehicle | 812.3 ± 248.4 | 84 | <0.0001 |

**Suppl. Table S3.** Summary of basal, TK inhibitor-induced, agonist-induced mean excited-state lifetimes of sensitized acceptor emission. Statistical test is one-way ANOVA with Dunnett's multiple comparison test.

# 10 A NANOBODY ACTIVATING METABOTROPIC GLUTAMATE RECEPTOR 4 DISCRIMINATES BETWEEN HOMO AND HETERODIMERS

The mGlu4 receptor is a constitutive dimeric receptor that forms both homo- and heterodimers. Studies suggest that the propensity to form heterodimers is significant. One heterodimer, the mGlu2-mGlu4 heterodimer (mGlu2-4), retains much attention because it was proven to exist and function in the rat brain and in human neurons.

The first subject is about the development and characterization of a nanobody. Nanobodies represent a group of molecules that can selectively bind or modulate a protein target. The nanobody is selective for the human mGlu4 receptor and fully activates it. Conversely, it does not activate, but potentiate the mGlu2-4 heterodimer, revealing a distinct pharmacology for these receptors.

Secondly, we investigate its mode of binding and mode of activation, by using biochemical approaches and molecular dynamics simulations. We reveal its epitope and a mode of action on the mGlu4 receptor, previously unknown for class C GPCRs.

In summary, we develop and characterize a novel selective pharmacological compound that could be used in deciphering the expression and function of the mGlu2-4 heterodimer in native tissues.

# A nanobody activating metabotropic glutamate receptor 4 discriminates between homo- and heterodimers

Jordi Haubrich[a,1], Joan Font[a,1], Robert B. Quast[b], Anne Goupil-Lamy[c], Pauline Scholler[a], Damien Nevoltris[d], Francine Acher[e], Patrick Chames[d], Philippe Rondard[a], Laurent Prézeau[a,2], and Jean-Philippe Pin[a,2]

[a]Institut de Génomique Fonctionnelle, University of Montpellier, CNRS, INSERM, 34094 Montpellier Cedex 5, France; [b]Centre de Biologie Structurale, University of Montpellier, CNRS, INSERM, 34090 Montpellier, France; [c]BIOVIA Science Council, Dassault Système, F-78140, Vélizy-Villacoublay Cedex, France; [d]Institut Paoli-Calmettes, Aix Marseille University, CNRS, INSERM, Centre de Recherche en Cancérologie de Marseille, 13009 Marseille, France; and [e]Faculté des Sciences Fondamentales et Biomédicales, Université de Paris, CNRS, 75270 Paris Cedex 06, France

Edited by Robert J. Lefkowitz, HHMI, Durham, NC, and approved July 6, 2021 (received for review March 26, 2021)

**There is growing interest in developing biologics due to their high target selectivity. The G protein–coupled homo- and heterodimeric metabotropic glutamate (mGlu) receptors regulate many synapses and are promising targets for the treatment of numerous brain diseases. Although subtype-selective allosteric small molecules have been reported, their effects on the recently discovered heterodimeric receptors are often not known. Here, we describe a nanobody that specifically and fully activates homodimeric human mGlu4 receptors. Molecular modeling and mutagenesis studies revealed that the nanobody acts by stabilizing the closed active state of the glutamate binding domain by interacting with both lobes. In contrast, this nanobody does not activate the heterodimeric mGlu2-4 but acts as a pure positive allosteric modulator. These data further reveal how an antibody can fully activate a class C receptor and bring further evidence that nanobodies represent an alternative way to specifically control mGlu receptor subtypes.**

G protein–coupled receptor | single-domain antibody | activation mechanism | agonist

There is more and more interest in developing antibodies as possible pharmacological and even therapeutic agents (1, 2). The single-domain antibodies, also named nanobodies, are prone for such activities, as their short variable loops can interact in surface cavities that can vary between the conformational states of a protein (1). As such, nanobodies regulating drug targets have already been reported (3, 4). Among the main drug targets are the G protein–coupled receptors (GPCRs) that play important roles in cell–cell communication (5).

Among the large GPCR family, class C receptors are those activated by the main neurotransmitters, glutamate and γ-amino butyric acid (GABA), as well as by $Ca^{2+}$ ions, sweet and umami compounds (6). There are eight genes encoding metabotropic glutamate (mGlu) receptor subunits. Although only considered as disulfide-linked homodimers, the complexity of the mGlu receptor family increased with the description of heterodimeric entities made of two different mGlu subunits (7). Indeed, the postsynaptic mGlu1 and -5 on one side and presynaptic mGlu2, -3, -4, -7, and -8 subunits on another side can form heterodimeric entities in recombinant cells, leading to the possible existence of 16 additional mGlu subtypes (7, 8). Among these, the mGlu2-4 heterodimer retained much attention. It was found to display a specific pharmacological profile and was identified in transfected neurons as well as in both cortico-striatal (9) and lateral perforant path (10) terminals. Identifying the various heterodimeric mGlu receptors in the brain and their possible roles is essential.

We recently reported nanobodies acting as positive allosteric modulators (PAMs) specific to the mGlu2 homodimer (11). Among the mGlu subtypes, the mGlu4 containing receptors, and especially mGlu4 homodimers, are of interest for the treatment of Parkinson's disease (12–14) and pain (15, 16). In the present study, we report the identification of DN45, a nanobody that specifically and fully activates human mGlu4 homodimers. We show that this nanobody acts by stabilizing the closed active state of the glutamate binding Venus flytrap domain (VFT). However, this nanobody was unable to directly activate the mGlu2-4 heterodimer, acting instead as a pure PAM. These data reveal a way a nanobody can activate a class C GPCR and confirm the potential of using nanobodies to discriminate between homo- and heterodimeric receptors.

## Results

**DN45 Is Specific to the Human mGlu4 Receptor.** To identify nanobodies targeting mGlu4, HEK293 cells transiently expressing either the human or the rat mGlu4 receptor were injected into a llama. Genes encoding $V_HH$ domains were amplified by RT-PCR from the total RNA of peripheral blood mononuclear cells and used to create a phage display library. This library was depleted on controlled Human Embryonic Kidney (HEK293) cells and enriched by two cycles of positive selection on human mGlu4 transfected cells in the presence of an excess of anti-HEK293 nanobodies (17). Nanobody containing *Escherichia coli* supernatants were screened by flow cytometry.

### Significance

**Biologics, and especially antibodies, are promising therapeutics. Antibodies are expected to show higher subtype selectivity and less off-target activity than small molecules. G protein–coupled receptors (GPCRs) being the main drug targets, there is a need for antibodies modulating these receptors. Here, we describe the first single-domain antibody fully activating a GPCR. This nanobody activates the homodimeric metabotropic glutamate receptor type 4 (mGlu4), an interesting target for the treatment of Parkinson's disease or pain. Using modeling tools, we show this nanobody acts by stabilizing the active form of the binding domain. It does not activate heterodimeric mGlu receptors containing the mGlu4 subunit. These data revealed that nanobodies can be useful tools to specifically control mGlu receptor subtypes.**

Author contributions: J.H., J.F., D.N., F.A., P.C., L.P., and J.-P.P. designed research; J.H., J.F., R.B.Q., A.G.-L., P.S., D.N., and F.A. performed research; J.H., J.F., R.B.Q., P.S., and F.A. analyzed data; and J.H., J.F., F.A., P.R., and J.-P.P. wrote the paper.

The authors declare no competing interest.

This article is a PNAS Direct Submission.



[1]J.H. and J.F. contributed equally to this work.

[2]To whom correspondence may be addressed. Email: laurent.prezeau@igf.cnrs.fr or jean-philippe.pin@igf.cnrs.fr.

This article contains supporting information online at https://www.pnas.org/lookup/suppl/doi:10.1073/pnas.2105848118/-/DCSupplemental.

Published August 12, 2021.

Among the selected clones, nanobody DN45 was further characterized. We performed a binding assay based on time-resolved fluorescence energy transfer (TR-FRET) between the SNAP-tagged receptor and an anti-c-Myc-antibody-d2 interacting with the c-Myc-tag inserted at the carboxyl-terminal end of the DN45 sequence (Fig. 1*A*). The nanobody binds to human mGlu4 exclusively when tested at 100 nM, and no binding was observed on any other human mGlu receptor (Fig. 1*B*) nor on the eight rat mGlu receptors (Fig. 1*C*). To avoid constitutive receptor activation by ambient glutamate produced by the cultured HEK293 cells, excitatory amino acid transporter 3 was cotransfected with the indicated receptors such that receptors were essentially in an inactive state under basal condition. Activating any of the mGlu receptors with an agonist did not allow binding of DN45 either, except on the human mGlu4, in which a higher signal was observed (Fig. 1 *B* and *C*). Indeed, DN45 had a preferred high binding affinity ($K_D$ = 3.1 nM) for the active conformation of the human mGlu4 receptor and a low binding affinity for the basal and antagonist-induced conformation (Fig. 1*D* and *SI Appendix*, Table S1).

**DN45 Is a Full Agonist of the mGlu4 Receptor.** In agreement with the higher binding affinity of DN45 for the active form of the hmGlu4 receptor, DN45 alone stabilizes the active conformation of the VFT dimer as revealed using a TR-FRET–based conformational biosensor (Fig. 2*A*) (7, 18). This biosensor measures the distance variation between the N-terminally inserted SNAP tags of the subunits such that a high TR-FRET is measured in the basal state (after random labeling with the SNAP substrates $O^6$-benzylguanine [BG]-Lumi4-Tb and BG-Green), while a lower TR-FRET is observed upon the reorientation of the VFTs upon activation (18). DN45 displays a potency and efficacy not significantly different from the group-III mGlu receptor agonist L-AP4 (Fig. 2*A* and *SI Appendix*, Table S2). Subsequently, we setup a single-molecule FRET (smFRET) approach to compare the agonist effect of L-AP4 and DN45 at the single-molecule level in an environment without ambient glutamate (Fig. 2*B* and *SI Appendix*, Fig. S1 and Table S3). There was no difference between the apo-state and the antagonist-stabilized state. However, both L-AP4 and DN45 acted as full agonists, as illustrated by the similar increase in the proportion of molecules in the low FRET, active conformation. DN45 also activated the natural Gi protein of the mGlu4 receptor with the same potency as L-AP4, as revealed with a Gi bioluminescence resonance energy transfer (BRET) sensor (Fig. 2*C* and *SI Appendix*, Fig. S2 and Table S2). The agonist activity of DN45 was further confirmed by measuring the accumulation of IP-1 upon activation of the chimeric G protein Gqi9 (Fig. 2*D*). DN45 potency and efficacy were similar to those obtained with L-AP4, both being more potent than glutamate (Fig. 2*D* and *SI Appendix*, Table S2). In the presence of LY341495, the potency of DN45 was decreased (Fig. 2*E*). Of note, the L-AP4 potency for accumulation of IP-1 was not significantly increased in the presence of nonsaturating DN45 concentrations (Fig. 2*F* and *SI Appendix*, Table S2).

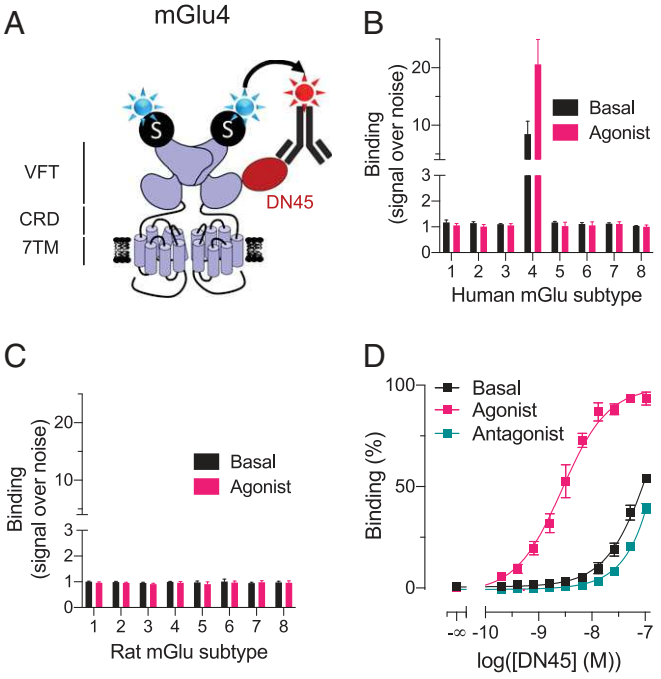


**Fig. 1.** DN45 is selective for the human mGlu4 receptor and preferentially binds to the active receptor. *(A)* Cartoon representing a TR-FRET–based binding assay. SNAP-mGlu receptors were labeled with 100 nM BG-Lumi4-Tb (blue star). Then, 100 nM DN45 containing a c-Myc epitope was labeled with 200 nM anti-c-Myc-antibody (gray) coupled to d2 (red star). *(B)* Specific binding of DN45 to human mGlu4 receptor without (black) and with (pink) a saturating concentration of agonist (mGlu group I: 1 μM quisqualic acid; group II: 100 nM LY379268; group III: 10 μM L-AP4), represented by an increase of signal compared to an irrelevant nanobody containing the c-Myc sequence. *(C)* No specific binding was observed between the nanobody and any rat mGlu receptors in the absence (black) or presence (pink) of agonist. *(D)* Binding of an increasing concentration of DN45 on hmGlu4 under basal condition (black) in the presence of the agonist L-AP4 (10 μM) or in the presence of the antagonist LY341495 (100 μM). Data in *B–D* are mean ± SEM of three individual experiments (*SI Appendix*, Table S1).

**Residues in Lobe 2 of the Human mGlu4 VFT Confer Subtype Selectivity to DN45.** To explain the subtype selectivity of DN45, we substituted any individual residue at the surface of the human mGlu4 VFT into its rat equivalent. We identified 12 residues on the surface of the VFT that are different in the human and rat proteins (Fig. 3*A*). Among the 12 mutations tested, three (i.e., I318S, H323R, and D485G) affected DN45 binding, with D485G suppressing binding completely (Fig. 3*B*). Consistent with these binding data, the DN45 agonist effect was largely affected or even suppressed in these human mGlu4 mutants (Fig. 3*C*), while L-AP4 could still activate them (*SI Appendix*, Fig. S3*A*).

**Molecular Modeling Identifies DN45-mGlu4 Interaction Site on Both Lobe 2 and Lobe 1.** We built three-dimensional (3D) models of both human mGlu4 (in an active closed conformation) and DN45 and performed docking experiments using ZDOCK (19) without any specific constraint. Our best-scored model using ZRANK (20), which keeps the main interactions with or without L-AP4 within the VFT binding site after a 10-ns dynamics simulation, revealed possible interaction sites of DN45 on the VFT (Fig. 3*A*). In the presence of bound L-AP4, more interactions between the partners were detected (*SI Appendix*, Fig. S4 *A* and *B*) in agreement with the higher binding affinity in the active state. A time-dependent analysis of the model revealed the mGlu4 residues maintaining interaction with DN45 during the 10-ns molecular dynamics simulations (*SI Appendix*, Fig. S5). These include the residues that are human-specific: I318, H323, D485 (lobe 2), and also residues on lobe 1 (*SI Appendix*, Fig. S5). The virtual mutagenesis analysis performed on our 3D model of the mGlu4–DN45 complex is perfectly in line with the evaluated impact of individually substituting the 12 human-specific residues for its rat equivalents (*SI Appendix*, Fig. S5 and Table S4). In addition, the model revealed other key residues such as L322 (*SI Appendix*, Fig. S6).

**DN45 Binding Was Restored on Rat mGlu4 Mutant Bearing At Least Four Human Residues.** The proposed model was further confirmed by introducing human-specific residues into the rat sequence, restoring DN45 binding and agonist activity on the mutated rat mGlu4 receptor. We considered five human-specific residues based on their proximity to the apparent epitope of DN45 (i.e., I318, H323, D485, V385, and H507 [Fig. 3*A*]). When the five rat residues

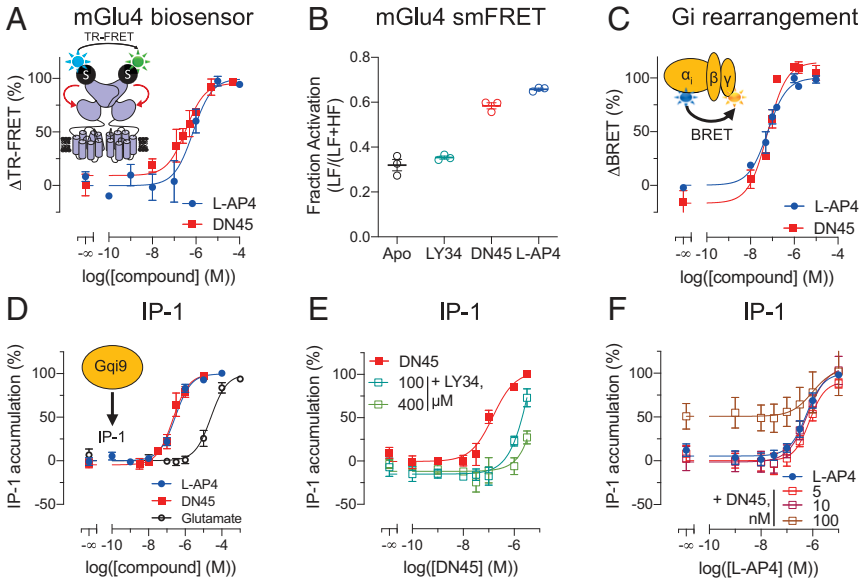


**Fig. 2.** DN45 is a full agonist of the hmGlu4 receptor. *(A)* Measurement of the change in TR-FRET induced upon stimulation with increasing concentrations of L-AP4 (blue) or DN45 (red). (*B*) Measurement of the fraction of activated receptor by single-molecule FRET in basal/apo state (black) in the presence of LY341495 (green), DN45 (red), or L-AP4 (blue). *(C)* Measurement of the rearrangement of the Gi protein in a BRET experiment upon stimulation with increasing concentrations of L-AP4 (blue) and DN45 (red). *(D)* Measurements of the activation of the Gq pathway via transient overexpression of Gqi9 upon stimulation with increasing concentrations of L-AP4 (blue), DN45 (red), or glutamate (black). *(E)* Measurements of the activation of the Gq pathway via transient overexpression of Gqi9 upon stimulation with increasing concentrations of DN45 alone (red) or in the presence of LY341495 (i.e., 100 or 400 μM). *(F)* Measurement of the activation of the Gq pathway upon stimulation with increasing concentrations of L-AP4 alone (blue) or L-AP4 with nonsaturating concentrations (i.e., 5, 10, or 100 nM) of DN45. Data in *A–F* are mean ± SEM of three or more individual experiments. Statistical analysis for *A–D* was performed using unpaired two-tailed *t* tests, and the statistical analysis of *F* was an ordinary one-way ANOVA with Dunnett's multiple comparisons test (*SI Appendix*, Tables S2 and S3).



were mutated to their human equivalent (rmG4-5M), DN45 bound (Fig. 3*D*) and activated the receptor (Fig. 3*E*) with an affinity ($K_D$ = 22.8 nM) and potency not different from those measured on the human mGlu4 receptor (*SI Appendix*, Tables S1 and S2). The substitutions G485D (rmG4-1M), G485D+R323H (rmG4-2M), and G485D+R323H+S318I (rmG4-3M) on the rat mGlu4 receptor were, however, not sufficient to recover binding of DN45 (Fig. 3*D*). Indeed, the model of rmG4-3M reveals that DN45 is not able to interact with the three mutated residues (i.e., S318I, R323H, and G485D) (*SI Appendix*, Fig. S4*A*) because a loop is closing the entrance of the epitope cavity (*SI Appendix*, Fig. S7). The additional mutation of I385V or Q507H restores the opening of the cavity and allows for interactions between DN45 and the three key human residues (*SI Appendix*, Fig. S7). This was further supported when binding of DN45 to the rat mGlu4 bearing the three main aforementioned substitutions plus I385V (rmG4-4MB) or Q507H (rmG4-4MA) was recovered (Fig. 3*D*) and both mutants were activated by DN45 (Fig. 3*E*). The observed affinities ($K_D$ = 13.6 nM and 10.4 nM, respectively) and potencies were not significantly different from those measured for human mGlu4 (Fig. 3 *D* and *E* and *SI Appendix*, Tables S1 and S2). All mutants were functional, as we successfully activated them with L-AP4 (*SI Appendix*, Fig. S3*B*).

Taken together, these modeling and mutagenesis data provide a reliable explanation for the species selectivity of DN45 by interacting with residues mainly located on lobe 2 of the VFT.

**DN45 Agonist Activity Needs Interaction with Both Lobes of the VFT.** The predictions of interactions between DN45 and lobe 1 of the VFT in a closed active state especially comprise residues H371 to E401 (Fig. 4 *A* and *B* and *SI Appendix*, Fig. S4*B*). Interactions with this region are expected to stabilize the closed conformation of the VFT, providing an explanation for the agonist activity of DN45 and its increased affinity for the active mGlu4 (Fig. 1*D*). In a first attempt to prevent the interaction between DN45 and lobe 1 of the mGlu4 VFT, an *N*-glycosylation site, A399N/E401S, was introduced. This resulted in a large decrease in DN45 agonist potency but did not suppress its agonist activity (Fig. 4*C*).

Single-point mutations H371A, K386A, H392A, D397A, E401A, and E403A did not lead to antagonist effects of DN45 on these mutants (*SI Appendix*, Fig. S8). Therefore, a virtual saturation mutagenesis was performed to predict the impact of multiple mutations of lobe 1 residues on the binding of DN45 and also the impact of these mutations on the overall stability of mGlu4. The best-predicted mutations were H371E, R391M, R393W, and A399K in a loop of lobe 1 (Fig. 4 *A* and *B*). The calculated binding energy revealed that the highest destabilizing values were found for the triple mutant R391M+R393W+A399K (4.82 kcal/mol) and quadruple mutant H371E+R391M+R393W+A399K (4.81 kcal/mol).

Experimental data support that this loop is involved in the agonist effect of DN45, as DN45 no longer activated either the triple or the quadruple mutant (Fig. 4 *D* and *E*). Of note, the quadruple mutant displays constitutive activity that is reduced by DN45, revealing that DN45 acts as an inverse agonist on this receptor (Fig. 4*E*). This is confirmed by the significant antagonistic effect of DN45 on this mutant upon activation by L-AP4 (Fig. 4*F* and *SI Appendix*, Table S2).

Taken together, these data reveal that DN45 primarily binds to lobe 2 but also to lobe 1 in the active state, an interaction increasing its affinity and required for its agonist activity.

**DN45 Acts as a Positive Allosteric Modulator on Heterodimeric mGlu2-4.** It is now recognized that the mGlu4 subunit can associate with other mGlu subunits to form heterodimeric mGlu receptors (7, 8). Among these, the mGlu2-4 heterodimer has retained much attention and has specific pharmacological properties that were used to illustrate its existence in the brain (9, 10).

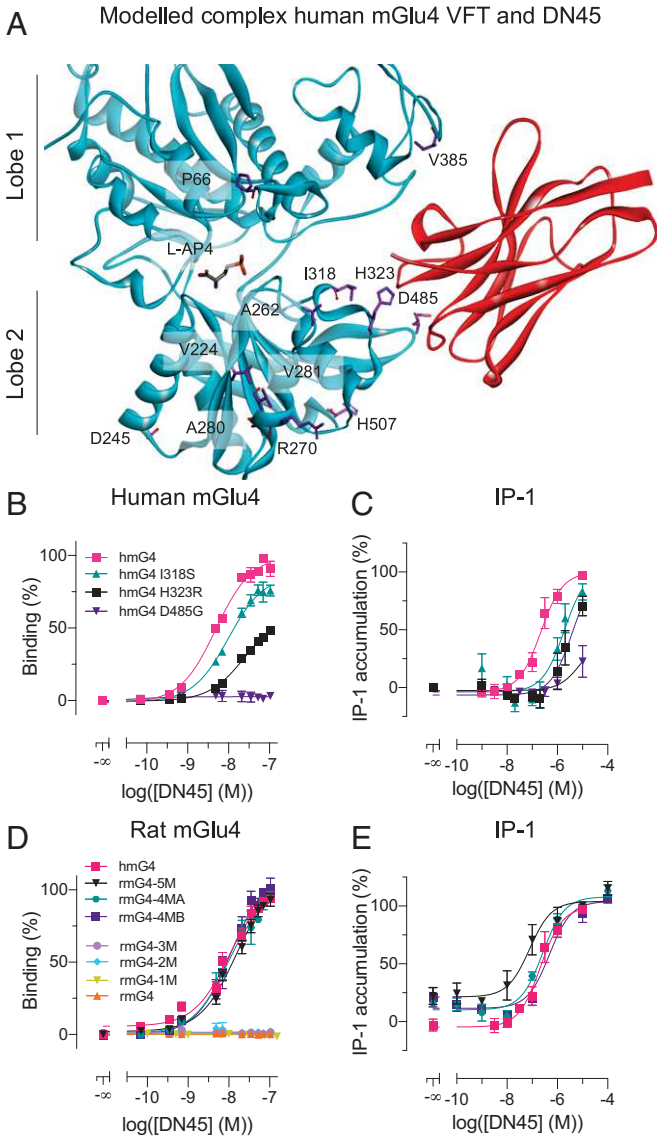


**Fig. 3.** Residues in lobe 2 of the human mGlu4 VFT confer subtype selectivity to DN45. *(A)* Front view of the closed conformation of the VFT of the human mGlu4 receptor, stabilized by DN45 (red) in the best-scored non-constrained docking followed by the 10-ns molecular dynamics simulation. Residues on the surface of the mGlu4 VFT that are specific for the human ortholog are highlighted in purple (side chains). *(B)* Binding of DN45 was determined in the TR-FRET binding assay as illustrated in Fig. 1*A* with human wild-type (hmG4) and mutated mGlu4 receptors (i.e., hmG4 I318S, hmG4 H323R, or hmG4 D485G) in the presence of 1 μM L-AP4. *(C)* Activation of the Gq pathway by hmG4, hmG4 I318S, hmG4 H323R, and hmG4 D485G with increasing concentrations of DN45. *(D)* Binding of DN45 to mutated rat mGlu4 receptors rmG4-5M ($K_D$ = 22.8 nM), rmG4-4MA ($K_D$ = 10.4 nM), and rmG4-4MB ($K_D$ = 13.6 nM) is not significantly different from binding to hmG4 ($K_D$ = 5.4 nM), and no binding is observed for rmG4-3M, rmG4-2M, rmG4-M1, or rmG4. *(E)* DN45 activation of the Gq pathway by rmG4-5M, rmG4-4MA, and rmG4-4MB. Data in *B–E* are mean ± SEM of three or more individual experiments. The $K_D$ values and statistical analysis for *B–E* was performed using an ordinary one-way ANOVA with Dunnett's multiple comparisons test and are presented in *SI Appendix*, Tables S1 and S2.

We first examined the binding of DN45 to the mGlu2-4 heterodimer using a combination of mGlu2 N-terminally labeled with CLIP-tag and carboxyl-terminal $GABA_{B1}$ endoplasmic reticulum retention sequence C1KKXX (21) (CLIP-mGlu2-C1KKXX) and mGlu4 N-terminally tagged with SNAP-tag and carboxyl-terminal $GABA_{B2}$ endoplasmic reticulum sequence C2KKXX (21) (SNAP-mGlu4-C2KKXX). After labeling CLIP-mGlu2-C1KKXX with Lumi4-Tb, binding of DN45 to the mGlu4 subunit should generate a TR-FRET signal between the Lumi4-Tb on the mGlu2 subunit and the d2 acceptor on an anti-c-Myc-antibody that binds to DN45 (Fig. 5*A*). A very low signal could be detected under basal condition that almost disappeared in the presence of the competitive antagonist LY341495 (Fig. 5*B*). However, a large signal could be measured in the presence of the mGlu4 agonist L-AP4, the general mGlu agonist glutamate, or the mGlu2 selective agonist LY379268 (Fig. 5*B*), revealing binding affinities of 5.0 nM, 3.1 nM, and 7.4 nM, respectively, close to the $K_D$ measured on the agonist-occupied mGlu4 homodimers (3.1 nM).

The effect of DN45 on the conformation of the mGlu2-4 heterodimer was then examined. Using CLIP-mGlu2-C1KKXX

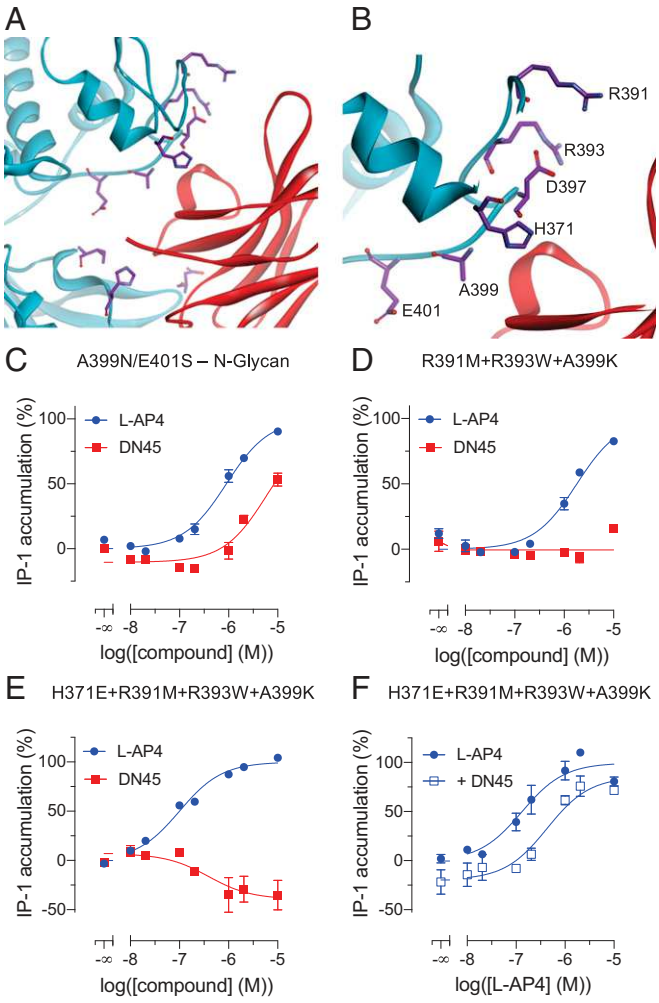


**Fig. 4.** DN45 agonist activity needs interactions with lobe 1 of the VFT. *(A)* A front view of the interactions between DN45 and lobe 1 and lobe 2 of the human mGlu4 receptor. Residues on lobe 1 in the loop spanning from H371 to E401 and residues I318, H323, and D485 are highlighted in purple (side chains). *(B)* A zoomed-in view of the loop comprising residues H371 to E401. *(C)* IP-1 production by L-AP4 (blue) and DN45 (red) of a human mGlu4 receptor bearing an *N*-glycosylation site at N399. *(D)* Effect of L-AP4 (blue) and DN45 (red) on IP-1 production by a human mGlu4 receptor bearing three mutations (i.e., R391M, R393W, and A399K). *(E)* Effect of L-AP4 (blue) and DN45 (red) on a human mGlu4 receptor bearing four mutations (i.e., H371E, R391M, R393W, and A399K). *(F)* Effect of L-AP4 alone (filled circles) and in the presence of 100 nM DN45 (open squares) on the activity of the quadruple hmGlu4 receptor mutant. Data of *C–F* are mean ± SEM of three individual experiments. Statistical analysis of *C* and F was performed using an unpaired one-tailed *t* test (*SI Appendix*, Table S2).

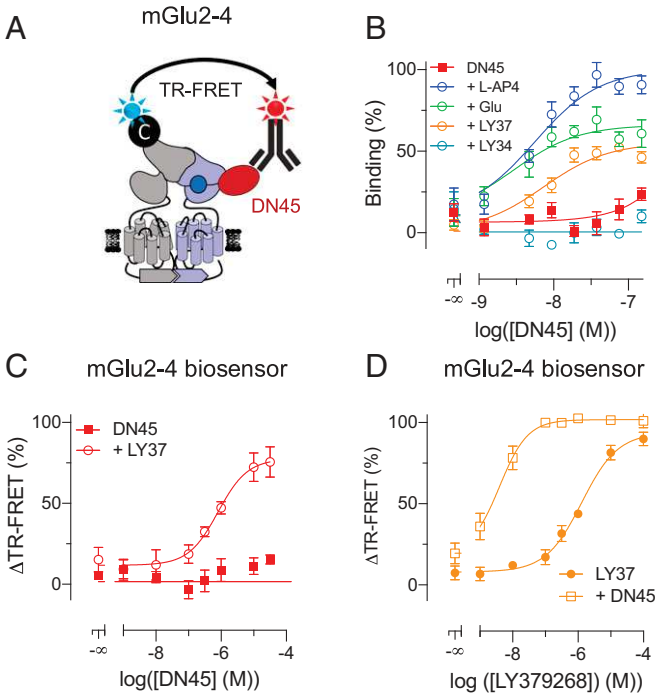


**Fig. 5.** DN45 acts as a positive allosteric modulator on heterodimeric mGlu2-4. *(A)* A cartoon representing a TR-FRET–based assay to measure binding of DN45 to the mGlu2-4 heterodimer using CLIP-mGlu2-C1KKXX and SNAP-mGlu4-C2KKXX. *(B)* Binding of DN45 to mGlu2-4 alone (red), in the presence of 100 μM mGlu4 antagonist LY341495 (light blue), of 1 mM glutamate (green), of 10 μM LY379268 (orange), or of 10 μM L-AP4 (blue). *(C)* Activation of the mGlu2-4 heterodimer by DN45 alone (red) or in the presence of the mGlu2 agonist LY379268 (50 nM) measured by a TR-FRET biosensor using CLIP-mGlu2-C1KKXX and SNAP-mGlu4-C2KKXX, labeled with 1 μM BC-Green and 100 nM BG-Lumi4Tb. Values are normalized to the maximal response to LY379268. *(D)* The response of LY379268 (filled circles) on the TR-FRET biosensor is potentiated by 10 μM DN45 (open squares). Values are normalized to the maximal response to LY379268. Data of *B–D* are mean ± SEM of three or more individual experiments. Statistical analysis of *B* was performed using an ordinary one-way ANOVA with Tukey's multiple comparisons test, and analysis of *D* was performed using an ordinary one-way ANOVA with Dunnett's multiple comparisons test (*SI Appendix*, Tables S1 and S2).

labeled with $O^6$-benzylcytosine (BC)-Lumi4Tb and SNAP-mGlu4-C2KKXX labeled with BG-Green, only the heterodimer generates a TR-FRET signal that is largely decreased upon activation (10, 18). As previously reported, the mGlu2 agonist LY379268 activated the heterodimer, while the mGlu4 agonist L-AP4 remains very partial (10, 18). DN45, on the other hand, could not activate the mGlu2-4 by itself (Fig. 5*C*). However, in the presence of 5% of the maximal effective concentration ($EC_5$) of LY379268 (50 nM), DN45 could activate the receptor, revealing a clear PAM effect (Fig. 5*C*). Indeed, DN45 largely increased the potency of the mGlu2 agonist LY379268 (Fig. 5*D*), demonstrating its potent pure PAM effect on the mGlu2-4 heterodimer.

## Discussion

The mGlu4 receptor has been proposed as a potential drug target for the treatment of Parkinson's disease (12, 22, 23) or pain (15). In the brain, mGlu4 can be found in a homodimeric form or associated with other mGlu subunits, like mGlu2, in heteromeric complexes. Using ligands with different properties at mGlu4 homo- and heterodimers, evidence has been provided supporting homodimers as the best targets for Parkinson's disease treatment (13). However, the respective role of both types of mGlu4 containing receptors remains to be clarified (8–10). In the present study, we report an mGlu4 nanobody with selective agonist activity at mGlu4 homodimers and with a pure PAM action on the mGlu2-4 heterodimers.

Nanobodies have become popular in pharmaceutical research. They have a high specificity and affinity and can stabilize specific conformations of their targets. Due to their small size compared to traditional IgG (~15 versus ~150 kDa), nanobodies have several advantages like lower immunogenicity, better pharmacokinetics, and the possibility to reach smaller cavities in proteins (3, 4). As such, nanobodies can stabilize specific conformations of their target, being interesting tools for structural studies (1) and innovative pharmacological agents (24). Moreover, some nanobodies can cross the blood–brain barrier and can then be used to target the central nervous system (25). Of course, nanobodies may have a much better subtype selectivity than orthosteric ligands acting at a binding site often conserved in various receptor subtypes activated by the same natural ligand. Most recently described nanobodies with pharmacological action at GPCRs act as antagonists (26, 27), as does the first Food and Drug Administration (FDA)-approved nanobody, caplacizumab (24).

Recently, nanobodies acting as selective PAMs for mGlu2 (11) and mGlu5 (28) homodimers were reported, the former having in vivo activities. Both nanobodies were found to stabilize the agonist-bound active orientation of the two VFTs of the dimers, with the mGlu2 nanobodies acting at the active interface of the VFTs (11), while the mGlu5 one acts on a loop on the top of the mGlu5 VFT (28). Here, we identified the mode of action of DN45 by combining state-of-the-art modeling and docking approaches and mutagenesis. We show that DN45 can stabilize the closed active state of each VFT in the mGlu4 homodimer, as the binding epitope includes residues from both lobe 1 and lobe 2. DN45, like L-AP4, increases the same proportion of mGlu4 in the active conformation, as shown by smFRET in the total absence of glutamate, demonstrating an agonist activity equivalent to that of L-AP4. While the primary binding epitope is located on lobe 2, further interaction between the VFT and DN45 occurs upon spontaneous closure of the VFT. These additional contacts increase the affinity of DN45 and lead to stabilization of the active state of the receptor, as does the agonist. This model is well supported by the observation that preventing contact between lobe 1 and the nanobody through mutations converts the nanobody into an antagonist or an inverse agonist, stabilizing the inactive receptor by preventing VFT closure. Taken together, our data confirm that stabilizing the closed VFTs is sufficient for receptor activation even in the absence of glutamate. Such a mode of action is, then, different from what has been proposed for the mGlu2 and mGlu5 PAM nanobodies and reveals ways for the development of selective agents acting at a specific mGlu subtype.

When tested on the mGlu2-4 heterodimer, DN45 was found unable to activate the receptor on its own. In contrast to the mGlu4 homodimer, on which two nanobodies are likely acting (one per VFT), only one is expected to bind to the heterodimer, on the mGlu4 VFT only. The fact that the nanobody cannot activate such a heterodimer suggests that the mGlu4 VFT may have less tendency to spontaneously close when associated with mGlu2. One may also consider the positive allosteric effect between each VFTs (21). The transient closure of one VFT may facilitate the closure of the other such that binding of a first nanobody may facilitate the binding of the second one in the homodimer, leading to the stabilization of the active state without agonist and then to the full agonist activity. Such an allosteric process is unlikely to occur in the heterodimer in the presence of DN45 alone, since DN45 only acts on one VFT. In agreement with this model, agonist binding in the mGlu2 VFT largely favored DN45 binding on the mGlu4 subunit. Such a model is consistent with the pure PAM effect of DN45 observed on the mGlu2-4 heterodimer.

Such a PAM action of DN45 on mGlu2-4 is also consistent with the effects of group-III agonists acting at the mGlu4 VFT. Indeed, L-AP4 could barely activate the heterodimer, while it largely

potentiates the effect of an mGlu2 agonist (10, 29). This supports the idea that the closure of the mGlu2 VFT is the driving force for the activation of the mGlu2-4 heterodimer that is then further stabilized in the active state through the closure of the mGlu4 VFT by DN45.

This model points to a transactivation mechanism within the mGlu2-4 receptor, as the mGlu4 TMD is mainly responsible for G-protein activation in this heterodimer (30). This is then similar to what is well established for the $GABA_B$ receptor in which GABA stabilizes the closed state of the GB1 VFT, leading to the G-protein activation by the GB2 7TM (31).

Overall, we describe a nanobody with a full agonist action at a GPCR. Such a tool will be useful to solve the active structure of human mGlu4. We show DN45 acts by stabilizing the closed state of the mGlu4 VFT by a distinct mode of action compared to other nanobodies that enhance the activity of class C GPCRs. Our study, then, provides insight into the activation mechanism of mGlu4 and mGlu2-4 receptors and illustrates how powerful nanobodies can be to decipher the function of these different receptor subtypes.

## Materials and Methods

Information on materials, llama immunization, selection, production, and purification of DN45, mutagenesis, cell culture and transfection, labeling of CLIP and SNAP-tag, the DN45 binding and selectivity assay, the IP-1 accumulation assay, the mGlu4 and mGlu2-4 biosensor assay, the BRET assay, statistical analysis, single-molecule FRET approach, and molecular modeling is provided in *SI Appendix*.

**Data Availability.** All data and associated protocols are available in the main paper and the *SI Appendix*. Materials described in this study are available upon request (to J.-P.P.).

**ACKNOWLEDGMENTS.** We thank the Arpège platform facilities at the Institut de Génomique Fonctionnelle for all fluorescence-based assays. J.-P.P. was supported by la Fondation pour la Recherche Médicale (Grant DEQ20170336747), Cisbio Bioassays (Eidos collaborative team Institut de Genomique Fonctionnelle-Cisbio, Grant 039293), the Fond Unique Interministériel (FUI) of the French government (grant Cell2Lead project), the Agence Nationale pour la Recherche (ANR) (Grant ANR-18-CE11-0004-01), and LabEx MAbImprove (Grant NR-10-LABX-5301). P.R. was supported by the ANR (Grant ANR-15-CE18-0020-01). J.-P.P., L.P., and P.R. were further supported by the Centre National de la Recherche Scientifique and the Institut National de la Santé et de la Recherche Médicale. P.C. and D.N. were supported by the FUI of the French government (FUI, Cell2Lead project). F.A. was supported by the Centre National de la Recherche Scientifique and the Science Ambassador Program from Dassault Système BIOVIA. J.H. was supported by a fellowship from la Région Occitanie and Cisbio Bioassays (TransACT, Grant 156544) and la Ligue contre le cancer (PhD Grant IP/SC-16487). J.F. was supported by la Fondation pour la Recherche Médicale (Grant DEQ20170336747). R.B.Q. was supported by a grant from the ANR (Grant ANR-18-CE11-0004-02). The Centre de Biologie Structurale belongs to the France-BioImaging national infrastructure supported by the ANR (Grant ANR-10-INBS-04, "Investments for the future").

1. K. D. Cromie, G. Van Heeke, C. Boutton, Nanobodies and their use in GPCR drug discovery. *Curr. Top. Med. Chem.* **15**, 2543–2557 (2015).
2. A. Gupta *et al*., Increased abundance of opioid receptor heteromers following chronic morphine administration. *Sci. Signal.* **3**, ra54 (2010).
3. C. J. Hutchings, M. Koglin, W. C. Olson, F. H. Marshall, Opportunities for therapeutic antibodies directed at G-protein-coupled receptors. *Nat. Rev. Drug Discov.* **16**, 787–810 (2017).
4. T. Hino *et al*., G-protein-coupled receptor inactivation by an allosteric inverse-agonist antibody. *Nature* **482**, 237–240 (2012).
5. A. S. Hauser, M. M. Attwood, M. Rask-Andersen, H. B. Schiöth, D. E. Gloriam, Trends in GPCR drug discovery: New agents, targets and indications. *Nat. Rev. Drug Discov.* **16**, 829–842 (2017).
6. J. Kniazeff, L. Prézeau, P. Rondard, J. P. Pin, C. Goudet, Dimers and beyond: The functional puzzles of class C GPCRs. *Pharmacol. Ther.* **130**, 9–25 (2011).
7. E. Doumazane *et al*., A new approach to analyze cell surface protein complexes reveals specific heterodimeric metabotropic glutamate receptors. *FASEB J.* **25**, 66–77 (2011).
8. J. Lee *et al*., Defining the homo- and heterodimerization propensities of metabotropic glutamate receptors. *Cell Rep.* **31**, 107605 (2020).
9. S. Yin *et al*., Selective actions of novel allosteric modulators reveal functional heteromers of metabotropic glutamate receptors in the CNS. *J. Neurosci.* **34**, 79–94 (2014).
10. D. Moreno Delgado *et al*., Pharmacological evidence for a metabotropic glutamate receptor heterodimer in neuronal cells. *eLife* **6**, 1–33 (2017).
11. P. Scholler *et al*., Allosteric nanobodies uncover a role of hippocampal mGlu2 receptor homodimers in contextual fear consolidation. *Nat. Commun.* **8**, 1967 (2017).
12. D. Charvin, $mGlu_4$ allosteric modulation for treating Parkinson's disease. *Neuropharmacology* **135**, 308–315 (2018).
13. C. M. Niswender *et al*., Development and antiparkinsonian activity of VU0418506, a selective positive allosteric modulator of metabotropic glutamate receptor 4 homomers without activity at mGlu2/4 heteromers. *ACS Chem. Neurosci.* **7**, 1201–1211 (2016).
14. P. Gubellini, C. Melon, E. Dale, D. Doller, L. Kerkerian-Le Goff, Distinct effects of mGlu4 receptor positive allosteric modulators at corticostriatal vs. striatopallidal synapses may differentially contribute to their antiparkinsonian action. *Neuropharmacology* **85**, 166–177 (2014).
15. B. Vilar *et al*., Alleviating pain hypersensitivity through activation of type 4 metabotropic glutamate receptor. *J. Neurosci.* **33**, 18951–18965 (2013).
16. C. Zussy *et al*., Dynamic modulation of inflammatory pain-related affective and sensory symptoms by optical control of amygdala metabotropic glutamate receptor 4. *Mol. Psychiatry* **23**, 509–520 (2018).
17. K. Even-Desrumeaux *et al*., Masked selection: A straightforward and flexible approach for the selection of binders against specific epitopes and differentially expressed proteins by phage display. *Mol. Cell. Proteomics* **13**, 653–665 (2014).
18. P. Scholler *et al*., HTS-compatible FRET-based conformational sensors clarify membrane receptor activation. *Nat. Chem. Biol.* **13**, 372–380 (2017).
19. R. Chen, L. Li, Z. Weng, ZDOCK: An initial-stage protein-docking algorithm. *Proteins* **52**, 80–87 (2003).
20. B. Pierce, Z. Weng, ZRANK: Reranking protein docking predictions with an optimized energy function. *Proteins* **67**, 1078–1086 (2007).
21. J. Kniazeff *et al*., Closed state of both binding domains of homodimeric mGlu receptors is required for full activity. *Nat. Struct. Mol. Biol.* **11**, 706–713 (2004).
22. S. Urwyler, Allosteric modulation of family C G-protein-coupled receptors: From molecular insights to therapeutic perspectives. *Pharmacol. Rev.* **63**, 59–126 (2011).
23. I. Sebastianutto, M. A. Cenci, mGlu receptors in the treatment of Parkinson's disease and L-DOPA-induced dyskinesia. *Curr. Opin. Pharmacol.* **38**, 81–89 (2018).
24. S. Duggan, Caplacizumab: First global approval. *Drugs* **78**, 1639–1642 (2018).
25. T. Li *et al*., Cell-penetrating anti-GFAP VHH and corresponding fluorescent fusion protein VHH-GFP spontaneously cross the blood-brain barrier and specifically recognize astrocytes: Application to brain imaging. *FASEB J.* **26**, 3969–3979 (2012).
26. S. Low *et al*., VHH antibody targeting the chemokine receptor CX3CR1 inhibits progression of atherosclerosis. *MAbs* **12**, 1709322 (2020).
27. C. McMahon *et al*., Synthetic nanobodies as angiotensin receptor blockers. *Proc. Natl. Acad. Sci. U.S.A.* **117**, 20284–20291 (2020).
28. A. Koehl *et al*., Structural insights into the activation of metabotropic glutamate receptors. *Nature* **566**, 79–84 (2019).
29. J. Levitz *et al*., Mechanism of assembly and cooperativity of homomeric and heteromeric metabotropic glutamate receptors. *Neuron* **92**, 143–159 (2016).
30. J. Liu *et al*., Allosteric control of an asymmetric transduction in a G protein-coupled receptor heterodimer. *eLife* **6**, 1–19 (2017).
31. T. Galvez *et al*., Allosteric interactions between GB1 and GB2 subunits are required for optimal $GABA_{(B)}$ receptor function. *EMBO J.* **20**, 2152–2159 (2001).

## Supplementary figures and tables

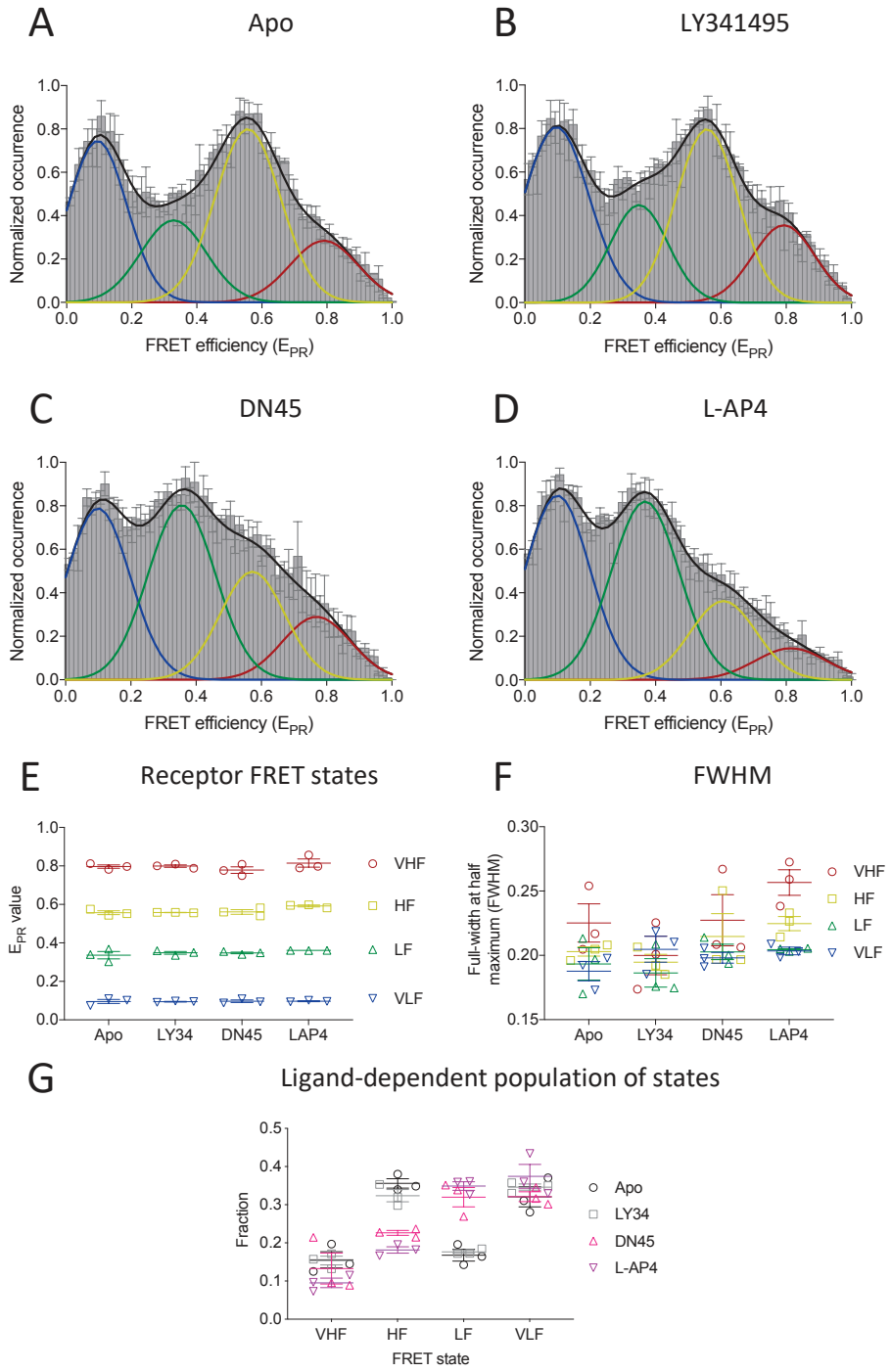


**Fig. S1.** Agonist action of DN45 nanobody on VFT reorientation analyzed by smFRET. *(A-D)* FRET efficiency histograms of mGlu4 dimers N-terminally SNAP-labeled with BG-Cy3b donor and BG-d2 acceptor fluorophores in the absence of ligand (Apo) or in the presence of DN45, LY341495 or L-AP4. The average global fit (black) as well as the very low FRET (VLF, blue), low FRET (LF, green), high FRET (HF, yellow)

and very high FRET (VHF, red) populations obtained by gaussian fitting using variable $E_{PR}$ and full width half maximum (FWHM) values are shown. E) Mean $E_{PR}$ and F) FWHM values for each of the four states under different ligand conditions. G) Fraction of each of the four states relative to all states under different ligand conditions. The histograms *A-D* show the mean number of molecules determined from three independent biological replicates each normalized to the maximum number per replicate with error bars given as SEM. Data of *E-G* are represented as mean ± SEM of three independent biological replicates.

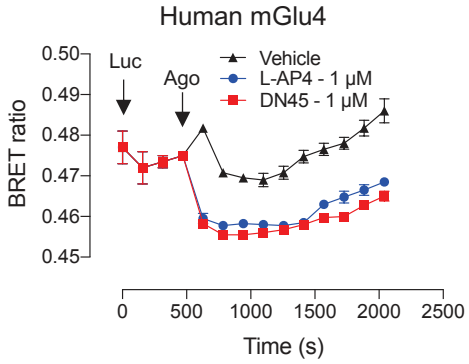


**Fig. S2.** Gi rearrangement kinetics visualized by change in BRET between Gαi-Rluc and Gγ-Venus. Signals were measured at 530 nm for the Venus and 480 nm for the Rluc. A basal signal was measured for 10 minutes after addition of coelenterazine (Luc). Next, the buffer and agonist conditions were added (Ago).

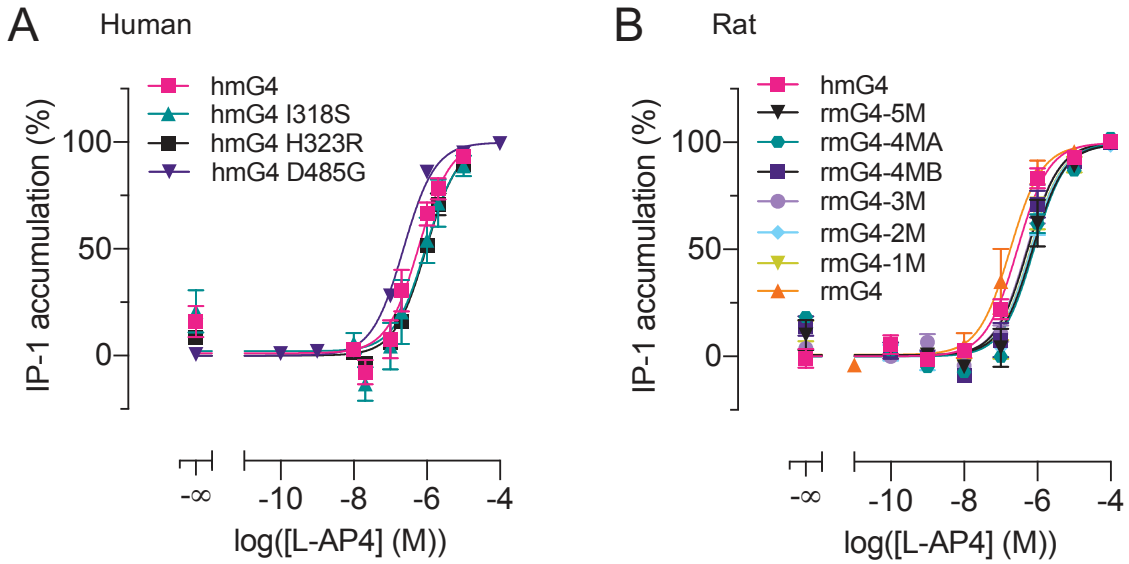


**Fig. S3.** Activation of human and rat mGlu4 constructs by L-AP4 in IP-1 accumulation assay. *(A)* IP-1 accumulation of human mGlu4 wild-type and mutated receptors. *(B)* IP-1 accumulation of the human and rat mGlu4 wild-type receptors and mutated rat mGlu4 receptors.

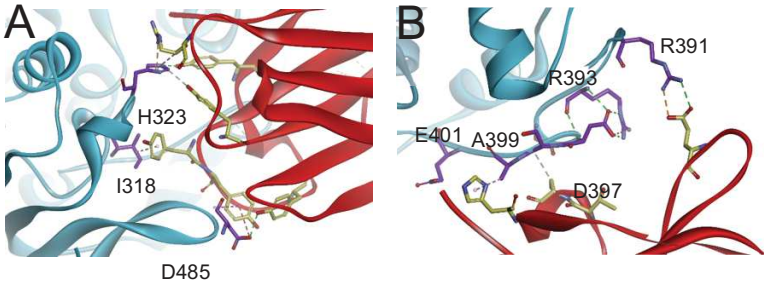


**Fig. S4.** Key interacting residues in the modelled complex of DN45 with human mGlu4 VFT (Fig. 3A). Residues of DN45 are displayed as yellow sticks, those of mGlu4 VFT in purple. *(A)* Lobe 2 and *(B)* lobe 1 interactions are shown as dashed lines (H-bonds are green, salt bridges are orange, hydrophobic interaction are purple).

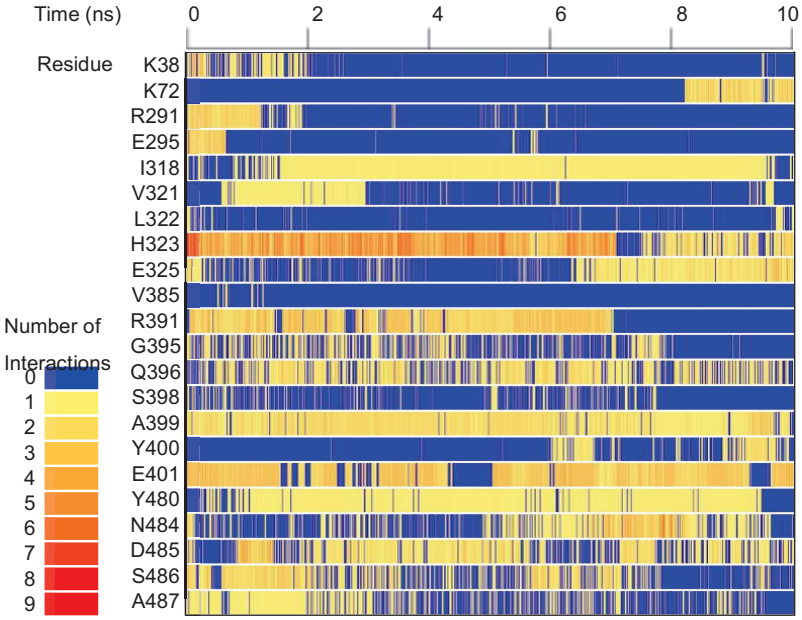


**Fig. S5.** Non-boned interactions as function of time for 10 ns molecular dynamics simulation of the docked DN45 mGlu4 complex for top interacting residues.

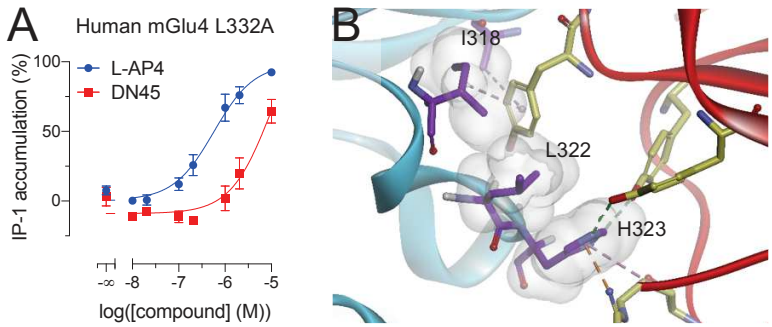


**Fig. S6.** Role of L322 in stabilizing interactions between the human mGlu4 VFT and DN45. *(A)* IP-1 accumulation induced by L-AP4 and DN45 on a human L322A mutated mGlu4 receptor. *(B)* Expanded view of Fig. 3A around residue L322 in the modelled complex of DN45 and the human mGlu4 VFT. Contacting residues in mGlu4 are displayed with light grey van der Waals surfaces.

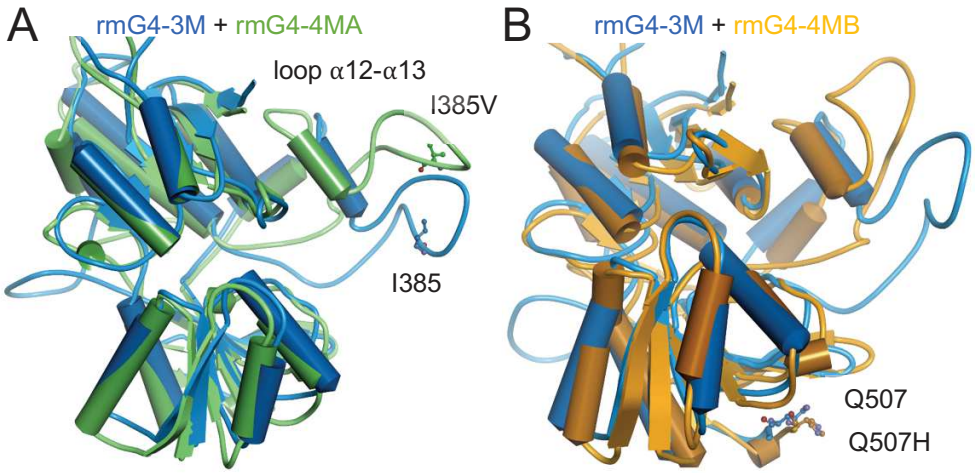


**Fig. S7.** Superimposition of VFTs of rmG4-3M and rmG4-4MA or rmG4-4MB models after 10 ns molecular dynamics simulation**.** *(A)* Superimposition of rmG4-3M and rmG4-4MA. *(B)* Superimposition of rmG4-3M and rmG4-4MB.

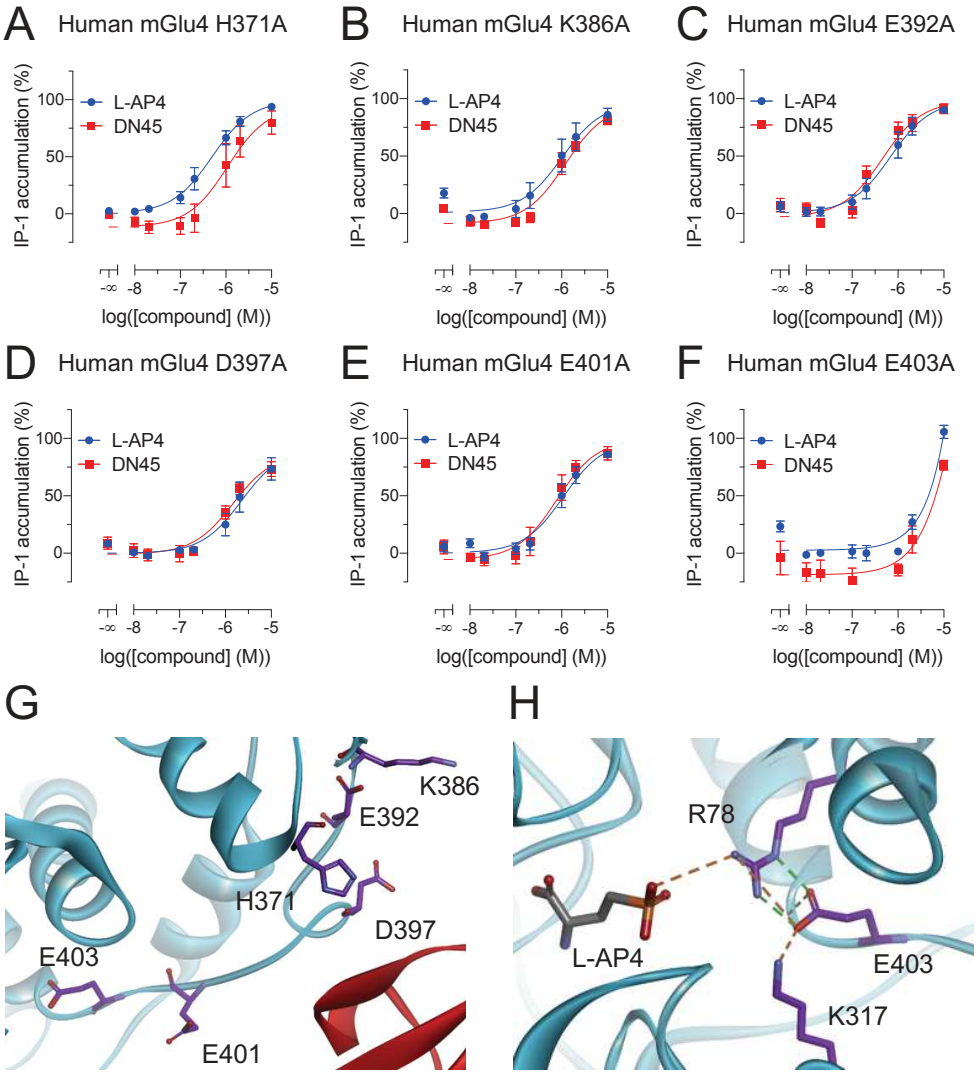


**Fig. S8.** Effect of alanine mutations on loop of lobe 1 of the human mGlu4 VFT. *(A-F)* Effect on the accumulation of IP-1 induced by L-AP4 and DN45 *(G-H)* 3D location of mutated residues in the modelled complex (Fig. 4). Note that E403 is stabilizing critical residues (R78 and K317) for L-AP4 binding explaining the decreased activation shown in panel F.

**Table S1.** Affinity ($pK_D$) and standard error of the mean (SEM) of DN45 for the different mGlu4 constructs. The used statistical analysis is mentioned in the main figure legends and values are compared with the control unless stated otherwise.

| Fig. | Receptor | Condition | pKD ± SEM | N | P-value |
|---|---|---|---|---|---|
| 1D | hmG4 | + 10 µM L-AP4 | 8.53 ± 0.09 | 3 | - |
| 3B | hmG4 | + 1 µM L-AP4 | 8.29 ± 0.02 | 3 | Control |
| | hmG4 I318S | + 1 µM L-AP4 | 8.00 ± 0.07 | 3 | 0.0168 |
| | hmG4 H323R | + 1 µM L-AP4 | 7.60 ± 0.06 | 3 | 0.0002 |
| 3D | hmG4 | + 1 µM L-AP4 | 8.28 ± 0.06 | 5 | Control |
| | rmG4-5M | + 1 µM L-AP4 | 7.70 ± 0.11 | 6 | 0.4613 |
| | rmG4-4MA | + 1 µM L-AP4 | 8.01 ± 0.10 | 3 | 0.9801 |
| | rmG4-4MB | + 1 µM L-AP4 | 7.93 ± 0.17 | 3 | 0.8392 |
| 5B | mGlu2-4 | + 10 µM L-AP4 | 8.34 ± 0.09 | 5 | (L-AP4 vs Glu) = 0.1130 |
| | | + 1 mM Glutamate | 8.54 ± 0.10 | 5 | (Glu vs LY37) = 0.0259 |
| | | + 10 µM LY379268 | 8.14 ± 0.07 | 3 | (LY37 vs L-AP4) = 0.4757 |

**Table S2.** Potency ($pEC_{50}$) and standard error of the mean (SEM) for the different mGlu4 constructs. The used statistical analysis is mentioned in the main figure legends and values are compared with the control.

| Fig. | Receptor | Condition | pEC50 ± SEM | N | P-value |
|---|---|---|---|---|---|
| 2A | hmG4 | L-AP4 | 6.12 ± 0.03 | 3 | Control |
| | | DN45 | 6.57 ± 0.23 | 3 | 0.1222 |
| 2C | hmG4 | L-AP4 | 7.22 ± 0.03 | 3 | Control |
| | | DN45 | 7.22 ± 0.11 | 3 | 0.9505 |
| 2D | hmG4 | L-AP4 | 6.54 ± 0.10 | 3 | Control |
| | | DN45 | 6.65 ± 0.21 | 3 | 0.6674 |
| | | Glutamate | 4.59 ± 0.15 | 3 | - |
| 2F | hmG4 | L-AP4 | 6.16 ± 0.18 | 4 | Control |
| | | + 5 nM DN45 | 5.96 ± 0.12 | 4 | 0.7166 |
| | | + 10 nM DN45 | 6.19 ± 0.19 | 4 | 0.9990 |
| | | + 100 nM DN45 | 5.74 ± 0.07 | 3 | 0.4949 |
| 3C | hmG4 | DN45 | 6.63 ± 0.20 | 3 | Control |
| | hmG4 I318S | DN45 | 5.68 ± 0.23 | 3 | 0.1794 |
| | hmG4 H323R | DN45 | 5.07 ± 0.54 | 3 | 0.0367 |
| 3E | hmG4 | DN45 | 6.65 ± 0.21 | 3 | Control |
| | rmG4-5M | DN45 | 6.59 ± 0.54 | 3 | 0.7939 |
| | rmG4-4MA | DN45 | 6.59 ± 0.02 | 3 | 0.9977 |
| | rmG4-4MB | DN45 | 6.31 ± 0.08 | 3 | 0.7524 |
| 4C | hmG4 (A399N/E401S - N-Glycan) | L-AP4 | 6.05 ± 0.08 | 3 | Control |
| | rmG4-4MA | DN45 | 5.18 ± 0.19 | 3 | 0.0070 |
| 4D | hmG4 (R391M+R393W+A399K) | L-AP4 | 5.74 ± 0.06 | 3 | - |
| 4E | hmG4 | L-AP4 | 7.00 ± 0.01 | 3 | - |
| | (H371E+R391M+R393W+A399K) | DN45 | 6.37 ± 0.06 | 3 | - |
| 4F | hmG4 | L-AP4 | 6.85 ± 0.16 | 3 | Control |
| | (H371E+R391M+R393W+A399K) | + DN45 | 6.33 ± 0.13 | 3 | 0.0351 |
| 5C | mGlu2-4 | + LY37 | 6.11 ± 0.19 | 3 | - |
| 5D | mGlu2-4 | LY37 | 6.02 ± 0.14 | 5 | Control |
| | | + 10 µM DN45 | 8.49 ± 0.14 | 4 | <0.0001 |

**Table S3.** Fraction and standard error of the mean (SEM) for single-molecule FRET analysis. The statistical analysis is mentioned in the main figure legend and values are compared to the control unless stated otherwise.

| Fig. | Receptor | Condition | Fraction ± SEM | N | P-value |
|---|---|---|---|---|---|
| 2B | hmG4 | Apo | 0.320 ± 0.025 | 3 | Control |
| | | LY34 | 0.353 ± 0.012 | 3 | 0.3263 |
| | | DN45 | 0.584 ± 0.014 | 3 | <0.0001 |
| | | L-AP4 | 0.658 ± 0.005 | 3 | <0.0001 |
| | | DN45 v. L-AP4 | | | 0.0073 |

**Table S4.** Impact on the binding of DN45 to hmGlu4 and overall stability of folding of the complex upon virtual mutation of twelve human residues to corresponding rat residues at the end of 10 ns simulation.

| # | Human | Rat | Mutation energy binding (kcal/mol) | Effect | Mutation energy stability (kcal/mol) | Effect |
|---|---|---|---|---|---|---|
| 66 | P | A | 0.07 | Neutral | 0.54 | Destabilizing |
| 224 | V | L | -0.04 | Neutral | 1.22 | Destabilizing |
| 245 | D | N | 0.12 | Neutral | 0.53 | Destabilizing |
| 262 | A | T | 0.11 | Neutral | -0.42 | Neutral |
| 270 | R | K | 0.02 | Neutral | 0.06 | Neutral |
| 280 | A | G | 0.09 | Neutral | 1.97 | Destabilizing |
| 281 | V | I | 0.01 | Neutral | -0.06 | Neutral |
| 385 | V | I | 0.01 | Neutral | -1.23 | Stabilizing |
| 507 | H | Q | 0.01 | Neutral | -0.3 | Neutral |
| 318 | I | S | 1.55 | Destabilizing | 3.14 | Destabilizing |
| 323 | H | R | 2.96 | Destabilizing | 2.92 | Destabilizing |
| 485 | D | G | 0.69 | Destabilizing | 0.89 | Destabilizing |

**Table S5.** Predicted difference in binding energy of DN45 to rat mGlu4 upon mutation of 5 selected rat residues to corresponding human residues.

| # | Rat | Human | Mutation energy binding (kcal/mol) | Effect |
|---|---|---|---|---|
| 385 | I | V | 0.02 | Neutral |
| 507 | Q | H | 0.02 | Neutral |
| 318 | S | I | -1.04 | Stabilizing |
| 323 | R | H | -2.52 | Stabilizing |
| 485 | G | D | -0.81 | Stabilizing |

# 11 DISCUSSION

## 11.1 INTRODUCTION

In this thesis, fluorescent biosensors were developed for studying conformational dynamics and pharmacology of transmembrane dimeric receptors. By using HTRF®-based techniques we provided insights in the role of dimerization on the function of transmembrane dimeric receptors, illustrated by the EGF receptor and mGlu4 receptor. HTRF® is a technique that is used for studying GPCR or receptor tyrosine kinase (RTK) activation pathways, receptor internalization, binding of ligands to GPCRs or kinases, cytokine release and protein interactions.[xvii] This technique has been discussed in '*Chapter 8: Materials and Methods*'. The toolbox that was generated in our team, providing multiple GPCRs and RTKs conformational biosensors, was a starting point for this thesis (Scholler, Moreno-Delgado, et al. 2017).

RTKs and GPCRs being the main drug targets, make them highly relevant to work on (Rask-Andersen, Masuram, and Schiöth 2014). Actually, both the EGF receptor and mGlu4 receptor are still subject to discussions about their conformation, dimerization, activation process and pharmacology. Innovative HTRF®-based conformational biosensors allow us to perform pharmacological investigations that could elucidate these processes.

### 11.1.1 Transactivation by GPCRs through intracellular ligand-free activation of the EGF receptor

Interestingly, it has been shown that GPCRs and the EGF receptor can cross-talk, or even associate, leading to a cross regulation of the activation and activity. Thus, understanding their respective activation and dimerization mechanism will also help understanding their complex cross-talk. Through transactivation of the EGF receptor, it has been shown that GPCRs are implicated in mitogenic signalling (Cattaneo et al. 2014), among them the mGlu5 receptor (Peavy et al. 2001), $GABA_B$ receptor (X. S. et al. 2017) and β2 adrenergic receptor (Drube et al. 2006; Maudsley et al. 2000). Transactivation occurs by two main pathways: 1) GPCR-dependent activation of a matrix metalloproteinase (MMP) and subsequent release of membrane-bound RTK agonists (Palanisamy et al. 2021), 2) GPCR-dependent activation of intracellular nRTKs (like the Src-family) and subsequent phosphorylation of RTKs on the intracellular domain (Fig. 33) (Liebmann 2011). Conversely, RTKs (i.e. IGF1-R) can also control GPCR (i.e. PACAP receptor) activity though transactivation (Delcourt et al. 2007). Importantly, transactivation increases the complexity of GPCR signalling and links them to many different physiological processes. Additionally, it shows that the EGF receptor can be activated via its intracellular domain, independently of its extracellular domain.

[xvii] https://fr.cisbio.eu/content/htrf-technology-basics

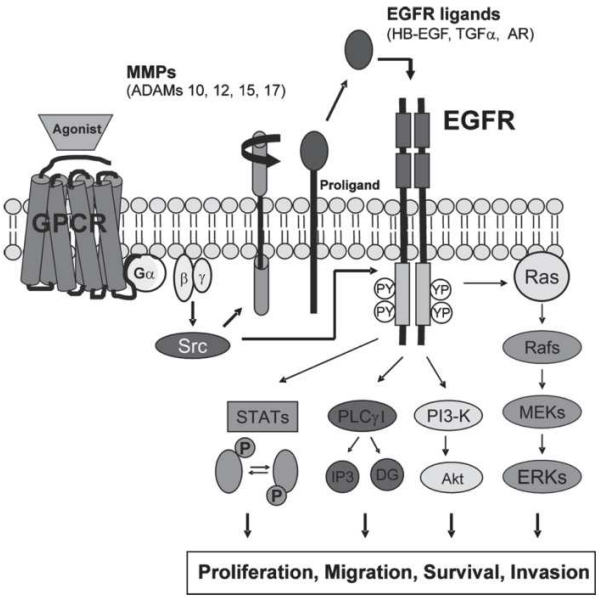


**Figure 33:** Transactivation of the EGF receptor by GPCRs. This image is copied from Liebmann *et al.* (2011) with permission from Elsevier.

## 11.2 EGF RECEPTOR DIMERIZATION, INTERNALIZATION AND FUTURE THERAPIES

### 11.2.1 EGF receptor activation process

The activation process of the EGF receptor remains a debated subject. The ligand-free EGF receptor has been described as mainly monomeric (Chung et al. 2010), dimeric (I. Maruyama 2014) or a mixture of monomers and dimers (Zanetti-Domingues et al. 2018) available for agonist binding. Through allosteric interactions, which is either leading to the availability of the dimerization arm and subsequent dimerization (Ferguson 2008) or a rotation of the TM domain (I. Maruyama 2014), two TK domains re-orientate into an asymmetric conformation, which is the active conformation of the receptor. During the thesis, we provide evidence that the EGF receptor is mainly monomeric, and that agonists induce dimer formation, rather than a conformational change on a pre-formed dimer.

In our study, we have used EGF receptor subunits with an N-terminal SNAP-tag labelled with a FRET compatible fluorophore pair to measure intersubunit FRET. We observed an increase in FRET after stimulation with some TK inhibitors and an even larger increase in FRET after stimulation with agonists. Because of the sensitivity of HTRF® for changes in FRET pair distance, this increase in FRET could be from ligand-induced dimerization as well as conformational changes. However, there are three main reasons, why the increase in FRET corresponds to ligand-induced dimerization:

Firstly, we showed that dimerization of the EGF receptor could be through the intracellular domain exclusively on an EGF receptor mutant lacking its dimerization arm. This proved that the intracellular domain is sufficient for dimer formation.

Secondly, an EGF-competitive antibody, cetuximab, that binds subdomains I and III, thereby preventing the appearance of the dimerization arm, was incubated with the EGF receptor. We showed that, while cetuximab is bound to the EGF receptor, TK inhibitors still induce intersubunit FRET with the same amplitude as without cetuximab. This proved that the induced intersubunit FRET by TK inhibitors is independent of the conformation of the extracellular domain.

Thirdly, we measured the excited-state lifetime of the FRET donor in presence of acceptor, the sensitized acceptor emission, and found that despite the difference in FRET amplitude induced by agonist and TK inhibitors, the lifetime of the sensitized acceptor emission remained the same. This means that the FRET efficiency was not changed and the difference in amplitude of the signal is due to a different number of receptors in FRET.

Overall, we concluded that: 1) the EGF receptor mainly follows ligand-induced dimerization, rather than ligand-induced conformational changes on a pre-formed dimer (Fig. 34A) and 2) the number of receptors in FRET can be modulated in a dose-dependent manner with TK inhibitors or agonist.

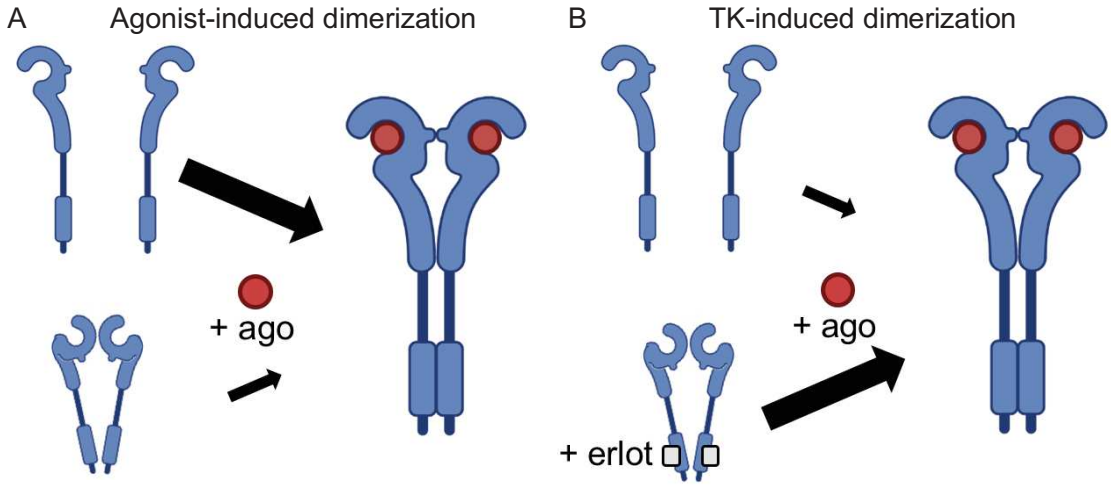


**Figure 34**: The activation process of the EGF receptor. A) Agonist-induced activation of the EGF receptor mainly follows ligand-induced dimerization. B) First-generation TK inhibitors and dacomitinib induce dimer formation, thereby altering the EGF receptor activation process. A TK inhibitor that induces dimer formation is represented in grey and "+ erlot".

### 11.2.2 A link between dimerization and internalization

In our experiments, we showed that AG1478, erlotinib, gefitinib, PD153035 and dacomitinib induce dimer formation, whereas lapatinib, GW583340, and osimertinib did not. The group of TK inhibitors that induce dimer formation all have small hydrophobic domains, thus they do not extend into the back of the cleft of the TK domain, thereby stabilizing an active conformation. Importantly, these TK inhibitors change the agonist-induced activation process of the EGF receptor by inducing dimer formation without activating the EGF receptor (Fig. 34B). Logically, this raised the question whether these groups may induce differential effects on the EGF receptor.

We determined phosphorylation of Y1068 of the EGF receptor and phosphorylation of ERK1/2 to measure *wild-type* EGF receptor activation. Except osimertinib, all TK inhibitors inhibited TK activity of the EGF receptor efficaciously, thereby not revealing any differential effect that could be linked to dimer formation. When measuring EGF-induced internalization of the EGF receptor, we did two exciting findings. Firstly, none of the TK inhibitors could fully inhibit EGF-induced internalization. Secondly, only TK inhibitors that

induce dimer formation could slow down EGF-induced internalization (i.e. maximal inhibition is around 50%).

For agonists, the induced internalization is dose-dependent, however in presence of TK inhibitors, and thus no or low Y1068 phosphorylation levels, internalization was not inhibited. This implies that internalization is not a direct consequence of Y1068 phosphorylation of the EGF receptor nor of the TK domain activity. This is supported by the finding that only TK inhibitors that induce dimer formation are capable of slowing down internalization, independently of the inhibition of TK activity. Previously, it was reported that EGF receptor internalization can follow clathrin-mediated and clathrin-independent endocytosis, which is regulated by a kinase, p38 (Tanaka et al. 2018). p38 phosphorylates inactive EGF receptors (monomers) and sorts them for recycling, whereas activated dimeric EGF receptors are degraded. As such, p38 could regulate EGF receptor sorting in case of no or low amounts of phosphorylation on the C-tail. Through this mechanism, inactive EGF receptor dimers (TK inhibitor-induced) could be sorted for recycling (Fig. 35A).

Additionally, dimer stability is important for EGF receptor signalling and may also be for internalization (Kiyatkin et al. 2020). Full agonists for the EGF receptor induce stable dimers, thereby swiftly activating the EGF receptor. As a consequence, negative feedback mechanisms like receptor dephosphorylation or internalization may occur (Fig. 35B) (Freed et al. 2017). In contrast, partial agonists like EREG and EPN, induce less stable dimers, resulting in sustained signalling and impaired internalization (Fig. 35A) (Freed et al. 2017). Arguably, some TK inhibitors that slow down internalization, induce less-stable dimers. This would be in line with increased negative cooperativity of EGF binding in presence of erlotinib compared to lapatinib (Hajdu et al. 2020). Importantly, erlotinib stabilizes both the active and inactive conformation of the TK domain (J. H. Park et al. 2012), resulting in an equal mix of symmetric and asymmetric TK domains (Fig. 35C). On the contrary, lapatinib only binds inactive TK domains (E. R. Wood et al. 2004), thereby stabilizing more symmetric TK domains (i.e. inactive-inactive) (Fig. 35D). Because of the absence of TK activity in presence of these TK inhibitors, we assume that most EGF receptors are bound by these TK inhibitors. Nevertheless, only half of the maximal signal could be inhibited by erlotinib, corresponding to half of the receptors. In agreement with this data, we propose that in presence of TK inhibitors only symmetric TK domains are internalized and asymmetric TK domains are less internalized (Fig. 35C, D). Unfortunately, we did not evaluate the physiological effects of these observations as this requires much additional work.

Overall, we have shown that the EGF receptor mainly follows ligand-induced dimerization in its activation process. The activation process can be altered by TK inhibitors that induce dimer formation. Despite most of the TK inhibitors block TK activity of the EGF receptor and phosphorylation of ERK1/2, internalization cannot be fully inhibited by TK inhibitors. This suggests that internalization is a process that is not a direct

consequence of the TK activity of the EGF receptor. Strikingly, only TK inhibitors that induce dimer formation slow down internalization. We propose that EGF-induced internalization is less favourable in presence of TK inhibitors that asymmetrically stabilize dimers (e.g. erlotinib) at the TK domain level. Taken together, our data support a link between EGF receptor dimerization and internalization.

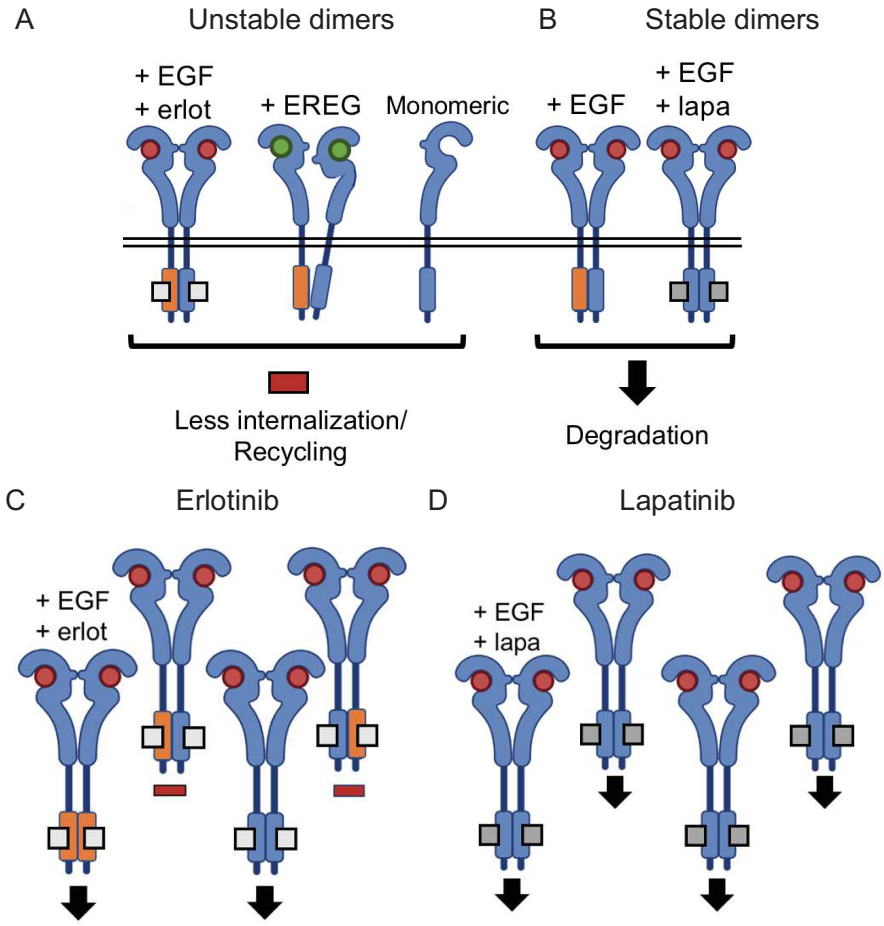


**Figure 35:** Hypothesis about the role of stability of dimers and dimerization status on internalization. A) Unstable dimers are less internalized or more recycled. B) Stable dimers are internalized and degraded. C) Erlotinib induces symmetric and asymmetric dimers. A portion of the erlotinib-induced dimers are less internalized. D) Lapatinib induces more symmetric dimers. Orange TK domains represent the active conformation and blue TK domains represent the inactive conformation.

### 11.2.3 Improving TK inhibitors

TK inhibitor-induced dimer formation may be an underexposed feature that alters the activation process of the EGF receptor and should be investigated further to understand its physiological relevance. In general, the EGFR family is targeted by many therapies (Table 4). Among them are the first EGF receptor TK inhibitor, gefitinib, and the first medicinal monoclonal antibody, trastuzumab (i.e. targeting the HER2). Both therapies significantly increase patient overall survival (Suzuki et al. 2013; Tang et al. 2019). Especially for TK inhibitors targeting the EGF receptor, an initial successful treatment period is followed by resistance to TK inhibitors. Resistance is due to different mechanisms, among them EGF receptor mutations in the TK domain, histological change and epithelial-to-mesenchymal transition (EMT) (Lindsey and Langhans 2015). The appearance of mutations in the TK domain are common. In between 10-35% of NSCLC-patients bear a primary mutation in the *EGFR* gene (i.e. 90% of these mutations are L858R or exon19del). Primary mutations increase sensitivity to first-generation TK inhibitors (i.e. erlotinib, gefitinib) (Lynch et al. 2004) and dacomitinib (Lau et al. 2019).

Additional mutations, that cause resistance to first and second-generation TK inhibitors, are common. The most common mutation is T790M (Pao et al. 2005), rendering resistance to first and second-generation TK inhibitors and subsequent C797S, causing resistance to covalent third-generation TK inhibitors (Grabe, Lategahn, and Rauh 2018). Therefore, new TK inhibitors of the EGF receptor need to be developed, overcoming resistance. Four possible ways to overcome resistance are: 1) by increasing the affinity of TK inhibitors for these mutants, 2) by using irreversible TK inhibitors, 3) by targeting a different binding pocket or 4) by combining TK inhibitors with a probe targeting the receptor for degradation.

1) Increasing affinity of TK inhibitors for mutations was applied for the design of third-generation TK inhibitors like osimertinib or rociletinib. These compounds are efficacious on the EGF receptor bearing T790M. It is however likely that new resistance could appear to these compounds, as is the case with C797S. C797S substitutes the residue that is covalently linking these TK inhibitors to the EGF receptor (Grabe, Lategahn, and Rauh 2018).

2) Generating irreversible TK inhibitors was also applied for the design of third-generation TK inhibitors and second-generation TK inhibitor dacomitinib. The appearance of C797S is also likely after treatment with irreversible TK inhibitors, thereby encountering the same problem as third-generation TK inhibitors (Grabe, Lategahn, and Rauh 2018).

3) Targeting a different binding pocket may be a promising strategy, as is the case for allosteric inhibitor EAI045 (Wang, Song, and Liu 2017). Its efficacy combined with cetuximab is still under investigation (Jia

et al. 2016; Maity, Pai, and Nayak 2020). Importantly, EAI045 is limited to the L858R primary mutation and not exon19del (Grabe, Lategahn, and Rauh 2018).

4) Combining TK inhibitors with an E3 ubiquitin ligase ligand-probe sorting the receptor for degradation (PROTAC), may be the most promising strategy (H. Zhang et al. 2020). By not or slightly inhibiting EGF receptor activity with allosteric inhibitors, resistance mechanism may be less induced and the low efficacy of EAI045 could be an advantage (Annex VI, Annex Fig. 6). Importantly, the number of EGF receptors is decreased by PROTAC, thereby reducing oncogenic signalling (Iradyan et al. 2019). An additional advantage is, that EAI045 is selective for the EGF receptor bearing T790M, thereby reducing potential *wild-type* EGF receptor-mediated side effects (Wang, Song, and Liu 2017).

| Drug | Compound | Target | Domain | Irreversible | Generation |
|---|---|---|---|---|---|
| Erlotinib | Small molecule | EGFR, $EGFR_{L858R}$ | TKD (Act./Inact.) | No | I |
| Gefitinib | Small molecule | EGFR, $EGFR_{L858R}$ | TKD (Act./Inact.) | No | I |
| PD153035 | Small molecule | EGFR, $EGFR_{L858R}$ | TKD (Act./Inact) | No | I |
| Dacomitinib | Small molecule | EGFR, $EGFR_{L858R}$, HER2 | TKD (Act./Inact.) | Yes: C797 | II |
| Lapatinib | Small molecule | EGFR, $EGFR_{L858R}$, HER2 | TKD (Inact.) | No | II |
| GW583340 | Small molecule | EGFR, $EGFR_{L858R}$, HER2 | TKD (Inact.) | No | II |
| Osimertinib | Small molecule | EGFR, $EGFR_{L858R}$, $EGFR_{L858R\ or\ exon19del/T790M}$ | TKD (Inact.) | Yes: C797 | III |
| EAI045 | Small molecule | $EGFR_{L858R/T790M(/C797S)}$ | TKD (Inact.) | No | Allosteric |
| Cetuximab | mAntibody | EGFR | ECD | No: Antibody | - |
| Trastuzumab | mAntibody | HER2 | ECD | No: Antibody | - |

**Table 4:** EGF receptor drugs. mAntibody means monoclonal antibody. EGFR means EGF receptor, HER2 means Human EGF receptor 2, TKD means Tyrosine kinase domain, Act. means active, Inact. means inactive, ECD means Extracellular domain.

### 11.2.4 Current and future clinical approaches

Improvement in treatment strategies are always ongoing, as is shown by the FLAURA (AstraZeneca & Paraxel, NCT02296125, 2014) (Ohe et al. 2019) and FLAURA2 (AstraZeneca, NCT04035486, 2019) clinical studies. Osimertinib has a preferred pharmacological and pharmacokinetic profile than first-generation TK inhibitors. Its affinity is better (i.e. 200 times) for double-mutated EGF receptor over *wild-type*, thereby reducing *wild-type* EGF receptor-related side effects (Cross et al. 2014). Besides, due to its favourable pharmacokinetics it crosses the BBB better than other TK inhibitors, and could inhibit potential brain metastases (Le and Gerber 2019).

In the FLAURA study, osimertinib was compared to erlotinib/gefitinib as first-line treatment strategy in advanced (i.e. stage IIIA, IIIB or IV) NSCLC. Osimertinib-treated patients had a progression-free survival[xviii] of 19.1 months compared to 13.8 months for gefitinib-treated patients, showing that osimertinib is superior as first-line therapy over gefitinib (Ohe et al. 2019). In the FLAURA2 study, which is still ongoing, the efficacy of osimertinib treatment with or without platinum/pemetrexed-based chemotherapy is under investigation. Some well-known chemotherapies are platinum complexes, 5-fluorouracil (5-FU) or permetrexed. Platinum complex chemotherapy is based on cross-linking platinum-based compounds (e.g. cisplatin) with the DNA, thereby preventing transcription of DNA into RNA and inducing apoptosis (Johnstone, Park, and Lippard 2014). 5-FU and permetrexed are other commonly used chemotherapies. Their main mechanism of action is to inhibit thymidylate synthase (TS), an enzyme that is implicated in DNA synthesis. Inhibition of TS leads to toxic imbalances of nucleotides and RNA and DNA damage, resulting in cell death (Longley, Harkin, and Johnston 2003). Much is expected from the FLAURA2 study as gefitinib and erlotinib had shown superior efficacy when combined with platinum/pemetrexed-based chemotherapy (Planchard et al. 2020; S. Liu et al. 2018). A meta-analysis showed that by combining first-line EGF receptor TK inhibitors (i.e. gefitinib/erlotinib) with chemotherapy, the objective response rate (ORR)[xix] is significantly increased (ORR = 1.18) compared to EGF receptor TK inhibitor monotherapy (Q. Wu et al. 2021). Despite an increase in chemotherapy-induced toxicity, treatment was well tolerated. Side effects of TK inhibitor treatment[xx] and chemotherapy[xxi] are present, but the combined treatment does not increase each other's' side effects, whilst efficacy of the treatment is increased (Q. Wu et al. 2021). Overall, current and future clinical approaches for treating advanced NSCLC seem to focus more on osimertinib and less on first-generation TK inhibitors. Combination therapy with chemotherapy is promising due to increased efficacy of the treatment, whilst side effects are not synergistically increased.

[xviii] The length of treatment in which the disease does not progress
[xix] The response rate of a treatment compared to another treatment (relative value)
[xx] Anemia, liver dysfunction, skin rash, diarrhea
[xxi] Thrombocytopenia, leukopenia, neutropenia, nausea and vomiting

### 11.2.5 Monomer preference for EGF receptor treatment

Even when focusing exclusively on the EGF receptor as target, combined therapy could improve treatment efficacy. There may be a central role for monoclonal antibodies like cetuximab.

Cetuximab is already used as treatment of several cancers, including NSCLC and cancers in the head and neck. Its mechanism of action is multivalent: firstly, cetuximab is a competitive antagonist for EGF receptor agonists, thereby reducing the apparent affinity of EGF for the EGFR. Secondly, it prevents the exposure of the dimerization arm, thereby inhibiting agonist-induced dimerization (S. Li et al. 2005). This leads to inhibition of phosphorylation and subsequent activation of the EGF receptor. Thirdly, cetuximab induces antibody-dependent cellular cytotoxicity (ADCC). ADCC is an immune response mediated by natural killer cells, targeted against antibodies bound to the cell surface (Kimura et al. 2007).

When cetuximab was combined with a TK inhibitor that induces dimer formation (i.e. dacomitinib or afatinib), tumour growth significantly decreased more than monotherapy of cetuximab or TK inhibitor alone(Oashi et al. 2019). This report provides evidence for the importance of the ability of TK inhibitors to induce dimer formation. It suggests that especially first-generation TK inhibitors (AG1478, gefitinib, erlotinib, PD153035) could benefit from combinatorial therapy with cetuximab.

Combining cetuximab with the newest generation of TK inhibitors, the allosteric TK inhibitors, has also been proposed as novel therapy. Especially, the novel "4$^{th}$ generation" TK inhibitor EAI045 retains much attention. EAI045 has a 1000-fold selectivity for triple-mutated (i.e. L858R/T790M/C797S) EGF receptor over *wild-type* EGF receptor and binds the allosteric binding pocket of the TK domain. This binding pocket is less well conserved in kinases than the ATP-binding pocket. Moreover, it interacts with M790, making it selective for EGF receptor mutants bearing this mutation. EAI045 has been tested in triple-mutated EGF receptor and showed an increased efficacy in monomeric EGF receptor (i.e. forced by cetuximab) (Jia et al. 2016).

I have discussed that TK inhibitors of the EGF receptor encounter resistance mechanisms and suggested ways to improve TK inhibitor design. PROTAC may be a promising future therapy, whereas osimertinib as first-line therapy with or without chemotherapy already has promising results in clinical trials. Our and other studies support the idea that the equilibrium between monomers and dimers plays an important role in TK inhibitor efficacy.

In conclusion, the activation process of the EGF receptor follows ligand-induced dimerization. TK inhibitors that induce dimer formation, alter the activation process of the EGF receptor and its internalization. Moreover, internalization could not be blocked by TK inhibitors. Importantly, this shows that internalization

is not a direct consequence of phosphorylation. We suggest that inducing dimer formation may play a significant role in internalization behaviour of the EGF receptor.

## 11.3 mGlu4, mGlu2-4 and DN45

### 11.3.1 mGlu4 receptor as drug target in Parkinson's Disease

The mGlu4 receptor has retained much attention as a potential target for treating neurological disorders like Parkinson's Disease (PD) (Marino et al. 2003) and pain (Vilar et al. 2013; Goudet et al. 2012). Moreover, the mGlu4 has been linked to cancers (Chang et al. 2005; Stepulak et al. 2014). In colorectal cancer, the mGlu4 was overexpressed and altered resistance to 5-FU. Resistance to 5-FU could even be increased in a dose-dependent manner by mGlu4 receptor antagonists (Yoo et al. 2004). Nevertheless, the mGlu4 has been linked primarily to PD. In our study, we characterize a nanobody that activates the mGlu4 and not the mGlu2-4 receptor. Such a pharmacological profile is favourable for inducing antiparkinsonian effects (Niswender et al. 2016).

First of all, the mGlu4 receptor is a promising target for improving the treatment of PD through an indirect way. PD is caused by a loss of dopaminergic neurons in the substantia nigra pars compacta (SNpc), causing a dysfunctional motor circuit in the basal ganglia. Moreover, GABAergic neurons in the globus pallidus internis (GPi) are hyperactive, causing motor symptoms (Marino et al. 2003). Due to glutamate toxicity, disease progression worsens. Following treatment with dopamine agonists (e.g. L-DOPA), patients suffer from L-DOPA-induced dyskinesia (LID) or returning PD symptoms. Indeed, mGlu4 receptor activation has been proposed to reduce GABA and glutamate release after treatment with L-DOPA (Dickerson and Conn 2012). Both PAMs and selective mGlu4 receptor agonists have been successfully tested in rodents as antiparkinsonian treatment (Niswender et al. 2016). However, PAMs may be preferred over orthosteric agonists, due to higher selectivity and a more physiological regulation, because they regulate activity only in presence of endogenous agonists (Christopoulos et al. 2004). Nevertheless, a clinical trial (Prexton Therapeutics, NCT03162874, 2017) involving foliglurax, a mGlu4 PAM, failed to significantly improve clinical outcomes (i.e. reducing motor symptoms and L-DOPA-induced dyskinesia (LID)) following L-DOPA treatment (Doller et al. 2020). Therefore, other strategies could be considered as well. An innovative strategy could be the use of activating nanobodies that have several advantages over PAMs and orthosteric agonists: high selectivity, non-toxic metabolites and adjustability[xxii] (Menzel et al. 2018). Indeed, DN45 being a high-affinity agonist for the mGlu4 receptor, could be suggested as potential drug. Nevertheless, in our view, DN45 is rather a pharmacological tool for research purposes for several reasons that will be discussed below.

[xxii] Increase *in vivo* half-life with PEG-linkers, target specific tissue with bi-valent nanobodies, increase affinity with bitopic nanobodies.

### 11.3.2 DN45 as therapeutic agent

Firstly, DN45 is selective for the human mGlu4 vs rodent mGlu4 receptor, making it difficult to conduct *in vivo* efficacy experiments in rodent models and proceeding in pre-clinical research. Nevertheless, there are 3 ways to overcome these issues:

1) Generation of transgenic mice expressing the human mGlu4 receptor (and not the mouse mGlu4 receptor).

2) Performing experiments on animals expressing the human-like mGlu4 receptor. Animals expressing similar mGlu4 receptors as humans are 2 primates: the chimpanzee and pygmy chimpanzee and 9 non-human primates (NHPs)[xxiii]. However, the use of primates and NHPs is strictly regulated in the European Union and should only be used when no other options are available (SCHEER 2017), which is not the case. Moreover, from an ethical point of view, efficacy studies should first be conducted in another animal model.

3) DN45 could be modified to make it bind to a rodent mGlu4 receptor. However, D485 (i.e. polar, acidic) of the human mGlu4 receptor plays a major role in DN45 binding (Annex VII). This residue is replaced by Glycine (i.e. non-polar, aliphatic) in rodents and it may be complicated to mimic such a strong interaction on a different receptor.

A second reason that DN45 is not proposed as potential therapeutic is because nanobodies encounter difficulties crossing the BBB, making them not very suitable as drugs for CNS receptors, yet. However, modified nanobodies with a basic isoelectric point (Tengfei Li et al. 2012), targeting the transferrin receptor (Niewoehner et al. 2014) or targeting the insulin receptor (Boado et al. 2013), were able to cross the BBB. Such studies show that nanobodies may be used for targeting receptors in the CNS in the near future.

Overall, DN45 is a nanobody with agonist properties on the mGlu4 receptor, which could be beneficial for treating Parkinson's Disease. Nonetheless, this nanobody is not directly suitable as drug for targeting the mGlu4 in the CNS, because of its selectivity for the human receptor, making it difficult to perform *in vivo* research and because it is not sure it crosses the BBB. Therefore, DN45 may be more suitable for researching the function of homo- and heterodimers of the mGlu4. How the DN45 activates the mGlu4 receptor will be discussed below.

[xxiii] crab-eating macaque, rhesus macaque, olive baboon, black snub-nosed monkey, pig-tailed macaque, ma's night monkey, green monkey, rhesus macaque, drill

### 11.3.3 Activation of the mGlu4 receptor by DN45

DN45 interacts with the two lobes of each VFT domain, thereby stabilizing a closed conformation of the extracellular domain (Fig. 36, 1.) (Haubrich et al. 2021). This involves a rotation of the VFT domains, leading to a rearrangement of the CRDs (Fig. 36, 2.).

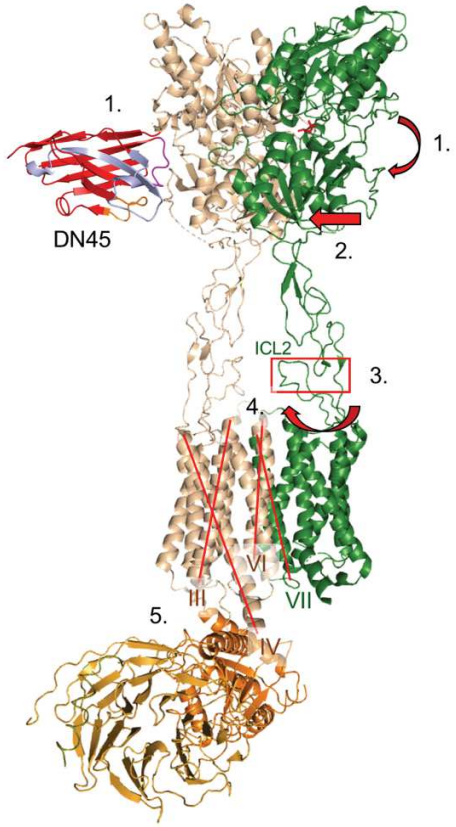


**Figure 36:** Activation of mGlu4 homodimer by DN45. 1. DN45 induces closure of VFT, 2. VFT domains rotate, 3. Interactions between ICL2 and CRD are established, causing a clockwise rotation of the 7TM domain, 4. Helix VI (G protein-bound) and helix VII (G protein-free) subunits interact, 5. G protein interacts with helix III and IV, and ICLs of 1 subunit. Figure is copied from Lin *et al.* (2021) with permission from Nature.

The CRDs are now in close proximity to extracellular loop (ECL) 2 of the 7TM domains, which is important for inducing a clockwise (from top view) rotation of the 7TM domain (Fig. 36, 3.) (Koehl et al. 2019).

The main interactions between the two mGlu4 subunits in an active receptor, at the 7TM domain level, are between helix VI of the G protein-bound and helix VII of the G protein-free mGlu4 (Fig. 36, 4.). Importantly, the cryo-EM structure reveals that only 1 subunit is G protein-bound at the same time (Lin et al. 2021).

The rotation of the 7TM domain re-orientates intracellular loop (ICL) 2, making it available for G protein recognition. G protein binding is then mediated through interactions with helices III and IV and all three ICLs (Fig. 36, 5.).

Importantly, structural data of the inactive mGlu2-7 heterodimer revealed that their 7TM interactions are similar to those of the mGlu7 homodimer, and not the mGlu2 homodimer, and G protein coupling is exclusively to the mGlu7 subunit, revealing the dominance of the mGlu7 in this heterodimer (Du et al. 2021). This is opposite of G protein coupling in the mGlu2-4 heterodimer, in which G protein coupling is shifted from the mGlu4 to the mGlu2 subunit by mGlu4 NAMs (J. Liu et al. 2017). This raises the question on how the allosteric interactions between the 7TM domains of the mGlu2 and mGlu4 in an mGlu2-4 heterodimer are regulated on the structural level and how mGlu4 NAMs change these.

These structural data reveal that class C GPCRs are asymmetrically activated. DN45 could be used as a selective mGlu4 agonist to elucidate asymmetric activation of the mGlu2-4 heterodimer.

**Regulation of heterodimeric mGlu2-4**

The physiological role of the mGlu2-4 heterodimer is unknown, partly because of a lack of tools that are selective enough to discriminate between homo- and heterodimers (McCullock and Kammermeier 2021). Nevertheless, some advances on deciphering its function have been made, as will be discussed.

The first experimental evidence showing that the mGlu2-4 heterodimer could exist was reported by Doumazane *et al.* (Doumazane et al. 2011). It is important to understand that mGlu receptors are strict dimers and as such they are coupled via disulphide bonds in the (rough) endoplasmic reticulum. That means that heterodimer expression on the cell surface could be regulated in a temporal way by controlling expression over time (Doumazane et al. 2011). Importantly, when they are expressed at the same time, their propensity to form heterodimers or their respective homodimers is comparable (Doumazane et al. 2011; Lee et al. 2020). Even though expression levels of the mGlu2 and mGlu4 are quite divergent in the brain, there is overlap in some areas: olfactory bulb, striatum and thalamus (Ferraguti and Shigemoto 2006). Moreover, in mouse cortical pyramidal neurons there is spatiotemporal overlap in RNA expression of mGlu2 and mGlu4 (Lee et al. 2020). Furthermore, functional mGlu2-4 heterodimers were demonstrated in corticostriatal synapses (Yin et al. 2014), hippocampal perforant pathway (Delgado et al. 2017) and medial prefrontal cortex synapses (Xiang et al. 2021), proving their existence *in vivo*.

The first pharmacological characterization of the mGlu2-4 heterodimer revealed that the mGlu4-coupled G protein could be activated by an mGlu2 agonist (Doumazane et al. 2011) (Fig. 37). Nevertheless, both subunits are necessary to fully activate the mGlu2-4 heterodimer (Kammermeier 2012). It was suggested that mGlu4 PAMs may not bind the mGlu4 when it is heterodimerized with the mGlu2, because they exert no function (Niswender et al. 2016; Kammermeier 2012). Additionally, Liu *et al.* showed that G protein-coupling is mainly to the mGlu4 and that mGlu4 NAMs and mGlu2 PAMs could shift the coupling to the mGlu2 subunit. Moreover, mGlu2 NAMs decreased total G protein-coupling (J. Liu et al. 2017). We show that the mGlu2-4 is heavily potentiated by closure of the mGlu4 subunit, when activated by a selective mGlu4 agonist, which is DN45 (Haubrich et al. 2021). Overall, the G protein coupling is to the mGlu4 subunit, which can be shifted to the mGlu2 subunit with mGlu2 PAMs or mGlu4 NAMs. The consequence of this asymmetric G protein-coupling remains elusive.

It was suggested that the mGlu7 receptor, due to its very low affinity for glutamate, has an *in vivo* function through forming heterodimers (Delgado et al. 2017). It is possible that the same accounts for the mGlu2 and mGlu4 receptors by forming mGlu2-4 heterodimers. However, the difference in glutamate affinity between

mGlu2 and mGlu4 receptors is small, so it would not make a big difference in activation (J. Liu et al. 2017). Imaginably, heterodimerization leads to spatial regulation of the mGlu4 receptor, because sole mGlu4 subunits with an unknown binding partner (i.e. likely the mGlu2 receptor) were found to be in inactive domains in neuronal synapses after mGlu4 activation (Siddig et al. 2020). It was suggested that the mGlu2 receptor traffics the mGlu4 receptor to oligomeric structures that regulate activity (Møller et al. 2018; Siddig et al. 2020). Such oligomeric signalling islands have been seen for the heterodimeric $GABA_B$ receptor (Comps-Agrar et al. 2011). Therefore, the function of the mGlu2-4 heterodimer may have more to do with mGlu4 trafficking as way of desensitization or inducing sustained signalling.

It is quite well understood how to pharmacologically control the mGlu2-4 heterodimer. Yet, there is almost no knowledge about its function *in vivo* and how the receptor is regulated (McCullock and Kammermeier 2021). Niswender *et al.* proposed that mGlu2-4 activation does not mediate antiparkinsonian effects (Niswender et al. 2016), but other recent studies investigating this heterodimer do not investigate its specific function *in vivo* (Scholler, Nevoltris, et al. 2017; J. Liu et al. 2017; Yin et al. 2014; Xiang et al. 2021). DN45 could help decipher its function, as will be discussed below.

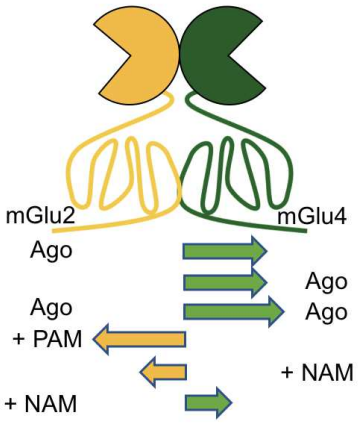


**Figure 37:** Regulation of the mGlu2-4 receptor activity with mGlu2 and mGlu4 ligands. Receptor coupling is to the subunit to which the arrows point. The size of the arrows is a measure for the amount of activation.

### 11.3.4 DN45 for investigating the function of the mGlu2-4 heterodimer

There are two ways we propose that the nanobody is used for investigating the function of the mGlu2-4 heterodimer. Firstly, DN45 could be used for localization of heterodimers in tissue. Secondly, DN45 is a pharmacological agent that specifically activates the mGlu4 receptor and that can be used to modulate activation of the mGlu2-4 receptor in native tissue.

DN45 being a human-selective nanobody, cannot be used for localization of the mGlu2-4 heterodimer in rat/mouse tissue. Therefore, research is limited to human(-like) primary neurons/neuronal cell lines. By combining DN45 and mGlu2 nanobodies (Scholler, Nevoltris, et al. 2017) with HTRF®, endogenous heterodimers could be detected in these tissues (Fig. 38A). Such studies could be performed for different brain regions (e.g. striatum, thalamus, olfactory bulb and others), thereby discovering the existence of heterodimers. Moreover, the mGlu4 has the propensity to form heterodimers with mGlu3, 7 and 8 (Doumazane et al. 2011). It is therefore of interest to determine what tissues contain these heterodimers.

Secondly, the mGlu2 subunit of an mGlu2-4 heterodimer is heavily potentiated by binding of DN45 to the mGlu4 subunit. Therefore, pharmacological responses are different in tissues that contain homodimers of mGlu2 or mGlu4 and mGlu2-4 heterodimers, which could be used to specifically control activation of neurons expressing heterodimers (Fig. 38B).

Overall, DN45 is unique in its properties and could be used to selectively target the mGlu4 or mGlu2-4 receptors in neurons or tissue. The precise localization, *in vivo* function and regulation of the heterodimeric mGlu2-4 is not well understood and compounds selectively targeting either mGlu2, mGlu4 or mGlu2-4 are necessary for further investigations. DN45 activates mGlu4 receptors, or potentiates the mGlu2-4 activation, thereby discriminating between homo- and heterodimers. Due to its agonist properties on the mGlu4, its therapeutic potential could be investigated as well. However, several obstacles need to be overcome: transgenic mice need to be generated and tested and it may be possible that DN45 needs to be optimized to efficaciously cross the BBB.

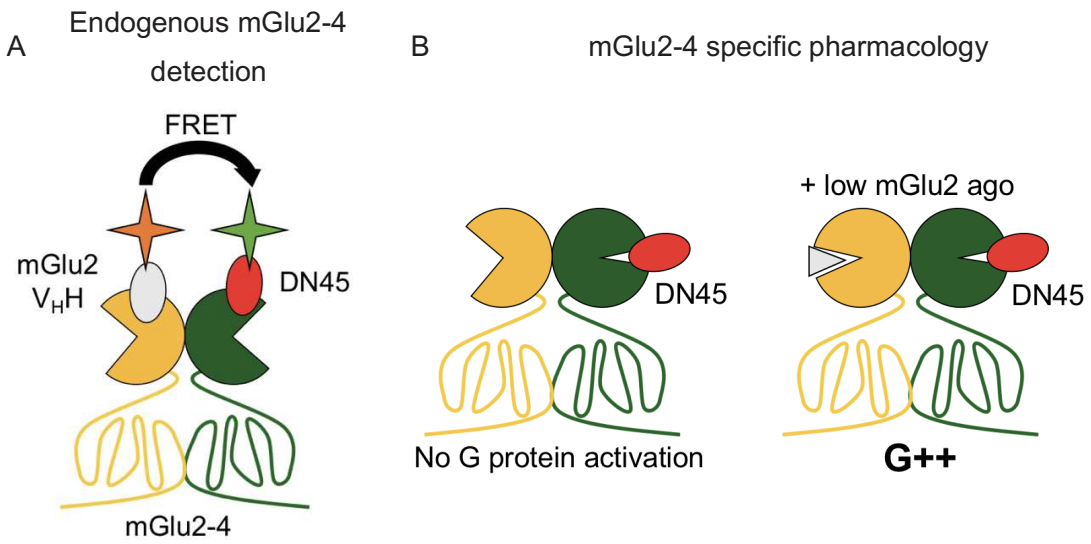


**Figure 38:** DN45 for researching mGlu2-4 heterodimers. A) A schematic proposal of an assay for the detection of endogenous mGlu2-4 heterodimer in assay. B) Specific pharmacological responses in tissues containing mGlu2-4 heterodimer. In orange is a FRET donor, in green is a FRET acceptor. The mGlu2 is in yellow, the mGlu4 is in green. The mGlu2 nanobody and agonist are in grey, DN45 is in red. The black arrow represents FRET.

### 11.3.5 Combining *in silico* and biochemical approaches for deciphering binding epitope and mode of action

DN45 is not the first nanobody that activates a membrane receptor. Previously, intracellular nanobodies (intrabodies) (Staus et al. 2014) and the first agonist nanobody (McMahon et al. 2020) for class A GPCRs have been described. However, DN45 is the first agonist nanobody for a class C GPCR. Its mode of action is unique, as DN45 interacts with both bottom and top part of the VFT domain (Chapter 9, Fig. 3 and 4). The crystal structure of the mGlu4 receptor was not known at the time of conducting the experiments, so models of the mGlu4 receptor and nanobody were generated by our collaborators. The mGlu4 receptor model was based on the mGlu8 structure of the VFT domain and a model for the DN45 structure was generated by SWISS model. Led by predicted interactions, mGlu4 mutants were generated and the binding site on the bottom lobe of the VFT domain was identified. Besides interactions between the nanobody and receptor, the computational model of the mGlu4 VFT domain predicted the stability of the VFT domain conformation as well. By this way, several key residues for the stability of the binding epitope of DN45 were identified, without these residues playing a direct role in binding (i.e. V385 and H507). To test the hypothesis of activation by stabilizing interactions with the top part of the VFT domain, it was important to show that the nanobody could be turned into an antagonist on a mGlu4 receptor mutant. Molecular dynamics simulations suggested triple and quadruple mutations to destabilize the nanobody-receptor interactions, while the mGlu4 receptor conformation and the binding of the nanobody remained stable. DN45 acted as antagonist and inverse agonist on these mutants, respectively. Such a study, shows the power of combining selective substances and computational modelling to determine in detail the binding epitope and mechanism of action.

## 11.4 TECHNICAL REMARKS

### 11.4.1 Expression in EGF receptor cell lines

In this thesis, I have shown that HTRF® is a very sensitive technique that is easily adaptable to receptors from different groups. Especially, in the EGF receptor research area, semi-quantitative methods like western blot to measure phosphorylation are still common, whereas HTRF® is a quantitative method that is precise enough to determine pharmacological parameters. To determine the receptor expression, we determined the relative expression to the A431, an epidermoid squamous carcinoma cell line (Sigma-Aldrich, ref. 85090402-1VL). Most importantly, receptor expression in the generated cell lines did not exceed that of cancerous cells as the expression of the EGF receptor was around 4-fold lower than in A431 cells (Fig. 39).

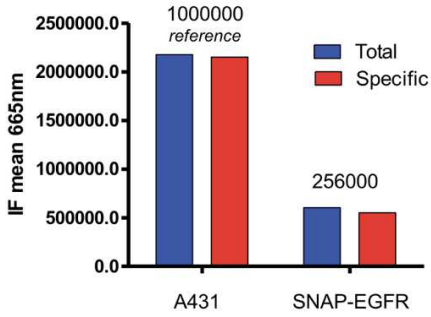


**Figure 39:** Expression of cancerous cell line (A431) and HEK293 stably expressing SNAP-EGFR (ST-EGFR cell line).

### 11.4.2 Internalization by confocal microscopy versus HTRF®

When internalization of the EGF receptor was observed with confocal microscopy, low fluorescence intensity, due to low receptor expression levels, complicated the experiments. The low signal and therefore relatively high background signal made it complicated to quantify internalization. More in general, cells are never completely homogenously spread on the lamellae and a zoom on a small region of the lamellae is therefore vulnerable to sampling bias. Moreover, confocal microscopy is a time-consuming technique, making it less compatible with pharmacology and kinetics. None of these issues appeared when measuring internalization with HTRF®. Despite relatively low receptor expression, results were very reproducible. With HTRF®, fluorescence of all labelled receptors in a well is measured and the experimenter cannot be biased because of heterogenous spread. Lastly, because these experiments are performed in 96-wells plates with fast acquisition of signal, many conditions can be measured continuously, thereby generating more (kinetic) data.

### 11.4.3 A future perspective: heterodimerization in EGFR family

Moreover, many different kinds of assays were performed using HTRF®-technique: dimerization/conformation, phosphorylation, internalization, antibody/nanobody binding, $G\alpha_q$-activation, dimerization being key subject in this thesis. As such, I showed dimerization of EGF receptor homodimers, $EGFR_{L858R+T790M}$ (and $EGFR_{L858R}$), heterodimers of the EGF receptor and $EGFR_{L858R+T790M}$, mGlu4 homodimers and mGlu2-4 heterodimers. The possibility to investigate other heterodimeric receptors like CLIP-EGFR with SNAP-HER2, SNAP-HER3, SNAP-HER4 could be interesting as well. Especially, pan-EGFR TK inhibitors may be of interest, as they can bind multiple EGFR receptors.

### 11.4.4 FRET-pair distance in EGF receptor

By analysing the excited-state lifetime of the sensitized emission, average distances of the FRET-pair could be calculated. Because of the complicated multiphase decay of Lumi4-Tb, any calculations to determine the average FRET-pair distance may not be reliable. Therefore, I did not include these calculations in chapter 10. Nonetheless, such calculations were performed with the formula to calculate the distance D, as described in '*Chapter 8: Materials and Methods*'. The results are found in annex V and show that the high FRET EGF receptor conformation has an average FRET-pair distance of 37 Å. The exact nature of the biphasic decay of Lumi4-Tb remains elusive, but it may be due to different conformations due to the attachment to the SNAP-tag on the receptor (Selvin 2002).

## 11.5 CONCLUDING REMARKS ABOUT DIMERIZATION

In this thesis, we have demonstrated and discussed the importance of dimer formation in different receptor types, how ligands and regulators modify dimerization properties and how dimerization regulates receptor activity and downstream events (Fig. 40). It turns out that dimerization is a central step in receptor function, either for activation, pharmacology, signalling or cellular trafficking.

### 11.5.1 Gene expression and pharmacological compounds regulate dimer formation

Firstly, dimerization is regulated on the level of gene expression, but can be modified by pharmacological compounds. All EGFR family members may form dimers on the cell surface depending on expression levels or available ligand. Importantly, we show that the EGF receptor is mainly monomeric and its dimerization induced by agonists leads to a specific conformation of the extracellular domains and association of intracellular domains. However, dimerization is also induced by non-competitive antagonists that do not activate the receptor, thereby showing that the dimeric conformation they induce does not allow activation, in contrast to that induced by agonists like EGF. Conversely, in the mGlu receptor family, dimerization is crucial for its activation. There is no ligand-induced dimerization, but ligand-induced rearrangements of the mGlu dimeric receptors. Indeed, dimeric partners are linked through a disulphide bond on the VFT domains, that is mediated by gene expression in a spatiotemporal way. Thus, ligand-induced dimerization processes add an extra level of complex regulation of some membrane receptor functioning.

### 11.5.2 Asymmetric interactions between dimeric partners are important for activation

Secondly, structural symmetry is a noteworthily hallmark of inactivity and asymmetry is necessary for activity of the EGF receptor and the mGlu4 receptor. Upon agonist binding to the EGF receptor and subsequent allosteric interactions, the association of TK domains of the EGF receptor removes auto-inhibitory interactions, thereby stabilizing an asymmetric active dimer of TK domains. Similarly, symmetric 7TM domains of mGlu receptors are inactive. Agonist-binding to the VFT domains, leads to allosteric interactions and a rotation of the 7TM domain, which then becomes structurally asymmetric. Asymmetry is needed for G protein coupling to the mGlu4 receptor.

### 11.5.3 Dimerization regulates activity and downstream events

Thirdly, dimerization is a key process in regulating downstream effects of receptors. We have shown that by inducing asymmetric, non-phosphorylated, EGF receptor dimers with TK inhibitors, internalization of the EGF receptor is slowed down. Conversely, internalization of symmetric, non-phosphorylated, EGF receptor dimers was not altered. The mGlu2-mGlu4 heterodimer strictly limits the efficacy of mGlu4 agonists, whereas mGlu2 agonists are potent in activating mGlu4 G protein signalling.

Overall, we show that the EGF receptor and mGlu4 receptor are illustrating examples of the complexity of transmembrane dimeric receptors. Despite these two receptors being regulated differently by gene expression or pharmacological compounds, they are sharing similarities on the level of asymmetric regulation. For both receptors asymmetric interactions within the dimer are necessary for activation.

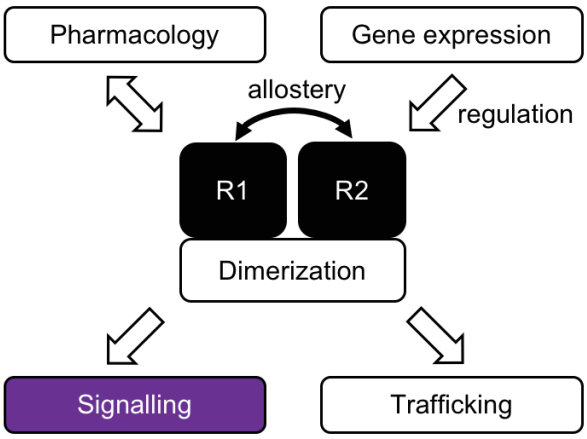


**Figure 40:** Dimerization is a central process in the regulation of receptor function. Highlighted processes are pharmacology, gene expression, signalling and trafficking.

# 12 CONCLUSIONS AND FUTURE PERSPECTIVES

In this thesis I report about conformational dynamics and pharmacology in transmembrane dimeric receptors. The goal was to investigate the role of dimerization on these receptors. The 2 main topics are: 1) The activation mechanism of the EGF receptor and the role of non-competitive antagonists on this process and 2) Selective control of homo- and heterodimeric mGlu4 activity by a nanobody.

We investigated the activation mechanism of the EGF receptor, because of the debated activation process of the EGF receptor: Does the EGF receptor follows ligand-induced dimerization or ligand-induced conformational changes of a pre-formed dimer? We show that the EGF receptor follows ligand-induced dimerization as principal activation mechanism. Importantly, we show that even though dimerization is necessary for activation, it is not crucial, as is demonstrated by erlotinib-like TK inhibitors inducing dimer formation. We demonstrate that 2 bound erlotinib-like TK inhibitors are necessary for inducing asymmetric EGF receptor dimers. We propose that a portion of the dimers that are induced by erlotinib do not internalize, due to an asymmetric conformation on the level of the TK domains. As such, dimerization is proposed as central step in the activity of the EGF receptor. Based on these findings, we suggest 3 future perspectives: 1) Investigation on the activation mechanism of heterodimeric EGFR family species, as it may reveal important information about the way heterodimerization is regulated by ligands, 2) The role of TK inhibitors on this process may be investigated as well. Especially, pan-EGFR TK inhibitors may be of interest, because they bind more than one EGFR family member, 3) Investigations on the physiological role of the observed EGF receptor internalization may be proceeded.

The mGlu4 forms homo- and heterodimers in the brain. Despite mGlu4 homodimers being a target for Parkinson's Disease, the role of mGlu2-4 heterodimers remains elusive. We developed and characterized a selective pharmacological tool, nanobody DN45, to specifically control activity of the mGlu4. DN45 promotes closure of the VFT domain of the mGlu4 through interactions with both lobes of the VFT domain, demonstrating full agonist activity. Importantly, DN45 does not activate the mGlu2-4 heterodimer, but acts as a potent PAM. Therefore, DN45 is a pharmacological tool that discriminates between homo- and heterodimers of the mGlu4. In view of these conclusions, 3 future perspectives are suggested as well: 1) DN45 may be used for localization of the mGlu2-4 heterodimer in native tissues, 2) DN45 could also be used as pharmacological tool for investigating mGlu2-4 heterodimer function in brain tissue, 3) For *in vivo* experiments, several optimizations are necessary in order to make DN45 bind the mGlu4 receptor in rodent brain. Overall, we demonstrate for two dimeric receptors that dimerization is a key process that is regulated by gene expression or pharmacological compounds. Importantly, dimerization is a central step in receptor function as it regulates receptor activation, pharmacology, signalling or cellular trafficking.

# 13 ANNEXES

## 13.1 ANNEX I: ABBREVIATIONS

| | |
|---|---|
| **#** | |
| 5-FU: | 5-Fluorouracil |
| 5-HT: | Serotonin |
| 7TM: | Seven transmembrane |
| **A** | |
| AC: | Adenylyl cyclase |
| ADAM: | A desintegrin and metalloproteinase |
| ADCC: | Antibody-dependent cellular cytotoxicity |
| ALK: | Anaplastic lymphoma kinase |
| AP2: | Adaptor protein 2 |
| AR: | Amphiregulin |
| ATP: | Adenosine triphosphate |
| **B** | |
| BBB: | Blood-brain-barrier |
| BC: | $O^6$-benzylcytosine |
| BG: | $O^6$-benzylguanine |
| BTC: | Betacellulin |
| BRET: | Bioluminescence resonance energy transfer |
| **C** | |
| C797: | Cysteine 797 |
| C797S: | Substition of cysteine 797 with serine |
| cAMP: | Cyclic adenosine monophosphate |
| CaSR: | Calcium-sensing receptor |
| CB: | Cannabinoid |
| Cb: | Cerebellum |
| Cbl: | Casita B-lineage Lymphoma |
| CDK: | Cyclin-dependent kinase |
| CDR: | Complementarity-determination region |
| CIN85: | Cbl-interacting protein of 85K |
| CLIP: | $O^6$-benzylcytosine |
| CME: | Clathrin-mediated endocytosis |
| CNS: | Central nervous system |
| CRD: | Cysteine-rich domain |
| Cryo-EM: | Cryogenic electron microscopy |
| CT: | Computed tomography |
| **D** | |
| D: | Distance between the FRET donor and acceptor |
| D855: | Aspartic acid 855 |
| DNA: | Deoxyribonucleic acid |
| **E** | |
| E: | FRET efficiency |
| E762: | Glutamic acid 762 |
| EAAT: | Excitatory amino acid transporter |
| EAI045: | EGF receptor allosteric inhibitor 045 |
| EC50: | Half maximal effect concentration/potency |
| ECD: | Extracellular domain |
| EGF: | Epidermal growth factor |
| EPN: | Epigen |
| ER: | Endoplasmic reticulum |
| EREG: | Epiregulin |
| ERK: | Extracellular signal-regulated kinase |
| Exon19del: | Deletion of residues 756 till 750 in exon 19 |
| **F** | |
| F856: | Phenylalanine 856 |
| FDA: | Federal Drug Administration |
| FRET: | Förster Resonance Energy Transfer |
| **G** | |
| G857: | Glycine 857 |
| Gab2: | Grb2 associated protein 2 |
| GABA: | γ-aminobutyric acid |
| GBM: | Glioblastoma multiforme |
| GDP: | Guanine diphosphate |
| GEF: | Guanine exchange factor |
| GPCR: | G protein-coupled receptor |
| GPe : | Globus pallidus externus |

| | |
|---|---|
| GPi: | Globus pallidus internus |
| Grb2: | Growth factor receptor-bound protein 2 |
| GRK: | G protein-coupled receptor kinase |
| GTP: | Guanine triphosphate |
| GTPase: | Guanine triphosphatase |
| **H** | |
| HB-EGF: | Heparin-binding EGF-like growth factor |
| HcAb: | Camelid heavy chain-only antibody |
| HER: | Human epidermal growth factor receptor |
| HGF: | Hepatocyte growth factor |
| HUGO: | Human Genome Project |
| HTRF®: | Homogenous Time Resolved Fluorescence |
| HTS: | High-throughput screening |
| **I** | |
| IC50: | Half maximal inhibitory concentration |
| ICD: | Intracellular domain |
| IgG: | Immunoglobulin G |
| iGlu: | Ionotropic glutamate |
| IL-33: | Interleukin-33 |
| INSR: | Insulin receptor |
| $IP_3$: | Inositol 1,4,5-triphosphate |
| **J** | |
| JxD: | Juxtamembrane domain |
| **K** | |
| K745: | Lysine 745 |
| Kd: | Dissociation constant |
| Ki: | Inhibition constant/affinity |
| $k_r$ : | Radiative decay rate |
| **L** | |
| L858: | Leucine 858 |
| L858R: | Substitution of leucine 858 with arginine |
| L-AP4: | L-2-amino-4-phosphonobuytric acid |
| LID: | L-DOPA-induced dyskinesia |
| LRET: | Lanthanide-based luminescence resonance energy transfer |
| **M** | |
| M-AP4: | (S)-2-methyl-2-amino-4-phosphonobutanoate |
| MET: | Mesenchymal-epithelial transition factor |
| MPEP: | 2-methyl-6-(2-phenylethynyl)pyridine |
| mGlu: | metabotropic glutamate |
| mRNA: | Messenger ribonucleic acid |
| MVB: | Multivesicular body |
| **N** | |
| *n*: | Hill coefficient |
| NAM: | Negative allosteric modulator |
| NGFR: | Nerve growth factor receptor |
| NHP: | Non-human primate |
| nRTK: | Non-receptor tyrosine kinase |
| NSCLC: | Non-small cell lung cancer |
| **O** | |
| Olf: | Olfactory bulb |
| OR: | Opioid receptor |
| **P** | |
| PAM: | Positive allosteric modulator |
| PD: | Parkinson's Disease |
| PD1: | Programmed cell death protein |
| PD-L1: | Programmed death-ligand 1 |
| pre-mRNA: | Pre-messenger ribonucleic acid |
| PDGFR: | Platelet-derived growth factor receptor |
| PI3K: | Phosphoinositide-3 kinase |
| $PIP_2$: | Phosphatidylinositol 4,5-biphosphate |
| $PIP_3$: | Phosphatidylinositol 3,4,5-triphosphate |
| PLC: | Phospholipase C |
| POI: | Protein of interest |
| **R** | |
| $R_0$: | Förster distance |
| RCPG: | Récepteur couple à une protéine G |
| RER: | Rough endoplasmic reticulum |
| RNA: | Ribonucleic acid |
| RTK: | Receptor tyrosine kinase |
| RSTK: | Receptor serine/threonine kinase |

**S**

SAM: Silent allosteric modulator
SCLC: Small cell lung cancer
SH: Src homology
smFRET: Single-molecule FRET
SN: Substantia nigra
SNAP: $O^6$-benzylguanine
SNpc: Substantia nigra pars compacta
SNpr: SUbstantia nigra pars reticulata
SOS: Sons of sevenless
STN: Subthalamic neurons

**T**

τ: Fluorescence lifetime
T790M: Substitution of threonine 790 with methionine
Tb: Terbium
$\tau_D$: Excited-state lifetime of the donor emission
$\tau_{DA}$: Excited-state lifetime of the acceptor emission
TGF-α: Transforming growth factor-α
TK: Tyrosine kinase
tRNA: Transfer ribonucleic acid
TS: Thymidylate synthase

**V**

VEGF: Vascular endothelial growth factor
VEGFR: Vascular endothelial growth factor receptor
VFT: Venus Flytrap
VGLUT: Vesicular glutamate transporter
$V_H$: Heavy chain
$V_HH$: Camelid variable heavy chain
$V_L$: Light chain
vWF: Von Willebrand factor

**Y**

Y: Tyrosyl

## 13.2 ANNEX II: LIST OF FIGURES AND TABLES

### Figures

*Introduction, Materials and Methods*



*Dimer formation and conformation of Epidermal Growth Factor Receptor control its activity and internalization*

*A nanobody activating metabotropic glutamate receptor 4 discriminates between homo- and heterodimers*



*Discussion*



**Tables**

## 13.3 ANNEX III: INTERNALIZATION ASSAY OPTIMIZATION FOR THE EGF RECEPTOR

### 13.3.1 Temperature (polyclonal *wild-type* SNAP-EGFR in HEK293)

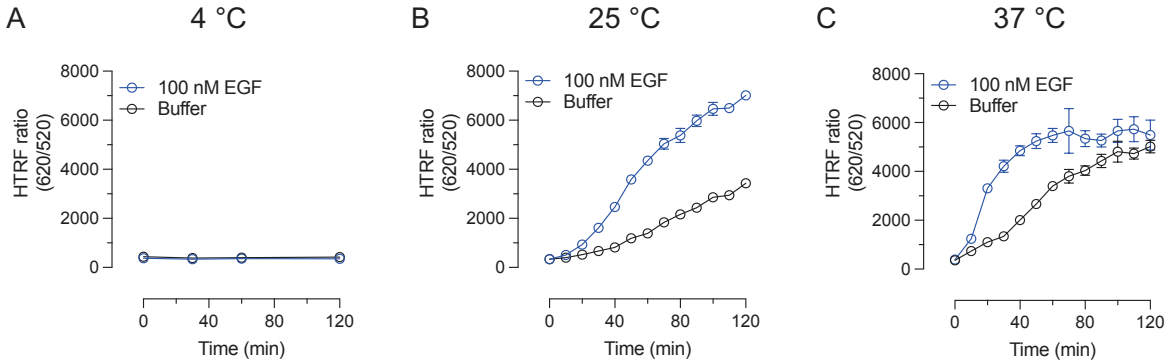


**Annex Fig. 1.** Internalization of the *wild-type* SNAP-EGFR in a polyclonal HEK293 cell line at different temperatures. A) 4 °C. B) 25 °C. C) 37 °C. Data is from a representative experiment: 190320 - Optimization - Internalization EGFR at 3 temperatures.

### 13.3.2 Polyclonal v. Monoclonal & wild-type v. mutated EGF receptor

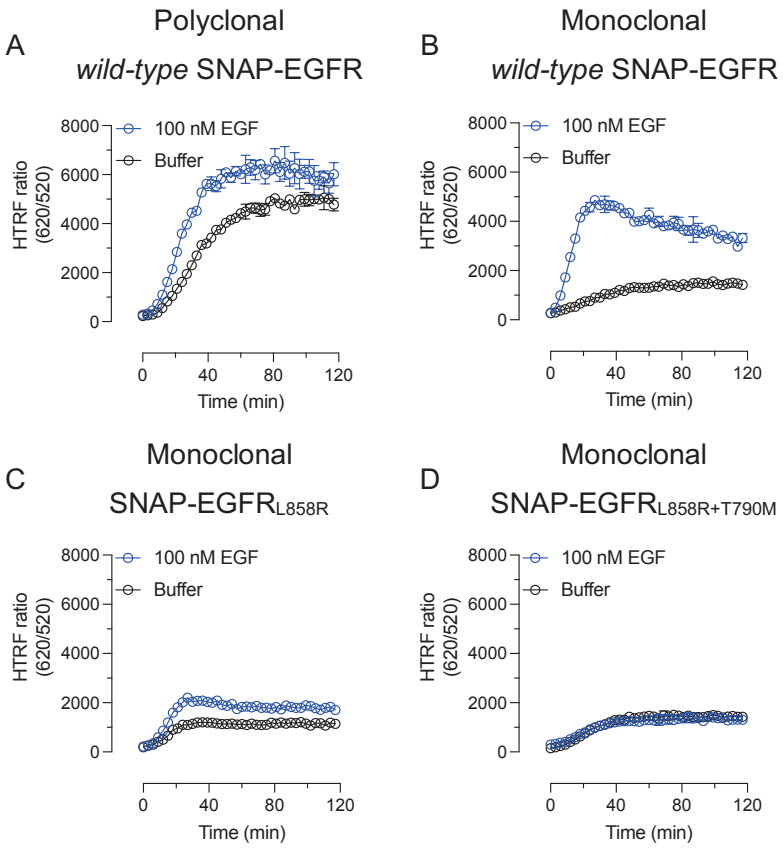


**Annex Fig. 2.** Internalization at 37 °C of poly- and monoclonal cell lines cell lines. A) Polyclonal *wild-type* SNAP-EGFR. B) Monoclonal *wild-type* SNAP-EGFR. C) Monoclonal SNAP-EGFR$_{L858R}$. D) Monoclonal SNAP-EGFR$_{L858R+T790M}$. Data is from a representative experiment: 190806_Monoclonal WT 858 790

## 13.4 ANNEX IV: GENERATION OF HEK293 CELLS STABLY EXPRESSING FLAG-SNAP-EGFR

### 13.4.1 Protocol

The generation of monoclonal stable cell lines can be done in 6 steps: 1) generation of plasmids of interest, 2) Transient transfection, 3) Selection of transfected cells with (eukaryote) antibiotic, 4) Growth of polyclonal cell line, 5) Selection of single cells with BD FACSMelody cell sorter™ and 6) Growth of monoclonal cell line.

#### *13.4.1.1 Generation of plasmids of interest*

Cisbio Bioassays kindly supplied us with a pcDNA3.1(+)-plasmid encoding for the wild-type FLAG-SNAP-EGFR containing G418 (also geneticin) resistance. Point mutations were introduced to obtain FLAG-SNAP-$EGFR_{L858R}$ and FLAG-SNAP-$EGFR_{L858R/T790M}$.

#### *13.4.1.2 Transient transfection*

On day 1, 250,000 HEK293 cells (from CLS that were kindly supplied by Cisbio Bioassays) were seeded in a 6-well plate (9.5 $cm^2$) and incubated at 37 °C and 5% $CO_2$. On day 2, 40 ng of the plasmid of interest supplemented with 1460 ng of a plasmid with an empty vector were transfected per well. On day 3, medium was replaced for normal growth medium.

#### *13.4.1.3 Selection of transfected cells with (eukaryote) antibiotic*

On day 5, cells were detached with trypsin and put in new 6-wells plates with fresh growth medium supplemented with 0.3 mg/mL G418. This value was determined by generation of a G418 kill curve (Annex Fig. 3).

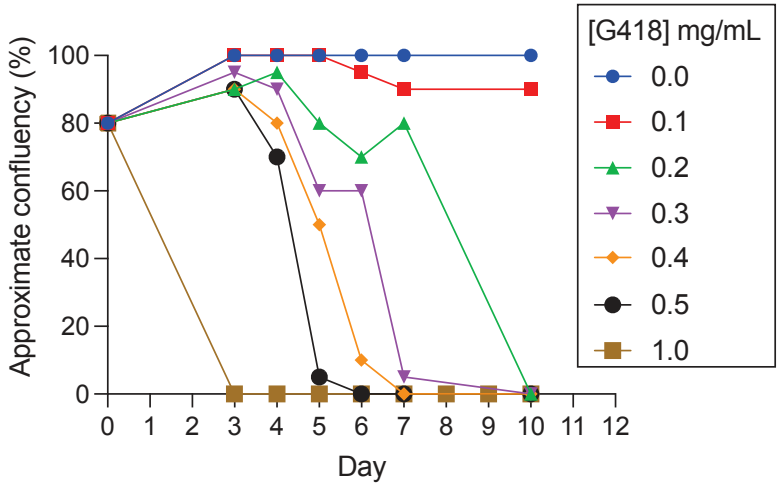


**Annex Fig. 3.** Kill curve G418. The toxic concentration of G418 was determined for HEK293 CLS cells to determine the lowest concentration of G418 that kills non-transfected HEK293 CLS after a transfection with plasmid containing resistance to G418.

*13.4.1.4 Growth of polyclonal cell line*

Cells were grown till 80% confluency of a 6-wells plate and on day 17, cells were transferred to a P100 petri dish (57 $cm^2$). On day 23, cells were transferred to a P150 petri dish (145 $cm^2$). Polyclonal cell lines were frozen in liquid nitrogen on day 24.

*13.4.1.5 Selection of single cells with BD FACSMelody cell sorter™*

On day 27, cells expressing the SNAP-tag on the cell surface, were sorted by BD FACSMelody cell sorter™ based on fluorescence. On the morning of the experiment, cells were labelled with SNAP-Green at 4 °C for 90 minutes and washed with Tag-Lite®-buffer. Gates for cell sorting were determined by selecting fluorescence at 520 nm of a non-transfected cell line (Annex Fig. X). Single cells with a high fluorescence were sorted in a well of a 96-wells plate (0.32 $cm^2$) filled with growth medium supplemented with 0.2 mg/mL G418.

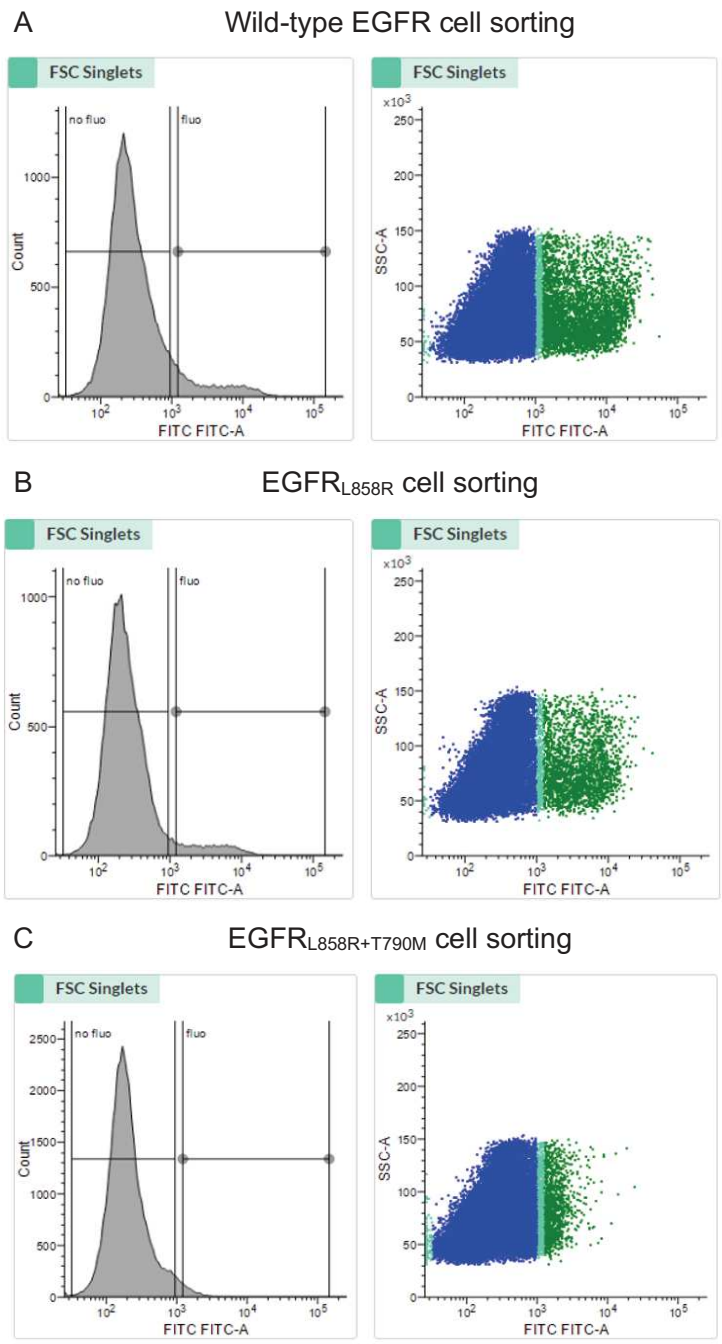


**Annex Fig. 4.** Cell sorting results for 3 EGF receptor cell lines. A) Results for wild-type EGFR cells. B) Results for $EGFR_{L858R}$ cells. C) Results for $EGFR_{L858R+T790M}$ cells.

*13.4.1.6 Growth of monoclonal cell line*

Single cells were regularly observed and on day 41, positive clones were transferred to 24-wells (1.9 $cm^2$) and subsequently 6-wells plates on day 46. Between day 46 and 59, large cell quantities were grown and cells were stored in liquid nitrogen for long-term freezing.

## 13.5 ANNEX V: SENSITIZED EMISSION FOR AVERAGE FRET-PAIR DISTANCE

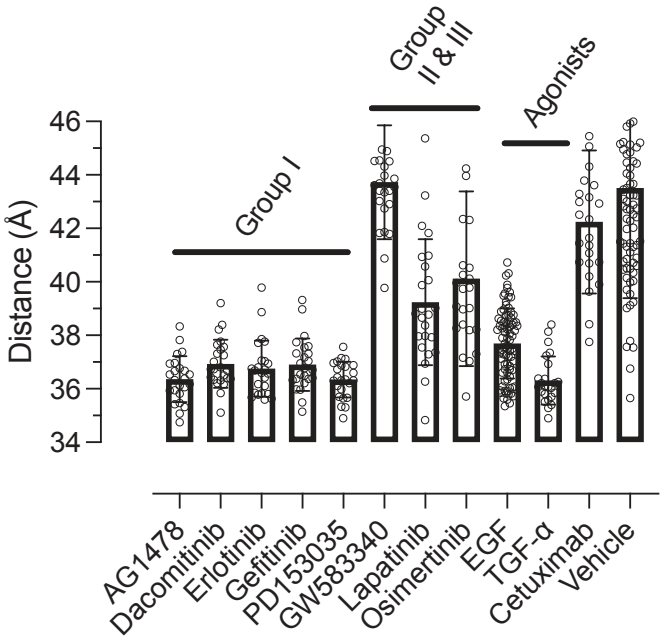


**Annex Fig. 5.** Calculated average FRET-pair distance. $\tau_D$ = 1954 and $R_0$ = 46.

## 13.6 ANNEX VI: EAI045 DIMERIZATION, PHOSPHORYLATION AND INTERNALIZATION

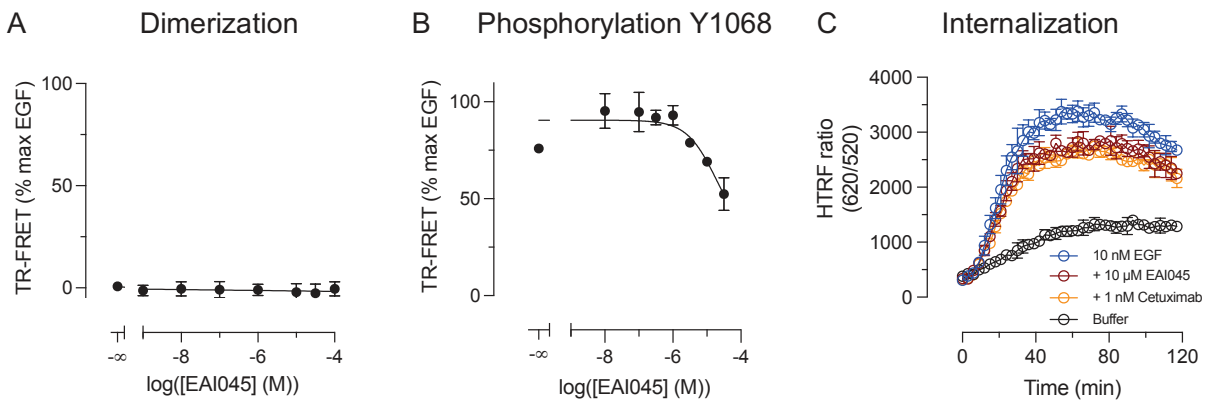


**Annex Fig. 6.** Effect of EAI045 on EGF receptor in intersubunit FRET, phosphorylation of Y1068 and internalization assays. A) Summary intersubunit FRET/dimerization assay. B) Summary of phosphorylation of Y1068 of the EGF receptor. C) Representative experiment showing internalization of SNAP-EGFR.

## 13.7 ANNEX VII: CRYO-EM STRUCTURE OF MGLU4 RECEPTOR (LIN *ET AL.* 2021)

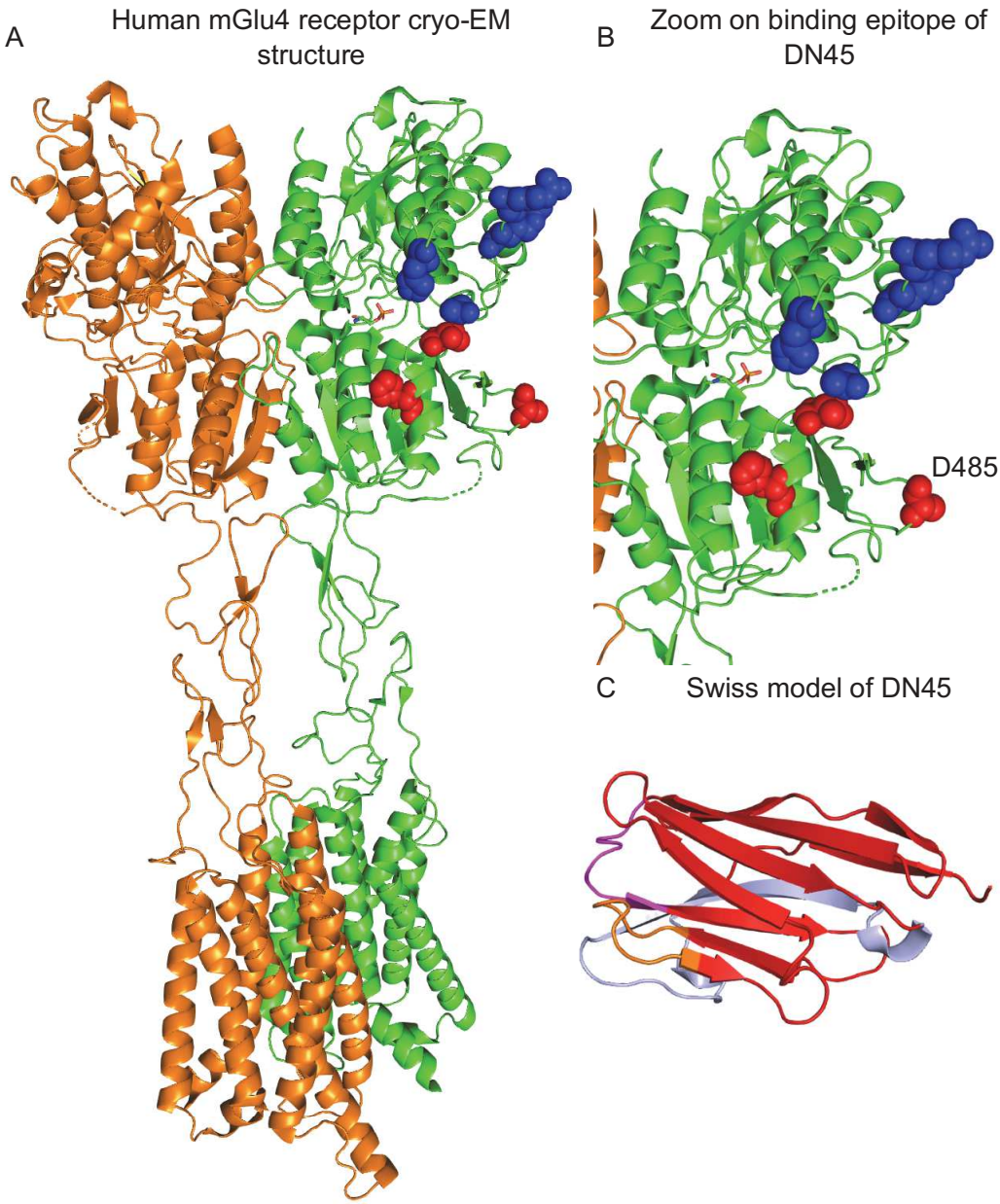


**Annex Fig. 7.** Cryo-electron microscopy images of the human mGlu4 receptor. A) Image of human mGlu4 homodimer. One subunit is in orange and one subunit is in green. Phosphoserine is bound to each of the VFT domains. B) Zoom on binding epitope and loop that is involved in agonist activity of DN45. In red: I318, H323 and D485 and in blue: H371, R391, R393 and A399. This figure is adapted from Lin *et al.* (2021), PDB: 7E9H. C) SWISS model structure prediction of DN45 with CDRs highlighted. In magenta: CDR1, in orange: CDR2, in light blue: CDR3. Interactions with D485 are in CDR2.

## 13.8 ANNEX VIII: SUPPLEMENTARY INFORMATION CHAPTER 9: "DIMER FORMATION AND CONFORMATION OF EPIDERMAL GROWTH FACTOR RECEPTOR CONTROL ITS ACTIVITY AND INTERNALIZATION"

### Supplementary Information

#### Reagents

CLIP-Lumi4Tb (cat. no. SCLPTBF), CLIP-Green (cat. no. SCLPGRNF), SNAP-Lumi4Tb (cat. no. SSNPTBX), SNAP-Green (cat. no. SSNPGRNZ), SNAP-Red (cat. no. SSNPREDZ), Tag-Lite® buffer (cat. no. LABMED), HEK293 cells (cat. no. 300192, CLS Cell Lines Service GmbH, Germany) and the plasmids for SNAP-$EGFR_{delCter}$ and SNAP-$EGFR_{del242-249}$ were provided by Cisbio Bioassays. LY379268 (cat. no. 2453) was bought from Tocris Bioscience. AG1478 (cat. no. T4182), EGF (cat. no. SRP3196), TGF- α (cat. no. T7924), dacomitinib (cat. no. PZ0330), PD153035 (cat. no. SML0564), gefitinib (cat. no. SML1657) GW583340 (cat. no. G3545) and lapatinib (cat. no. SML2259) were bought from Sigma-Aldrich. Erlotinib (cat. no. S7786) and cetuximab (cat. no. A2000) were bought from Selleckchem. Osimertinib (cat. no. I-9701) was bought from Achemblock. AG1024 (cat. no. 121767) was bought from Calbiochem.

#### Cell culture

HEK293 (CLS) cells and HEK293 cells stably expressing SNAP-EGFR and SNAP-$EGFR_{L858R+T790M}$ were cultured in DMEM medium supplemented with 10% fetal calf serum (cat. no. F2442, Sigma-Aldrich), 50 IU/mL penicillin (P4333, Sigma-Aldrich) and 50 µg/mL streptomycin (P4333, Sigma-Aldrich), 1% non-essential amino acids (11140-035, Invitrogen) and 2 mM HEPES (EGFR medium) at 37° C and 5% $CO_2$. Cells were grown in P150 petri dishes and cell splitting was performed every two or three days. The culture medium was removed by aspiration and cells were washed with 10 mL PBS. Cells were detached by incubating them in 3 mL of Trypsin-EDTA (0,05%) (cat. no. 25300054, ThermoFisher Scientific) for 3 minutes at 37 °C and 5% $CO_2$. Cells were then diluted to the desired concentration and added to new P150 petri dishes with fresh culture medium.

#### Cell preparation for experiments

A black 96-well plate was coated with of poly-L-ornithine (ref. P4957, Sigma-Aldrich) by incubating for 30 minutes at 37 °C. After 30 minutes, wells were washed with PBS to remove any non-bound poly-L-ornithine (PLO). HEK293 cells were grown in EGFR medium at 37 °C and 5% $CO_2$ in P150 petri dishes till 80% confluency. To detach cells, they were incubated for 3 minutes at 37 °C and 5% $CO_2$ in 3 mL 0.05% trypsin-EDTA. Trypsin was inactivated by addition of an excess of EGFR medium and cells were centrifuged and added to a 96-well plate at a concentration of 5,000, 50,000 or 100,000 cells/well in EGFR medium depending on the experiment and incubated for 24 hours at 37 °C and 5% $CO_2$.

#### Generation of non-small cell lung cancer mutated-EGFR and CLIP-EGFR plasmids

The SNAP-$EGFR_{NSCLC}$ and CLIP-EGFR plasmids were generated by modifying the previously described SNAP-EGFR plasmid (Scholler, Moreno-Delgado, et al. 2017). To generate the two single-point mutations (i.e. L858R and T790M) in the SNAP-EGFR construct, firstly the L858R point mutation was generated in SNAP-EGFR to obtain SNAP-$EGFR_{L858R}$-plasmid. Next, a T790M point mutation was generated in the $EGFR_{L858R}$-plasmid to obtain the SNAP-$EGFR_{L858R+T790M}$-plasmid (SNAP-$EGFR_{NSCLC}$). Corresponding sense and antisense primers were bought from Eurofins Genomics and introduced in the SNAP-EGFR by site-directed mutagenesis following the manufacturer's protocol (Agilent). For the generation of the CLIP-EGFR plasmid a gene containing the CLIP-tag was generated and substituted for the SNAP-tag by GeneCust through the generation of a synthetic gene.

**Lipofectamine transfection for experiments (for transient receptor transfection)**

Cells were prepared following the ‘’cell preparation for experiments’’ protocol. Transient plasmid transfection was done following the reverse lipofectamine transfection manufacturer’s (Lipofectamine™ 2000, Invitrogen). In short, a DNA mixture of 150 ng pcDNA (i. 4 ng of SNAP-EGFR, ii. 100 ng of CLIP-EGFR or iii. 40 ng SNAP-mGlu4-C2 and 80 ng CLIP-mGlu2-C1 qsp 150 ng with empty pRK6 vector) and 0.375 µL Lipofectamine 2000™ reagent qsp 50 µL OptiMEM (cat. no. 31985062, Thermo Fisher) per well was prepared. The prepared DNA mixture was added to HEK293 cells or a monoclonal HEK293 stable cell line in a 96-well plate depending on the experiment. The cell/DNA mixture was then incubated for 24 hours at 37 °C and 5% $CO_2$.

**Generation of HEK293 cells stably expressing SNAP-EGFR and SNAP-EGFR$_{NSCLC}$**

We incubated 250,000 HEK293 cells per well in DMEM supplemented with 10% FBS in a 6 wells plate for cell culture for 24 hours at 37 °C and 5% $CO_2$. After 24 hours we removed the medium by aspiration and added 1 mL of DMEM supplemented with 10% FBS and 1 mL OptiMEM containing 3,75 µL lipofectamine 2000™ reagents and 1500 ng DNA (i.e. 40 ng of the plasmid coding for SNAP-EGFR and 1460 ng of the plasmid coding for an empty DNA vector). Cell splitting was performed when confluency reached 80% and medium was refreshed every 2 or 3 days. At day 4 after lipofectamine transfection, medium was replaced by DMEM supplemented with 10% FBS and 0.3 mg/mL G418 (selection medium), a neomycin analog, to start selection as the used vector contains neomycin resistance. Cells were grown in 6-wells plates and at day 16 after transfection, cells were transferred into P100 plates and further grown in selection medium. At day 26 after transfection, cells were labelled at 16 °C for 1 hour with SNAP-Green and washed to remove unbound SNAP-Green. Next, cells were released from the plates with enzyme-free dissociation buffer (cat. No. 13151014, Gibco™) and diluted in PBS to a concentration of less than 1 million cells/mL. Single cell sorting was performed by the BD FACSMelody™ Cell Sorter based on signal at 488 nm, corresponding to the emission spectrum of SNAP-Green. Before cell sorting, we set the negative gate according to the counts measured for non-transfected HEK293 cells incubated with SNAP-Green. Cells that were positive were sorted in clear-bottomed black 96-wells plates and grown in selection medium. Positive clones were identified and transferred to clear 24-wells plates 40 days after transfection and 6-wells plates 45 days after transfection. After 46 days of transfection, cells were transferred to P100 plates. At 48 days after transfection, expression levels were regularly verified.

**Intersubunit FRET assay**

For the measurement of the intersubunit FRET, 50,000 monoclonal HEK293 cells stably expressing SNAP-EGFR or SNAP-EGFR$_{NSCLC}$ were incubated at 37 °C and 5% $CO_2$ in a black PLO-coated 96-wells plate 24 hours prior to the start of the experiment. EGFR medium was replaced 90 minutes before the start of the experiment by 50 µL cold serum-free DMEM supplemented with 100 nM SNAP-Lumi4-Tb and 125 nM SNAP-Green for the SNAP-SNAP-labelling or 125 nM SNAP-Green and 1 µM CLIP-Lumi4-Tb for SNAP-CLIP-labelling and cells were stored at 4 °C. Cells were then washed four times with Tag-lite buffer and 50 µL Tag-Lite containing ligands were added. Cetuximab was always pre-incubated 30 minutes before addition of the other compounds. After addition of the ligands, the cells were incubated at 37 °C and 5% $CO_2$ for 30 minutes. Next, the plates were read in the PHERAstar FS microplate reader with 30 flashes/well of a 337 nm UV-pulsed nitrogen laser. Emmission levels at 520 nm and 620 nm were integrated between 50 and 450 µs. The HTRF®-ratio was then calculated as follows:

$$HTRF® - ratio = \frac{\int_{50}^{450} 520\,nm\,signal}{\int_{50}^{450} 620\,nm\,signal} * 10{,}000.$$

Curve fitting was performed with GraphPad Prism software using nonlinear regression log(agonist) vs. response (three parameters) analysis. Values were normalized to the maximum and minimum response of EGF.

**Binding and displacement of Ab58-d2**

For the measurement of the binding of Ab58-d2 to SNAP-EGFR, 50,000 monoclonal HEK293 cells stably expressing SNAP-EGFR were incubated at 37 °C and 5% $CO_2$ in a black PLO-coated 96-wells plate 24 hours prior to the start of the experiment. EGFR medium was replaced by cold serum-free DMEM supplemented with 100 nM SNAP-Lumi4-

Tb 90 minutes prior to the experiment. Cells were then washed four times with Tag-lite buffer. Then, vehicle, 10 µM erlotinib or 10 nM EGF and Ab58-d2 were added to the cells for binding of Ab58-d2. For the displacement of Ab58-d2, vehicle or 10 µM erlotinib, 3.75 nM Ab58-d2 and cetuximab were added to the cells. The cells were incubated for 30 minutes at 37 °C and 5% $CO_2$. After incubation, the 96-well plate was read in the PHERAstar FS microplate reader using a 30 flashes/well with a 337 nm UV-pulsed nitrogen laser. Emission levels at 665 nm and 620 nm were integrated between 50 and 450 µs. The HTRF®-ratio was then calculated as follows:

$$HTRF® - ratio = \frac{\int_{50}^{450} 665\ nm\ signal}{\int_{50}^{450} 620\ nm\ signal} * 10{,}000.$$

**ERK1/2 phosphorylation**

For measuring phosphorylation and total ERK1/2 we added 5,000 monoclonal HEK293 cells stably expressing SNAP-EGFR per well to a black PLO-coated 96-well plate 24 hours prior to starting the experiment. EGFR medium was replaced by 50 µL pre-heated serum-free DMEM 3 hours prior to the experiment and cells were kept at 37 °C and 5% $CO_2$. Ligands were prepared in serum-free DMEM and heated to 37 °C. Inhibitors were pre-incubated for 10 minutes after which EGF was added. After 5 minutes of stimulation with EGF, the medium was removed by plate flicking and cells were lysed in 50 µL lysis buffer directly. After cells were lysed, 16 µL of lysate was transferred to a white 384-well plate and 4 µL of an anti-phospho-ERK1/2 antibody mixture (cat. no. 64AERPEH, Cisbio Bioassays) was added to the lysate. During the optimization, we determined that total ERK1/2 levels were not influenced by any of the ligands and therefore 16 µL of lysate of cells stimulated with vehicle was transferred to a 384-wells plate and 4 µL of an anti-ERK1/2 antibody mixture (cat. no. 64NRKPEH, Cisbio Bioassays) was added to the lysate. Both antibody mixtures consist of antibodies labelled with $Eu^{3+}$-cryptate and d2, TR-FRET-compatible fluorophores. The lysate and antibody mixtures were incubated for minimally 4 hours at room temperature. After incubation, 384-wells plates were read in the PHERAstar FS microplate reader using 30 flashes/well with a 337 nm UV-pulsed nitrogen laser. Emission levels at 665 nm and 620 nm were integrated between 50 and 450 µs. The HTRF®-ratio was then calculated as follows:

$$HTRF® - ratio = \frac{\int_{50}^{450} 665\ nm\ signal}{\int_{50}^{450} 620\ nm\ signal} * 10{,}000.$$

For each sample, the HTRF®-ratios of the phospho-ERK1/2 and total ERK1/2 were divided to calculate the signal over noise ratio (S/N):

$$S/N = \frac{HTRF®{-}ratio\ (phospho\ ERK1/2)}{HTRF®{-}ratio\ (total\ ERK1/2)}.$$

S/N values were plotted as a negative logarithmic function of ligand concentrations and a curve was fitted with GraphPad Prism software, using a log(agonist) vs. response (three parameters) analysis for agonists and log(inhibitor) vs. response – response (three parameters) analysis for inhibitors. Values were normalized and the bottom of the curve of EGF was set as 0% and the top of the curve of EGF was set at 100%. The best fit values of the logEC50 and logIC50 values were determined by performing a least-squares fit.

**Phosphorylation of Y1068 of the EGFR**

The phosphorylation and total EGFR were measured by adding 50,000 polyclonal HEK293 cells expressing SNAP-EGFR per well to a black PLO-coated 96-well plate 24 hours prior to starting the experiment. EGFR medium was replaced by 50 µL pre-heated serum-free DMEM 3 hours prior to the experiment and cells were kept at 37 °C and 5% $CO_2$. Ligands were prepared in serum-free DMEM and heated to 37 °C. Inhibitors were pre-incubated for 30 minutes after which EGF was added. After 30 minutes of stimulation with EGF, the medium was removed by plate flicking

and cells were lysed in 50 µL lysis buffer directly. After cells were lysed, 16 µL of lysate was transferred to a white 384-well plate and 4 µL of an anti-phospho-Y1068-EGFR antibody mixture was added to the lysate. During the optimization, we determined that total EGFR levels were not influenced by any of the ligands. The antibody mixture consists of antibodies labelled with $Eu^{3+}$-cryptate and d2. The lysate and antibody mixture were incubated for minimally 4 hours at room temperature. After incubation, 384-wells plates were read in the PHERAstar FS microplate reader using 30 flashes/well of a 337 nm UV-pulsed nitrogen laser. Emission levels at 665 nm and 620 nm were integrated between 50 and 450 µs. The HTRF®-ratio was then calculated as follows:

$$HTRF® - ratio = \frac{\int_{50}^{450} 665\ nm\ signal}{\int_{50}^{450} 620\ nm\ signal} * 10{,}000$$

HTRF®-ratio values were plotted as a negative logarithmic function of ligand concentrations and a curve was fitted with GraphPad Prism 9.0 software (ref.), using a log(agonist) vs. response (three parameters) analysis for agonists and log(inhibitor) vs. response (three parameters) analysis for inhibitors. Values were normalized and the bottom of the curve of EGF was set as 0% and the top of the curve of EGF was set at 100%. The best fit values of the logEC50 and logIC50 values were determined by performing a least-squares fit.

**Internalization**

To measure internalization of the EGFR, we adapted an internalization assay previously described for GPCRs labelled with a SNAP-tag (Levoye et al. 2015). We added 100,000 monoclonal HEK293 cells stably expressing SNAP-EGFR in EGFR medium per well to a flat-bottomed white PLO-coated 96-well plate 24 hours prior to starting the experiment and were kept at 37 °C and 5% $CO_2$. After removal of the EGFR medium by aspiration, cold 100 nM SNAP-Lumi4Tb in serum-free DMEM was added and incubated at 4 °C during 90 minutes. Labelling of the receptors at the cell surface was performed at 4 °C to prevent constitutive internalization. Ligands were prepared in a 25 µM fluorescein solution in Tag-lite buffer (FB) and kept on ice. After 90 minutes, plates were washed three times with Tag-lite buffer and inhibitors in pre-cooled FB were added to the plate and incubated for 30 or 120 minutes. After incubation, agonists (i.e. EGF or TGF-α) in pre-cooled FB were added to the plate and the plate was put in the PHERAstar FS microplate reader that was pre-heated at 37 °C and measurements were started. Each 3 minutes for 120 minutes, cells were excited by a UV-pulsed nitrogen laser at 337 nm and emission spectra at 620 nm between 1500 and 3000 µs and 520 nm emission spectra between 160 and 560 µs were integrated. HTRF®-ratio was calculated as follows:

$$HTRF® - ratio = \frac{\int_{1500}^{3000} 620\ signal}{\int_{160}^{560} 520\ signal} * 10{,}000$$

HTRF®-ratio values for agonists were plotted as a negative logarithmic function of ligand concentrations and a curve was fitted with GraphPad Prism 9.0 software (ref.), using a log(agonist) vs. response three parameters analysis. The bottom of the curve of EGF was set as 0% and the top of the curve of EGF was set at 100%. The best fits of the logEC50 and logIC50 values were determined by a least-squares fit.

To determine the slowing down of the rate of internalization, values were normalized and the HTRF®-ratio at time-point 0 was set as 0% and the top of the peak value of the response to 100 nM of EGF (typically after 30 to 39 minutes) was set as 100%. We then used the normalized value of inhibitor in presence of 10 nM EGF at the time point of the peak of 100 nM EGF and inversed the normalization by setting 0% as 100 and 100% as 0. These values were used to calculate the % of slowing down the rate of internalization.

To determine whether Lumi4Tb was not photo-bleached, we labelled SNAP-EGFR with Lumi4Tb and added tag-lite buffer instead of FB to the wells. We measured the 620 nm signal each 3 minutes for 120 minutes. The emission levels at 620 nm for Lumi4-Tb remained stable over time.

**Fluorescence microscopy**

Cells were prepared 48 hours before the start of the experiment. Lab-Tek®II 8-chamber #1.5 German Coverglass System plates (cat. no. 155409, Nunc) were coated with PLO and 25,000 cells per well in DMEM supplemented with 10% FBS were added. Cells were incubated at 37 °C and 5% $CO_2$. At 4 hours before the start of the experiment, 200 nM of BG-Red in ice-cold serum-free DMEM was added and cells were incubated at 4 °C for 90 minutes. Next, wells were washed 4 times with Tag-Lite®-buffer and 250 µL ice-cold Tag-Lite®-buffer containing 1 µM erlotinib, 1 µM osimertinib, 10 nM cetuximab or vehicle was added and incubated for 2 hours at 4 °C. A pre-heated LSM780 confocal microscope (Zeiss) at 37 °C with 63X Plan Apochromat 1.4 NA oil DIC (Zeiss) and X-Cite 120LED Boost High-Power LED illumination system (Excelitas Technologies) was used for image acquisition. SNAP-Red was excited by a helium-neon laser at 633 nm. Images were taken in brightfield and red acceptor emission spectrum, right before addition of 250 µL pre-heated EGF (final concentration of 10 nM) or vehicle and after 30 minutes incubation at 37 °C. Image brightness was optimized by ImageJ (Version 2.1.0/1.53c, Fiji) for each condition. The same brightness settings were used for the same condition at 0 and 30 minutes.

**Data analysis**

All experiments have been performed at least three times and all graphs present the means and standard error of the mean (SEM) of at least three individually performed experiments unless stated otherwise. Curve fitting and statistical analysis was done with GraphPad Prism software (version 9.0) and is explained in the corresponding figure legends.

## 13.9 ANNEX IX: SUPPLEMENTARY INFORMATION CHAPTER 10: "A NANOBODY ACTIVATING METABOTROPIC GLUTAMATE RECEPTOR 4 DISCRIMINATES BETWEEN HOMO- AND HETERODIMERS"

### Materials

L-AP4 (Cat. No. 0103), LY341495 (Cat. No. 1209/1), LY379268 (Cat. No. 2453) and L-Quisqualic acid (Cat. No. 0.188) were bought from Tocris Bioscience. Isopropyl β-D-1-thiogalactopyranoside (IPTG) (ref. I6758), L-glutamic acid hydrochloride (ref. G2128) and Poly-L-Ornithine (ref. P4957) were from Sigma-Aldrich. $O^6$-benzylcytosine (BC)-Lumi4-Tb (ref. SCLPTBF), BC-Green (ref. SCLPGRNF), $O^6$-benzylguanine (BG)-Lumi4Tb (ref. SSNPTBX), BG-Green (ref. SSNPGRNZ), anti-c-Myc-d2 (ref. 61MYCDAF) and Tag-lite® buffer (ref. LABMED) were kindly supplied by Cisbio Bioassays. BG-Cy3b was custom designed by Cisbio Bioassays. The plasmids encoding for the N-terminal SNAP-tag and CLIP-tag-labelled wild-type human and rat mGlu4 (Scholler, Moreno-Delgado, et al. 2017), rat mGlu2-C1KKXX (Doumazane et al. 2011) and rat SNAP-mGlu4-C2KKXX (J. Liu et al. 2017) have been described previously.

### Methods

**Llama immunization, selection, production and purification of DN45**

The llama immunization, selection, production and purification of DN45 were performed as described previously (Scholler, Nevoltris, et al. 2017). In brief, two llamas were immunized by four subcutaneous injections with $5 \times 10^7$ HEK293T cells, transfected with rat or human mGlu4 receptors. The $V_HH$ library constructions were performed in E. Coli TG1 strains and the library diversity was above $10^9$ transformants.

Bacteria were then infected by KM13 helper phage and phage-containing pellets were purified by two selection rounds on human mGlu4 receptor transfected in HEK293T ($2 \times 10^7$) cells. Each round was preceded by a depletion step on cells that were not transfected and positive selections were performed in the presence of an excess of anti-HEK293 cells (Even-Desrumeaux et al. 2014). E. Coli TG1 bacteria were infected with eluted phages and could be used for production of the nanobody.

The production of DN45 was done by transforming E. Coli BL21DE3 strain bacteria. They were grown overnight at 37 °C while agitating. Protein production was induced the day after by addition of 1 mM IPTG and bacteria were grown overnight at 28 °C while agitating. Bacteria were then collected and lysed in TES-buffer containing Tris, EDTA and sucrose. After centrifugation, the periplasmic extract was recovered and the His-tagged nanobodies were purified by Ni-NTA purification (Qiagen).

**Mutagenesis**

For the generation of rmG4-2M, rmG4-3M, rmG4-4MA, rmG4-4MB and rmG4-5M, synthethic genes encoding for the rat mGlu4 with corresponding mutations were ordered at GeneCust. The synthetic gene was inserted in a N-terminally SNAP-tagged rat mGlu4 receptor with the DNA ligation kit from Agilent Technologies. SNAP-rmG4-5M-C2KKXX was generated by introducing the synthetic gene encoding for rmG4-5M into a N-terminally SNAP-tagged rat mGlu4 receptor with a C-terminal endoplasmic reticulum sequence C2KKXX. All other mutations were done by site-directed mutagenesis following the QuickChange mutagenesis protocol from Agilent Technologies.

**Cell culture and transfection**

HEK-293 (ATCC® CRL-1573™) cells were cultured in Dulbecco's Modified Eagle Medium (DMEM) (ref. 41965, Gibco™) containing 10% fetal bovine serum (FBS) (ref. F2442, Sigma-Aldrich). For each experiment we used 100,000 cells/well of a black 96-wells plate (ref. 655086, Greiner bio-one) coated with poly-L-ornithine (ref. P4957, Sigma-Aldrich). Cells were detached from the petridish (~80% confluency) with trypsin-EDTA

(0.05%) (ref. 25300054, Gibco™) and after removal of the trypsin-EDTA by centrifuging, diluted in DMEM supplemented with 10% FBS.

Depending on the experiment, HEK-293 cells were transfected by electroporation (Brabet, Parmentier, and Colle 1998) or reverse lipofectamine transfection following the manufacturer's protocol (Invitrogen™ Lipofectamine 2000™). To prevent toxic concentrations of glutamate in the medium, excitatory amino acid transporter 3 (EAAC1) was co-transfected. For binding experiments 9 µg of plasmid of the receptor and 1 µg EAAC1 were co-transfected by electroporation. For IP-1 accumulation experiments, 8 µg of plasmid of the receptor, 1 µg Gqi9 and 1 µg EAAC1 were co-transfected by electroporation. For the Gi-BRET assay, 4 µg of plasmid of the receptor, 0.8 µg Gi-Rluc, 0.8 µg Gβ, 1.6 µg Gγ-Venus and 1 µg EAAC1 were co-transfected by electroporation. For the mGlu2-4 biosensor experiment, 80 ng CLIP-mGlu2-C1KKXX, 40 ng SNAP-rmG4-5M-C2KKXX, 20 ng EAAC1 and 10 ng pRK6 empty vector per well were transfected by reverse lipofectamine transfection. Cells were incubated for 24 hours at 37 °C and 5% $CO_2$ and medium was changed for pre-heated serum-free DMEM Glutamax (ref. 10566016, Gibco™) 2 hours before the start of the experiment.

**Labelling of CLIP and SNAP-tag**
Labelling of the CLIP and SNAP-tag with fluorescent molecules was done for 1 hour and 30 minutes at 37 °C in serum-free DMEM Glutamax. For expression and binding experiments for the mGlu4, the cells were incubated with 100 nM BG-Lumi4Tb. For measuring expression levels of the mGlu2-4, the cells were incubated with 1 µM BC-Lumi4Tb and 100 nM BG-Lumi4Tb. For binding on the mGlu2-4, the cells were incubated with 1 µM BC-Lumi4Tb. For the TR-FRET biosensor assay of the mGlu4, the cells were incubated with 100 nM BG-Lumi4Tb and 60 nM BG-Green. For the TR-FRET biosensor assay of the mGlu2-4, the cells were incubated with 100 nM BG-Lumi4Tb and 1 µM BC-Green. Unbound substrate was removed by washing each well four times with Tag-lite®-buffer.

**DN45 binding and selectivity assay**
Eight rat and eight human mGlu receptors were overexpressed in HEK293 cells as described in cell culture and transfection and incubated in a black 96-wells plate. Expression levels of the receptors were measured by the PHERAstar FS as the signal at 620 nm after excitation at 337 nm by a UV-pulsed nitrogen laser. Next, cells were pre-incubated for 30 minutes at 37 °C and 5% $CO_2$ with 10 µM L-AP4, 100 nM LY379268, 1 µM quisqualic acid or 100 µM LY341495 in Tag-lite®-buffer depending on the overexpressed receptor. Then,105 nM of DN45 and 200 nM anti-c-Myc-d2 were added at the same time and cells were incubated for 3 hours at 20 °C. As a negative control, a nanobody against β-arrestin 2 containing the c-Myc sequence was added instead of DN45. TR-FRET was measured with the PHERAstar FS after excitation at 337 nm by a UV-pulsed nitrogen laser. Signals at 620 nm and 665 nm were integrated and the HTRF®-ratio was calculated as follows:

$$HTRF® - ratio = \frac{Signal\ 665\ nm}{Signal\ 620\ nm} \times\ 10{,}000$$

Values were normalized as the signal over the signal of the negative control.

**IP-1 accumulation assay**
Inositol phosphate (IP-1) accumulation was determined with the IP-One assay kit from Cisbio Bioassays (ref. 62IPAPEC). Cells had been prepared in a black 96-wells plate. Dilution ranges of DN45 and L-AP4 were prepared in stimulation buffer, added to the cells and incubated for 30 minutes at 37 °C and 5% $CO_2$. Then, cells were lysed by addition of IP1 labelled with d2 and anti-IP1 antibody labelled with Lumi4Tb in lysis buffer. The lysate was incubated for 1 hour at 20 °C and TR-FRET was measured with the PHERAstar FS and the HTRF®-ratio was determined. Values were normalized as the percentage of response to L-AP4.

**mGlu2-4 and mGlu4 biosensor assay**
Compounds were added to each well of a black 96-wells plate containing cells and incubated for 30 minutes at 37 °C and 5% $CO_2$ in Tag-lite®-buffer. In case of pre-incubation steps, compounds were pre-incubated 30 minutes at 37 °C and 5% $CO_2$ prior to addition of the other compounds. TR-FRET was measured with the PHERAstar FS after excitation at 337 nm by a UV-pulsed nitrogen laser. The signal at 520 nm was integrated and an acceptor ratio was calculated as described before (Scholler, Moreno-Delgado, et al. 2017):

$$Acceptor\ ratio\ (\mu s) = \frac{\int_{100}^{50} Signal\ at\ 520\ nm}{\int_{1600}^{1200} Signal\ at\ 520\ nm}$$

Values were normalized as the percentage of response to L-AP4.

**BRET assay**
Cells had been prepared in a black 96-wells plate. Coelenterazine and dilution ranges of DN45, L-AP4 were prepared in PBS buffer. The signals at 530 nm and 480 nm were measured by the Mithras LB 940 (Berthold). Coelenterazine was added and signals were measured for 10 minutes. Then, coelenterazine and compounds were added directly after each other. Signals were measured for 25 minutes and BRET-values were calculated by dividing the signals at 530 nm and 480 nm. Values were normalized as percentage of response to L-AP4.

**Statistical analysis**
Curve fitting and statistical analysis was done with Graphpad Prism software (version 9.0). Data are expressed as mean ± SEM of three or more individually performed experiments. The performed statistical analysis is explained in the corresponding figure legend. P-values<0.05 were considered significant.

## Single-molecule FRET approach

**Sample preparation and smFRET measurements**
Sample preparation and smFRET measurements were done as previously described(Cao et al. 2021) with a few modifications as specified in the following.

**Cell culture, transfection and membrane fraction preparation**
HEK293T cells (ATCC CRL-3216, LGC Standards S.a.r.l., France) were grown in Gibco™ DMEM, high glucose, GlutaMAX™ Supplement, pyruvate (Thermo Fisher Scientific, France) supplemented with 10% (vol/vol) FBS (Sigma-Aldrich, France) at 37°C, 5% $CO_2$ in 25cm$^2$ flasks to approximately 80 % confluence. Transfection was carried out by mixing 4 µg SNAP-mGlu4 plasmid DNA and 8 µl Lipofectamine 2000 (Thermo Fisher Scientific, France) in 500 µl Gibco™ Opti-MEM™ I reduced serum medium (Thermo Fisher Scientific, France) and incubation at room temperature for 25 minutes. The mixture was then added to the cells in DMEM GlutaMax supplemented with10 % FBS and expression was carried out for 72h at 37°C and 5% $CO_2$. The medium was replaced once with fresh DMEM GlutaMax with 10 % FBS after 48h. SNAP-tag labeling was achieved by addition of 2 mL DMEM GlutaMax supplemented with 900 nM BG-Cy3b and 300 nM BG-d2 and carried out for 1.5 hours at 37°C and 5 % $CO_2$, followed by three washes with 5 mL PBS DPBS w/o $Ca^{2+}$ and $Mg^{2+}$ (Thermo Fischer Scientific, France) at ambient temperature. Then cells were detached mechanically using a cell scraper in DPBS and collected at 1000 x g and 22°C for 5 minutes. Cells were resuspended in cold hypotonic lysis buffer (10 mM HEPES pH 7.4, cOmplete™ protease inhibitor (Sigma-Aldrich, France)), frozen and stored at -80°C. For the preparation of membrane fractions cells were thawed on ice and passed 30-times through a 200 µL pipette tip. After two rounds of centrifugation at 500 x g and 4°C for 5 min, the supernatant was aliquoted and centrifuged at 21,000 x g and 4°C for 30 min to collect crude membranes. The pellets were washed once with 20 mM HEPES pH 7.4, 118 mM NaCl, flash frozen in liquid $N_2$ and stored at -80°C.

**Detergent solubilization**
Receptors were solubilized on ice by resuspension of crude membranes in acquisition buffer (20 mM Tris-HCl pH7.4, 118 mM NaCl, 1.2 mM $KH_2PO_4$, 1.2 mM $MgSO_4$, 4.7 mM KCl, 1.8 mM $CaCl_2$) supplemented with 1 % (w/v) lauryl maltose neopentyl glycol (LMNG, Anatrace purchased through CliniSciences, France) + 0.2 % (w/v) cholesteryl hemisuccinate tris salt (CHS Tris, Anatrace purchased through CliniSciences, France) for 5 min. Then Glyco-diosgenin (GDN, Avanti Polar Lipids purchased through Merck) was added (final detergent concentration 0.83 % LMNG + 0.167 % CHS Tris + 0.83 % GDN) and the solution was centrifuged for 10 min at 21,000 x g and 4°C. The supernatant was diluted 8.33-times in acquisition buffer and applied to a Zeba Spin Desalting Column (7 kDa cut-off, Thermo Fisher Scientific, France) equilibrated in acquisition buffer containing 0.005 %

LMNG + 0.001 % CHS Tris + 0.005 % GDN and centrifuged 2 min at 1,500 x g and 4°C. The flow-through was then immediately diluted 10-times in cold acquisition buffer and kept on ice in the dark until use.

**smFRET measurements**
The pulsed interleaved excitation (PIE) – multiparameter fluorescence detection (MFD) setup, data acquisition and analysis were previously described.(Cao et al. 2021) Measurements were performed at a 4 times dilution of the sample in acquisition buffer without detergent and further dilution in acquisition buffer containing 0.0025 % LMNG, 0.0005 CHS tris, 0.0025 % GDN to achieve single molecule-compatible concentrations of labeled receptors (approximately 30-50 pM) in the absence of ligand or in presence of 100 µM LY34, 10 µM DN45 or 10 µM L-AP4. Apparent FRET efficiencies ($E_{PR}$) corrected for direct acceptor excitation and donor leakage into the acceptor channel were determined using the Software Package for Multiparameter Fluorescence Spectroscopy, Full Correlation and Multiparameter Fluorescence Imaging developed in C.A.M. Seidel's lab (http:// www.mpc.uni-duesseldorf.de/seidel/) as previously described.(Olofsson et al. 2014) FRET histograms were fitted using Origin 6 (Microcal Software, Inc.) and displayed in GraphPad Prism 7.05.

## Molecular modelling

**Homology model of mGlu4 VFT**
The model for the mGlu4 homodimer was built using MODELER (Sali and Blundell 1993) as implemented in Discovery Studio. Two PDB structures 6BSZ (Human mGlu8 Receptor complexed with glutamate at 2.65 Å resolution) and 6BT5 (Human mGlu8 Receptor complexed with L-AP4 at 2.92 Å resolution) were used as templates. A disulfide bridge was defined between the Cys 136 of the two loops. The ligand L-AP4 from 6BT5 was used when constructing the model. We generated 100 models and the one with the lowest probability density factor (PDF) and lowest discrete optimized protein energy (DOPE) (Shen and Sali 2006) score was selected.

**Homology model of DN45**
We then built the homology model of DN45 with the Model Antibody Cascade protocol from Discovery Studio 2020. This protocol automatically identified most similar PDB structures to model the framework and used 5GXB, 5IMM, 4LGS and 5M2W. The protocol also identifies the best templates for each CDR loop. For loop H1, it used loop H1 from PDB structures 5LMJ and EJ1. For loop H2, the templates were the H2 loop from 6EHG, 4TVS. Finally, for loop H3, the templates loops where from 5LWF and 1U0Q.

**Docking of DN45 to mGlu4 VFT**
The docking of DN45 to mGlu4 VFT was performed with ZDOCK (R. Chen, Li, and Weng 2003) as implemented in Discovery Studio (BIOVIA, Dassault Systèmes, Discovery Studio Modeling Environment, Release 2020, San Diego: Dassault Systèmes, 2020). After generating 54000 poses, a filtering was then used to keep only poses where CDRs from the nanobody DN45 were interacting with mGlu4. The distance criterion was 10 Å. The two first poses with the best ZRANK (Pierce and Weng 2007) score were in the same cluster, at the interface of the two lobes.

**Refinement of Docked Structures**
In order to refine the best pose generated with ZDOCK, we solvated the mGlu4 dimer-DN45 complex and the mGlu4 dimer-DN45-L-AP-4 complex in an orthorhombic periodic box of water with a minimum distance from boundary of 15.0 Å and performed with NAMD (Phillips et al. 2005) a molecular dynamics simulation for 10 ns for each system. Analysis of trajectories and non-bonded interactions have been performed with Discovery Studio.

**Virtual mutations**
Using the last frame of the molecular dynamics simulation, we performed a virtual mutagenesis to identify residues in mGlu4 that are critical for binding to DN45. We used the Discovery Studio Calculate Mutation Energy Binding protocol (Spassov and Yan 2012) that evaluates the effect of mutations on the binding affinity of molecular partners in protein-protein and protein-ligand complexes. It performs combinatorial amino-acid scanning mutagenesis on a set of selected amino-acid residues by mutating them to one or more specified amino-acid types. The energy effect of each mutation on the binding affinity ($\Delta\Delta G_{mut}$) is calculated as the difference between the binding free energy ($\Delta\Delta G_{bind}$) in the mutated structure and wild type protein: $\Delta\Delta G_{mut}$ =

$\Delta\Delta G_{bind}$(mutant) - $\Delta\Delta G_{bind}$(wild type). The $\Delta\Delta G_{bind}$ is defined as the difference between the free energy of the complex and unbound state. All energy terms are calculated by CHARMm and the electrostatics energy is calculated using a Generalized Born implicit solvent model. The total energy is calculated as an empirical weighted sum of van der Waals interactions ($E_{vdW}$), electrostatic interactions ($\Delta G_{elec}$), an entropy contribution (-$TS_{sc}$) related to the changes in side-chain mobility, and a non-polar, surface dependent, contribution to solvation energy ($\Delta G_{np}$).

This protocol was used to predict the impact of single or a combination of mutations of human residues to their rat counterpart. Finally, the full interaction surface between DN45 and human mGlu4 was scanned.

We also calculated the impact of a single point mutation of each of these interface residues to the overall stability of mGlu4 using the Calculate Mutation Energy Stability protocol (Spassov and Yan 2016). It performs combinatorial amino-acid scanning mutagenesis on a set of selected amino-acid residues by mutating each of them to one or more specified amino-acid types. The energy effect of each mutation on the protein stability (mutation energy, $\Delta\Delta G_{mut\text{-}stab}$) is calculated as the difference of the free energy of folding ($\Delta\Delta G_{folding}$) between the mutated structure and the wild type protein: $\Delta\Delta G_{mut\text{-}stab} = \Delta\Delta G_{folding}$(mutant) - $\Delta\Delta G_{folding}$(wild type). The $\Delta\Delta G_{folding}$ is defined as the free energy difference between the folded ($\Delta G_{fld}$) and unfolded (denaturated) states ($\Delta G_{unf}$) of the protein: $\Delta\Delta G_{folding} = \Delta G_{fld} - \Delta G_{unf}$. Note that a negative value of $\Delta\Delta G_{mut}$ indicates the mutation has a stabilizing effect, and conversely, a positive value indicates the mutation has a destabilizing effect. The energy of the folded state of the wild type is derived from the input structure. The structures of the mutants in the folded state are modeled by keeping the backbone rigid while optimizing the side-chains using the ChiRotor algorithm (Spassov, Yan, and Flook 2007). Before evaluating the folding energy terms, the structures of the wild type and mutants are energy minimized using CHARMm. The unfolded state is modeled as a relaxed penta-peptide in an extended conformation with the mutated residue in the center. The peptide model is applied only to the short range interactions involving the mutated residues and it is extended with a Gaussian chain model to account for the long-range electrostatic interactions. This is based on the hypothesis that most of the contacts between amino acid residues in the unfolded protein are only sporadic if the residues are not immediate neighbors along the sequence. Considering that van der Waals interactions decline sharply with distance and contribute only at very close contacts; the method neglects the non-polar interactions between the residues that are separated by more than two peptide bonds in sequence.

All energy terms are calculated by CHARMm, and the electrostatics energy is calculated using a Generalized Born implicit solvent model. The total energy is calculated as an empirical weighted sum of van der Waals ($E_{vdW}$) interaction, electrostatic interaction ($\Delta G_{elec}$), an entropy contribution (-$TS_{sc}$) related to side-chain mobility, and a non-polar, surface dependent, contribution to solvation energy ($\Delta G_{np}$). The calculations were performed in pH-dependent mode.

# 14 BIBLIOGRAPHY


Abou-Fayçal, Cherine, Anne Sophie Hatat, Sylvie Gazzeri, and Beatrice Eymin. 2017. "Splice Variants of the RTK Family: Their Role in Tumour Progression and Response to Targeted Therapy." *International Journal of Molecular Sciences* 18 (2). https://doi.org/10.3390/ijms18020383.

Acher, Francine C, and Tocris. 2006. "Metabotropic Glutamate Receptors Molecular Pharmacology." *Cell and Tissue Research, TOCRIS*. http://www.springerlink.com/index/XJ5N003452023770.pdf.

Alberts, Bruce, Alexander Johnson, Julian Lewis, Martin Raff, Keith Roberts, and Peter Walter. 2002. "Signaling through Enzyme-Linked Cell-Surface Receptors." In *Molecular Biology of the Cell*, 4th ed. New York: Garland Science.

Arts, Remco, Stijn J A Aper, and Maarten Merkx. 2017. "Chapter Three - Engineering BRET-Sensor Proteins." In *Enzymes as Sensors*, edited by Richard B Thompson and Carol A Fierke, 589:87–114. Methods in Enzymology. Academic Press. https://doi.org/https://doi.org/10.1016/bs.mie.2017.01.010.

Bader, Arjen N., Erik G. Hofman, Jarno Voortman, Paul M.P. Van Bergen En Henegouwen, and Hans C. Gerritsen. 2009. "Homo-FRET Imaging Enables Quantification of Protein Cluster Sizes with Subcellular Resolution." *Biophysical Journal* 97 (9): 2613–22. https://doi.org/10.1016/j.bpj.2009.07.059.

Berger, Miles, John A. Gray, and Bryan L. Roth. 2009. "The Expanded Biology of Serotonin." *Annual Review of Medicine* 60: 355–66. https://doi.org/10.1146/annurev.med.60.042307.110802.

Boado, Ruben J., Eric K.W. Hui, Jeff Zhiqiang Lu, Rachita K. Sumbria, and William M. Pardridge. 2013. "Blood-Brain Barrier Molecular Trojan Horse Enables Imaging of Brain Uptake of Radioiodinated Recombinant Protein in the Rhesus Monkey." *Bioconjugate Chemistry* 24 (10): 1741–49. https://doi.org/10.1021/bc400319d.

Bockaert, J., J. Pin, and L. Fagni. 1993. "Metabotropic Glutamate Receptors: An Original Family of G Protein-coupled Receptors." *Fundamental & Clinical Pharmacology* 7 (9): 473–85. https://doi.org/10.1111/j.1472-8206.1993.tb00252.x.

Boerckel, Winfield, Johannes Bruns, Jesme Fox, Adityawati Ganggaiswari, Patricia Mondragón, Maureen Rigney, and Christina Sit. 2019. "Personalizing Treatment for Patients with Non – Small-Cell Lung Cancer :" *Conquer: The Patient Voice*, no. August. https://conquer-magazine.com/issues/special-issues/august-2019-personalizing-treatment-for-patients-with-non-small-cell-lung-cancer-the-important-role-of-biomarker-testing.

Bolander, F F. 2004. "Chapter 7: Membrane Receptors." In *Molecular Endocrinology (Third Edition)*, 3:147–213. https://doi.org/10.1146/annurev.bi.43.070174.001125.

Boucrot, Emmanuel, Antonio P.A. Ferreira, Leonardo Almeida-Souza, Sylvain Debard, Yvonne Vallis, Gillian Howard, Laetitia Bertot, Nathalie Sauvonnet, and Harvey T. McMahon. 2015. "Endophilin Marks and Controls a Clathrin-Independent Endocytic Pathway." *Nature* 517 (7535): 460–65. https://doi.org/10.1038/nature14067.

Brabet, Isabelle, Marie-laure Parmentier, and Cyril De Colle. 1998. "Comparative Effect of L -CCG-I , DCG-IV and k -Carboxy- L -Glutamate on All Cloned Metabotropic Glutamate Receptor Subtypes." *Neuropharmacology* 37: 1043–51.

Brewer, Monica Red, Hee Choi Sung, Diego Alvarado, Katarina Moravcecic, Ambra Pozzi, Mark A Lemmon, and Graham Carpenter. 2009. "The Juxtamembrane Region of the EGF Receptor Functions as an Activation Domain." *Molecular Cell* 34 (6): 641–51. https://doi.org/10.1016/j.molcel.2009.04.034.

Brice, N. L., A. Varadi, S. J.H. Ashcroft, and E. Molnar. 2002. "Metabotropic Glutamate and GABAB Receptors Contribute to the Modulation of Glucose-Stimulated Insulin Secretion in Pancreatic Beta Cells." *Diabetologia* 45 (2): 242–52. https://doi.org/10.1007/s00125-001-0750-0.

Briggs, C A, and M Gopalakrishnan. 2007. "2.22 - Ion Channels – Ligand Gated." In *Comprehensive Medicinal Chemistry II*, edited by John B Taylor and David J Triggle, 877–918. Oxford: Elsevier. https://doi.org/https://doi.org/10.1016/B0-08-045044-X/00067-5.

Bublil, E. M., G. Pines, G. Patel, G. Fruhwirth, T. Ng, and Y. Yarden. 2010. "Kinase-Mediated Quasi-Dimers of EGFR." *The FASEB Journal* 24 (12): 4744–55. https://doi.org/10.1096/fj.10-166199.

Buhrow, S. A., S. Cohen, D. L. Garbers, and J. V. Staros. 1983. "Characterization of the Interaction of 5'-p-Fluorosulfonylbenzoyl Adenosine with the Epidermal Growth Factor Receptor/Protein Kinase in A431 Cell Membranes." *Journal of Biological Chemistry* 258 (12): 7824–27.

Burgess, Antony W., Hyun Soo Cho, Charles Eigenbrot, Kathryn M. Ferguson, Thomas P.J. Garrett, Daniel J. Leahy, Mark A. Lemmon, Mark X. Sliwkowski, Colin W. Ward, and Shigeyuki Yokoyama. 2003. "An Open-and-Shut Case? Recent Insights into the Activation of EGF/ErbB Receptors." *Molecular Cell* 12 (3): 541–52. https://doi.org/10.1016/S1097-2765(03)00350-2.

Burtness, Barbara, Milan Anadkat, Surendra Basti, Miranda Hughes, Mario E. Lacouture, Joan S. McClure, Patricia L. Myskowski, et al. 2009. "NCCN Task Force Report: Management of Dermatologic and Other Toxicities Associated with EGFR Inhibition in Patients with Cancer." *Journal of the National Comprehensive Cancer Network* 7 (SUPPL. 1): 5–21. https://doi.org/10.6004/jnccn.2009.0074.

Cao, Anne-marinette, Robert B Quast, Fataneh Fatemi, and Philippe Rondard. 2021. "Allosteric Modulators Enhance Agonist Efficacy by Increasing the Residence Time of a GPCR in the Active State." *Nature Communications* in press.

Carpenter, G., and S. Cohen. 1979. "Epidermal Growth Factor." *Journal of Biological Chemistry* 48: 193–216.

Cattaneo, Fabio, Germano Guerra, Melania Parisi, Marta De Marinis, Domenico Tafuri, Mariapia Cinelli, and Rosario Ammendola. 2014. "Cell-Surface Receptors Transactivation Mediated by G Protein-Coupled Receptors." *International Journal of Molecular Sciences* 15 (11): 19700–728. https://doi.org/10.3390/ijms151119700.

Chang, Hee Jin, Byong Chul Yoo, Seok Byung Lim, Seung Yong Jeong, Woo Ho Kim, and Jae Gahb Park. 2005. "Metabotropic Glutamate Receptor 4 Expression in Colorectal Carcinoma and Its Prognostic Significance." *Clinical Cancer Research* 11 (9): 3288–95. https://doi.org/10.1158/1078-0432.CCR-04-1912.

Charvin, Delphine. 2018. "MGlu4 Allosteric Modulation for Treating Parkinson's Disease." *Neuropharmacology* 135: 308–15. https://doi.org/10.1016/j.neuropharm.2018.03.027.

Chen, Jianchun, Fenghua Zeng, Steven J. Forrester, Satoru Eguchi, Ming Zhi Zhang, and Raymond C. Harris. 2016. "Expression and Function of the Epidermal Growth Factor Receptor in Physiology and Disease." *Physiological Reviews* 96 (3): 1025–69. https://doi.org/10.1152/physrev.00030.2015.

Chen, Lingfeng, Weitao Fu, Lulu Zheng, Zhiguo Liu, and Guang Liang. 2018. "Recent Progress of Small-Molecule Epidermal Growth Factor Receptor (EGFR) Inhibitors against C797S Resistance in Non-Small-Cell Lung Cancer." Review-article. *Journal of Medicinal Chemistry* 61 (10): 4290–4300. https://doi.org/10.1021/acs.jmedchem.7b01310.

Chen, Rong, Li Li, and Zhiping Weng. 2003. "ZDOCK : An Initial-Stage Protein-Docking Algorithm." *PROTEIN: Structure, Function, and Genetics* 52: 80–87.

Christopoulos, A, L T May, V A Avlani, and P M Sexton. 2004. "G-Protein-Coupled Receptor Allosterism: The Promise and the Problem(S)." *Biochemical Society Transactions* 32 (Pt 5): 873–77. https://doi.org/10.1042/BST0320873.

Chung, Inhee, Robert Akita, Richard Vandlen, Derek Toomre, Joseph Schlessinger, and Ira Mellman. 2010. "Spatial Control of EGF Receptor Activation by Reversible Dimerization on Living Cells." *Nature* 464 (7289): 783–87. https://doi.org/10.1038/nature08827.

Clark, Alfred J. 1933. *The Mode of Action of Drugs on Cells. The Mode of Action of Drugs on Cells*. London, England: Arnold.

Claus, Jeroen, Gargi Patel, Flavia Autore, Audrey Colomba, Gregory Weitsman, Tanya N. Soliman, Selene Roberts, et al. 2018. "Inhibitor-Induced HER2-HER3 Heterodimerisation Promotes Proliferation through a Novel Dimer Interface." *ELife* 7: 1–23. https://doi.org/10.7554/eLife.32271.

Coban, Oana, Laura C. Zanetti-Dominguez, Daniel R. Matthews, Daniel J. Rolfe, Gregory Weitsman, Paul R. Barber, Jody Barbeau, et al. 2015. "Effect of Phosphorylation on EGFR Dimer Stability Probed by Single-Molecule Dynamics and FRET/FLIM." *Biophysical Journal* 108 (5): 1013–26. https://doi.org/10.1016/j.bpj.2015.01.005.

Cohen, S., H. Ushiro, C. Stoscheck, and M. Chinkers. 1982. "A Native 170,000 Epidermal Growth Factor Receptor-Kinase Complex from Shed Plasma Membrane Vesicles." *Journal of Biological Chemistry* 257 (3): 1523–31.

Comps-Agrar, Laétitia, Julie Kniazeff, Lenea Nørskov-Lauritsen, Damien Maurel, Martin Gassmann, Nathalie Gregor, Laurent Prézeau, et al. 2011. "The Oligomeric State Sets GABA B Receptor Signalling Efficacy." *EMBO Journal* 30 (12): 2336–49. https://doi.org/10.1038/emboj.2011.143.

Conti, Fiorenzo, Silvia DeBiasi, Andrea Minelli, Jeffrey D. Rothstein, and Marcello Melone. 1998. "EAAC1, a High-Affinity Glutamate Transporter, Is Localized to Astrocytes and Gabaergic Neurons besides Pyramidal Cells in the Rat Cerebral Cortex." *Cerebral Cortex* 8 (2): 108–16. https://doi.org/10.1093/cercor/8.2.108.

Corti, C., L. Aldegheri, P. Somogyi, and F. Ferraguti. 2002. "Distribution and Synaptic Localisation of the Metabotropic Glutamate Receptor 4 (MGluR4) in the Rodent CNS." *Neuroscience* 110 (3): 403–20. https://doi.org/10.1016/S0306-4522(01)00591-7.

Cortot, Alexis B., and Pasi A. Jänne. 2014. "Molecular Mechanisms of Resistance in Epidermal Growth Factor Receptor-Mutant Lung Adenocarcinomas." *European Respiratory Review* 23 (133): 356–66. https://doi.org/10.1183/09059180.00004614.

Cottet, Martin, Orestis Faklaris, Damien Maurel, Pauline Scholler, Etienne Doumazane, Eric Trinquet, Jean Philippe Pin, and Thierry Durroux. 2012. "BRET and Time-Resolved FRET Strategy to Study GPCR Oligomerization: From Cell Lines toward Native Tissues." *Frontiers in Endocrinology* 3 (JUL). https://doi.org/10.3389/fendo.2012.00092.

Cromie, Karen D, and Gino Van Heeke and Carlo Boutton. 2015. "Nanobodies and Their Use in GPCR Drug Discovery." *Current Topics in Medicinal Chemistry*. https://doi.org/http://dx.doi.org/10.2174/1568026615666150701113549.

Cross, Darren A.E., Susan E. Ashton, Serban Ghiorghiu, Cath Eberlein, Caroline A. Nebhan, Paula J. Spitzler, Jonathon P. Orme, et al. 2014. "AZD9291, an Irreversible EGFR TKI, Overcomes T790M-Mediated Resistance to EGFR Inhibitors in Lung Cancer." *Cancer Discovery* 4 (9): 1046–61. https://doi.org/10.1158/2159-8290.CD-14-0337.

Dagogo-Jack, Ibiayi, and Alice T. Shaw. 2018. "Tumour Heterogeneity and Resistance to Cancer Therapies." *Nature Reviews Clinical Oncology* 15 (2): 81–94. https://doi.org/10.1038/nrclinonc.2017.166.

Dankort, D L, Z Wang, V Blackmore, M F Moran, and W J Muller. 1997. "Distinct Tyrosine Autophosphorylation Sites Negatively and Positively Modulate Neu-Mediated Transformation." *Molecular and Cellular Biology* 17 (9): 5410–25. https://doi.org/10.1128/mcb.17.9.5410.

Dar, Arvin C., and Kevan M. Shokat. 2011. "The Evolution of Protein Kinase Inhibitors from Antagonists to Agonists of Cellular Signaling." *Annual Review of Biochemistry* 80: 769–95. https://doi.org/10.1146/annurev-biochem-090308-173656.

Dawson, Jessica P, Mitchell B Berger, Chun-Chi Lin, Joseph Schlessinger, Mark A Lemmon, and Kathryn M Ferguson. 2005. "Epidermal Growth Factor Receptor Dimerization and Activation Require Ligand-Induced Conformational Changes in the Dimer Interface." *Molecular and Cellular Biology* 25 (17): 7734–42. https://doi.org/10.1128/MCB.25.17.7734.

Delcourt, Nicolas, Eric Thouvenot, Benjamin Chanrion, Nathalie Galéotti, Patrick Jouin, Joël Bockaert, and Philippe Marin. 2007. "PACAP Type I Receptor Transactivation Is Essential for IGF-1 Receptor Signalling and Antiapoptotic Activity in Neurons." *EMBO Journal* 26 (6): 1542–51. https://doi.org/10.1038/sj.emboj.7601608.

Delgado, David Moreno, Thor C. Møller, Jeanne Ster, Jesús Giraldo, Damien Maurel, Xavier Rovira, Pauline Scholler, et al. 2017. "Pharmacological Evidence for a Metabotropic Glutamate Receptor Heterodimer in Neuronal Cells." *ELife* 6: 1–33. https://doi.org/10.7554/eLife.25233.

Dickerson, Jonathan W, and P Jeffrey Conn. 2012. "Therapeutic Potential of Targeting Metabotropic Glutamate Receptors for Parkinson's Disease." *Neurodegenerative Disease Management* 2 (2): 221–32. https://doi.org/10.2217/nmt.12.6.

Dijkman, Patricia M., Oliver K. Castell, Alan D. Goddard, Juan C. Munoz-Garcia, Chris De Graaf, Mark I. Wallace, and Anthony Watts. 2018. "Dynamic Tuneable G Protein-Coupled Receptor Monomer-Dimer Populations." *Nature Communications* 9 (1). https://doi.org/10.1038/s41467-018-03727-6.

Diwanji, Devan, Tarjani Thaker, and Natalia Jura. 2019. "More than the Sum of the Parts: Toward Full-Length Receptor Tyrosine Kinase Structures." *IUBMB Life* 71 (6): 706–20. https://doi.org/10.1002/iub.2060.

Doller, Dario, Anton Bespalov, Rob Miller, Malgorzata Pietraszek, and Mikhail Kalinichev. 2020. "A Case Study of Foliglurax, the First Clinical MGluR4 PAM for Symptomatic Treatment of Parkinson's Disease: Translational Gaps or a Failing Industry Innovation Model?" *Expert Opinion on Investigational Drugs* 29 (12): 1323–38. https://doi.org/10.1080/13543784.2020.1839047.

Doumazane, Etienne, Pauline Scholler, Jurriaan M. Zwier, Eric Trinquet, Philippe Rondard, and Jean-Philippe Pin. 2011. "A New Approach to Analyze Cell Surface Protein Complexes Reveals Specific Heterodimeric Metabotropic Glutamate Receptors." *The FASEB Journal* 25 (1): 66–77. https://doi.org/10.1096/fj.10-163147.

Drube, Sebastian, Jörg Stirnweiss, Christina Valkova, and Claus Liebmann. 2006. "Ligand-Independent and EGF Receptor-Supported Transactivation: Lessons from B2-Adrenergic Receptor Signalling." *Cellular Signalling* 18 (10): 1633–46. https://doi.org/10.1016/j.cellsig.2006.01.003.

Du, Juan, Dejian Wang, Hongcheng Fan, Chanjuan Xu, Linhua Tai, Shuling Lin, Shuo Han, et al. 2021. "Structures of Human MGlu2 and MGlu7 Homo- and Heterodimers." *Nature* 594 (7864): 589–93. https://doi.org/10.1038/s41586-021-03641-w.

Duggan, Sean. 2018. "Caplacizumab : First Global Approval." *Drugs* 78 (15): 1639–42. https://doi.org/10.1007/s40265-018-0989-0.

Dzubay, Jeffrey A., and Craig E. Jahr. 1999. "The Concentration of Synaptically Released Glutamate Outside of the Climbing Fiber-Purkinje Cell Synaptic Cleft." *Journal of Neuroscience* 19 (13): 5265–74. https://doi.org/10.1523/jneurosci.19-13-05265.1999.

Ebrahimi, Zahra, Nazanin Kahvandi, Alireza Komaki, Seyed Asaad Karimi, Marzieh Naderishahab, and Abdolrahman Sarihi. 2021. "The Role of MGlu4 Receptors within the Nucleus Accumbens in Acquisition and Expression of Morphine-Induced Conditioned Place Preference in Male Rats." *BMC Neuroscience* 22 (1): 1–10. https://doi.org/10.1186/s12868-021-00627-2.

Eriksen, Lisbeth, and Christian Thomsen. 1995. "[3H]-L-2-amino-4-phosphonobutyrate Labels a Metabotropic Glutamate Receptor, MGluR4a." *British Journal of Pharmacology* 116 (8): 3279–87. https://doi.org/10.1111/j.1476-5381.1995.tb15136.x.

Ettinger, David S., Douglas E. Wood, Wallace Akerley, Lyudmila A. Bazhenova, Hossein Borghaei, David Ross Camidge, Richard T. Cheney, et al. 2015. "Non-Small Cell Lung Cancer, Version 6.2015: Featured Updates to the NCCN Guidelines." *JNCCN Journal of the National Comprehensive Cancer Network* 13 (5): 515–24. https://doi.org/10.6004/jnccn.2015.0071.

Even-Desrumeaux, Klervi, Damien Nevoltris, Marie Noelle Lavaut, Karima Alim, Jean Paul Borg, Stephane Audebert, Brigitte Kerfelec, Daniel Baty, and Patrick Chames. 2014. "Masked Selection: A Straightforward and Flexible Approach for the Selection of Binders against Specific Epitopes and Differentially Expressed Proteins by Phage Display." *Molecular and Cellular Proteomics* 13 (2): 653–65. https://doi.org/10.1074/mcp.O112.025486.

Fallarino, Francesca, Claudia Volpi, Francesco Fazio, Serena Notartomaso, Carmine Vacca, Carla Busceti, Silvio Bicciato, et al. 2010. "Metabotropic Glutamate Receptor-4 Modulates Adaptive Immunity and Restrains

Neuroinflammation." *Nature Medicine* 16 (8): 897–902. https://doi.org/10.1038/nm.2183.

Fazio, Francesco, Martina Ulivieri, Claudia Volpi, Marco Gargaro, and Francesca Fallarino. 2018. "Targeting Metabotropic Glutamate Receptors for the Treatment of Neuroinflammation." *Current Opinion in Pharmacology* 38: 16–23. https://doi.org/10.1016/j.coph.2018.01.010.

Ferguson, Kathryn M., Mitchell B. Berger, Jeannine M. Mendrola, Hyun Soo Cho, Daniel J. Leahy, and Mark A. Lemmon. 2003. "EGF Activates Its Receptor by Removing Interactions That Autoinhibit Ectodomain Dimerization." *Molecular Cell* 11 (2): 507–17. https://doi.org/10.1016/S1097-2765(03)00047-9.

Ferguson, Kathryn M. 2008. "Structure-Based View of Epidermal Growth Factor Receptor Regulation." *Annual Review of Biophysics* 37: 353–73. https://doi.org/10.1146/annurev.biophys.37.032807.125829.

Fernandes, Helen, Stanley Cohen, and Subal Bishayee. 2001. "Glycosylation-Induced Conformational Modification Positively Regulates Receptor-Receptor Association." *The Journal of Biological Chemistry* 276 (7): 5375–83. https://doi.org/10.1074/jbc.M005599200.

Ferraguti, Francesco, and Ryuichi Shigemoto. 2006. "Metabotropic Glutamate Receptors." *Cell Tissue* 326 (2): 483–504.

Finlay, Clare, and Susan Duty. 2014. "Therapeutic Potential of Targeting Glutamate Receptors in Parkinson's Disease." *Journal of Neural Transmission* 121 (8): 861–80. https://doi.org/10.1007/s00702-014-1176-4.

Flynn, Daniel C. 2001. "Adaptor Proteins." *Oncogene* 20: 6270–72. https://doi.org/https://doi.org/10.1038/sj.onc.1204769.

Freed, Daniel M., Diego Alvarado, and Mark A. Lemmon. 2015. "Ligand Regulation of a Constitutively Dimeric EGF Receptor." *Nature Communications* 6 (May): 1–7. https://doi.org/10.1038/ncomms8380.

Freed, Daniel M, Nicholas J Bessman, Anatoly Kiyatkin, Emanuel Salazar-Cavazos, Patrick O Byrne, Jason O Moore, Christopher C Valley, et al. 2017. "EGFR Ligands Differentially Stabilize Receptor Dimers to Specify Signaling Kinetics." *Cell* 171 (3): 683–95. https://doi.org/10.1016/j.cell.2017.09.017.

Freyd, Thibaud, Dawid Warszycki, Stefan Mordalski, Andrzej J Bojarski, Ingebrigt Sylte, and Mari Gabrielsen. 2017. "Ligand-Guided Homology Modelling of the GABA B2 Subunit of the GABA B Receptor." *PLoS ONE*, 1–21.

Fulton, Mark G., Matthew T. Loch, Alice L. Rodriguez, Xin Lin, Jonathan A. Javitch, P. Jeffrey Conn, Colleen M. Niswender, and Craig W. Lindsley. 2020. "Synthesis and Pharmacological Evaluation of Bivalent Tethered Ligands to Target the MGlu2/4 Heterodimeric Receptor Results in a Compound with MGlu2/2 Homodimer Selectivity." *Bioorganic & Medicinal Chemistry Letters* 2 (April): 127212. https://doi.org/10.1016/j.bmcl.2020.127212.

Gan, Hui K., Anna N. Cvrljevic, and Terrance G. Johns. 2013. "The Epidermal Growth Factor Receptor Variant III (EGFRvIII): Where Wild Things Are Altered." *FEBS Journal* 280 (21): 5350–70. https://doi.org/10.1111/febs.12393.

Gan, Hui K., Francesca Walker, Antony W. Burgess, Angela Rigopoulos, Andrew M. Scott, and Terrance G. Johns. 2007. "The Epidermal Growth Factor Receptor (EGFR) Tyrosine Kinase Inhibitor AG1478 Increases the Formation of Inactive Untethered EGFR Dimers: Implications for Combination Therapy with Monoclonal Antibody 806." *Journal of Biological Chemistry* 282 (5): 2840–50. https://doi.org/10.1074/jbc.M605136200.

Gangemi, Sebastiano, Tindara Franchina, Paola Lucia Minciullo, Mirella Profita, Mariangela Zanghì, Antonio David, Ivanna Kennez, and Vincenzo Adamo. 2013. "IL-33/IL-31 Axis: A New Pathological Mechanisms for EGFR Tyrosine Kinase Inhibitors-Associated Skin Toxicity." *Journal of Cellular Biochemistry* 114 (12): 2673–76. https://doi.org/10.1002/jcb.24614.

Gautier, Arnaud, Alexandre Juillerat, Christian Heinis, Ivan Reis Corrêa, Maik Kindermann, Florent Beaufils, and Kai Johnsson. 2008. "An Engineered Protein Tag for Multiprotein Labeling in Living Cells." *Chemistry and Biology* 15 (2): 128–36. https://doi.org/10.1016/j.chembiol.2008.01.007.

Ghayad, Sandra E., Julie A. Vendrell, Sabrina Ben Larbi, Charles Dumontet, Ivan Bieche, and Pascale A. Cohen. 2010.

"Endocrine Resistance Associated with Activated ErbB System in Breast Cancer Cells Is Reversed by Inhibiting MAPK or PI3K/Akt Signaling Pathways." *International Journal of Cancer* 126 (2): 545–62. https://doi.org/10.1002/ijc.24750.

Goudet, Cyril, Julie Kniazeff, Veronika Hlavackova, Fanny Malhaire, Damien Maurel, Francine Acher, Jaroslav Blahos, Laurent Prézeau, and Jean Philippe Pin. 2005. "Asymmetric Functioning of Dimeric Metabotropic Glutamate Receptors Disclosed by Positive Allosteric Modulators." *Journal of Biological Chemistry* 280 (26): 24380–85. https://doi.org/10.1074/jbc.M502642200.

Goudet, Cyril, Bruno Vilar, Tiphanie Courtiol, Thierry Deltheil, Thomas Bessiron, Isabelle Brabet, Nadia Oueslati, et al. 2012. "A Novel Selective Metabotropic Glutamate Receptor 4 Agonist Reveals New Possibilities for Developing Subtype Selective Ligands with Therapeutic Potential." *The FASEB Journal* 26 (4): 1682–93. https://doi.org/10.1096/fj.11-195941.

Grabe, Tobias, Jonas Lategahn, and Daniel Rauh. 2018. "C797S Resistance: The Undruggable EGFR Mutation in Non-Small Cell Lung Cancer?" Editorial. *ACS Medicinal Chemistry Letters* 9: acsmedchemlett.8b00314. https://doi.org/10.1021/acsmedchemlett.8b00314.

Graus-Porta, Diana, Roger R. Beerli, John M. Daly, and Nancy E. Hynes. 1997. "ErbB-2, the Preferred Heterodimerization Partner of All ErbB Receptors, Is a Mediator of Lateral Signaling." *EMBO Journal* 16 (7): 1647–55. https://doi.org/10.1093/emboj/16.7.1647.

Hajdu, Tímea, Tímea Váradi, István Rebenku, Tamás Kovács, János Szöllösi, and Peter Nagy. 2020. "Comprehensive Model for Epidermal Growth Factor Receptor Ligand Binding Involving Conformational States of the Extracellular and the Kinase Domains." *Frontiers in Cell and Developmental Biology* 8 (776): 1–16. https://doi.org/10.3389/fcell.2020.00776.

Han, Guangming, and David R. Hampson. 1999. "Ligand Binding to the Amino-Terminal Domain of the MGluR4 Subtype of Metabotropic Glutamate Receptor." *Journal of Biological Chemistry* 274 (15): 10008–13. https://doi.org/10.1074/jbc.274.15.10008.

Haubrich, Jordi, Joan Font, Robert B. Quast, Anne Goupil-Lamy, Pauline Scholler, Damien Nevoltris, Francine Acher, et al. 2021. "A Nanobody Activating Metabotropic Glutamate Receptor 4 Discriminates between Homo- And Heterodimers." *Proceedings of the National Academy of Sciences of the United States of America* 118 (33): 2–7. https://doi.org/10.1073/pnas.2105848118.

Hauser, Alexander S, Misty M Attwood, Mathias Rask-andersen, Helgi B Schiöth, and David E. Gloriam. 2017. "Trends in GPCR Drug Discovery : New Agents , Targets and Indications." *Nat Rev Drug Discov* 16 (12): 829–42. https://doi.org/10.1038/nrd.2017.178.Trends.

Henriksen, Lasse, Michael Vibo Grandal, Stine Louise Jeppe Knudsen, Bo van Deurs, and Lene Melsæther Grøvdal. 2013. "Internalization Mechanisms of the Epidermal Growth Factor Receptor after Activation with Different Ligands." *PLoS ONE* 8 (3). https://doi.org/10.1371/journal.pone.0058148.

Herlitze, Stefan, David E. Garcla, Ken Mackle, Bertil Hille, Todd Scheuer, and William A. Catterall. 1996. "Modulation of Ca2+ Channels by G-Protein Bγ Subunits." *Nature*. https://doi.org/10.1038/380258a0.

Heydt, Carina, Sebastian Michels, Kenneth S. Thress, Sven Bergner, Jürgen Wolf, and Reinhard Buettner. 2018. "Novel Approaches against Epidermal Growth Factor Receptor Tyrosine Kinase Inhibitor Resistance." *Oncotarget* 9 (20): 15418–34. https://doi.org/10.18632/oncotarget.24624.

Heyduk, Tomasz, and Ewa Heyduk. 2001. "Luminescence Energy Transfer with Lanthanide Chelates: Interpretation of Sensitized Acceptor Decay Amplitudes." *Analytical Biochemistry* 289 (1): 60–67. https://doi.org/10.1006/abio.2000.4925.

Hlavackova, Veronika, Cyril Goudet, Julie Kniazeff, Alice Zikova, Damien Maurel, Claire Vol, Johana Trojanova, Laurent Prézeau, Jean Philippe Pin, and Jaroslav Blahos. 2005. "Evidence for a Single Heptahelical Domain Being Turned on upon Activation of a Dimeric GPCR." *EMBO Journal* 24 (3): 499–509. https://doi.org/10.1038/sj.emboj.7600557.

Hood, Leroy, and David Galas. 2003. "The Digital Code of DNA." *Nature* 421 (6921): 444–48. https://doi.org/10.1038/nature01410.

Huang, Fangtian, Donald Kirkpatrick, Xuejun Jiang, Steven Gygi, and Alexander Sorkin. 2006. "Differential Regulation of EGF Receptor Internalization and Degradation by Multiubiquitination within the Kinase Domain." *Molecular Cell* 21 (6): 737–48. https://doi.org/10.1016/j.molcel.2006.02.018.

Huang, Yongjian, Shashank Bharill, Deepti Karandur, Sean M. Peterson, Morgan Marita, Xiaojun Shi, Megan J. Kaliszewski, Adam W. Smith, Ehud Y. Isacoff, and John Kuriyan. 2016. "Molecular Basis for Multimerization in the Activation of the Epidermal Growth Factor Receptor." *ELife* 5 (MARCH2016): 1–27. https://doi.org/10.7554/eLife.14107.

Hubbard, Stevan R. 2006. "EGF Receptor Activation: Push Comes to Shove." *Cell* 125 (6): 1029–31. https://doi.org/10.1016/j.cell.2006.05.028.

Iacovelli, Luisa, Antonietta Arcella, Giuseppe Battaglia, Simonetta Pazzaglia, Eleonora Aronica, Paola Spinsanti, Alessandra Caruso, et al. 2006. "Pharmacological Activation of MGlu4 Metabotropic Glutamate Receptors Inhibits the Growth of Medulloblastomas." *Journal of Neuroscience* 26 (32): 8388–97. https://doi.org/10.1523/JNEUROSCI.2285-06.2006.

Inoue, Asuka, Francesco Raimondi, Francois Marie Ngako Kadji, Gurdeep Singh, Takayuki Kishi, Akiharu Uwamizu, Yuki Ono, et al. 2019. "Illuminating G-Protein-Coupling Selectivity of GPCRs." *Cell*, 1–15. https://doi.org/10.1016/j.cell.2019.04.044.

Iradyan, Iradyan, Hulin, Hambardzumyan, Gyulkhandanyan, Alves de Sousa, Hessani, et al. 2019. "Targeting Degradation of EGFR through the Allosteric Site Leads to Cancer Cell Detachment-Promoted Death." *Cancers* 11 (8): 1094. https://doi.org/10.3390/cancers11081094.

Ishizawar, Rumey, and Sarah J. Parsons. 2004. "C-Src and Cooperating Partners in Human Cancer." *Cancer Cell* 6 (3): 209–14. https://doi.org/10.1016/j.ccr.2004.09.001.

Ishkakova, Liliya, and Yoland Smith. 2016. "MGluR4-Containing Corticostriatal Terminals: Synaptic Interactions with Direct and Indirect Pathway Neurons in Mice." *Brain Structure and Function* 221 (9): 4589–99. https://doi.org/10.1007/s00429-016-1187-z.

Jänne, Pasi A., James Chih-Hsin Yang, Dong-Wan Kim, David Planchard, Yuichiro Ohe, Suresh S. Ramalingam, Myung-Ju Ahn, et al. 2015. "AZD9291 in EGFR Inhibitor–Resistant Non–Small-Cell Lung Cancer." *New England Journal of Medicine* 372 (18): 1689–99. https://doi.org/10.1056/NEJMoa1411817.

Jia, Yong, Cai-hong Yun, Eunyoung Park, Dalia Ercan, Mari Manuia, Jose Juarez, Chunxiao Xu, et al. 2016. "Overcoming EGFR T790M and C797S Resistance with Mutant-Selective Allosteric Inhibitors." *Nature* 534 (7605): 129–32. https://doi.org/10.1038/nature17960.Overcoming.

Jiang, Tao, Chunxia Su, Shengxiang Ren, Federico Cappuzzo, Gaetano Rocco, Joshua D Palmer, Nico Van Zandwijk, et al. 2018. "A Consensus on the Role of Osimertinib in Non-Small Cell Lung Cancer from the AME Lung Cancer Collaborative Group." *Journal of Thoracic Disease* 10 (7): 3909–21. https://doi.org/10.21037/jtd.2018.07.61.

Johnstone, Timothy C., Ga Young Park, and Stephen J. Lippard. 2014. "Understanding and Improving Platinum Anticancer Drugs - Phenanthriplatin." *Anticancer Research* 34 (1): 471–76.

Jura, Natalia, Yibing Shan, Xiaoxian Cao, David E. Shaw, and John Kuriyan. 2009. "Structural Analysis of the Catalytically Inactive Kinase Domain of the Human EGF Receptor 3." *Proceedings of the National Academy of Sciences of the United States of America* 106 (51): 21608–13. https://doi.org/10.1073/pnas.0912101106.

Kado, Yuji, Eiichi Mizohata, Satoru Nagatoishi, Mariko Iijima, Keiko Shinoda, Takamitsu Miyafusa, Taisuke Nakayama, et al. 2016. "Epiregulin Recognition Mechanisms by Anti-Epiregulin Antibody 9E5: Structural, Functional, and Molecular Dynamics Simulation Analyses." *Journal of Biological Chemistry* 291 (5): 2319–30. https://doi.org/10.1074/jbc.M115.656009.

Kammermeier, Paul J. 2012. "Functional and Pharmacological Characteristics of Metabotropic Glutamate Receptors

2/4 Heterodimers." *Molecular Pharmacology* 82 (3): 438–47. https://doi.org/10.1124/mol.112.078501.

Karachaliou, Niki, Manuel Fernandez-Bruno, Jillian Wilhelmina Paulina Bracht, and Rafael Rosell. 2019. "EGFR First- and Second-Generation TKIs-There Is Still Place for Them in EGFR-Mutant NSCLC Patients." *Translational Cancer Research* 8 (Suppl 1): S23–47. https://doi.org/10.21037/tcr.2018.10.06.

Kaszuba, Karol, Adam Orlowski, Reinis Danne, Tomasz Róg, Kai Simons, Ünal Coskun, and Ilpo Vattulainen. 2015. "N -Glycosylation as Determinant of Epidermal Growth Factor Receptor Conformation in Membranes." *Proceedings of the National Academy of Sciences* 112 (14): 4334–39. https://doi.org/10.1073/pnas.1503262112.

Kenakin, Terry. 2011. "Functional Selectivity and Biased Receptor Signaling." *Journal of Pharmacology and Experimental Therapeutics* 336: 296–302. https://doi.org/10.1124/jpet.110.173948.

Kennedy, Sean P., Jordan F. Hastings, Jeremy Z.R. Han, and David R. Croucher. 2016. "The Under-Appreciated Promiscuity of the Epidermal Growth Factor Receptor Family." *Frontiers in Cell and Developmental Biology* 4 (AUG). https://doi.org/10.3389/fcell.2016.00088.

Keppler, Antje, Susanne Gendreizig, Thomas Gronemeyer, Horst Pick, Horst Vogel, and Kai Johnsson. 2003. "A General Method for the Covalent Labeling of Fusion Proteins with Small Molecules in Vivo." *Nature Biotechnology* 21 (1): 86–89. https://doi.org/10.1038/nbt765.

Kimura, Hideharu, Kazuko Sakai, Tokuzo Arao, Tatsu Shimoyama, Tomohide Tamura, and Kazuto Nishio. 2007. "Antibody-Dependent Cellular Cytotoxicity of Cetuximab against Tumor Cells with Wild-Type or Mutant Epidermal Growth Factor Receptor." *Cancer Science* 98 (8): 1275–80. https://doi.org/10.1111/j.1349-7006.2007.00510.x.

Kingston, A. E., P. L. Ornstein, R. A. Wright, B. G. Johnson, N. G. Mayne, J. P. Burnett, R. Belagaje, S. Wu, and D. D. Schoepp. 1998. "LY341495 Is a Nanomolar Potent and Selective Antagonist of Group II Metabotropic Glutamate Receptors." *Neuropharmacology* 37 (1): 1–12. https://doi.org/10.1016/S0028-3908(97)00191-3.

Kiyatkin, Anatoly, Iris K. van Alderwerelt van Rosenburgh, Daryl E. Klein, and Mark A. Lemmon. 2020. "Kinetics of Receptor Tyrosine Kinase Activation Define ERK Signaling Dynamics." *Science Signaling* 13 (645): eaaz5267. https://doi.org/10.1126/scisignal.aaz5267.

Koehl, Antoine, Hongli Hu, Dan Feng, Bingfa Sun, Yan Zhang, Michael J. Robertson, Matthew Chu, et al. 2019. "Structural Insights into the Activation of Metabotropic Glutamate Receptors." *Nature* 566 (7742): 79–84. https://doi.org/10.1038/s41586-019-0881-4.

Kofuji, Paulo, Norman Davidson, and Henry A. Lester. 1995. "Evidence That Neuronal G-Protein-Gated Inwardly Rectifying K+ Channels Are Activated by Gβγ Subunits and Function as Heteromultimers." *Proceedings of the National Academy of Sciences of the United States of America* 92 (14): 6542–46. https://doi.org/10.1073/pnas.92.14.6542.

Kondo, I, and N Shimizu. 1983. "Mapping of the Human Gene for Epidermal Growth Factor Receptor (EGFR) on the P13 Leads to Q22 Region of Chromosome 7." *Cytogenetics and Cell Genetics* 35 (1): 9–14. https://doi.org/10.1159/000131829.

Kovacs, Erika, Rahul Das, Qi Wang, Timothy S. Collier, Aaron Cantor, Yongjian Huang, Kathryn Wong, et al. 2015. "Analysis of the Role of the C-Terminal Tail in the Regulation of the Epidermal Growth Factor Receptor." *Molecular and Cellular Biology* 35 (17): 3083–3102. https://doi.org/10.1128/mcb.00248-15.

Kozer, Noga, and Andrew H.A. Clayton. 2019. "In-Cell Structural Dynamics of an EGF Receptor during Ligand-Induced Dimer–Oligomer Transition." *European Biophysics Journal* 49 (1): 21–37. https://doi.org/10.1007/s00249-019-01410-2.

Kris, Mark G, Bruce E Johnson, Lynne D Berry, David J Kwiatkowski, A John Iafrate, Ignacio I Wistuba, Marileila Varella-garcia, et al. 2014. "Using Multiplexed Assays of Oncogenic Drivers in Lung Cancers to Select Targeted Drugs." *Jama* 311 (19): 1998–2006. https://doi.org/10.1001/jama.2014.3741.Using.

Kunishima, Naoki, Yoshimi Shimada, Yuji Tsuji, Toshihiro Sato, Masaki Yamamoto, Takashi Kumasaka, Shigetada Nakanishi, Hisato Jingami, and Kosuke Morikawa. 2000. "Structural Basis of Glutamate Recognition by a

Dimeric Metabotropic Glutamate Receptor." *Nature* 407 (6807): 971–77. https://doi.org/10.1038/35039564.

Langley, J. N. 1901. "On the Stimulation and Paralysis of Nerve-cells and of Nerve-endings: Part I." *The Journal of Physiology* 27 (3): 224–36. https://doi.org/10.1113/jphysiol.1901.sp000868.

Langley, J. N. 1905. "On the Reaction of Cells and of Nerve-endings to Certain Poisons, Chiefly as Regards the Reaction of Striated Muscle to Nicotine and to Curari." *The Journal of Physiology* 33 (4–5): 374–413. https://doi.org/10.1113/jphysiol.1905.sp001128.

Lau, Sally C.M., Ullas Batra, Tony S.K. Mok, and Herbert H. Loong. 2019. "Dacomitinib in the Management of Advanced Non-Small-Cell Lung Cancer." *Drugs* 79 (8): 823–31. https://doi.org/10.1007/s40265-019-01115-y.

Lazareno, S., and N. J.M. Birdsall. 1993. "Estimation of Competitive Antagonist Affinity from Functional Inhibition Curves Using the Gaddum, Schild and Cheng-Prusoíf Equations." *British Journal of Pharmacology* 109 (4): 1110–19. https://doi.org/10.1111/j.1476-5381.1993.tb13737.x.

Le, Tri, and David E. Gerber. 2019. "Newer-Generation EGFR Inhibitors in Lung Cancer: How Are They Best Used?" *Cancers* 11 (3): 1–14. https://doi.org/10.3390/cancers11030366.

Lee, Joon, Hermany Munguba, Vanessa A. Gutzeit, Melanie Kristt, Jeremy S. Dittman, and Joshua Levitz. 2020. "Defining the Homo- and Heterodimerization Propensities of Metabotropic Glutamate Receptors." *Cell Reports* 31 (5): 107605. https://doi.org/10.1016/j.celrep.2020.107605.

Lemmon, Mark A., Daniel M. Freed, Joseph Schlessinger, and Anatoly Kiyatkin. 2016. "The Dark Side of Cell Signaling: Positive Roles for Negative Regulators." *Cell* 164 (6): 1172–84. https://doi.org/10.1016/j.cell.2016.02.047.

Lemmon, Mark A., Joseph Schlessinger, and Kathryn M. Ferguson. 2014. "The EGFR Family: Not so Prototypical Receptor Tyrosine Kinases." *Cold Spring Harbor Perspectives in Biology* 6 (a020768). https://doi.org/10.1101/cshperspect.a020768.

Levoye, Angélique, Jurriaan M. Zwier, Agnieszka Jaracz-Ros, Laurence Klipfel, Martin Cottet, Damien Maurel, Sara Bdioui, et al. 2015. "A Broad G Protein-Coupled Receptor Internalization Assay That Combines SNAP-Tag Labeling, Diffusion-Enhanced Resonance Energy Transfer, and a Highly Emissive Terbium Cryptate." *Frontiers in Endocrinology* 6 (167). https://doi.org/10.3389/fendo.2015.00167.

Li, Shiqing, Karl R. Schmitz, Philip D. Jeffrey, Jed J.W. Wiltzius, Paul Kussie, and Kathryn M. Ferguson. 2005. "Structural Basis for Inhibition of the Epidermal Growth Factor Receptor by Cetuximab." *Cancer Cell* 7 (4): 301–11. https://doi.org/10.1016/j.ccr.2005.03.003.

Li, Tao, Fayez K. Ghishan, and Liqun Bai. 2005. "Molecular Physiology of Vesicular Glutamate Transporters in the Digestive System." *World Journal of Gastroenterology* 11 (12): 1731–36. https://doi.org/10.3748/wjg.v11.i12.1731.

Li, Tengfei, Jean Pierre Bourgeois, Susanna Celli, Fabienne Glacial, Anne Marie Le Sourd, Salah Mecheri, Babette Weksler, et al. 2012. "Cell-Penetrating Anti-GFAP VHH and Corresponding Fluorescent Fusion Protein VHH-GFP Spontaneously Cross the Blood-Brain Barrier and Specifically Recognize Astrocytes: Application to Brain Imaging." *FASEB Journal* 26 (10): 3969–79. https://doi.org/10.1096/fj.11-201384.

Liebmann, Claus. 2011. "EGF Receptor Activation by GPCRs: An Universal Pathway Reveals Different Versions." *Molecular and Cellular Endocrinology* 331 (2): 222–31. https://doi.org/10.1016/j.mce.2010.04.008.

Lin, Shuling, Shuo Han, Xiaoqing Cai, Qiuxiang Tan, Kexiu Zhou, Dejian Wang, Xinwei Wang, et al. 2021. "Structures of Gi-Bound Metabotropic Glutamate Receptors MGlu2 and MGlu4." *Nature*. https://doi.org/10.1038/s41586-021-03495-2.

Lindsey, Stephan, and Sigrid A Langhans. 2015. "Epidermal Growth Factor Signaling in Transformed Cells." *Int Rev Cell Mol Biol.* 314: 1–41. https://doi.org/10.1016/bs.ircmb.2014.10.001.

Litschig, Stephane, Fabrizio Gasparini, Doris Rueegg, Natacha Stoehr, Peter Josef Flor, Ivo Vranesic, Laurent Prézeau, Jean-Philippe Pin, Christian Thomsen, and Rainer Kuhn. 1999. "CPCCOEt, a Noncompetitive Metabotropic

Glutamate Receptor 1 Antagonist, Inhibits Receptor Signaling Without Affecting Glutamate Binding." *Molecular Pharmacology* 55 (3): 453 LP – 461. http://molpharm.aspetjournals.org/content/55/3/453.abstract.

Littlefield, Peter, Lijun Liu, Venkatesh Mysore, Yibing Shan, David E Shaw, and Natalia Jura. 2015. "Structural Analysis of the EGFR/HER3 Heterodimer Reveals the Molecular Basis for Activating HER3 Mutations." *Scientific Signaling* 7 (354): ra114. https://doi.org/10.1126/scisignal.2005786.

Liu, Junke, Zongyong Zhang, David Moreno-Delgado, James A.R. Dalton, Xavier Rovira, Ana Trapero, Cyril Goudet, et al. 2017. "Allosteric Control of an Asymmetric Transduction in a G Protein-Coupled Receptor Heterodimer." *ELife* 6: 1–19. https://doi.org/10.7554/eLife.26985.

Liu, Ping, Thankiah Sudhaharan, Rosita M.L. Koh, Ling C. Hwang, Sohail Ahmed, Ichiro N. Maruyama, and Thorsten Wohland. 2007. "Investigation of the Dimerization of Proteins from the Epidermal Growth Factor Receptor Family by Single Wavelength Fluorescence Cross-Correlation Spectroscopy." *Biophysical Journal* 93 (2): 684–98. https://doi.org/10.1529/biophysj.106.102087.

Liu, Sangtian, Yayi He, Tao Jiang, Shengxiang Ren, Fei Zhou, Chao Zhao, Xuefei Li, et al. 2018. "EGFR-TKIs plus Chemotherapy Demonstrated Superior Efficacy than EGFR-TKIs Alone as First-Line Setting in Advanced NSCLC Patients with EGFR Mutation and BIM Deletion Polymorphism." *Lung Cancer* 120 (April): 82–87. https://doi.org/10.1016/j.lungcan.2018.04.004.

Longley, Daniel B., D. Paul Harkin, and Patrick G. Johnston. 2003. "5-Fluorouracil: Mechanisms of Action and Clinical Strategies." *Nature Reviews Cancer* 3 (5): 330–38. https://doi.org/10.1038/nrc1074.

Lopez, Sebastien, Nathalie Turle-Lorenzo, Francine Acher, Elvira De Leonibus, Andrea Mele, and Marianne Amalric. 2007. "Targeting Group III Metabotropic Glutamate Receptors Produces Complex Behavioral Effects in Rodent Models of Parkinson's Disease." *Journal of Neuroscience* 27 (25): 6701–11. https://doi.org/10.1523/JNEUROSCI.0299-07.2007.

Lu, Chafen, Li-Zhi Mi, Michael J. Grey, Jieqing Zhu, Elizabeth Graef, Shigeyuki Yokoyama, and Timothy A. Springer. 2010. "Structural Evidence for Loose Linkage between Ligand Binding and Kinase Activation in the Epidermal Growth Factor Receptor." *Molecular and Cellular Biology* 30 (22): 5432–43. https://doi.org/10.1128/mcb.00742-10.

Lynch, Thomas J., Daphne W. Bell, Raffaella Sordella, Sarada Gurubhagavatula, Ross A. Okimoto, Brian W. Brannigan, Patricia L. Harris, et al. 2004. "Activating Mutations in the Epidermal Growth Factor Receptor Underlying Responsiveness of Non–Small-Cell Lung Cancer to Gefitinib." *The New England Journal of Medicine* 350 (21): 2129–39. https://doi.org/10.1056/NEJMoa1303342.

Lyu, Hui, Amy Han, Erik Polsdofer, Shuang Liu, and Bolin Liu. 2018. "Understanding the Biology of HER3 Receptor as a Therapeutic Target in Human Cancer." *Acta Pharmaceutica Sinica B* 8 (4): 503–10. https://doi.org/10.1016/j.apsb.2018.05.010.

Madshus, I. H., and E. Stang. 2009. "Internalization and Intracellular Sorting of the EGF Receptor: A Model for Understanding the Mechanisms of Receptor Trafficking." *Journal of Cell Science* 122 (19): 3433–39. https://doi.org/10.1242/jcs.050260.

Maity, Swastika, K. Sreedhara Ranganath Pai, and Yogendra Nayak. 2020. "Advances in Targeting EGFR Allosteric Site as Anti-NSCLC Therapy to Overcome the Drug Resistance." *Pharmacological Reports* 72 (4): 799–813. https://doi.org/10.1007/s43440-020-00131-0.

Marino, Michael J., David L. Williams, Julie A. O'Brien, Ornella Valenti, Terrence P. McDonald, Michelle K. Clements, Rulping Wang, et al. 2003. "Allosteric Modulation of Group III Metabotropic Glutamate Receptor 4: A Potential Approach to Parkinson's Disease Treatment." *Proceedings of the National Academy of Sciences of the United States of America* 100 (23): 13668–73. https://doi.org/10.1073/pnas.1835724100.

Marshall, C. J. 1995. "Specificity of Receptor Tyrosine Kinase Signaling: Transient versus Sustained Extracellular Signal-Regulated Kinase Activation." *Cell* 80: 197–185.

Maruyama, Ichiro. 2014. "Mechanisms of Activation of Receptor Tyrosine Kinases: Monomers or Dimers." *Cells* 3

(2): 304–30. https://doi.org/10.3390/cells3020304.

Maruyama, Ichiro N. 2015. "Activation of Transmembrane Cell-Surface Receptors via a Common Mechanism? The 'Rotation Model.'" *BioEssays* 37 (9): 959–67. https://doi.org/10.1002/bies.201500041.

Mathiesen, Jesper Mosolff, and M. Teresa Ramirez. 2006. "The Metabotropic Glutamate Receptor 4 Is Internalized and Desensitized upon Protein Kinase C Activation." *British Journal of Pharmacology* 148 (3): 279–90. https://doi.org/10.1038/sj.bjp.0706733.

Mathiesen, Jesper Mosolff, Nannette Svendsen, Hans Bräuner-Osborne, Christian Thomsen, and M. Teresa Ramirez. 2003. "Positive Allosteric Modulation of the Human Metabotropic Glutamate Receptor 4 (HmGluR4) by SIB-1893 and MPEP." *British Journal of Pharmacology* 138 (6): 1026–30. https://doi.org/10.1038/sj.bjp.0705159.

Matsumoto, Taro, and Hideo Mugishima. 2006. "Signal Transduction via Vascular Endothelial Growth Factor (VEGF) Receptors and Their Roles in Atherogenesis." *Journal of Atherosclerosis and Thrombosis* 13 (3): 130–35. https://doi.org/10.5551/jat.13.130.

Maudsley, Stuart, Kristen L. Pierce, A. Musa Zamah, William E. Miller, Seungkirl Ahn, Yehia Daaka, Robert J. Lefkowitz, and Louis M. Luttrell. 2000. "The B2-Adrenergic Receptor Mediates Extracellular Signal-Regulated Kinase Activation via Assembly of a Multi-Receptor Complex with the Epidermal Growth Factor Receptor." *Journal of Biological Chemistry* 275 (13): 9572–80. https://doi.org/10.1074/jbc.275.13.9572.

Maurel, Damien, Laëtitia Comps-Agrar, Carsten Brock, Marie Laure Rives, Emmanuel Bourrier, Mohammed Akli Ayoub, Hervé Bazin, et al. 2008. "Cell-Surface Protein-Protein Interaction Analysis with Time-Resolved FRET and Snap-Tag Technologies: Application to GPCR Oligomerization." *Nature Methods* 5 (6): 561–67. https://doi.org/10.1038/nmeth.1213.

McCullock, Tyler W, and Paul J Kammermeier. 2021. "The Evidence for and Consequences of Metabotropic Glutamate Receptor Heterodimerization." *Neuropharmacology* Pre-proof. https://doi.org/https://doi.org/10.1016/j.neuropharm.2021.108801.

McMahon, Conor, Dean P. Staus, Laura M. Wingler, Jialu Wang, Meredith A. Skiba, Matthias Elgeti, Wayne L. Hubbell, Howard A. Rockman, Andrew C. Kruse, and Robert J. Lefkowitz. 2020. "Synthetic Nanobodies as Angiotensin Receptor Blockers." *Proceedings of the National Academy of Sciences*, 202009029. https://doi.org/10.1073/pnas.2009029117.

Mellone, Manuela, and Fabrizio Gardoni. 2018. "Glutamatergic Mechanisms in L-DOPA-Induced Dyskinesia and Therapeutic Implications." *Journal of Neural Transmission* 125 (8): 1225–36. https://doi.org/10.1007/s00702-018-1846-8.

Meng, Delong, Anderson R. Frank, and Jenna L. Jewell. 2018. "MTOR Signaling in Stem and Progenitor Cells." *Development* 145 (1): dev152595. https://doi.org/10.1242/dev.152595.

Menzel, Stephan, Nicole Schwarz, Friedrich Haag, and Friedrich Koch-Nolte. 2018. "Nanobody-Based Biologics for Modulating Purinergic Signaling in Inflammation and Immunity." *Frontiers in Pharmacology* 9 (MAR): 1–7. https://doi.org/10.3389/fphar.2018.00266.

Møller, Thor C., Jerome Hottin, Caroline Clerté, Jurriaan M. Zwier, Thierry Durroux, Philippe Rondard, Laurent Prézeau, et al. 2018. "Oligomerization of a G Protein-Coupled Receptor in Neurons Controlled by Its Structural Dynamics." *Scientific Reports* 8 (1): 1–15. https://doi.org/10.1038/s41598-018-28682-6.

Mota, Jose Mauricio, Katharine Ann Collier, Ricardo Lima Barros Costa, Timothy Taxter, Aparna Kalyan, Caio A. Leite, Young Kwang Chae, Francis J. Giles, and Benedito A. Carneiro. 2017. "A Comprehensive Review of Heregulins, HER3, and HER4 as Potential Therapeutic Targets in Cancer." *Oncotarget* 8 (51): 89284–306. https://doi.org/10.18632/oncotarget.18467.

Nagai, Takeharu, Keiji Ibata, Eun Sun Park, Mie Kubota, Katsuhiko Mikoshiba, and Atsushi Miyawaki. 2002. "A Variant of Yellow Fluorescent Protein with Fast and Efficient Maturation for Cell-Biological Applications." *Nature Biotechnology* 20 (1): 87–90. https://doi.org/10.1038/nbt0102-87.

Niederst, Matthew J, Haichuan Hu, Hillary E Mulvey, Elizabeth L Lockerman, Angel R Garcia, Zofia Piotrowska,

Lecia V Sequist, Jeffrey A Engelman, General Hospital, and Massachusetts General Hospital. 2015. "The Allelic Context of the C797S Mutation Acquired upon Treatment with Third Generation EGFR Inhibitors Impacts Sensitivity to Subsequent Treatment Strategies." *Clinical Cancer Research* 21 (17): 3924–33. https://doi.org/10.1158/1078-0432.CCR-15-0560.

Nieto, Yago, Fatima Nawaz, Roy B. Jones, Elizabeth J. Shpall, and Samia Nawaz. 2007. "Prognostic Significance of Overexpression and Phosphorylation of Epidermal Growth Factor Receptor (EGFR) and the Presence of Truncated EGFRvIII in Locoregionally Advanced Breast Cancer." *Journal of Clinical Oncology* 25 (28): 4405–13. https://doi.org/10.1200/JCO.2006.09.8822.

Niewoehner, Jens, Bernd Bohrmann, Ludovic Collin, Eduard Urich, Hadassah Sade, Peter Maier, Petra Rueger, et al. 2014. "Increased Brain Penetration and Potency of a Therapeutic Antibody Using a Monovalent Molecular Shuttle." *Neuron* 81 (1): 49–60. https://doi.org/10.1016/j.neuron.2013.10.061.

Niswender, Colleen M., Carrie K. Jones, Xin Lin, Michael Bubser, Analisa Thompson Gray, Anna L. Blobaum, Darren W. Engers, et al. 2016. "Development and Antiparkinsonian Activity of VU0418506, a Selective Positive Allosteric Modulator of Metabotropic Glutamate Receptor 4 Homomers without Activity at MGlu2/4 Heteromers." *ACS Chemical Neuroscience* 7 (9): 1201–11. https://doi.org/10.1021/acschemneuro.6b00036.

Niswender, Colleen M, and P Jeffrey Conn. 2010. "Metabotropic Glutamate Receptors: Physiology, Pharmacology, and Disease." *Annual Reviews of Pharmacology and Toxicology* 50: 295–322.

Niswender, Colleen M, Kari A Johnson, C David Weaver, Carrie K Jones, Zixiu Xiang, Qingwei Luo, Alice L Rodriguez, et al. 2008. "Discovery, Characterization, and Antiparkinsonian Effect of Novel Positive Allosteric Modulators of Metabotropic Glutamate Receptor 4." *Molecular Pharmacology* 74 (5): 1345–58. https://doi.org/10.1124/mol.108.049551.

Nosaki, Kaname, Miyako Satouchi, Takayasu Kurata, Tatsuya Yoshida, Isamu Okamoto, Nobuyuki Katakami, Fumio Imamura, et al. 2016. "Re-Biopsy Status among Non-Small Cell Lung Cancer Patients in Japan: A Retrospective Study." *Lung Cancer* 101: 1–8. https://doi.org/10.1016/j.lungcan.2016.07.007.

Novak, Ulrike, Francesca Walker, and Andrew Kaye. 2001. "Expression of EGFR-Family Proteins in the Brain: Role in Development, Health and Disease." *Journal of Clinical Neuroscience* 8 (2): 106–11. https://doi.org/10.1054/jocn.2000.0799.

Oashi, Ayano, Hiroyuki Yasuda, Keigo Kobayashi, Tetsuo Tani, Junko Hamamoto, Keita Masuzawa, Tadashi Manabe, et al. 2019. "Monomer Preference of EGFR Tyrosine Kinase Inhibitors Influences the Synergistic Efficacy of Combination Therapy with Cetuximab." *Molecular Cancer Therapeutics* 18 (9): 1593–1601. https://doi.org/10.1158/1535-7163.MCT-18-1036.

Ogiso, Hideo, Ryuichiro Ishitani, Osamu Nureki, Shuya Fukai, Mari Yamanaka, Jae Hoon Kim, Kazuki Saito, et al. 2002. "Crystal Structure of the Complex of Human Epidermal Growth Factor and Receptor Extracellular Domains." *Cell* 110 (6): 775–87. https://doi.org/10.1016/S0092-8674(02)00963-7.

Ohe, Yuichiro, Fumio Imamura, Naoyuki Nogami, Isamu Okamoto, Takayasu Kurata, Terufumi Kato, Shunichi Sugawara, et al. 2019. "Osimertinib versus Standard-of-Care EGFR-TKI as First-Line Treatment for EGFRm Advanced NSCLC: FLAURA Japanese Subset." *Japanese Journal of Clinical Oncology* 49 (1): 29–36. https://doi.org/10.1093/jjco/hyy179.

Olanow, C. Warren, Matthew B. Stern, and Kapil Sethi. 2009. "The Scientific and Clinical Basis for the Treatment of Parkinson Disease (2009)." *Neurology* 72 (21 SUPPL. 4). https://doi.org/10.1212/WNL.0b013e3181a1d44c.

Olofsson, Linnea, Suren Felekyan, Etienne Doumazane, Pauline Scholler, Ludovic Fabre, Jurriaan M. Zwier, Philippe Rondard, Claus A.M. Seidel, Jean Philippe Pin, and Emmanuel Margeat. 2014. "Fine Tuning of Sub-Millisecond Conformational Dynamics Controls Metabotropic Glutamate Receptors Agonist Efficacy." *Nature Communications* 5. https://doi.org/10.1038/ncomms6206.

Pal Choudhuri, S., R. J. Delay, and E. R. Delay. 2016. "Metabotropic Glutamate Receptors Are Involved in the Detection of IMP and L-Amino Acids by Mouse Taste Sensory Cells." *Neuroscience* 316: 94–108. https://doi.org/10.1016/j.neuroscience.2015.12.008.

Palanisamy, Srikanth, Carolyn Xue, Shun Ishiyama, Sathyamangla Venkata Naga Prasad, and Kathleen Gabrielson. 2021. "GPCR-ErbB Transactivation Pathways and Clinical Implications." *Cellular Signalling* 86 (110092). https://doi.org/10.1016/j.cellsig.2021.110092.

Palczewski, Krzysztof, Takashi Kumasaka, Tetsuya Hori, Craig A Behnke, Hiroyuki Motoshima, Brian A Fox, Isolde Le Trong, et al. 2000. "Crystal Structure of Rhodopsin : A G Protein-Coupled Receptor P." *Science* 289 (5480): 739–45.

Pao, William, Vincent A. Miller, Katerina A. Politi, Gregory J. Riely, Romel Somwar, Maureen F. Zakowski, Mark G. Kris, and Harold Varmus. 2005. "Acquired Resistance of Lung Adenocarcinomas to Gefitinib or Erlotinib Is Associated with a Second Mutation in the EGFR Kinase Domain." *PLoS Medicine* 2 (3): 0225–35. https://doi.org/10.1371/journal.pmed.0020073.

Pao, William, Vincent Miller, Maureen Zakowski, Jennifer Doherty, Katerina Politi, Inderpal Sarkaria, Bhuvanesh Singh, et al. 2004. "EGF Receptor Gene Mutations Are Common in Lung Cancers from 'Never Smokers' and Are Associated with Sensitivity of Tumors to Gefitinib and Erlotinib." *Proceedings of the National Academy of Sciences of the United States of America* 101 (36): 13306–11. https://doi.org/10.1073/pnas.0405220101.

Papasergi-Scott, Makaía M., Michael J. Robertson, Alpay B. Seven, Ouliana Panova, Jesper M. Mathiesen, and Georgios Skiniotis. 2020. "Structures of Metabotropic GABAB Receptor." *Nature* 584 (7820): 310–14. https://doi.org/10.1038/s41586-020-2469-4.

Park, D., D. Y. Jhon, C. W. Lee, K. H. Lee, and Sue Goo Rhee. 1993. "Activation of Phospholipase C Isozymes by G Protein Bγ Subunits." *Journal of Biological Chemistry* 268 (7): 4573–76. https://doi.org/10.1016/S0021-9258(18)53431-1.

Park, Jin H., Yingting Liu, Mark A. Lemmon, and Ravi Radhakrishnan. 2012. "Erlotinib Binds Both Inactive and Active Conformations of the EGFR Tyrosine Kinase Domain." *Biochemical Journal* 448 (3): 417–23. https://doi.org/10.1042/BJ20121513.

Peavy, Richard D., Mike S. S. Chang, Elaine Sanders-Bush, and P. Jeffrey Conn. 2001. "Metabotropic Glutamate Receptor 5-Induced Phosphorylation of Extracellular Signal-Regulated Kinase in Astrocytes Depends on Transactivation of the Epidermal Growth Factor Receptor." *J. Neurosci.* 21 (24): 9619–28. http://www.jneurosci.org/content/21/24/9619.long.

Pertea, Mihaela, Alaina Shumate, Geo Pertea, Ales Varabyou, Yu-Chi Chang, Anil Madugundu, Akhilesh Pandey, and Steven Salzberg. 2018. "Thousands of Large-Scale RNA Sequencing Experiments Yield a Comprehensive New Human Gene List and Reveal Extensive Transcriptional Noise." *BioRxiv*, 332825. https://doi.org/10.1101/332825.

Phillips, James C, Rosemary Braun, Wei Wang, James Gumbart, Emad Tajkhorshid, Elizabeth Villa, Christophe Chipot, Robert D Skeel, Laxmikant Kalé, and Klaus Schulten. 2005. "Scalable Molecular Dynamics with NAMD." *Journal of Computational Chemistry* 26 (16): 1781–1802.

Pierce, Brian, and Zhiping Weng. 2007. "ZRANK: Reranking Protein Docking Predictions With an Optimized Energy Function." *PROTEIN: Structure, Function, and Genetics* 67: 1078–86.

Pin, J. P., and R. Duvoisin. 1995. "The Metabotropic Glutamate Receptors: Structure and Functions." *Neuropharmacology* 34 (1): 1–26. https://doi.org/10.1016/0028-3908(94)00129-G.

Pin, Jean Philippe, Thierry Galvez, and Laurent Prézeau. 2003. "Evolution, Structure, and Activation Mechanism of Family 3/C G-Protein-Coupled Receptors." *Pharmacology and Therapeutics* 98 (3): 325–54. https://doi.org/10.1016/S0163-7258(03)00038-X.

Planchard, D., P-H. Feng, N. Karaseva, S-W. Kim, T.M. Kim, C.K. Lee, A. Poltoratskiy, et al. 2020. "1401P Osimertinib plus Platinum/Pemetrexed in Newly-Diagnosed EGFR Mutation (EGFRm)-Positive Advanced NSCLC: Safety Run-in Results from the FLAURA2 Study." *Annals of Oncology* 31: S888. https://doi.org/10.1016/j.annonc.2020.08.1715.

Purba, Endang, Ei-ichiro Saita, and Ichiro Maruyama. 2017. "Activation of the EGF Receptor by Ligand Binding and

Oncogenic Mutations: The 'Rotation Model.'" *Cells* 6 (2): 13. https://doi.org/10.3390/cells6020013.

Rask-Andersen, Mathias, Surendar Masuram, and Helgi B Schiöth. 2014. "The Druggable Genome: Evaluation of Drug Targets in Clinical Trials Suggests Major Shifts in Molecular Class and Indication." *Annual Review of Pharmacology and Toxicology* 54 (August 2013): 9–26. https://doi.org/10.1146/annurev-pharmtox-011613-135943.

Rasmussen, Søren G.F., Hee Jung Choi, Daniel M. Rosenbaum, Tong Sun Kobilka, Foon Sun Thian, Patricia C. Edwards, Manfred Burghammer, et al. 2007. "Crystal Structure of the Human B2 Adrenergic G-Protein-Coupled Receptor." *Nature* 450 (7168): 383–87. https://doi.org/10.1038/nature06325.

Ribas, Antoni, and Siwen Hu-Lieskovan. 2016. "What Does PD-L1 Positive or Negative Mean?" *Journal of Experimental Medicine* 213 (13): 2835–40. https://doi.org/10.1084/jem.20161462.

Romano, Carmelo, Wan Lin Yang, and Karen L. O'Malley. 1996. "Metabotropic Glutamate Receptor 5 Is a Disulfide-Linked Dimer." *Journal of Biological Chemistry* 271 (45): 28612–16. https://doi.org/10.1074/jbc.271.45.28612.

Rosemond, Erica, Vanya Peltekova, Mark Naples, Henning Thøgersen, and David R. Hampson. 2002. "Molecular Determinants of High Affinity Binding to Group III Metabotropic Glutamate Receptors." *Journal of Biological Chemistry* 277 (9): 7333–40. https://doi.org/10.1074/jbc.M110476200.

Roskoski, Robert. 2016. "Classification of Small Molecule Protein Kinase Inhibitors Based upon the Structures of Their Drug-Enzyme Complexes." *Pharmacological Research* 103: 26–48. https://doi.org/10.1016/j.phrs.2015.10.021.

Roskoski, Robert. 2019. "Small Molecule Inhibitors Targeting the EGFR/ErbB Family of Protein-Tyrosine Kinases in Human Cancers." *Pharmacological Research* 139: 395–411. https://doi.org/10.1016/j.phrs.2018.11.014.

Rovira, Xavier, Ana Trapero, Silvia Pittolo, Charleine Zussy, Adèle Faucherre, Chris Jopling, Jesús Giraldo, et al. 2016. "OptoGluNAM4.1, a Photoswitchable Allosteric Antagonist for Real-Time Control of MGlu4 Receptor Activity." *Cell Chemical Biology* 23 (8): 929–34. https://doi.org/10.1016/j.chembiol.2016.06.013.

S., Candace, Candace S Bever, Jie-Xian Dong, Natalia Vasylieva, Bogdan Barnych, Yongliang Cui, Zhen-Lin Xu, Bruce D Hammock, and Shierley J Gee. 2016. "VHH Antibodies: Emerging Reagents for the Analysis of Environmental Chemicals." *Analytical and Bioanalytical Chemistry* 408 (22): 5985–6002. https://doi.org/10.1007/s00216-016-9585-x.

S., Xia, He C., Zhu Y., Wang S., Li H., Zhang Z., and Jiang X. 2017. "GABABR-Induced EGFR Transactivation Promotes Migration of Human Prostate Cancer Cells." *Molecular Pharmacology* 92 (3): 265–77. https://doi.org/http://dx.doi.org/10.1124/mol.116.107854.

Sali, Andrej, and Tom L Blundell. 1993. "Comparative Protein Modelling by Satisfaction of Spatial Restraints." *Journal of Molecular Biology* 234: 779–815.

Salt, T. E., J. P. Turner, and A. E. Kingston. 1999. "Evaluation of Agonists and Antagonists Acting at Group I Metabotropic Glutamate Receptors in the Thalamus in Vivo." *Neuropharmacology* 38 (10): 1505–10. https://doi.org/10.1016/S0028-3908(99)00081-7.

Sato, Ken-ichi. 2013. "Cellular Functions Regulated by Phosphorylation of EGFR on TYR845." *International Journal of Molecular Sciences* 14 (6): 10761–90. https://doi.org/10.3390/ijms140610761.

Savage, C. R., T. Inagami, and S. Cohen. 1972. "The Primary Structure of Epidermal Growth Factor." *Journal of Biological Chemistry* 247 (23): 7612–21.

Savage, Richard C, John H Hash, and Stanley Cohen. 1973. "Epidermal Growth Factor Location of Disulfide Bonds." *Journal of Biological Chemistry* 248 (22): 7669–73.

SCHEER. 2017. "SCHEER (Scientific Committee on Health Environmental and Emerging Risks) Final Opinion on 'The Need for Non-Human Primates in Biomedical Research, Production and Testing of Products and Devices."

Scholler, Pauline, David Moreno-Delgado, Nathalie Lecat-Guillet, Etienne Doumazane, Carine Monnier, Fabienne

Charrier-Savournin, Ludovic Fabre, et al. 2017. “HTS-Compatible FRET-Based Conformational Sensors Clarify Membrane Receptor Activation.” *Nature Chemical Biology* 13 (4): 372–80. https://doi.org/10.1038/nchembio.2286.

Scholler, Pauline, Damien Nevoltris, Dimitri De Bundel, Simon Bossi, David Moreno-delgado, Xavier Rovira, Thor C Møller, et al. 2017. “Allosteric Nanobodies Uncover a Role of Hippocampal MGlu2 Receptor Homodimers in Contextual Fear Consolidation.” *Nature Communications* 8 (1967): 1. https://doi.org/10.1038/s41467-017-01489-1.

Ségaliny, Aude I., Marta Tellez-Gabriel, Marie Françoise Heymann, and Dominique Heymann. 2015. “Receptor Tyrosine Kinases: Characterisation, Mechanism of Action and Therapeutic Interests for Bone Cancers.” *Journal of Bone Oncology* 4 (1): 1–12. https://doi.org/10.1016/j.jbo.2015.01.001.

Selvin, Paul R. 2002. “Principles and Biophysical Applications of Lanthanide-Based Probes.” *Annual Review of Biophysics and Biomolecular Structure* 31: 275–302. https://doi.org/10.1146/annurev.biophys.31.101101.140927.

Shajahan, Ayesha N., Chinnaswamy Tiruppathi, Alan V. Smrcka, Asrar B. Malik, and Richard D. Minshall. 2004. “Gβγ Activation of Src Induces Caveolae-Mediated Endocytosis in Endothelial Cells.” *Journal of Biological Chemistry* 279 (46): 48055–62. https://doi.org/10.1074/jbc.M405837200.

Shen, Min-yi, and Andrej Sali. 2006. “Statistical Potential for Assessment and Prediction of Protein Structures.” *Protein Science* 15: 2507–24. https://doi.org/10.1110/ps.062416606.Instead.

Shi, Fumin, Shannon E. Telesco, Yingting Liu, Ravi Radhakrishnan, and Mark A. Lemmona. 2010. “ErbB3/HER3 Intracellular Domain Is Competent to Bind ATP and Catalyze Autophosphorylation.” *Proceedings of the National Academy of Sciences of the United States of America* 107 (17): 7692–97. https://doi.org/10.1073/pnas.1002753107.

Shigematsu, Hisayuki, Li Lin, Takao Takahashi, Masaharu Nomura, Makoto Suzuki, Ignacio I. Wistuba, Kwun M. Fong, et al. 2005. “Clinical and Biological Features Associated with Epidermal Growth Factor Receptor Gene Mutations in Lung Cancers.” *Journal of the National Cancer Institute* 97 (5): 339–46. https://doi.org/10.1093/jnci/dji055.

Siddig, Sana, Sarah Aufmkolk, Sören Doose, Marie Lise Jobin, Christian Werner, Markus Sauer, and Davide Calebiro. 2020. “Super-Resolution Imaging Reveals the Nanoscale Organization of Metabotropic Glutamate Receptors at Presynaptic Active Zones.” *Science Advances* 6 (16). https://doi.org/10.1126/sciadv.aay7193.

Sigismund, Sara, Tanja Woelk, Claudia Puri, Elena Maspero, Carlo Tacchetti, Pietro Transidico, Pier Paolo Di Fiore, and Simona Polo. 2005. “Clathrin-Independent Endocytosis of Ubiquitinated Cargos.” *Proceedings of the National Academy of Sciences of the United States of America* 102 (8): 2760–65. https://doi.org/10.1073/pnas.0409817102.

Simmons, Rosa Maria A., Amy A. Webster, Anshu B. Kalra, and Smriti Iyengar. 2002. “Group II MGluR Receptor Agonists Are Effective in Persistent and Neuropathic Pain Models in Rats.” *Pharmacology Biochemistry and Behavior* 73 (2): 419–27. https://doi.org/10.1016/S0091-3057(02)00849-3.

Singh, Bhuminder, Graham Carpenter, and Robert J. Coffey. 2016. “EGF Receptor Ligands: Recent Advances.” *F1000Research* 5 (0): 2270. https://doi.org/10.12688/f1000research.9025.1.

Singh, Deo R., Christopher King, Matt Salotto, and Kalina Hristova. 2020. “Revisiting a Controversy: The Effect of EGF on EGFR Dimer Stability.” *Biochimica et Biophysica Acta - Biomembranes* 1862 (1): 183015. https://doi.org/10.1016/j.bbamem.2019.07.003.

Sladeczek, F, J P Pin, M Recasens, J Bockaert, and S Weiss. 1985. “Glutamate Stimulates Inositol Phosphate Formation in Striatal Neurones.” *Nature* 317 (6039): 717–19.

Slieker, Lawrence J, Todd M Martensen, and M Daniel Lane. 1988. “Biosynthesis of the Epidermal Growth Factor Receptor: Post-Translational Glycosylation-Independent Acquisition of Tyrosine Kinase Autophosphorylation Activity.” *Biochemical and Biophysical Research Communications* 153 (1): 96–103.

Soini, Erkki, Timo Lövgren, and Charles B Reimer. 1987. "Time-Resolved Fluorescence of Lanthanide Probes and Applications in Biotechnology." *Critical Reviews in Analytical Chemistry* 18 (2): 105–54.

Spassov, Velin Z, and Lisa Yan. 2012. "PH-Selective Mutagenesis of Protein–Protein Interfaces: In Silico Design of Therapeutic Antibodies with Prolonged Half-Life." *PROTEINS: Structure, Function and Bioinformatics* 81: 704–14. https://doi.org/10.1002/prot.24230.

Spassov, Velin Z, and Lisa Yan. 2016. "A PH-Dependent Computational Approach to the Effect of Mutations on Protein Stability." *Journal of Computational Chemistry* 37 (29): 2573–87. https://doi.org/10.1002/jcc.24482.

Spassov, Velin Z, Lisa Yan, and Paul K Flook. 2007. "The Dominant Role of Side-Chain Backbone Interactions in Structural Realization of Amino Acid Code. ChiRotor: A Side-Chain Prediction Algorithm Based on Side-Chain Backbone Interactions." *Protein Science* 16: 494–506. https://doi.org/10.1110/ps.062447107.

Sriram, Krishna, and Paul A. Insel. 2018. "G Protein-Coupled Receptors as Targets for Approved Drugs: How Many Targets and How Many Drugs?" *Molecular Pharmacology* 93 (4): 251–58. https://doi.org/10.1124/mol.117.111062.

Stamos, Jennifer, Mark X. Sliwkowski, and Charles Eigenbrot. 2002. "Structure of the Epidermal Growth Factor Receptor Kinase Domain Alone and in Complex with a 4-Anilinoquinazoline Inhibitor." *Journal of Biological Chemistry* 277 (48): 46265–72. https://doi.org/10.1074/jbc.M207135200.

Staus, Dean P., Laura M. Wingler, Ryan T. Strachan, Soren G.F. Rasmussen, Els Pardon, Seungkirl Ahn, Jan Steyaert, Brian K. Kobilka, and Robert J. Lefkowitz. 2014. "Regulation of B2-Adrenergic Receptor Function by Conformationally Selective Single-Domain Intrabodies." *Molecular Pharmacology* 85 (3): 472–81. https://doi.org/10.1124/mol.113.089516.

Stepulak, Andrzej, Radoslaw Rola, Krzysztof Polberg, and Chrysanthy Ikonomidou. 2014. "Glutamate and Its Receptors in Cancer." *Journal of Neural Transmission* 121 (8): 933–44. https://doi.org/10.1007/s00702-014-1182-6.

Suzuki, Hidekazu, Tomonori Hirashima, Norio Okamoto, Tadahiro Yamadori, Motohiro Tamiya, Naoko Morishita, Takayuki Shiroyama, Tomoyuki Otsuka, Kanako Kitai, and Ichiro Kawase. 2013. "The Relationship between Tyrosine Kinase Inhibitor Therapy and Overall Survival in Patients with Non-Small Cell Lung Cancer Carrying EGFR Mutations." *Chinese Journal of Cancer* 32 (3): 136–40. https://doi.org/10.5732/cjc.012.10160.

Takei, Kohji, and Volker Haucke. 2001. "Clathrin-Mediated Endocytosis: Membrane Factors Pull the Trigger." *Trends in Cell Biology* 11 (9): 385–91. https://doi.org/10.1016/S0962-8924(01)02082-7.

Tan, Chee Seng, Nesaretnam Barr Kumarakulasinghe, Yi Qing Huang, Yvonne Li En Ang, Joan Rou En Choo, Boon Cher Goh, and Ross A. Soo. 2018. "Third Generation EGFR TKIs: Current Data and Future Directions." *Molecular Cancer* 17 (1): 1–14. https://doi.org/10.1186/s12943-018-0778-0.

Tanaka, Tomohiro, Yue Zhou, Tatsuhiko Ozawa, Ryuya Okizono, Ayako Banba, Tomohiro Yamamura, Eiji Oga, Atsushi Muraguchi, and Hiroaki Sakurai. 2018. "Ligand-Activated Epidermal Growth Factor Receptor (EGFR) Signaling Governs Endocytic Trafficking of Unliganded Receptor Monomers by Non-Canonical Phosphorylation." *Journal of Biological Chemistry* 293 (7): 2288–2301. https://doi.org/10.1074/jbc.M117.811299.

Tang, Monica, Andrea Schaffer, Belinda E. Kiely, Benjamin Daniels, Robert J. Simes, Chee K. Lee, and Sallie Anne Pearson. 2019. "Treatment Patterns and Survival in HER2-Positive Early Breast Cancer: A Whole-of-Population Australian Cohort Study (2007–2016)." *British Journal of Cancer* 121 (11): 904–11. https://doi.org/10.1038/s41416-019-0612-5.

Tanner, Caroline M. 2020. "Exploring the Clinical Burden of OFF Periods in Parkinson Disease." *American Journal of Managed Care* 26 (12): S255–64. https://doi.org/10.1007/s11910-018-0829-3.

Teramura, Yuji, Junya Ichinose, Hiroaki Takagi, Kenji Nishida, Toshio Yanagida, and Yasushi Sako. 2006. "Single-Molecule Analysis of Epidermal Growth Factor Binding on the Surface of Living Cells." *EMBO Journal* 25 (18): 4215–22. https://doi.org/10.1038/sj.emboj.7601308.

Thibado, Jordana K., Jean Yves Tano, Joon Lee, Leslie Salas-Estrada, Davide Provasi, Alexa Strauss, Joao Marcelo Lamim Ribeiro, et al. 2021. "Differences in Interactions between Transmembrane Domains Tune the Activation of Metabotropic Glutamate Receptors." *ELife* 10: 1–32. https://doi.org/10.7554/ELIFE.67027.

Threadgill, David W., Andrzej A. Dlugosz, Laura A. Hansen, Tamar Tennenbaum, Ulrike Lichti, Della Yee, Christian LaMantia, et al. 1995. "Targeted Disruption of Mouse EGF Receptor: Effect of Genetic Background on Mutant Phenotype." *Science* 269 (5221): 230–34. https://doi.org/10.1126/science.7618084.

Uchikawa, Emiko, Eunhee Choi, Guijun Shang, Hongtao Yu, and Bai Xiao-Chen. 2019. "Activation Mechanism of the Insulin Receptor Revealed by Cryo-EM Structure of the Fully Liganded Receptor-Ligand Complex." *ELife* 8: 1–23. https://doi.org/10.7554/eLife.48630.

Vilar, Bruno, Jérôme Busserolles, Bing Ling, Sophie Laffray, Lauriane Ulmann, Fanny Malhaire, Eric Chapuy, et al. 2013. "Alleviating Pain Hypersensitivity through Activation of Type 4 Metabotropic Glutamate Receptor." *Journal of Neuroscience* 33 (48): 18951–65. https://doi.org/10.1523/JNEUROSCI.1221-13.2013.

Wang, Shuhang, Yongping Song, and Delong Liu. 2017. "EAI045: The Fourth-Generation EGFR Inhibitor Overcoming T790M and C797S Resistance." *Cancer Letters* 385: 51–54. https://doi.org/10.1016/j.canlet.2016.11.008.

Wang, Shuhang, Stella T. Tsui, Christina Liu, Yongping Song, and Delong Liu. 2016. "EGFR C797S Mutation Mediates Resistance to Third-Generation Inhibitors in T790M-Positive Non-Small Cell Lung Cancer." *Journal of Hematology & Oncology* 9 (1): 59. https://doi.org/10.1186/s13045-016-0290-1.

Warmuth, Markus, Robert Damoiseaux, Yi Liu, Doriano Fabbro, and Nathanael Gray. 2005. "Src Family Kinases: Potential Targets for the Treatment of Human Cancer and Leukemia." *Current Pharmaceutical Design* 9 (25): 2043–59. https://doi.org/10.2174/1381612033454126.

Wee, Ping, and Zhixiang Wang. 2017. "Epidermal Growth Factor Receptor Cell Proliferation Signaling Pathways." *Cancers* 9 (5): 1–45. https://doi.org/10.3390/cancers9050052.

Wettschureck, Nina, and Stefan Offermanns. 2005. "Mammalian G Proteins and Their Cell Type Specific Functions." *Physiological Reviews* 85 (4): 1159–1204. https://doi.org/10.1152/physrev.00003.2005.

William, Doreen, Poroshista Mokri, Nora Lamp, Michael Linnebacher, Carl Friedrich Classen, Andreas Erbersdobler, and Björn Schneider. 2017. "Amplification of the EGFR Gene Can Be Maintained and Modulated by Variation of EGF Concentrations in in Vitro Models of Glioblastoma Multiforme." *PLoS ONE* 12 (9): 1–13. https://doi.org/10.1371/journal.pone.0185208.

Wilson, Kristy J, Jennifer L Gilmore, John Foley, Mark A Lemmon, and David J Riese II. 2009. "Functional Selectivity of EGF Family Peptide Growth Factors: Implications for Cancer." *Pharmacology and Therapeutics* 122 (1): 1–8. https://doi.org/110.1016/j.pharmthera.2008.11.008.

Witebsky, Ernest. 1954. "Witebsky : Ehrlich ' s Side-Chain Theory." *Annals of the New York Academy of Sciences*, 168–81.

Wood, Edgar R, Anne T Truesdale, Octerloney B Mcdonald, Derek Yuan, Anne Hassell, Scott H Dickerson, Byron Ellis, et al. 2004. "A Unique Structure for Epidermal Growth Factor Receptor Bound to GW572016 ( Lapatinib ): Relationships among Protein Conformation , Inhibitor Off-Rate , and Receptor Activity in Tumor Cells." *Cancer Research* 64: 6652–59.

Wood, Michael R., Corey R. Hopkins, John T. Brogan, P. Jeffrey Conn, and Craig W. Lindsley. 2011. "'Molecular Switches' on MGluR Allosteric Ligands That Modulate Modes of Pharmacology." *Biochemistry* 50 (13): 2403–10. https://doi.org/10.1021/bi200129s.

Wu, Huixian, Chong Wang, Karen J Gregory, Gye Won Han, Hyekyung P Cho, Colleen M Niswender, Vsevolod Katritch, et al. 2014. "Structure of a Class C GPCR Metabotropic Glutamate Receptor 1 Bound to an Allosteric Modulator." *Science* 344 (6179): 58–64. https://doi.org/10.1126/science.1249489.

Wu, Qiang, Wuxia Luo, Wen Li, Ting Wang, Lin Huang, and Feng Xu. 2021. "First-Generation EGFR-TKI Plus Chemotherapy Versus EGFR-TKI Alone as First-Line Treatment in Advanced NSCLC With EGFR Activating

Mutation: A Systematic Review and Meta-Analysis of Randomized Controlled Trials." *Frontiers in Oncology* 11 (April): 1–12. https://doi.org/10.3389/fonc.2021.598265.

Xiang, Zixiu, Xiaohui Lv, Xin Lin, Daniel E O'Brien, Molly K Altman, Craig W Lindsley, Jonathan A Javitch, Colleen M Niswender, and Jeffrey P Conn. 2021. "Input-Specific Regulation of Glutamatergic Synaptic Transmission in the Medial Prefrontal Cortex by MGlu 2/MGlu 4 Receptor Heterodimers." *Science Signaling* 14 (677): eabd2319.

Xu, Jide, Todd M Corneillie, Evan G Moore, Ga-Lai Law, Nathaniel G Butlin, and Kenneth N Raymond. 2011. "Octadentate Cages of Tb(III) 2-Hydroxyisophthalamides: A New Standard for Luminescent Lanthanide Labels." *Journal of the American Chemical Society* 133 (49): 19900–910. https://doi.org/10.1021/ja2079898.

Xue, Li, Qian Sun, Han Zhao, Xavier Rovira, Siyu Gai, Qianwen He, Jean Philippe Pin, Jianfeng Liu, and Philippe Rondard. 2019. *Rearrangement of the Transmembrane Domain Interfaces Associated with the Activation of a GPCR Hetero-Oligomer*. *Nature Communications*. Vol. 10. https://doi.org/10.1038/s41467-019-10834-5.

Yamashita, Hirotaka, Yoshiaki Yano, Kenichi Kawano, and Katsumi Matsuzaki. 2015. "Oligomerization-Function Relationship of EGFR on Living Cells Detected by the Coiled-Coil Labeling and FRET Microscopy." *Biochimica et Biophysica Acta - Biomembranes* 1848 (6): 1359–66. https://doi.org/10.1016/j.bbamem.2015.03.004.

Yavas, Sibel, Radek Macháň, and Thorsten Wohland. 2016. "The Epidermal Growth Factor Receptor Forms Location-Dependent Complexes in Resting Cells." *Biophysical Journal* 111 (10): 2241–54. https://doi.org/10.1016/j.bpj.2016.09.049.

Yin, Shen, Meredith J. Noetzel, Kari A. Johnson, Rocio Zamorano, Nidhi Jalan-Sakrikar, Karen J. Gregory, P. Jeffrey Conn, and Colleen M. Niswender. 2014. "Selective Actions of Novel Allosteric Modulators Reveal Functional Heteromers of Metabotropic Glutamate Receptors in the CNS." *Journal of Neuroscience* 34 (1): 79–94. https://doi.org/10.1523/JNEUROSCI.1129-13.2014.

Yoo, Byong Chul, Eunkyung Jeon, Sung Hye Hong, Young Kyoung Shin, Hee Jin Chang, and Jae Gahb Park. 2004. "Metabotropic Glutamate Receptor 4-Mediated 5-Fluorouracil Resistance in a Human Colon Cancer Cell Line." *Clinical Cancer Research* 10 (12 I): 4176–84. https://doi.org/10.1158/1078-0432.CCR-1114-03.

Yu, Xiaochun, Kailash D. Sharma, Tsuyoshi Takahashi, Ryo Iwamoto, and Eisuke Mekada. 2002. "Ligand-Independent Dimer Formation of Epidermal Growth Factor Receptor (EGFR) Is a Step Separable from Ligand-Induced EGFR Signaling." *Molecular Biology of the Cell* 13 (6): 2170–79. https://doi.org/10.1091/mbc.01.

Yun, C.-H., K. E. Mengwasser, A. V. Toms, M. S. Woo, H. Greulich, K.-K. Wong, M. Meyerson, and M. J. Eck. 2008. "The T790M Mutation in EGFR Kinase Causes Drug Resistance by Increasing the Affinity for ATP." *Proceedings of the National Academy of Sciences* 105 (6): 2070–75. https://doi.org/10.1073/pnas.0709662105.

Zanetti-Domingues, Laura C., Dimitrios Korovesis, Sarah R. Needham, Christopher J. Tynan, Shiori Sagawa, Selene K. Roberts, Antonija Kuzmanic, et al. 2018. "The Architecture of EGFR's Basal Complexes Reveals Autoinhibition Mechanisms in Dimers and Oligomers." *Nature Communications* 9 (1): 4325. https://doi.org/10.1038/s41467-018-06632-0.

Zhang, Hao, Hong Yi Zhao, Xiao Xiao Xi, Yan Jie Liu, Minhang Xin, Shuai Mao, Jun Jie Zhang, A. Xin Lu, and San Qi Zhang. 2020. "Discovery of Potent Epidermal Growth Factor Receptor (EGFR) Degraders by Proteolysis Targeting Chimera (PROTAC)." *European Journal of Medicinal Chemistry* 189: 112061. https://doi.org/10.1016/j.ejmech.2020.112061.

Zhang, Xuewu, Jodi Gureasko, Kui Shen, Philip A. Cole, and John Kuriyan. 2006. "An Allosteric Mechanism for Activation of the Kinase Domain of Epidermal Growth Factor Receptor." *Cell* 125 (6): 1137–49. https://doi.org/10.1016/j.cell.2006.05.013.

Zhang, Zhichao, Xiaoyan Zheng, Yan Luan, Yingfei Liu, Xingxing Li, Chongxiao Liu, Haixia Lu, Xinlin Chen, and Yong Liu. 2018. "Activity of Metabotropic Glutamate Receptor 4 Suppresses Proliferation and Promotes Apoptosis with Inhibition of Gli-1 in Human Glioblastoma Cells." *Frontiers in Neuroscience* 12 (MAY): 1–16. https://doi.org/10.3389/fnins.2018.00320.

Zhao, Peng, Ming Yu Yao, Su Jie Zhu, Ji Yun Chen, and Cai Hong Yun. 2018. "Crystal Structure of EGFR T790M/C797S/V948R in Complex with EAI045." *Biochemical and Biophysical Research Communications* 502 (3): 332–37. https://doi.org/10.1016/j.bbrc.2018.05.154.

Zhen, Yuejun, Richard M. Caprioli, and James V. Staros. 2003. "Characterization of Glycosylation Sites of the Epidermal Growth Factor Receptor." *Biochemistry* 42 (18): 5478–92. https://doi.org/10.1021/bi027101p.

Zussy, C., X. Gómez-Santacana, X. Rovira, D. De Bundel, S. Ferrazzo, D. Bosch, D. Asede, et al. 2018. "Dynamic Modulation of Inflammatory Pain-Related Affective and Sensory Symptoms by Optical Control of Amygdala Metabotropic Glutamate Receptor 4." *Molecular Psychiatry* 23: 509–20. https://doi.org/10.1038/mp.2016.223.

Zwier, Jurriaan M., Herve Bazin, Laurent Lamarque, and Gérard Mathis. 2014. "Luminescent Lanthanide Cryptates: From the Bench to the Bedside." *Inorganic Chemistry* 53 (4): 1854–66. https://doi.org/10.1021/ic402234k.